University of Nottingham
UK | CHINA | MALAYSIA

inspire
European Training Network in Safety Pharmacology

Cardiovascular safety liabilities of VEGFR-2 inhibitors

Patrizia Pannucci, MPharm

Thesis submitted to the University of Nottingham for the Degree of Doctor of Philosophy

October 2023

This thesis is entirely the candidate's own work. The experiments described in *Methods 2.1, 2.2.1, Chapter 3 and Chapter 4* of this thesis were performed between October 2020 and October 2023 in the Cell Signalling Research Group at the Centre of Membrane Proteins and Receptors, University of Nottingham, UK. All *in vitro* experiments were completely solely by the author. All *in vivo* work was performed as part of a collaborative research team comprising of Patrizia Pannucci (The Author: Experimenter, Surgeon and Surgical Assistant), Julie March (Surgeon and Senior Lab Technician), Sam Cooper (Experimenter, Surgeon and Surgical Assistant), Jeanette Woolard (Principal Investigator, Project Licence Holder and Surgical Assistant), Edward Wragg (Experimenter and Surgical Assistant), Marleen Groenen (Surgical Assistant) and Marieke Van Daele (Surgical Assistant).

The experiments described in *Methods 2.2.2, 2.2.3, 2.3* and *Chapter 5* of this thesis were performed between October 2022 and April 2023 in the Laboratory of Physiopharmacology, University of Antwerp, Belgium. All *ex vivo* work was performed as part of a collaborative research team comprising of Patrizia Pannucci (The Author, Experimenter), Dustin Krüger (Experimenter), Callan Wesley (Experimenter), Cédric Neutel (Experimenter), Pieter-Jan Guns (Principal Investigator, Project Licence Holder). All *in vivo* work was performed by Patrizia Pannucci (The Author, Experimenter, Surgeon), Dustin Krüger (Experimenter, Surgeon), Pieter-Jan Guns (Principal Investigator, Project Licence Holder). Histological staining was performed by Mandy Vermont (Lab Technician), histology imaging and analysis were performed by Patrizia Pannucci and Dustin Krüger.

No part of this material has been submitted previously for a degree or any other qualification at any University.

Funding: This work was supported financially by the by the H2020 Marie Skłodowska-Curie Actions (grant number GA 858070).

Conflicts of Interest: The author declares no conflicts of interest.

I. Abstract

The identification of the vascular endothelial growth factor (VEGF) as a crucial determinant in neoangiogenesis, as well as the role of its overexpression in tumour growth and dissemination, have provided an attractive target for more specific cancer treatments. In particular, since the clinical approval of the first receptor tyrosine kinase inhibitor (RTKI) in 2001, several agents targeting vascular endothelial growth factor receptor (VEGFR) signalling have been approved for the treatment of a variety of malignancies. However, the improved clinical outcomes associated with these therapeutics have been accompanied by unanticipated cardiovascular toxicities, in particular hypertension, resulting in both acute- and long-term cardiovascular dysfunctions, which still represent a major cause of morbidity and mortality in cancer survivors. As a result, cardiovascular safety of VEGFR inhibitors remains a major challenge in oncology, since unanticipated and poorly controlled cardiovascular toxicities induced by these therapeutics often result in a reduction of therapeutic dosage or treatment interruption, therefore influencing cancer management. To that end, this project aimed to comprehensively characterise the cardiovascular safety liabilities associated with two VEGFR-2 inhibitors, in particular axitinib and lenvatinib, as well as investigate the involvement of endothelin-1 (ET-1) system in the development of RTKI-induced hypertension. Combining diverse *in vitro*, *ex vivo* and *in vivo* approaches, the purpose of this study was also the identification of sensitive approaches to readily detect cardiovascular risk of these novel targeted therapies in preclinical settings.

As the incidence of hypertension seems to be correlated to the potency of these therapeutics against VEGFR-2, we first quantified the inhibitory activity of a spectrum of RTKIs on VEGFR-2 mediated responses. The five RTKIs targeting VEGFR-2 tested in this study (axitinib, linifanib, vatalanib, SU-14813 and lenvatinib) showed a potent inhibition of $VEGF_{165}$a-stimulated nuclear factor of activated T-cell (NFAT) response with IC_{50} values in nanomolar range, with axitinib and lenvatinib showing highest relative potency for the receptor. These two RTKIs were then selected for the characterisation of their haemodynamic effects in conscious and freely moving rats. Both axitinib and lenvatinib caused a significant hypertensive response, which was associated with an increased vascular tone in hindquarters and mesenteric arteries. Additionally, given the onset time for hypertension in the animal model used (24-48 hours), this *in vivo* model has proven to be a sensitive and translational

approach for the prediction and early detection of haemodynamic effects of these novel targeted anticancer therapies.

Second, we investigated the role of dual ET_A/ET_B receptor blockade with bosentan and selective ET_A receptor antagonism with sitaxentan in the prevention of axitinib- and lenvatinib-induced hypertension. In conscious and freely moving rats, sitaxentan completely prevented the hypertensive response to axitinib and lenvatinib. These findings established the contribution of ET-1 to RTKI-induced hypertension. In particular, our results have demonstrated that such increase in BP is purely regulated by ET_A receptors. The simultaneous evaluation of the role of endothelin receptors antagonism in preventing the RTKI-mediated alterations of vascular tone in regional vascular beds showed that axitinib- and lenvatinib-induced increase of mesenteric vascular tone could be independent of their hypertensive effect, and it may be mainly mediated by ET_B receptors.

Third, *ex vivo* studies were used to investigate the effect of axitinib and lenvatinib on vascular reactivity and endothelial function, while also assessing the role of arterial stiffness in the haemodynamic responses associated with these agents. Experiments on isolated mouse aortic segments showed that the treatment with axitinib and lenvatinib was not associated with endothelial dysfunction, as reported by the unaltered endothelium-dependent relaxation in response to acetylcholine (ACh). Endothelium-independent relaxation in response to nitric oxide (NO) donor was not affected by both axitinib and lenvatinib, suggesting a preserved vascular smooth muscle cells (VSMCs) function. In addition, the rodent oscillatory set-up to study arterial compliance (ROTSAC) was used to investigate the effect of axitinib and lenvatinib on arterial stiffness; no evidence was found that these agents affect arterial compliance in the time period evaluated in this study.

Finally, *in vivo* experiments were performed to assess cardiac functional and structural changes induced by axitinib and lenvatinib in a mouse model. Echocardiographic measurements and pressure-volume loops analysis revealed an impairment of systolic function in response to lenvatinib. The treatment with this RTKI was also associated with structural changes of the left ventricle (LV), including left ventricular wall thinning and cavity enlargement, suggestive of drug-induced dilated cardiomyopathy.

II. Publications

RESEARCH PAPERS

Wragg ES*, Pannucci P*, Hill SJ, Woolard J, Cooper SL (2022). Involvement of β-adrenoceptors in the cardiovascular responses induced by selective adenosine A_{2A} and A_{2B} receptor agonists. *Pharmacology Research & Perspectives*. 10:e00975. doi:10.1002/prp2.975

Cooper SL*, Wragg ES*, Pannucci P, Soave M, Hill SJ, Woolard J (2022). Regionally selective cardiovascular responses to adenosine A_{2A} and A_{2B} receptor activation. *The FASEB Journal.* 36:e22214. doi:10.1096/fj.202101945R

*Authors contributed equally to this work.

REVIEW ARTICLES

Pannucci P, Jefferson SR, Hampshire J, Cooper SL, Hill SJ, Woolard J (2023). COVID-19-Induced Myocarditis: Pathophysiological Roles of ACE2 and Toll-like Receptors. *International Journal of Molecular Sciences*. 24(6):5374. https://doi.org/10.3390/ijms24065374

Van Daele M, Cooper SL, Pannucci P, Wragg ES, March J, de Jong I, Woolard J (2022). Monitoring haemodynamic changes in rodent models to better inform safety pharmacology: Novel insights from in vivo studies and waveform analysis. *JRSM Cardiovascular Disease*. 11. doi:10.1177/20480040221092893

CONFERENCE PROCEEDINGS

Pannucci P, Krüger D, Wesley CD, Neutel CHG, Guns PJ Hill SJ, Woolard J (2023). Cardiovascular functional and structural alterations induced by VEGFR-2 inhibitors axitinib and lenvatinib.
(Poster presentation at Safety Pharmacology Society Annual Meeting 2023, Brussels, Belgium).

Pannucci P, Krüger D, Wesley CD, Neutel CHG, Guns PJ Hill SJ, Woolard J (2023). Cardiovascular functional and structural alterations induced by VEGFR-2 inhibitors axitinib and lenvatinib.
(Oral communication at University of Nottingham PGR Symposium, 2023).

Pannucci P, March J, Cooper SL, Hill SJ, Woolard J (2023). Assessing the cardiovascular safety liabilities of growth factor inhibitors.
(Oral communication at the Bunnett Lab, New York University, 2023).

Pannucci P, March J, Cooper SL, Hill SJ, Woolard J (2022). Role of dual versus selective endothelin receptor antagonism in the prevention of axitinib-induced cardiovascular haemodynamic changes in conscious, freely moving rats.
(Poster presentation at Safety Pharmacology Society Annual Meeting 2022, Montréal, Canada).

Pannucci P, March J, Cooper SL, Hill SJ, Woolard J (2022). Assessing the cardiovascular safety liabilities of growth factor inhibitors.
(Oral communication at COMPARE Symposium, University of Nottingham, 2022).

Pannucci P, March J, Cooper SL, Hill SJ, Woolard J (2022). Effects of axitinib and lenvatinib on cardiovascular function and haemodynamic.
(Oral communication at University of Nottingham PGR Symposium, 2022).

Pannucci P, March J, Cooper SL, Hill SJ, Woolard J (2022). Effects of axitinib and lenvatinib on cardiovascular function and haemodynamic.
(Poster presentation at Frontiers in Cardiovascular Biomedicine 2022, Budapest, Hungary. Abstract published for *Cardiovascular Research*, Volume 118, Issue Supplement_1, cvac066.210).

III. Acknowledgments

First, I am extremely grateful to my supervisors, Prof. Jeanette Woolard and Prof. Steve Hill, for their invaluable advice, continuous support, and patience during my PhD. You have pushed and supported me while also providing an environment where I felt comfortable seeking help and advice. Thank you for being fantastic supervisors and for helping me through countless difficult situations. I am sure that your professional and personal guidance will guide me for the rest of my career.

A big thank you to the "F-floor" team, without whose support large part of my *in vivo* work would have not been possible. Working with animals is amazing but also quite challenging. The "F-floor" team allowed me to maintain my passion for *in vivo* research, while also helping me navigating the continuous challenges that this entails. I would like to thank Julie March for her incredible work and help in the lab. A special thanks to Marleen Groenen for assisting the experiments while also providing immense personal support. I also want to thank Dr. Eddy Wragg, for his precious help with the last *in vivo* experiments. Finally, I am deeply thankful to Dr. Sam Cooper, whose mentorship and encouragement have been instrumental in the successful completion of this thesis. Thank you not only for teaching me how to carry out *in vivo* experiments but also for consistently making time for me, discussing ideas, and answering my countless questions.

I would also like to express my appreciation to Dr. Laura Kilpatrick, who has taught me everything about the NFAT assay and whose kindness helped me since the first day I arrived in Nottingham.

I would not have been able to do this project without the financial support provided by INSPIRE EU Horizon 2020 Research and Innovation programme under Marie Skłodowska-Curie Action. A special thanks to Prof. Pieter-Jan Guns and Paz Yanez for putting together the INSPIRE team and for coordinating such a great network over the past 3 years.

I want to thank everyone in the INSPIRE network. Every single person deserves a paragraph of appreciation. Being part of this collaboration was a transformative journey, not only in terms of professional growth but mostly for the personal aspect. In this context, I want to express my gratitude to Prof. Pieter-Jan Guns for hosting me at the University of Antwerp and making Chapter 5 of this thesis possible. His expertise and dedication have been inspiring. I am truly thankful to my colleagues (now friends) at the University of Antwerp, in particular Callan Wesley and Dustin Krüger, for being a great bunch of people in and out of the lab. Our discussions, exchange of ideas and shared moments enriched my academic and personal life.

To my incredible friend Silvia Tomellini. You have not only been a friend but a constant reminder that the journey is as important as the destination. Your friendship has been a reassuring presence during the inevitable challenges of this adventure.

I am profoundly grateful to Dr. Francesco Volse, Dr. Giovanna Palumbo, Dr. Alessandra Violet Bacca and Dr. Carlo Enrico Ambrosini for their extraordinary role during the most challenging moments of my life. Your medical expertise, resolution, sincere compassion and personal support have left an indelible mark on my life.

Finally, an immensely big thank you to my family. To my Mum and Dad, your sacrifices, support, and belief in my abilities have been a tremendous source of strength. A special thank you to my sister, my biggest cheerleader. You brought laughter and joy to my life, ensuring that I never lost sight of the lighter side of life. Being far from you has not been easy, but I felt your presence every single moment of this journey. A very special mention to Clayton Wesley. For the moments we have shared, the growth we have experienced together and the bright future we are building.

Abbreviations

ACh	Acetylcholine
ADR	Adverse drug reaction
AMPK	Adenosine monophosphate-activated protein kinase
ATP	Adenosine triphosphate
AUC	Area under the curve
BP	Blood pressure
bpm	Beats per minute
BSA	Bovine serum albumin
DAG	Diacylglycerol
DBP	Diastolic blood pressure
DEANO	Diethylamine NONOate
Dll4	Delta-like ligand 4
DMEM	Dulbecco's modified Eagle's medium
DMSO	Dimethyl sulfoxide
EC	Endothelial cell
ECD	Extracellular ligand-binding domain
ECE	Endothelin converting enzyme
ECG	Electrocardiogram
ECM	Extracellular matrix
EDPVR	End-diastolic pressure-volume relationship
EF	Ejection fraction
EMA	European Medicines Agency
eNOS	Endothelial nitric oxide synthase
ERK1/2	Extracellular signal-regulated protein kinase 1/2
ESPVR	End-systolic pressure-volume relationship
ET-1	Endothelin 1
ET_A	Endothelin receptor type A
ET_B	Endothelin receptor type B
FCS	Foetal calf serum
FDA	Food and Drug Administration
FGFR	Fibroblast growth factor receptor
FS	Fractional shortening

hERG	Human ether-a-go-go related gene
HIF-1	Hypoxia-inducible factor-1
HPβCD	Hydroxypropyl-β-cyclodextrin
HR	Heart rate
HRE	Hypoxia response element
HSP27	Heat shock protein 27
HSPG	Heparan sulphate proteoglycan
HTN	Hypertension
IP_3	Inositol-1,4,5-trisphosphate
IVCO	Inferior vena cava occlusion
L-NAME	L^{ω}-Nitro-L-arginine methyl ester hydrochloride
LV	Left ventricle
LVAW	Left ventricular anterior wall
LVD	Left ventricular dysfunction
LVEDP	Left ventricular end-diastolic pressure
LVEF	Left ventricular ejection fraction
LVID	Left ventricular internal diameter
LVPW	Left ventricular posterior wall
LVV	Left ventricular volume
MAP	Mean arterial pressure
MAPK	Mitogen-activated protein kinase
MMP-9	Matrix metalloproteinase-9
mRCC	Metastatic renal cell carcinoma
mRNA	Messenger ribonucleic acid
MV	Mitral valve
NFAT	Nuclear factor of activated T-cells
NNH	Number needed to harm
NO	Nitric oxide
NRP-1	Neuropilin 1
NRP-2	Neuropilin 2
NRP	Neuropilin
OR	Odds ratio
OS	Overall survival
PAI-1	Plasminogen activator inhibitor-1

PDGF	Platelet-derived growth factor
PDGFR	Platelet-derived growth factor receptor
PDL	Poly-D-lysine
PE	Phenylephrine
PFS	Progression-free survival
PGI_2	Prostaglandin I2
PI3K	Phosphatidylinositol 3-kinase
PIP_2	Phosphatidylinositol -4,5- bisphosphate
PKB	Protein kinase B
PKC	Protein kinase C
PLAX	Parasternal long-axis
PLCγ	Phospholipase C gamma
PlGF	Placental growth factor
PP	Pulse pressure
PRF	Pulse repetition frequency
PSAX	Parasternal short-axis
PV	Pressure-volume
RCC	Renal cell carcinoma
RR	Respiratory rate
RTK	Receptor tyrosine kinase
RTKI	Receptor tyrosine kinase inhibitor
RVU	Relative value unit
SBP	Systolic blood pressure
SP	Safety Pharmacology
SR	Sarcoplasmic reticulum
SV	Stroke volume
TKI	Tyrosine kinase inhibitor
TNF-α	Tumour necrosis factor α
TSAd	T cell specific adaptor protein
uPA	Urokinase-type plasminogen activator
VEGF	Vascular endothelial growth factor
VEGFR	Vascular endothelial growth factor receptor
VC	Vascular conductance
VSMC	Vascular smooth muscle cell

1 General Introduction

Cancer represents a leading cause of death worldwide (Nagai & Kim, 2017; Bray et al., 2021), with an incidence that increased from 12.7 to 19.3 million new cancer cases in the period from 2008 to 2020 (Ferlay et al., 2010; Sung et al., 2021). Globally, new cancer cases are expected to rise to 28.4 million by 2040 (Hulvat, 2020; Sung et al., 2021). However, the mortality rate among cancer patients has significantly reduced in the last 20 years, primarily as a result of considerable advances in terms of tumour prevention, diagnosis and treatment (Barac et al., 2015; Miller et al., 2022). In the past decade, a growing understanding of the biological processes underlying cancer initiation and progression has redefined the therapeutic approach in the oncology field (Lee et al., 2018; Malone et al., 2020). In particular, the introduction of novel cancer treatments targeting the VEGF pathway has led to a considerable reduction in morbidity and mortality among cancer patients (Bhargava & Robinson, 2011; Vasudev & Reynolds, 2014; Iacovelli et al., 2015; Lee et al., 2018). Indeed, VEGF, by binding its receptor tyrosine kinase (RTK), acts as a proangiogenic factor, whose overexpression correlates with tumour invasive growth and metastasis (Shibuya, 2011; Apte et al., 2019; Elebiyo et al., 2022). Given the implication of VEGF and RTKs in the pathogenesis of several types of malignancies, new therapeutics, which inhibit functional activity of these proteins, have shown improvements both in terms of progression-free survival (PFS) and overall survival (OS) (R. Siegel et al., 2012; Vasudev & Reynolds, 2014; Iacovelli et al., 2015; Roviello et al., 2017; Baek Moller et al., 2019), although variable results have been obtained depending on the type of cancer, the stage of malignancy and the combination with traditional antineoplastic treatments (Vasudev & Reynolds, 2014; Melincovici et al., 2018). Nevertheless, along with these improved clinical outcomes, soon after the introduction of VEGF inhibitors in clinical practice, unanticipated cardiotoxicities emerged, leading to both acute and long term cardiovascular dysfunctions (Zuppinger & Suter, 2010; Guha et al., 2019), which still represent a major cause of morbidity and mortality in cancer survivors (Barac et al., 2015; Mohammed, Parekh, et al., 2021). Even if from clinical practice it is clear that VEGF inhibition strongly affects the haemodynamic balance in patients treated with RTKIs (Bair et al., 2013; Mäki-Petäjä et al., 2021), the molecular mechanisms underpinning these cardiovascular toxicities are still largely unknown. Many hypotheses have been proposed but a clear understanding of the cardiovascular biology of VEGF and the processes by which its inhibition impairs cardiovascular function remains to be elucidated (Dhaun & Webb, 2010; Small et al., 2014; Touyz et al., 2018; Dorst et al., 2021). The lack of clarity regarding the mechanisms and the extent to which VEGF inhibition affects cardiovascular function complicates the therapeutic management of cancer patients who develop such adverse

effects (Steingart et al., 2012; Dobbin et al., 2018). In particular, the severity of cardiovascular toxicities associated with VEGFR inhibitors often requires a dose reduction, temporary discontinuation or permanent interruption of these potentially lifesaving therapies (Copur & Obermiller, 2011; Mellor et al., 2011; Small et al., 2014; Mohammed, Parekh, et al., 2021). Identifying the specific mechanisms of RTKIs-related cardiovascular toxicities can strongly contribute to develop novel targeted cancer therapies which do not alter the signalling pathway responsible for such complications. Moreover, a clear comprehension of the pathophysiology of RTKI-induced cardiovascular diseases would represent a key point in the therapeutic management of these cardiovascular events in cancer population. Indeed, antihypertensive strategies currently used in in the cancer patients who develops RTKI-induced hypertension are generic and not pathophysiologically targeted (Lankhorst, Saleh, et al., 2015b; Dorst et al., 2021). Presently, evidence for an effective approach to assess and treat RTKIs-related cardiovascular dysfunctions is limited and specific guidelines for the management of cardiovascular events in RTKI-treated patients are lacking (Dorst et al., 2021; Mohammed, Parekh, et al., 2021). The majority of data relative to cardiovascular adverse effects of VEGFIs derives from clinical trials or retrospective meta-analyses (Bair et al., 2013). This phenomenon sheds light on the urgent need to identify strategies to assess cardiovascular safety of VEGFR inhibitors during preclinical studies and to detect potential cardiovascular impairment during drug development, in addition to clearly defining the effects of these therapies on the cardiovascular system. In the field of safety pharmacology, these three aspects represent both the theoretical and practical knowledge gaps that this PhD project aims to address. In this context, the vision of the INSPIRE programme (INnovation in Safety Pharmacology for Integrated cardiovascular safety assessment to REduce adverse events and late-stage drug attrition) (Guns et al., 2020), within which my project is supported, is to identify and mitigate cardiovascular complications in an early-stage of the drug development, thus contributing to a substantial progress within the context of the safety pharmacology. Indeed, drug-induced changes in haemodynamic, as well as structural and functional cardiovascular toxicities, represent an emerging problem in safety pharmacology, requiring an unequivocal and urgent identification of predictive preclinical models to define the cardiovascular safety profile of novel anticancer therapeutics, as well as a better understanding of the mechanistic basis of their cardiovascular liabilities, by means of *in vitro*, *ex vivo* and *in vivo* approaches. Combining all these strategies, this project has a key role in the refinement of cardiovascular safety pharmacology assays. This research, aiming to identify the relationship between VEGF signalling inhibition and cardiovascular dysfunctions,

plays a critical role in the future prediction and prevention of cardiovascular risk in patients treated with RTKIs. Considering the success of these drugs in cancer treatment, fully understanding the pathophysiological events behind their cardiovascular toxicity, as well as identifying more sensitive predictive tools to identify and/or reduce their cardiovascular risk, may have a significant impact in the cardiovascular safety of cancer patients. Indeed, the inadequacy to readily detect cardiovascular risk of these novel targeted therapies in preclinical settings resulted in unanticipated adverse effects both during clinical trials and post-marketing phase, leading to a reduced translational value of the existing investigating approaches (Laverty et al., 2011; Bhatt et al., 2019).

1.1 SAFETY PHARMACOLOGY

Starting from the 1970s, it became clear that the standard studies to preclinically evaluate the toxicity of therapeutics were not sufficient to adequately identify pharmacodynamic adverse effects on physiological functions (Williams, 1990; Bass et al., 2004; Bass et al., 2015). In particular, preclinical safety studies carried out until that period failed to appropriately predict the safety endpoint in humans. From this urgent need to examine the impact of drugs on vital functions prior to human exposure (Pugsley, 2015), safety pharmacology has emerged as a new field, the aim of which is to investigate any functional adverse effect of therapeutics on critical organ systems (e.g. cardiovascular, respiratory and central nervous systems), as officially defined in the International Conference on Harmonization (ICH) S7A (Anon, 2001e). The assessment of pharmacologically based toxicity from the evaluation of drug effects, both on intended therapeutic target and on target distinct from the primary one, represents therefore the major goal of safety pharmacology itself (Anon, 2001e; Pugsley, 2015). As a result, along with preclinical toxicology studies, safety pharmacology plays an essential role within the non-clinical safety profiling of new therapeutics (Claude & Claude, 2004; Morimoto et al., 2015). In the context of drug development, this new approach is seen as an essential strategy to ensure both drug safety and effectiveness, reducing safety-related attrition rate both in preclinical, clinical and post-marketing phase (Bowes et al., 2012; Trame et al., 2016).

Cardiovascular safety liabilities represent the leading cause of drug attrition from preclinical development to post-approval phase (Laverty et al., 2011; Ferri et al., 2013; Weaver & Valentin, 2018), where the incidence of cardiovascular-related attrition may reach up to 45% (Redfern WS, 2010; Valentin, 2010) (Figure 1). The major concern is represented by the subtle, but high-risk, cardiovascular complications which emerge when therapeutics are

clinically used on large scale and for long periods of time, without being either preclinically anticipated or defined as clinically significant during non-clinical and clinical evaluation (Redfern WS, 2010). This phenomenon often results in the temporary or permanent treatment interruption in order to limit cardiovascular toxicities (Laverty et al., 2011). Complications in cardiovascular function are linked to the administration of both cardiovascular and non-cardiovascular therapeutics and include alterations in terms of blood pressure (BP), cardiac function and vascular system (Laverty et al., 2011; Belcik et al., 2012; Ancker et al., 2017; Versmissen et al., 2019). An emerging challenge is represented by cardiovascular toxicity related to novel molecular targeted therapies used in oncology, with particular reference to RTKIs (Barac et al., 2015; Campia et al., 2019). However, the relationship between these drugs and the impairment of cardiovascular status is still far from being clearly understood (Small et al., 2014; Camarda et al., 2022). As a result, predicting and managing cardiovascular adverse effects associated with RTK inhibitors is not only relevant to reduce drug attrition, development times and costs, but it is also essential to improve patient safety (Laverty et al., 2011; Yang & Papoian, 2018). Characterising their impact on cardiovascular physiology, as well as improving the predictive and translational value of existing preclinical investigations, is fundamental in order to determine and limit cardiovascular safety liabilities of these drugs (Laverty et al., 2011; Yang & Papoian, 2012; Chaar et al., 2018).

Phase	Non-clinical	Phase I	Phase I-III	Approval	Post-approval	Post-approval
Information	Cause of attrition	Serious ADRs	Cause of attrition	ADRs on label	Serious ADRs	Withdrawal from sale
Source	Car (2006)	Sibille et al (1998)	Olson (2000)	Krejsa (2003)	Budnitz et al (2006)	Stevens & Baker (2008)
Sample size	88 CDs stopped	1015 subjects	82 CDs stopped	1138 drugs	21298 patients	47 drugs
Cardiovascular system	27%	9%	21%	36%	15%	45%
Hepatic system	8%	7%	21%	13%	0%	32%
Nervous system	14%	28%	21%	67%	39%	2%
Respiratory system	2%	0%	0%	32%	8%	2%

0% 1-10% 10-20% >20%

Figure 1. *Prevalence of safety liabilities relating to the cardiovascular, hepatic, nervous and respiratory systems from the preclinical stage to the post-approval phase and their impact in terms of drug attrition. ADRs = adverse drug reactions; CDs = candidate drugs. Information was compiled from*

published articles (Sibille et al., 1998; Olson et al., 2000; Krejsa et al., 2003; Budnitz et al., 2006; Car, 2006; Stevens & Baker, 2009). Adapted from (Redfern WS, 2010)

1.1.1 Haemodynamic assessment in Safety Pharmacology

Significant attention in cardiovascular safety assessment has been dedicated on drug-induced alterations of the electrocardiogram (ECG) and proarrhythmic potential, mainly via the evaluation of human ether-a-go-go related gene (hERG) potassium channel blockade and *in vivo* assessment of QT interval prolongation potential (Pollard et al., 2010; Valentin, 2010; Pugsley, 2015). An alteration of hERG, which is responsible for encoding for the subunit of one of the most important channel involved in the repolarization of the ventricular cardiomyocyte action potential, leads to an excessive prolongation of the action potential and to an increased dispersion of ventricular repolarization (Sanguinetti & Keating, 1997; Monitillo et al., 2016). A prolongation of the QT interval, representative of a delayed ventricular repolarization, is a critical safety issue in drug development, being in fact associated with an increased risk for potentially fatal ventricular tachyarrhythmia, also known as torsade de pointes (Finlayson et al., 2004; Kannankeril et al., 2010; Sheng et al., 2016; Li & Ramos, 2017). To implement the prediction of clinical proarrhythmic risk, a comprehensive proarrhythmia assay paradigm has been established through an extensive cooperation between industries, regulatory agencies and academia (Colatsky et al., 2016). However, the situation is much less definite when it comes to other cardiovascular alterations such as hypertension and left ventricular dysfunction (LVD) (Valentin, 2010; Pugsley et al., 2015). Indeed, the unclear clinical relevance of elevated BP and changes in cardiac function detected by the existing preclinical models reduces the predicting power of such non-clinical strategies (Valentin, 2010; Pugsley et al., 2015). Specifically, considering that hypertension is the major risk factor for stroke and cardiovascular diseases, a more precise prediction of prohypertensive risk in preclinical models and its clinical implications should be pursued (Authier et al., 2015; Pugsley et al., 2015). Indeed, the relationship between elevated BP and cardiovascular impairment makes arterial BP an essential parameter within safety pharmacology (Valentin, 2010; Authier et al., 2015). A number of methods are available to detect changes in arterial BP in preclinical studies. In particular, significant alterations in BP can be readily detected in preclinical setting and their clinical meaning is easily translatable (Valentin, 2010). Conversely, the major challenge is represented by small alterations in BP, which cannot always be accurately identified in preclinical setting and, when they are detected, their clinical translatability remains difficult

to be interpreted (Valentin, 2010; Authier et al., 2015; Pugsley, 2015). This highlights the need for more sensitive and translational preclinical approaches to assess the hypertensive potential of therapeutics in safety pharmacology studies.

The VEGF signalling inhibitors represent a good example of drugs that have a significant impact on BP, which became evident only when they were used widely within the general population (Minotti et al., 2010; Small et al., 2014). Moreover, the mechanisms by which they cause such hypertensive effect is still unclear (Kamba & McDonald, 2007; Mohammed, Parekh, et al., 2021; Camarda et al., 2022). Using preclinical safety pharmacology models for the haemodynamic assessment of VEGFR-TKIs represents a valuable opportunity to develop new tools able to identify and predict haemodynamic changes associated with these drugs (Belcik et al., 2012; Pugsley, 2015; Bhatt et al., 2019), in addition to permitting the understanding of the mechanisms responsible for RTKIs-related cardiovascular toxicities.

1.1.2 Cardiovascular safety assessment of cancer therapies: the need for cardio-oncology

During the last decade, cancer treatment has undergone a revolutionary progress, moving from non-selective cytotoxic therapies to novel targeted drugs, specifically addressed to cellular pathways overexpressed in cancer cells but not in normal cells (Gerber, 2008). In particular, novel targeted anticancer treatments can be mainly categorized as small molecule (e.g., RTK inhibitors) and large molecule drugs (cytokines, monoclonal antibodies and antibody-drug conjugates) (Martin, 2015; Lee et al., 2018; Zhong et al., 2021). If the high selectivity of large molecule biopharmaceuticals reduces their likelihood of binding unintended targets or exerting toxicity directly related to their mechanism of action (Scott et al., 2012), small molecules, not being characterised by the same elevated specificity, have an increased potential for cross-reactivity with other targets (Davis et al., 2011). As a result of this lack of specificity, low molecular weight therapeutics may lead to complications both related to their mechanism of action ("on-target" toxicity) as well as not linked to their primary target ("off-target" toxicity) (Schmidinger, 2013; Martin, 2015; Touyz et al., 2018; Lin et al., 2019). In this context, RTK inhibitors targeting VEGFRs are a good example of drugs which have been shown to determine cardiovascular impairment although it is not yet clear whether this toxicity results from an "on-target" effect on the intended kinase target (i.e., VEGFR-2) and/or "off-target" interaction with additional kinases (Mellor et al., 2011; Baek Moller et al., 2019). These small molecules, inhibiting VEGF signalling via blockade of VEGFR-2, suppress the pro-angiogenic response associated with this signalling pathway, preventing

the vascularisation and the growth of the primary tumour and metastases (Ferrara, 2004a; Ellis & Hicklin, 2008). Whilst these therapeutics have significantly improved cancer prognosis and survivorship, multiple cardiovascular complications have been identified as associated to these agents, without being anticipated in preclinical studies (Barac et al., 2015; Li et al., 2015; Sheng et al., 2016). This discrepancy draws attention to the lack of predictive and sensitive preclinical strategies to anticipate the cardiovascular liabilities of these therapies, which mainly include severe hypertension, heart failure and thromboembolism (Sheng et al., 2016; Arjun K Ghosh, 2017; Touyz et al., 2018; Camarda et al., 2022). Indeed, within the toxicological assessment of these drugs, the standard repeated-dose studies have not been able to predict and detect these cardiotoxicities (Martin, 2015). As a result of these cardiac and vascular sequelae associated with novel anticancer target therapies, the new translational discipline of cardio-oncology has emerged (Bellinger et al., 2015; Campia et al., 2019; Kostakou et al., 2019; Tan & Lyon, 2021). This multidisciplinary field is focused on limiting and predicting cardiovascular complications in cancer patients and survivors (Yeh & Bickford, 2009; Guha et al., 2019), with the dual aim of reducing both short- and long-term risk for cardiovascular diseases in cancer population, as well as improving our understanding of signalling events implicated in these events (Campia et al., 2019; Versmissen et al., 2019; Tan & Lyon, 2021).

Multitarget tyrosine kinase inhibitors, notably sunitinib and sorafenib, have been reported to produce hypertension and other cardiovascular impairments, such as LVD and heart failure (Chu et al., 2007; Force et al., 2007; Khakoo et al., 2008; Choueiri et al., 2010; Abdel-Rahman & Fouad, 2014). Among cancer patients treated with VEGFR inhibitors, 30% to 80% of them developed hypertension, and a quarter of patients experienced an asymptomatic LVD, resulting in symptomatic heart failure for 4-8% of them (Wu et al., 2008; Yeh & Bickford, 2009; Richards et al., 2011; Chaar et al., 2018; Chung et al., 2020; Mäki-Petäjä et al., 2021). Nevertheless, the inadequacy of primary literature about the cardiovascular adverse events rate of novel anticancer treatments, with particular reference to the most recent RTK inhibitors, represents an additional relevant issue within cardio-oncology (Dong & Chen, 2018; Baek Moller et al., 2019; Chung et al., 2020). These drugs, as inhibitors of the vascular endothelial growth factor (VEGF) signalling pathway, provide an effective strategy in oncology, and are used to treat several malignancies, such as breast, colorectal, lung, pancreatic and hematologic cancer, as well as renal cell and hepatocellular carcinoma (Markman & Markman, 2018; Versmissen et al., 2019; Liu et al., 2022). Even if highly effective

in treating cancer, VEGFR inhibitors have a significant limitation due to their detrimental impact on cardiovascular function (Markman & Markman, 2018; Dobbin et al., 2021). In this regard, the aim of cardio-oncology is therefore to identify new strategies to early detect and appropriately manage alterations on cardiac function and haemodynamic parameters in cancer patients and survivors (Yeh & Bickford, 2009; Barac et al., 2015; Kostakou et al., 2019).

1.2 VEGF SIGNALLING

VEGFs play a key role in regulating a wide range of physiological and pathological responses in different tissues, being master regulators of blood vessel growth and development (Nieves et al., 2009; Shibuya, 2011). The pathways activated by VEGFs mediate both vascular development from precursor cells during embryogenesis (vasculogenesis) and the formation of new blood vessels from pre-existing vasculature (angiogenesis) (Ferrara et al., 2003; Koch & Claesson-Welsh, 2012; Melincovici et al., 2018; Wiszniak & Schwarz, 2021). Along with the regulation of vascular development and angiogenesis, the binding between VEGFs and their cognate receptors, with the contribution of several co-receptors, controls metabolic homeostasis, cell proliferation, migration, survival and permeability (Smith et al., 2015; Apte et al., 2019; di Somma et al., 2020; Wiszniak & Schwarz, 2021). All these responses are the result of a refined and complex signal transduction pathway activated by ligand-mediated VEGFR dimerization and co-receptors recruitment, namely neuropilins (NRPs), heparan sulphate proteoglycans (HSPGs) and integrins (Figure 2) (Jakobsson et al., 2006; Grünewald et al., 2010; Chiodelli et al., 2011; Koch & Claesson-Welsh, 2012; M. Simons et al., 2016). In particular, five different VEGF ligands, and their related splice isoforms, interact in an overlapping manner with three diverse VEGF receptors, which belong to the family of tyrosine kinase receptors (Olsson et al., 2006; Shibuya, 2011; M. Simons et al., 2016). In addition to modulate physiological outcomes, VEGF signalling, if upregulated, has also a role in the pathogenesis of several diseases, including cancer, where uncontrolled angiogenesis and metastatic spreading support tumour growth and invasion (Smith et al., 2015; Apte et al., 2019; Wang et al., 2020). As a result, considering the involvement of VEGFs in vascular development both in health and disease, it is crucial to understand their biology, as well as the events associated with their pathways in physiological and pathological conditions (E. M. Siegel et al., 2012; Smith et al., 2015; Wang et al., 2020; Qi et al., 2022).

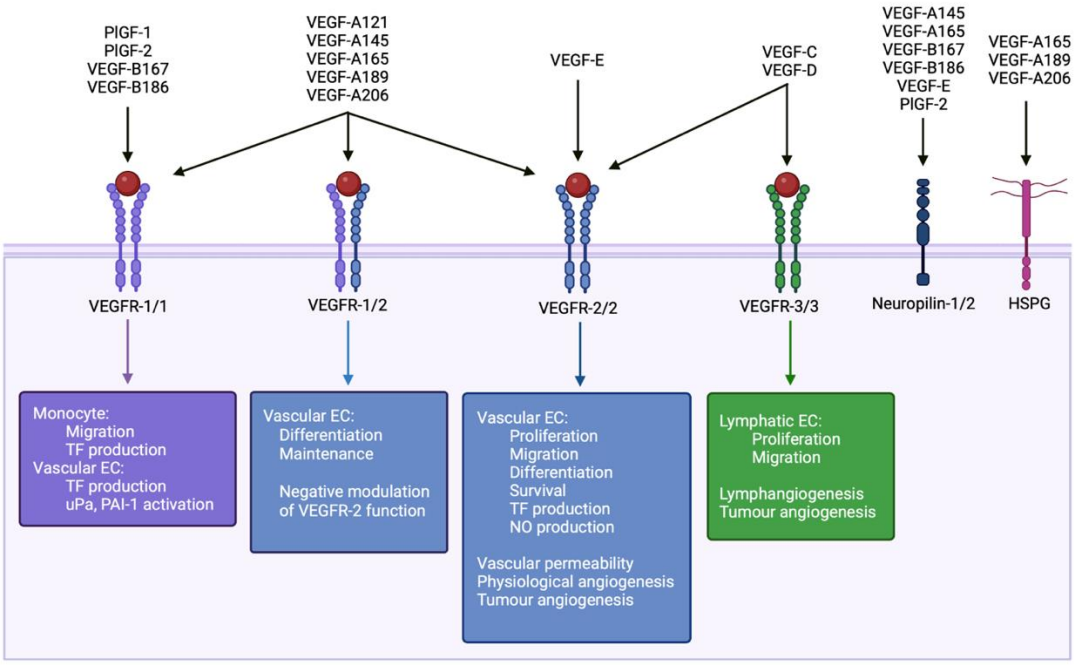

Figure 2. *Interaction between the members of the VEGF family and their cognate receptors. VEGF-A isoforms act as ligands both for VEGFR-1 and VEGFR-2, whereas VEGF-B interact selectively with VEGFR-1. VEGF-C and VEGF-D bind to VEGFR-3 and, if proteolytically processed, bind also VEGFR-2. In addition, $VEGFA_{165}$, $VEGFA_{189}$ and $VEGFA_{206}$, heparin-binding isoforms of VEGF-A, additionally interact with heparan sulphate proteoglycans (HSPG), for a finer modulation of VEGF-A activity. VEGFR-2 can form homodimer or heterodimers with both VEGFR-1 and VEGFR-3. VEGFR-2 homodimer-mediated signalling is finely modulated through the interaction with various co-receptors, in particular HSPG and neuropilins (NRP-1/2). Adapted from (Matsumoto & Claesson-Welsh, 2001; Olsson et al., 2006). Figure created with BioRender.com*

1.2.1 VEGF isoforms

VEGFs are secreted dimeric glycoproteins of 45 kDa (Ferrara & Davis-Smyth, 1997). In mammals, the VEGF family consists of five diverse members: VEGF-A, VEGF-B, VEGF-C, VEGF-D and PlGF (placental growth factor) (Olsson et al., 2006; Shibuya, 2011; Shibuya, 2012). Structurally related to platelet-derived growth factors (PDGFs), VEGFs are characterized by a cysteine knot motif, where interchain and intrachain disulphide bonds occur between eight cysteine residues (Muller et al., 1997; Olsson et al., 2006; Iyer & Acharya, 2011). VEGFs exert their biological activities as dimers, preferentially as homodimers, with VEGF-A and PlGF which are active even as heterodimers (Olsson et al., 2006; Koch et al., 2011; Shibuya, 2011; Shaik et al., 2020).

1.2.1.1 VEGF-A

VEGF-A, also denoted VEGF, is the prototype member of VEGF family, whose activation stimulates endothelial cells (ECs) proliferation and migration, apoptosis inhibition, vasodilation and enhances vascular permeability, leading to a potent proangiogenic response (Ferrara & Adamis, 2016; Melincovici et al., 2018). The human *Vegf-A* gene comprises eight exons and seven introns (Robinson & Stringer, 2001). Alternative splicing results in several isoforms with diverse biological activity (Figure 3) (Holmes & Zachary, 2005; Olsson et al., 2006), including pro-angiogenic isoforms ($VEGF_{121}a$, $VEGF_{145}a$, $VEGF_{148}a$, $VEGF_{165}a$, $VEGF_{183}a$,$VEGF_{189}a$, $VEGF_{206}a$) and anti-angiogenic isoforms ($VEGF_{121}b$, $VEGF_{145}b$, $VEGF_{165}b$, $VEGF_{183}b$, $VEGF_{189}b$) (Bates et al., 2002; Woolard et al., 2009; Smith et al., 2015) where the three-digit number indicates the number of amino acids after signal sequence cleavage (Tischer et al., 1991). In all these variants, exons 1-5 (also called "constitutive exons") are maintained and are responsible for encoding the signal sequence (exon1), the N-terminus dimerization domain (exon 2), the VEGFR1-binding and N-glycosylation (exon 3), the VEGFR2-binding site (exon 4) and the plasmin cleavage site (exon 5) (Smith et al., 2015; Stevens et al., 2019). By contrast, the other exons may be missing in the different isoforms, therefore determining their biological properties (Figure 3). Exons 6a, 6b, 7a and 7b encode the heparin-binding domain and determine the binding with neuropilin and extracellular matrix (ECM). Exons 6a and 7 mediate the interaction with electronegative heparan sulphate in the ECM, defining a diverse bioavailability for each isoform (Peach et al., 2018). Those isoforms lacking exons 6 and 7, such as $VEGF_{111}$ and $VEGF_{121}$, do not bind ECM and are therefore highly diffusible, whereas $VEGF_{145}$, $VEGF_{189}$ and $VEGF_{206}$, where exons 6a and 7 are maintained, remain bound to the ECM (Houck et al., 1991). Another important site of alternative splicing is represented by exon 8, given its crucial function in physiological and pathological angiogenesis (Dehghanian et al., 2014). Indeed, isoforms containing exon 8b, identified as $VEGF_{xxx}b$, have been defined as anti-angiogenic, due to their ability to negatively regulate $VEGF_{xxx}a$-mediated pro-angiogenic activity (Woolard, Wang, et al., 2004; Olsson et al., 2006). This event on exon 8 plays a key role in determining the balance between anti-angiogenic isoforms and those with pro-angiogenic function (Dehghanian et al., 2014). In particular, downregulation of $VEGF_{xxx}b$ isoforms has been shown in several malignancies, where, by contrast, $VEGF_{xxx}a$ is highly expressed, leading to a pathological pro-angiogenic switch. (Woolard, Wang, et al., 2004; Nowak et al., 2008). However, it is worth noting that there is some controversy over whether $VEGF\text{-}A_{xxx}b$ isoforms exist *in vivo* (Bridgett et al., 2017).

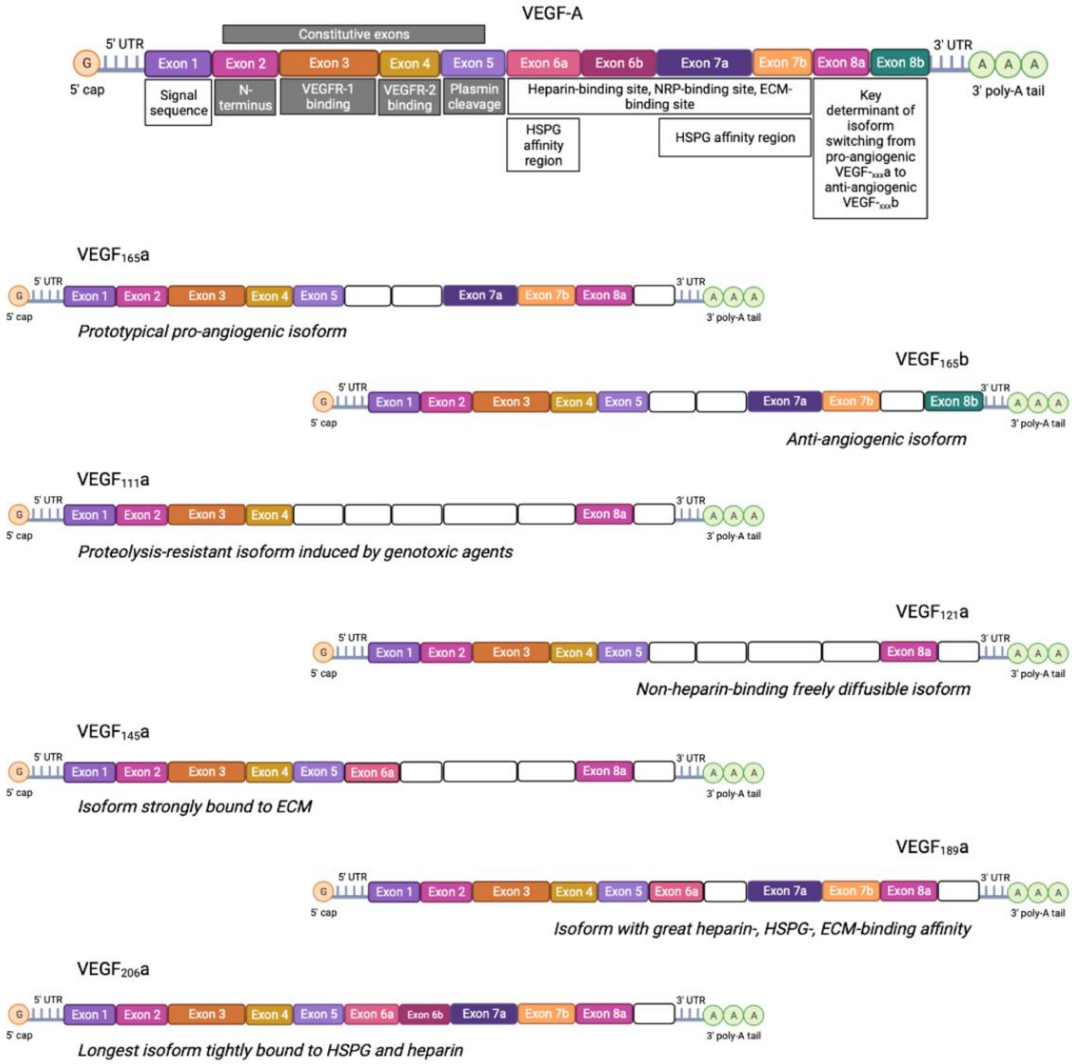

Figure 3. *Alternative splicing in VEGF-A isoforms and their corresponding properties. Adapted from (Peach et al., 2018). Figure created with BioRender.com*

VEGF-A is produced by ECs, but under hypoxic conditions is also secreted by other cells, including cancer cells, macrophages, platelets, keratinocytes, activated T-cells, renal mesangial cells, astrocytes and osteoblasts (Klagsbrun & D'Amore, 1996; Yamazaki & Morita, 2006; Al Kawas et al., 2022). Notably, under low oxygen conditions, stabilized hypoxia-inducible factors (HIFs) interact with specific elements on promoter region of VEGF-A, resulting in an increased transcription and expression of this ligand (Pugh & Ratcliffe, 2003; Déry et al., 2005; Ziello et al., 2007). In terms of receptors, VEGF-A binds both to VEGFR-1 and VEGFR-2, although it shows a 10-fold higher affinity for VEGFR-1 (Shibuya, 2011; Melincovici et al., 2018; Shaik et al., 2020). VEGF-A has also been shown to bind platelet-

derived growth factor receptor alpha (PDGFR-α) and beta (PDGFR-β), promoting both recruitment and proliferation of mesenchymal stem cells (Ball et al., 2007).

1.2.1.2 OTHER ISOFORMS

VEGF-B, abundantly expressed in the myocardium and skeletal muscle, is mainly involved in the embryological development of cardiovascular system and vascular survival, although its contribution in adult angiogenesis is limited (Hoeben et al., 2004; Li et al., 2009; F. Zhang et al., 2009; Räsänen et al., 2021). Two isoforms have been identified as a result of alternative splicing (VEGF-B_{167} and VEGF-B_{186}), both interacting with VEGFR-1 (Lal et al., 2018; Melincovici et al., 2018).

Through their interaction with VEGFR-3 on endothelial lymphatic cells, VEGF-C and VEGF-D control the formation of new lymphatic vessels (lymphangiogenesis), playing only a marginal role in angiogenesis (Shibuya, 2011; Deng et al., 2015).

Placental growth factor (PlGF), mainly secreted by placental tissues and uterine mucosa, is crucial in regulating trophoblast development and blastocyst implantation (De Falco, 2012; Binder et al., 2016). In addition, a specific synergism with VEGF-A determines the pro-angiogenic function of PlGF in pathological conditions (Ziche et al., 1997; Carmeliet et al., 2001; Shibuya, 2011).

1.2.2 VEGF receptors

VEGF-induced biological responses are the result of the interaction between VEGF ligands and specific tyrosine kinase receptors (Smith et al., 2015; Park et al., 2018), precisely denoted as VEGFR-1 (Fms-like tyrosine kinase 1 or Flt-1), VEGFR-2 (kinase insert domain receptor or KDR in human; fetal liver kinase 1 or Flk-1 in mouse) and VEGFR-3 (Fms-like tyrosine kinase 4 or Flt-4) (Melincovici et al., 2018; Stevens & Oltean, 2019). VEGFR-1 and VEGFR-2 are primarily expressed on vascular ECs, although they have been also detected in non-ECs, including cancer cells (Duffy AM, 2000–2013; Matsumoto & Claesson-Welsh, 2001; Olsson et al., 2006). During early embryonic development, VEGFR-3 is expressed both on blood ECs and lymphatic ECs, becoming essentially confined to the lymphatic ECs at later stages (Matsumoto & Claesson-Welsh, 2001; Norgall et al., 2007; Deng et al., 2015).

Structurally related, these membrane-bound receptors consist of an extracellular ligand-binding domain (ECD) with a seven immunoglobulin (Ig)-like domain, a transmembrane domain, a juxtamembrane domain, an intracellular domain with tyrosine kinase domains split by a kinase insert domain and a carboxy-terminal domain (Neufeld et al., 1999; Smith et al.,

2015). Following the receptor dimerization due to the interaction between VEGFs and the extracellular receptor domain, the cytoplasmatic kinase domain is activated, leading to the phosphorylation of the tyrosine residues both on the receptor dimer and on downstream signal transducers, thus activating various signalling pathways (Lemmon & Schlessinger, 2010; Koch & Claesson-Welsh, 2012).

1.2.2.1 VEGFR-1

VEGFR-1 interacts with VEGF-A, VEGF-B and PlGF (Figure 4), whose binding sites have been identified on the second Ig-like domain, responsible for both ligand binding and initiation of signal transduction cascade (Ferrara et al., 2003; Ye et al., 2021). VEGFR-1 shows a lower tyrosine kinase activity in comparison with VEGFR-2 (Shibuya, 2011; Koch & Claesson-Welsh, 2012). Indeed, the interaction between VEGFR-1 and its ligands triggers a weak kinase activity, resulting in a reduced phosphorylation of intracellular tyrosine residues (Rahimi, 2006; Smith et al., 2015). Due to its high affinity for VEGF-A but weak tyrosine kinase activity, VEGFR-1 is also described as a decoy receptor that negatively regulates VEGF-A signalling amplitude (Boucher et al., 2017). Specifically, the tyrosine residues which can be subjected to autophosphorylation are: Y794, Y1169, Y1213, Y1242, Y1309, Y1327 and Y1333 (Figure 4) (Vieira et al., 2010; Smith et al., 2015). In addition to ECs, VEGFR-1 is also expressed on inflammatory cells, monocytes, macrophages, hematopoietic stem cells, trophoblastic cells, mesangial renal cells, vascular smooth muscle cells and tumour cells (Neufeld et al., 1999; Autiero et al., 2003; Yao et al., 2011). Whilst VEGFR-1 has a marginal role in vasculogenesis, it is largely involved in several pathological conditions, including inflammatory process and tumour growth (Melincovici et al., 2018). In this regard, the tyrosine kinase domain of this receptor has been identified as crucial in determining pathological formation of new blood vessels (Murakami et al., 2008; Koch & Claesson-Welsh, 2012). Indeed experiments on animals which did not express VEGFR-1 tyrosine kinase region showed a reduced metastatic process compared to wild-type group (Ferrara, 2004b). Furthermore, once activated, VEGFR-1 releases proteolytic enzymes into the ECM, such as matrix metalloproteinase-9 (MMP-9), facilitating tumour dissemination (Melincovici et al., 2018). A proteolytic cleavage of VEGFR-1 mRNA gives rise to a soluble isoform namely sVEGFR-1 (sFlt-1) (Olsson et al., 2006), which lacks both the transmembrane domain and the intracellular region typical of VEGFR-1 (Melincovici et al., 2018). This soluble form of VEGFR-1 is responsible for a negative regulation of VEGFR-2 activity (Koch & Claesson-Welsh, 2012). Indeed sVEGFR-1 inhibits the

interaction between VEGF family members and VEGFR-2, thus exerting an anti-angiogenic effect (Ferrara, 2004b).

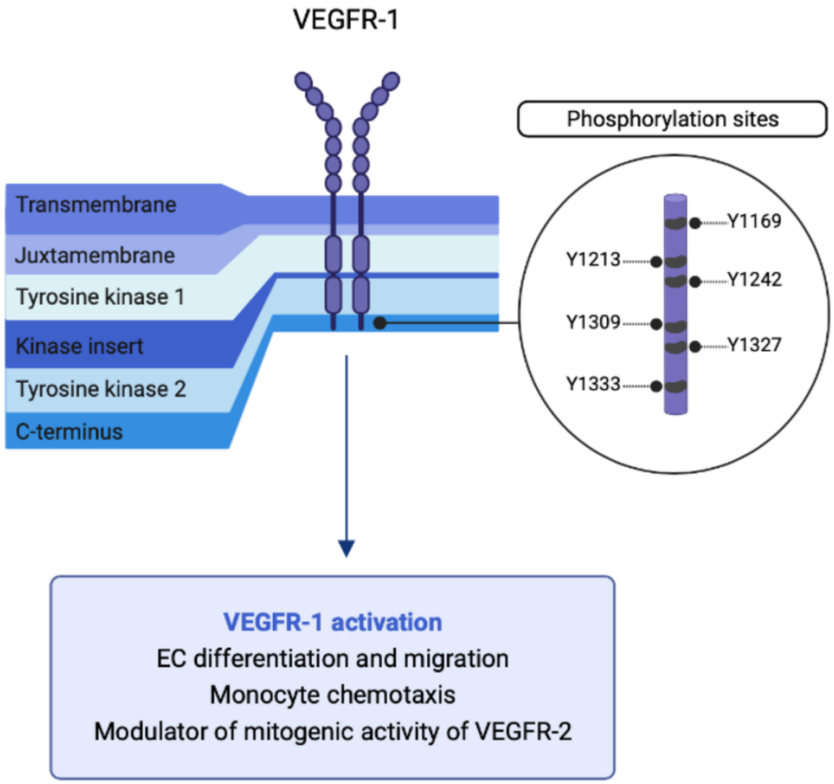

Figure 4. *VEGFR-1: schematic structure, phosphorylation sites and biological activity. EC = endothelial cell. Adapted from (Olsson et al., 2006). Figure created with BioRender.com*

Additional biological responses induced by VEGFR-1 signalling pathway comprise monocyte migration, fatty acid uptake and control of pathological angiogenesis (Koch & Claesson-Welsh, 2012). In particular, by binding to VEGFR-1 and NRP-1, VEGF-B determines fatty acid recruitment in ECs, whereas the binding between VEGFR-1 and PlGF is mainly involved in pathological formation of new blood vessels (Koch & Claesson-Welsh, 2012). By intensifying bone marrow-derived macrophage recruitment, VEGFR-1 signalling also promotes lymphangiogenesis, as well as indirectly controlling EC migration (Murakami et al., 2008; Smith et al., 2015).

1.2.2.2 VEGFR-2

VEGFR-2, the most expressed VEGF receptor, has a high affinity for VEGF-A, resulting in a potent pro-angiogenic response (Hoeben et al., 2004; Niu & Chen, 2010). Proteolytically processed forms of VEGF-C and VEGF-D also bind VEGFR-2, resulting in a subsequent

stimulation of lymphangiogenesis (Olsson et al., 2006; Bui et al., 2016). Extracellular Ig-like domains 2 and 3 have been identified as VEGF-A binding sites on VEGFR-2 (Fuh et al., 1998; Wang et al., 2020). The interaction between VEGFR-2 and its ligands leads to the activation and autophosphorylation of several tyrosine residues: Y801, Y951, Y1054, Y1059, Y1175, Y1214, Y1223, Y1305, Y1309 and Y1319 (Figure 5) (Smith et al., 2015; Wang et al., 2020). This receptor is predominantly expressed on ECs of blood vessels and lymphatic vessels, in addition to being detected also on embryonic tissues, hematopoietic cells, retinal stem cells, megakaryocytes, neurons, pancreatic ductal cells, osteoblasts and tumour cells (Neufeld et al., 1999; Takahashi & Shibuya, 2005; Smith et al., 2010). VEGFR-2 expression is downregulated in quiescent blood vessels, in order to minimize its pro-angiogenic signal (Smith et al., 2015). Conversely, under hypoxic conditions, increased levels of HIFs result in an upregulation of its expression (Pugh & Ratcliffe, 2003; Shibuya, 2011). Together with its role in the embryonic development of the vascular system (Ferrara, 2004b; Haigh, 2008), the predominant function of VEGFR-2 is associated with a crucial control of angiogenesis, both in physiological conditions and during pathological processes, including tumour angiogenesis (Hoeben et al., 2004; Koch & Claesson-Welsh, 2012). By promoting EC differentiation, proliferation, migration, survival, vascular permeability and tubulogenesis, VEGFR-2 is the primary mediator of all VEGF-A-related effects, such as pro-angiogenic response, mitogenic activity and increased permeability (Ferrara et al., 2003; Wang et al., 2020). Alternative splicing of *VEGFR-2 gene* produces a soluble VEGFR-2 (sVEGFR-2), expressed in plasma, heart, skin, ovary, kidney and spleen (Pavlakovic et al., 2010; Smith et al., 2015). By binding VEGF-C with high affinity, sVEGFR-2 prevents the interaction between this ligand and VEGFR-3, exerting a negative control both on lymphatic ECs proliferation and lymphangiogenesis (Hoeben et al., 2004; Pavlakovic et al., 2010). In addition, it has been observed that VEGFR-2 is also activated by PDGFs (Mamer et al., 2017), therefore reinforcing the hypothesis about a possible VEGF/PDGF cross-family interaction (Ball et al., 2007; Mamer et al., 2017).

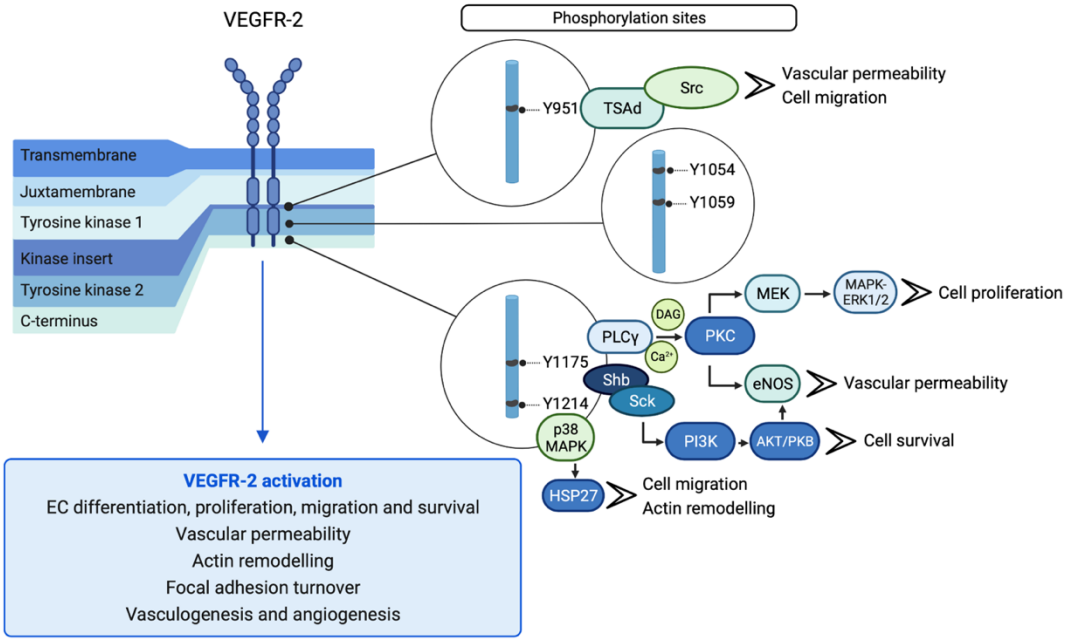

Figure 5. *VEGFR-2: schematic structure, phosphorylation sites and biological activity. DAG = diacylglycerol; eNOS = endothelial* nitric oxide *synthase; ERK 1/2 = Extracellular signal-regulated kinase 1/2; HSP27 = heat-shock protein 27; MAPK = Mitogen-activated protein kinases; MEK = Mitogen-activated* protein *kinase kinase; PI3K = phosphatidylinositol 3-kinases; Akt/PKB = protein kinase B or Akt; PKC = protein kinase C; PLCγ = Phospholipase C gamma; Sck = Shc-like* protein; *Shb = SH2 Domain Containing Adaptor* Protein *B; TSAd = T cell–specific adapter* protein. *Adapted from (Olsson et al., 2006). Figure created with BioRender.com*

Following the activation of VEGFR-2 by VEGF-A, the phosphorylation of Y951 in the kinase insert domain allows this epitope to bind T cell-specific adapter molecule (TSAd) with the subsequent formation of a complex between TSAd and Src (proto-oncogene tyrosine-protein kinase Src), which mediates vascular permeability and EC migration (Figure 5) (Olsson et al., 2006; Wang et al., 2020). In the tyrosine kinase 2 domain, phosphorylated Y1054 and Y1059 represent crucial regulators of kinase activity, determining phosphorylation of other tyrosine kinase residues (Koch & Claesson-Welsh, 2012; Smith et al., 2015). In the carboxy-terminal domain, phosphorylation of Y1175 promotes the recruitment of phospholipase C gamma (PLCγ), with consequent production of diacylglycerol (DAG) and activation of protein kinase C (PKC), in turn responsible for the release of endothelial NO synthase (eNOS) and subsequent increase of vascular permeability (Smith et al., 2015; Wang et al., 2020). In addition, PKC also promotes the activation of MAPK (mitogen-activated protein kinase)-ERK1/2 (extracellular signal-regulated kinase 1/2) cascade, resulting in cell proliferation (Smith et al., 2015; Song & Finley, 2020; Wang et al., 2020). Phosphorylated Y1175 activates

the adaptor proteins Shb and Sck, leading to phosphatidylinositol 3-kinase (PI3K) production and consequent activation of protein kinase B (PKB, also known as Akt) and eNOS, which respectively control cell survival and vascular permeability (Olsson et al., 2006; Smith et al., 2015; Wang et al., 2020). In the carboxy-terminal domain, phosphorylated Y1214 activates p38 MAPK, thereby regulating vascular permeability (Olsson et al., 2006; Koch & Claesson-Welsh, 2012; Wang et al., 2020). Activation of p38 MAPK determines the phosphorylation of heat-shock protein 27 (HSP27), which modulates cell migration and actin remodelling (Kobayashi et al., 2006; Smith et al., 2015). VEGFR-2 also mediates cell migration and focal adhesion turnover via focal-adhesion kinase (FAK) and its substrate paxillin (Olsson et al., 2006; Koch & Claesson-Welsh, 2012).

1.2.2.3 VEGFR-3

This receptor is mainly expressed in lymphatic ECs, where regulating their differentiation, proliferation, migration and survival plays a crucial role in the formation of lymphatic vessels (Hoeben et al., 2004; Olsson et al., 2006; Zhang et al., 2010; Monaghan et al., 2021), as well as being identified in non-ECs, including macrophages and osteoblasts (Koch & Claesson-Welsh, 2012). VEGFR-3 mainly acts as a crucial regulator of lymphangiogenesis, both during embryonic stage and in adult life (Figure 6) (Takahashi & Shibuya, 2005; Shibuya, 2011).

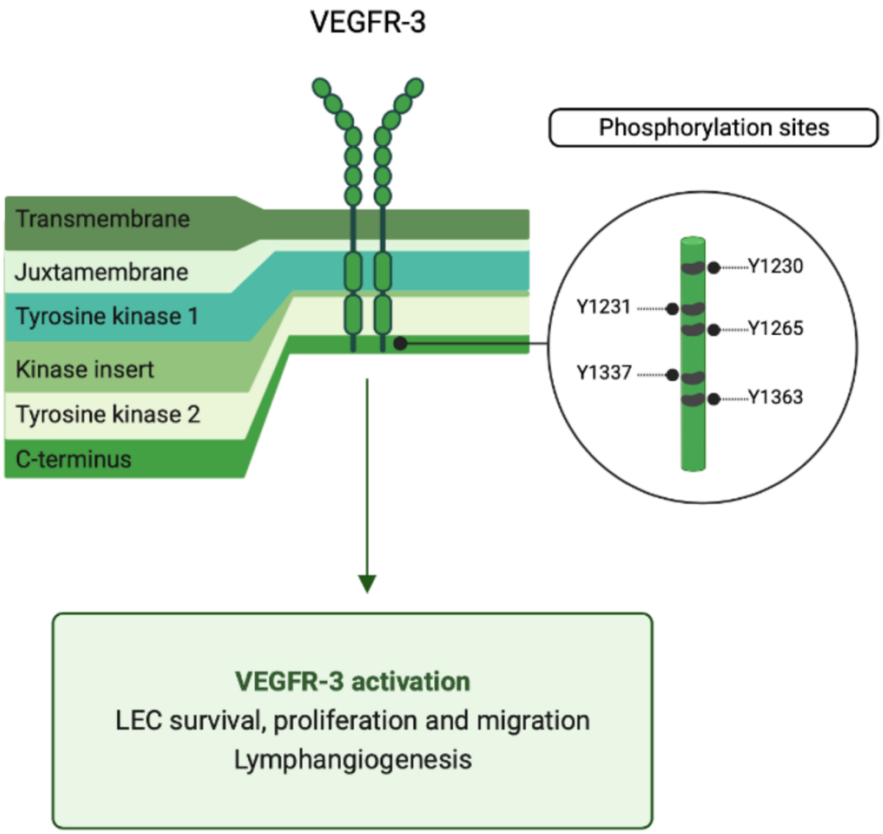

Figure 6. *VEGFR-3: schematic structure, phosphorylation sites and biological activity. LEC = lymphatic endothelial cells. Adapted from (Olsson et al., 2006). Figure created with BioRender.com*

1.2.3 Regulation of VEGF receptors signal transduction

In addition to being predominantly modulated by availability of VEGF ligands, VEGFR activity is also regulated by a variety of additional elements (Koch & Claesson-Welsh, 2012; Sarkar et al., 2022), such as different dimerization patterns, formation of complexes with specific proteins, as well as receptor internalisation, therefore resulting in a specific biological response (Koch & Claesson-Welsh, 2012). First of all, the diverse ability of forming homodimers and/or heterodimers contributes to define the final cellular response mediated by VEGFRs (Mac Gabhann & Popel, 2007; Koch & Claesson-Welsh, 2012). In this context, both VEGFR-1/VEGFR-2 heterodimers and VEGFR-2 homodimers promote angiogenic signal, whereas VEGFR-1 homodimers have not been associated with such a pro-angiogenic response (Carmeliet & Jain, 2011; Sarkar et al., 2022). Furthermore, the formation of VEGFR-2/VEGFR-3 heterodimers, consequent to the binding of VEGF-C or VEGF-D, is critical in the modulation of specific mechanisms, such as lymphangiogenesis (Alam et al., 2004; Koch & Claesson-Welsh, 2012). The interaction between VEGFR-2 and its co-receptor NRP-1 has also

a crucial role in the modulation of VEGF-induced cellular responses (Soker et al., 1998; Herzog et al., 2011; Koch & Claesson-Welsh, 2012). NRP-1, expressed by arterial ECs, selectively binds to exon 7-containing VEGF-A isoforms (e.g. VEGF-A_{165}), leading to the formation of a ternary complex with VEGFR-2, essential for the promotion of anti-apoptotic and pro-angiogenic responses (Olsson et al., 2006; Lyu et al., 2020). In addition to acting as co-receptor for VEGFR-2, NRP-1 is also able to modulate VEGFR-1 signalling (Fuh et al., 1998; Fuh et al., 2000). By contrast, NRP-2, expressed on ECs in veins and lymphatic vessels, acts as co-receptor for VEGFR-3 (Fuh et al., 1998). In resting ECs, VEGFR-2 is retained in intracellular Rab4- and Rab11- negative vesicles (Koch & Claesson-Welsh, 2012). Following stimulation with NRP-1-binding VEGF-A, the internalised receptor is delivered to the plasma membrane, where its activity is restored (Ballmer-Hofer et al., 2011). Conversely, in absence of NRP-1, VEGFR-2 undergoes lysosomal degradation via Rab7-positive vesicles (Ballmer-Hofer et al., 2011; Peach et al., 2018). As a result of this elaborate interaction between VEGFRs and these transmembrane proteins, the overexpression or disruption of NRP-1 and NRP-2 is associated with pathological processes, such as tumour angiogenesis, cancer growth and metastasis (Koch & Claesson-Welsh, 2012). Moreover, VEGFR signalling is also modulated by the interaction with transmembrane heterodimers, namely integrins (e.g., collagen, fibronectin, vitronectin and laminin), which potentiate VEGF-mediated responses (Byzova et al., 2000; Koch & Claesson-Welsh, 2012). In particular, VEGFR-2 forms a complex with integrin $\alpha v\beta 3$, resulting in an enhanced angiogenic signal, as well as the binding between VEGF-A and integrin $\alpha 9\beta 1$ has been associated with pathological angiogenesis (Vlahakis et al., 2007; Somanath et al., 2009; Koch & Claesson-Welsh, 2012). Finally, internalisation of VEGFRs, especially VEGFR-2 and VEGFR-3, is significantly involved in the modulation of their pro-angiogenic activity (Koch & Claesson-Welsh, 2012; Lessen et al., 2015; Basagiannis et al., 2016). More specifically, following the binding with VEGF-A, VEGFR-2 dissociates from caveolin-1 or VE-cadherin, thus passing from its inactive conformation to an active form, which is thus internalised into endosomes (Lampugnani et al., 2006; Koch & Claesson-Welsh, 2012). Receptor signalling is not terminated with its internalisation; indeed, the internalised VEGFR-2 undergoes phosphorylation, therefore continuing to signal from endosomes (Lampugnani et al., 2006; Koch & Claesson-Welsh, 2012). As a result, internalisation plays an important role in promoting the pro-angiogenic activity mediated by VEGFR-2 (Koch & Claesson-Welsh, 2012; Basagiannis et al., 2016).

1.3 VEGF IN HEALTH AND DISEASE

As previously described, VEGF acts on vascular ECs with high specificity and potency (Dvorak et al., 1995; Rosen, 2002), controlling several processes, such as vascular growth, permeability, EC mitogenesis and angiogenesis (Dvorak et al., 1995; Shibuya, 2011). A variety of physiological outcomes are associated with VEGF signalling, starting with the differentiation of blood islands into ECs during embryonic development (Ferrara, 2004b; Takahashi & Shibuya, 2005). In postnatal development, VEGF induces EC proliferation, migration and survival, as well as acting as a promoter both of tubulogenesis and vascular permeability, which is the result of VEGF-mediated fenestration in ECs (Neufeld et al., 1999; Takahashi & Shibuya, 2005; Bates, 2010). In adult life, VEGF maintains its crucial role as a pro-angiogenic factor in diverse processes, such as wound healing and the menstrual cycle (Ferrara, 2004b; Eelen et al., 2020). However, in addition to mediating these physiological responses, VEGF signalling alterations are heavily involved in the pathogenesis of several diseases, including preeclampsia, diabetic retinopathy and cancer (Ferrara & Davis-Smyth, 1997; Bergers & Benjamin, 2003).

1.3.1 Physiological angiogenesis

Our complex network of blood vessels is the result of two processes, namely vasculogenesis and angiogenesis, which both begin during embryogenesis and persist in adult life, even if at a reduced level (Ferrara, 2004a; Lugano et al., 2020; Barrasa-Ramos et al., 2022). Indeed, in physiological conditions, the adult vascular network generally remains quiescent and angiogenesis rarely occurs, being essentially associated with maintenance of such vasculature (Welti et al., 2013; Eelen et al., 2020). The inner wall of arteries, veins and capillaries is defined by a monolayer of ECs, whose junctional integrity is highly maintained by specific molecules, such as VE-cadherins and claudins (Viallard & Larrivee, 2017; Duong & Vestweber, 2020). Mural cells, specifically smooth muscle cells and pericytes, interacting with ECs, keep them in contact with the basal membrane and, preventing excessive vascular permeability and vascular leakage, support long-term stabilisation of the vasculature (Armulik et al., 2011; Viallard & Larrivee, 2017). If the *de novo* formation of blood vessels from endothelial precursors is defined as vasculogenesis, angiogenesis represents the formation of blood vessels from existing vasculature (Carmeliet & Jain, 2011). In particular, angiogenesis requires a complex synergism between ECs and the extracellular environment and it is the result of elaborate steps, which include EC activation, basement membrane degradation, EC migration, ECM invasion, EC proliferation and lumen formation (Ucuzian et

al., 2010; Senger & Davis, 2011; Welti et al., 2013). The major stimulus for angiogenesis is represented by hypoxia, even if other conditions, such as hypertension, inflammation, hypoglycaemia, metabolic acidosis and mechanical stress, may also trigger the expansion of vascular network (Rosen, 2002; Carmeliet & Jain, 2011; Cheng & Ma, 2015). These pro-angiogenic stimuli, among which VEGF plays a predominant role, determine the activation of ECs and mural cells, resulting in vasodilation and structural alterations of existing vasculature (Welti et al., 2013; Melincovici et al., 2018; Lugano et al., 2020). Specifically, upon VEGF stimulation, activated ECs migrate into the ECM, thus initiating the sprouting process (Lamalice et al., 2007; Raza et al., 2010; Song & Finley, 2022).

In physiological angiogenesis, the formation of growing sprouts is initiated by a particular phenotype of ECs, known as tip cells, which, being invasive and motile, lead the growing blood vessels (Phng & Gerhardt, 2009; Elorza Ridaura et al., 2021). By contrast, stalk cells, other ECs which follow the tip cells, proliferate and are responsible for the integrity of the nascent sprout and the lumen formation (Phng & Gerhardt, 2009; Viallard & Larrivee, 2017; Elorza Ridaura et al., 2021). The Notch signalling pathway has a key function in the morphogenesis of new vessels, being involved in the differential conversion of ECs in tip or stalk phenotype (Phng & Gerhardt, 2009; Blanco & Gerhardt, 2013; Viallard & Larrivee, 2017). The potential of an EC to switch into the tip or stalk phenotype primarily relies on VEGF expression, VEGFR-2 availability and Dll4 (Delta like canonical Notch ligand 4) expression (Jakobsson et al., 2010; Herbert & Stainier, 2011; Elorza Ridaura et al., 2021). On the tip cell, the binding between VEGFR-2 and VEGF-A upregulates the expression of Dll4 ligand, which interacts with Notch 1 receptor in neighbouring cells (stalk cells) (Phng & Gerhardt, 2009; Blanco & Gerhardt, 2013; Welti et al., 2013; Chen et al., 2019). The low levels of Dll4 and the increased Notch activity on stalk cells, determining an upregulation of VEGFR-1 and a downregulation of VEGFR-2, makes them less responsive to VEGF, therefore suppressing the tip cell phenotype (Phng & Gerhardt, 2009; Jakobsson et al., 2010; Chen et al., 2019). In turn, stalk cells, due to reduced level of Dll4, cannot activate Notch signalling on tip cells, which therefore maintain higher expression of VEGFR-2 and NRP-1 (Chen et al., 2019). The activation of Notch signalling pathway reduces VEGFR-2 expression on stalk cells, resulting in their stabilisation and in the inhibition of excessive conversion of stalk cells into tip cells (Chen et al., 2019).

Endothelial tip cells, through their filopodia responsive to pro-angiogenic mediators, guide the vasculature expansion (Phng & Gerhardt, 2009; Welti et al., 2013; Lugano et al., 2020).

The consequent lumen formation and vasculature stabilisation complete the sprouting process (Iruela-Arispe & Davis, 2009; Ucuzian et al., 2010; Blanco & Gerhardt, 2013). ECs internalise pinocytic vesicles of the plasma membrane, which coalesce, hence creating the novel vascular lumen (Iruela-Arispe & Davis, 2009; Carmeliet & Jain, 2011). Under physiological conditions, a functional vasculature requires mature and stable blood vessels (Welti et al., 2013). In this context, a key role is played by PDGF-β/PDGFR-β pathway (Sounni et al., 2011), which, activated by membrane type-1 matrix metalloproteinase (MT1-MMP), promotes pericytes migration, recruitment of mural cells, as well as stabilisation of intercellular adhesion (Sounni et al., 2011; Viallard & Larrivee, 2017). This process is also supported by adhesion molecules (e.g., VE-cadherins) which reinforce adhesion among ECs, therefore preventing vascular hyperpermeability (Welti et al., 2013; Viallard & Larrivee, 2017).

Furthermore, during physiological angiogenesis, VE-cadherins maintain vascular quiescence by inducing the dephosphorylation of VEGFR-2 (Giannotta et al., 2013; Viallard & Larrivee, 2017). The appropriate balance between pro-angiogenic and anti-angiogenic mechanisms, as well as cessation of all the pro-angiogenic stimuli, are the essential prerequisites of physiological formation of new quiescent blood vessels (Ferrara, 2004a; Lugano et al., 2020).

1.3.2 Tumour angiogenesis

In addition to being a physiological requirement, a new vascular network is also essential in the context of pathological conditions, such as cancer (Viallard & Larrivee, 2017; Lugano et al., 2020; Wang et al., 2020). The hypoxic environment typical of cancer cells allows them to grow up to 1 mm^3, at which point their high proliferative rate requires a vascular supply of oxygen and nutrients (Bergers & Benjamin, 2003; Ferrara, 2004a; Sebestyén et al., 2021). The formation of a tumour vasculature, also defined neoangiogenesis, is characterized by a critical upregulation of pro-angiogenic factors (angiogenic switch), as well as by oncogene activation and mutation of tumour suppressor genes (Bergers & Benjamin, 2003; Lugano et al., 2020; Saman et al., 2020).

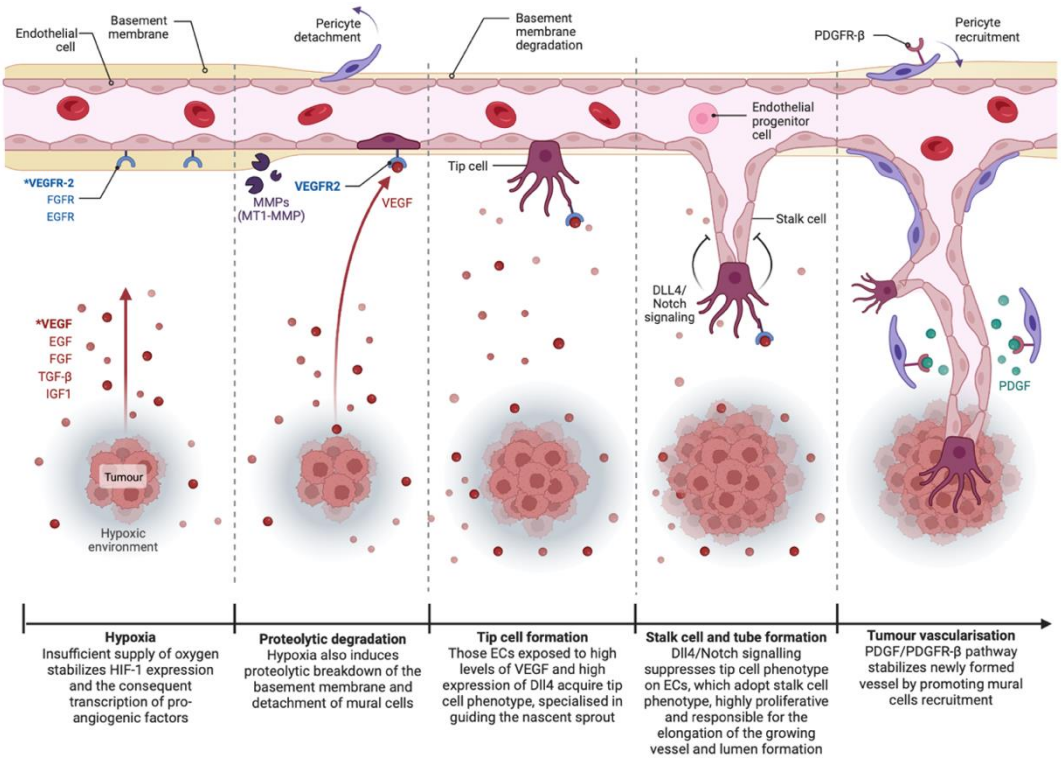

Figure 7. *Tumour-induced angiogenesis. Pro-angiogenic stimuli, such as hypoxic conditions and pro-angiogenic factors, promote the activation of endothelial cells and mural cells, with consequent disruption of the vascular barrier and the formation of new vessels guided by tip and stalk cells. Adapted from (García-Caballero et al., 2022). Figure created with BioRender.com*

Insufficient supply of oxygen is the main stimulus for tumour angiogenesis (Figure 7) (Emami Nejad et al., 2021). Indeed, hypoxia-induced HIF-1 stabilisation and its subsequent binding with hypoxia response elements (HREs) promote the transcription of multiple pro-angiogenic and anti-apoptotic genes (Viallard & Larrivee, 2017; Rodriguez et al., 2021). Moreover, the activation of oncogenic signalling pathways (e.g., ERK/MAPK pathway) also contributes to enhance HIF-1 transcriptional activity (Semenza, 2002), further switching the balance in favour of pro-angiogenic factors (Bergers & Benjamin, 2003; Liu et al., 2023). However, significant differences exist between tumour angiogenesis and normal angiogenesis, the first being characterized by atypical morphological organization, impaired EC-pericytes interactions, hyperpermeability and abnormal blood flow (Figure 8) (Folkman, 1995; Lugano et al., 2020). First of all, the tumour vascular network is not quiescent and undergoes ongoing angiogenesis (Bergers & Benjamin, 2003; Lugano et al., 2020). Even the architecture of tumour vasculature, presenting a chaotic arrangement, with dilated, tortuous and aberrant structures, differs from that of normal blood vessels (Folkman, 1995; Nagy et al., 2009). In addition, tumour blood vessels appear haemorrhagic and characterized by excessive

permeability, due the overexpression of VEGF and impaired connection between perivascular cells (Viallard & Larrivee, 2017; Lugano et al., 2020). Indeed, high levels of VEGF promote the formation of a VEGFR-2/PDGFR-β complex, resulting in a reduced barrier integrity, also supported by the secretion of metalloproteinases (MMPs) from cancer cells (Greenberg et al., 2008; Yuan et al., 2023). Moreover, under pathological conditions and in presence of VEGF and HIF-1, angiopoietin-2 causes a further impairment of EC interactions, leading to disorganized and instable blood vessels (Ucuzian et al., 2010; Rodriguez et al., 2021). Once initiated, tumour angiogenesis plays a fundamental role not only in the progression of the primary tumour but also in the metastatic dissemination (Ferrara, 2004a; Baghban et al., 2020). An high vascular density and the metastatic process have been associated with a poor prognosis (Rosen, 2002), making angiogenesis an important target of the newly introduced antineoplastic drugs (Carmeliet & Jain, 2011; Rajabi & Mousa, 2017; Saman et al., 2020; Qi et al., 2022).

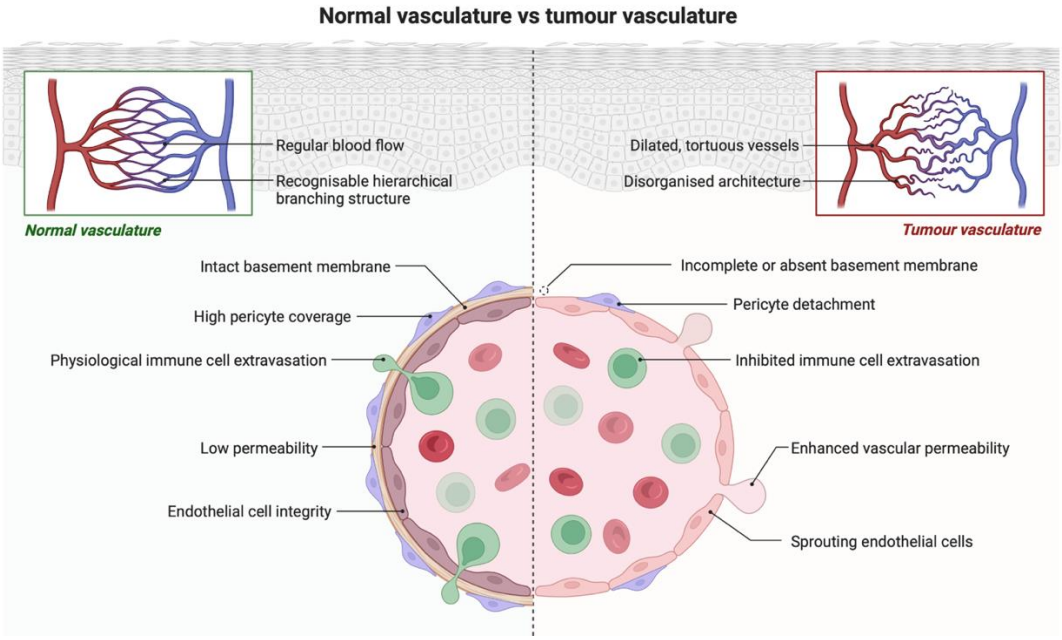

Figure 8. *Main differences between normal and tumour vasculature. Tumour vasculature is characterised by excessive branching and flow patterns. Tumour endothelial cell basement membrane is disrupted, as well as the interaction between pericytes and endothelial cells is altered in tumour vasculature. Adapted from (Magnussen & Mills, 2021). Figure created with BioRender.com*

1.3.2.1 ROLE OF VEGF IN CANCER GROWTH AND METASTASES

In the complex formation of new blood vessels to support cancer growth and progression, VEGF exerts a crucial role (Ferrara, 2004a; Lugano et al., 2020). Overexpression of this factor

has been associated with tumorigenesis, angiogenesis and metastasis (Rosen, 2002; Goel & Mercurio, 2013; Matsumoto & Ema, 2014; Ceci et al., 2020). As previously described, VEGF is crucial in determining the specification of tip/stalk cells in tumour tissues, stimulating the upregulation of Dll4 ligand in tip cells and Jagged 1 ligand mainly in stalk cells (Matsumoto & Ema, 2014; Michael Simons et al., 2016; Chen et al., 2019). In addition to controlling the mechanisms involved in tumour neovascularization, VEGF also acts as an anti-apoptotic mediator, enhancing the survival of cancer cells by upregulating the antiapoptotic factors Bcl-2 and survivin (Harmey & Bouchier-Hayes, 2002; Ferrara, 2004a; Masoumi Moghaddam et al., 2012). Moreover, VEGF has been associated with inhibition of dendritic cell differentiation, leading to the hypothesis that its pathological overexpression may have a role in the suppression of tumour immune surveillance (Gabrilovich et al., 1996; Ferrara, 2004a; Li et al., 2016). Indeed, dendritic cells have a decisive function in promoting immune response against pathogens, including cancer cells (Banchereau et al., 2000; Marciscano & Anandasabapathy, 2021). Tumour-released VEGF prevents the formation of mature dendritic cells, leading to an inadequate presentation of tumour antigens and consequent immune tolerance of cancer cells (Gabrilovich et al., 1996; Del Prete et al., 2023). This VEGF-mediated immune deficiency, preventing the host immune system from attacking tumour cells, has been correlated with tumour growth and poor prognosis in several types of malignancies (Saito et al., 1998; J.-W. Kim et al., 2013; de Aguiar & de Moraes, 2019). Given that VEGF expression is significantly increased in a variety of malignancies, its levels are used as prognostic factor in defining the clinical outcome of cancer patients (Poon et al., 2001; Guo & Lu, 2018). In particular, high levels of VEGF are associated with a poor prognosis in several malignancies, such as breast cancer, ovarian cancer, non-small cell lung cancer, colon cancer, acute myeloid leukaemia and hepatocellular carcinoma (Seo et al., 2000; Poon et al., 2001; Ferrara, 2004a; Sopo et al., 2019). As a result of its implications in several aspects of carcinogenesis, VEGF signalling pathway has been evaluated as an antineoplastic target, and its inhibition has become an effective therapeutic strategy in oncology (Ferrara & Alitalo, 1999; Ferrara, 2004a; Matsumoto & Ema, 2014; Lugano et al., 2020; Patel et al., 2023).

1.4 VEGF AS A TARGET FOR CANCER THERAPY

The identification of the VEGF signalling as a crucial determinant in neoangiogenesis, as well as the role of its overexpression in tumour growth and metastasis, have provided an attractive target for more specific cancer treatments (Ferrara, 2004a; Ellis & Hicklin, 2008; Marmé, 2018). In particular, molecular targeted therapies against the VEGF pathway include

small molecules tyrosine kinase inhibitors, monoclonal antibodies and immunotherapy (Lee et al., 2018; Min & Lee, 2022). Among these, several VEGFR inhibitors have shown a considerable clinical success in effectively treating a variety of malignancies (Lee et al., 2018; Liu et al., 2022). In addition to being used as single agents, VEGF-targeted drugs are often used in conjunction with conventional therapies (e.g., cisplatin, gemcitabine, fluorouracil and paclitaxel) (Ellis & Hicklin, 2008; Ansari et al., 2022). Indeed, chemotherapy and radiotherapy often promote VEGF upregulation mainly through stabilisation and upregulation of HIF-1, thus contributing to antineoplastic resistance (Ferrara, 2004a; Moeller et al., 2004; Riedel et al., 2004; Zips et al., 2005; Xia et al., 2018; Kanthou & Tozer, 2019). In addition, even VEGFR-2 inhibitors have been associated with resistance, whose mechanisms of action mainly include the activation of alternative proangiogenic pathways (e.g., angiopoietin, platelet derived growth factor β, fibroblast growth factor, matrix metalloproteinases), as well as recruitment of bone marrow-derived cells and stromal cells to override VEGF-induced angiogenesis (Abdullah & Perez-Soler, 2012; Haibe et al., 2020). In this context, coadministration of traditional therapeutic strategies and VEGF inhibitors ensures maximum effectiveness of both treatments (Moeller et al., 2004; Ellis & Hicklin, 2008; Kanthou & Tozer, 2019). Nevertheless, cardiovascular safety of VEGFR inhibitors remains a major challenge in oncology, since unanticipated and poorly controlled cardiovascular toxicities induced by these therapeutics often result in a reduction of therapeutic dosage or treatment interruption, therefore influencing cancer management (Mellor et al., 2011; Jiang et al., 2020).

1.4.1 VEGF inhibitors

Since the clinical approval of the first TKI imatinib in 2001 (Savage & Antman, 2002), a variety of agents aimed at inhibiting VEGFR signalling have been developed and several of them have been approved to be clinically used in the treatment of numerous malignancies (Ellis & Hicklin, 2008; Zhong et al., 2021). All the inhibitors of the kinase activity of VEGFRs currently approved by FDA and EMA are listed in Table 1 (Roskoski, 2020; Zhong et al., 2021), whereas many others (e.g., cediranib, vatalanib, brivanib, zanzalintinib, ningetinib and golvatinib) are in phase I, II or III of clinical development (Scott et al., 2007; Lindsay et al., 2009; Schlumberger et al., 2009; Molife et al., 2014; Chan et al., 2017; Zhao et al., 2020; Sharma et al., 2022). The efficacy of VEGFR-2 inhibitors, in particular when used as single-agents, may differ depending on the specific mechanism that VEGFR inhibitors exert on different malignancies (Ellis & Hicklin, 2008). Indeed, it has been observed that in certain type of cancer, such as renal cell carcinoma (RCC) and colorectal cancer (CRC) and neuroendocrine

tumours, the clinical efficacy of VEGF-RTKIs is particularly relevant, whereas it seems limited in other malignancies (Ellis & Hicklin, 2008; Sitohy et al., 2012; Vasudev & Reynolds, 2014; Haibe et al., 2020). This may be attributed to the fact that cancers with a high responsiveness to anti VEGF therapy rely on a highly VEGF-dependent angiogenesis, while tumours that are dependent on angiogenic factors other than VEGF show a reduced susceptibility to VEGF inhibition (e.g., pancreatic cancer, breast cancer and prostate cancer) (Casanovas et al., 2005; Ellis & Hicklin, 2008; Haibe et al., 2020).

The inhibition of the VEGFR signalling pathway and the consequent impact on tumour growth have been proposed as the result of multiple mechanisms, not necessarily mutually exclusive (Ellis & Hicklin, 2008; Lugano et al., 2020). In particular, VEGF-targeted therapies exert a cytostatic effect on blood vessels, thus resulting in the blockade of neovascularization (Folkman, 1971; Niu & Chen, 2010). Additionally, as VEGF promotes a variety of cell survival pathways in ECs, including the activation of anti-apoptotic factors like Bcl-2, Akt, survivin and inhibitor of apoptosis proteins (IAPs), its inhibition through these novel therapeutics has been associated with tumour ECs apoptosis (Gerber et al., 1998; Dimmeler & Zeiher, 2000; Ellis & Hicklin, 2008; Apte et al., 2019). When combined with chemotherapeutic agents, the reduction of survival signalling in tumour ECs due to RTKIs also makes these cells more susceptible to chemotherapy-induced apoptosis (Ellis & Hicklin, 2008; Ansari et al., 2022). Tyrosine kinase inhibitors targeting VEGFRs also act on the heterogenous tumour vasculature, restoring a more structurally and functionally normal vascular network (Goel et al., 2011; Shibuya, 2011; Viallard & Larrivee, 2017; Wu et al., 2018). In this regard, VEGFR inhibitor-induced vascular normalisation re-establishes a balance between pro- and anti-angiogenic factors, resulting in an attenuation of vascular hyperpermeability, stabilisation of pericyte coverage and reduction of basement membrane thickness (Winkler et al., 2004; Goel et al., 2011; Viallard & Larrivee, 2017). VEGFR signalling being crucial in the expression of vasodilating factors, such as NO and prostacyclin (Dvorak et al., 1995; Niu & Chen, 2010), its blockade has been associated with vascular constriction and a decreased tumour perfusion (Ellis & Hicklin, 2008; Wu et al., 2018). In addition, the expression of VEGFR not only on ECs but also on tumour cells extends its contribution in tumorigenesis, going beyond angiogenesis and vascular permeability (Tian et al., 2001; Goel & Mercurio, 2013; Mercurio, 2019). Specifically, autocrine and paracrine VEGFR signalling pathways within cancer cells have also been associated with several aspects of tumorigenesis, including cancer cell stemness (Goel & Mercurio, 2013; Yamagishi et al., 2013). As a result, some of the

therapeutic effects observed with VEGFRs inhibitors have been also ascribed to a direct apoptotic effect on tumour cells (Harmey & Bouchier-Hayes, 2002; Yamagishi et al., 2013; Li et al., 2016). VEGF-A also inhibits dendritic cell maturation and enhances the expression of immune suppressive checkpoints (e.g., programmed cell death protein 1 or PD-1), thus having an immunosuppressive role (Voron et al., 2015). The blockade of its signalling pathway could also promote antitumour immunity by improving dendritic cell function and immune recognition of cancer cells (Ellis & Hicklin, 2008; Ribatti, 2022). All these pharmacological responses are the result of a complex interaction between RTK inhibitors and VEGF receptors (Gotink & Verheul, 2010). In particular, the majority of VEGFR-TKIs exerts its activity by competing with adenosine triphosphate (ATP), thus blocking catalytic activity of VEGF receptor (Gotink & Verheul, 2010; Modi & Kulkarni, 2019). According to the kinase conformation which they recognise, RTK inhibitors are classified as type I, type II and type III inhibitors (Gotink & Verheul, 2010; Modi & Kulkarni, 2019). Type I inhibitors, also called ATP competitive inhibitors, bind to the active conformation of the kinase in the ATP-binding pocket and include sunitinib, pazopanib, vandetanib, axitinib and lenvatinib (Gotink & Verheul, 2010; Modi & Kulkarni, 2019). Those RTKIs interacting with the inactive conformation of the kinase are classified as type II inhibitors and include sorafenib, cabozantinib and regorafenib (Gotink & Verheul, 2010; Modi & Kulkarni, 2019; Liu et al., 2022). They indirectly compete with ATP by occupying the allosteric pocket region adjacent to the ATP-binding site (Gotink & Verheul, 2010; Ghorab et al., 2017; Zhao, 2020; Liu et al., 2022). Type III inhibitors (e.g., vatalanib), also known as covalent inhibitors, irreversibly bind to cysteine residue at specific sites on the kinase (Wood et al., 2000; Ghorab et al., 2017; Modi & Kulkarni, 2019; Abdeldayem et al., 2020; Liu et al., 2022).

Drug	Brand name, developer	Year of approval	Targets	Type	Indication	References
Sorafenib (BAY 43-9006)	Nevaxar®, Bayer Pharmaceuticals	2005 (FDA) 2006 (EMA)	VEGFR-1/2/3, FLT3, KIT, C-Raf, PDGFR-ß, DDR2, RET, FGFR1, CDK19, CDK8, B-Raf	Type II	HCC RCC DTC	(Wilhelm et al., 2006; Llovet et al., 2008)
Sunitinib (SU11248)	Sutent®, Pfizer	2006 (FDA, EMA)	VEGFR-1/2/3, KIT, PDGFR-ß, FLT3, RET, FGFR1, CSF1R	Type I	GIST RCC NETs	(Faivre et al., 2007)
Pazopanib (GW 786034)	Votrient®, Novartis	2009 (FDA) 2010 (EMA)	VEGFR-1/2/3, PDGFR-ß, KIT, FGFR-1, CSF1R	Type I	RCC STSs	(Sloan & Scheinfeld, 2008; Sternberg et al., 2013)
Vandetanib (ZD-6474)	Capelsa®, Genzyme	2011 (FDA) 2012 (EMA)	VEGFR-2, RET, EGFR, KIT	Type I	MTC	(Morabito et al., 2009)
Axitinib (AG-013736)	Inlyta®, Pfizer	2012 (FDA, EMA)	VEGFR-1/2/3, PDGFR-ß, KIT, PLK4	Type I	RCC	(Schiller et al., 2009; Rini et al., 2011)
Regorafenib (BAY 73-4506)	Stivarga®, Bayer Pharmaceuticals	2012 (FDA) 2013 (EMA)	VEGFR-1/2/3, B-Raf	Type II	CRC GIST	(Dhillon, 2018)
Cabozantinib (XL-184)	Cometriq® and Cabometyx®, Exelixis	2012 (FDA) 2014 (EMA)	VEGFR-2, MET, RET, KIT	Type II	MTC RCC HCC	(Elisei et al., 2013; Abou-Alfa et al., 2018)
Nintedanib (BIBF-1120)	Ofev® and Vargatef®, Boehringer Ingelheim	2014 (FDA, EMA)	VEGFR-1/2/3, PDGFRα/β, FGFR-1/2/3, BCRP, MDR1	Type I	NSCLC	(Dhillon, 2015; Zhao, 2020)
Lenvatinib (E 7080)	Lenvima®, Eisai	2015 (FDA, EMA)	VEGFR-2/3, PDGFR-α, FGFR-1/2/3/4, RET, KIT	Type I	DTCs EC HCC RCC	(Cabanillas & Habra, 2016)
Tivozanib (AV-951)	Fotivda®, AVEO Pharmaceuticals	2017 (EMA) 2021 (FDA)	VEGFR-1/2/3, PDGFRα, FGFR-1-2-3-4, KIT, RET	Type II	RCC	(Escudier et al., 2018; Modi & Kulkarni, 2019)

Table 1. *FDA- and EMA-approved VEGFR inhibitors, their primary targets and therapeutic indications. BCRP = breast cancer resistance protein; CDK8 = cyclin dependent kinase 8; CDK19 = cyclin dependent kinase 19; CRC = colorectal carcinoma; CSF1R = colony-stimulating factor 1 receptor; DDR2 = discoidin domain receptor tyrosine Kinase 2; DTC = differentiated thyroid carcinoma; EC= endometrial carcinoma; EGFR = epidermal growth factor receptor; FGFR-1/2/3 = fibroblast growth factor receptor 1/2/3; FLT3 = FMS-like tyrosine kinase 3; GIST = gastrointestinal stromal tumour; HCC = hepatocellular carcinoma; MDR1 = multidrug resistance protein 1; MTC = medullary thyroid cancer; NETs = pancreatic neuroendocrine tumours; NSCLC = non-small cell lung cancer; PDGFR-α/ß = platelet derived growth factor receptor α/ß; PLK4 = Polo-like kinase 4; Raf = rapidly accelerated fibrosarcoma; RCC = renal cell carcinoma; STSs = soft-tissue sarcomas; VEGFR-1/2/3 = vascular endothelial growth factor receptor 1/2/3.*

1.4.1.1 "MULTI-KINASE" INHIBITORS: SELECTIVITY RATHER THAN SPECIFICITY

Given that their primary site of action is within the cell, small molecule RTK inhibitors, including those targeting VEGF pathway, have the advantage of being able to cross biological membranes (Ellis & Hicklin, 2008; Zhong et al., 2021). Although RTKIs are designed to inhibit a particular kinase, they have been shown to exert their activity even on unintended targets (Ghoreschi et al., 2009; Davis et al., 2011). Understanding their potential targets, as well as their affinity both for intended and unintended pathways, is essential for a clear assessment of their safety (Martin, 2015; Pugsley, 2015). The majority of antiangiogenic RTKIs designed to target VEGFRs interacts with several different kinases, being therefore also defined as multi-kinase inhibitors (Ellis & Hicklin, 2008; Knight et al., 2010). Tyrosine kinases show a high similarity within their kinase domain, where the ATP-binding site, essential for their activity, is in fact largely conserved across the kinome (Gotink & Verheul, 2010). Considering that most RTKIs bind to the ATP-binding site of their target, their specificity is therefore limited, establishing a cross-reaction with related kinases (Wellstein et al., 2018; Pottier et al., 2020). It has been observed that type I RTK inhibitors, binding to the highly-conserved adenine region in the ATP-binding site, tend to be less selective in comparison with type II RTK inhibitors, which, interacting with a more variable and kinase-specific region adjacent to the ATP-binding site, show a relatively higher selectivity (Davis et al., 2011). However, there are some exceptions, so the development of type II inhibitors does not guarantee the desired selectivity (Davis et al., 2011). In addition, a quantitative analysis of the overall selectivity of RTKIs, as well as of their selectivity across kinases closely related to the intended kinase, showed that even if some compounds are group-selective, revealing a large selectivity for a particular kinase subfamily, they also exhibit a selectivity outside the primary group (Davis et al., 2011). As a result, the evaluation of the RTKIs selectivity for kinases which belong to the same group of the intended kinase proved not to be a reliable means to determine the overall selectivity (Davis et al., 2011). In light of their way of interacting with ATP-binding site, RTKIs are therefore defined as selective rather than specific for a precise kinase (Ellis & Hicklin, 2008; Karaman et al., 2008; Pottier et al., 2020). As an example, sorafenib and sunitinib, both targeting VEGFRs, show a significant interaction even with other receptor tyrosine kinases, such as PDGFR-β, fibroblast growth factor receptor (FGFR), FMS-like tyrosine kinase 3 (FLT3), KIT and colony-stimulating factor 1 receptor (CSF1R) (Karaman et al., 2008; Gotink & Verheul, 2010). This extended activity on additional targets, such as PDGFRs, may lead to a more effective treatment, but it also increases the likelihood for unintended toxicities (Ellis &

Hicklin, 2008). Identifying the full range of kinases targeted by a RTK inhibitor, as well as where they are expressed, plays a crucial role in the prevention of potential toxicities (J. Zhang et al., 2009). In this regard, besides any "on-target" cardiovascular complications associated with primary pharmacology, a safety concern about promiscuity of RTKIs includes also the "off-target"-associated cardiovascular risks, which lead to parallel toxicities (Mellor et al., 2011).

1.4.1.2 AXITINIB

Axitinib (AG-013736), commercially known as Inlyta®, is an oral ATP-competitive tyrosine kinase inhibitor of VEGFR-1/2/3, PDGFR-β, KIT and Polo-like kinase 4 (PLK4) (Rini et al., 2005; Rini et al., 2011). Developed by Pfizer and fully approved by EMA and FDA in 2012, axitinib is clinically used for second-line treatment of adult patients with advanced renal cell carcinoma (Rixe et al., 2007; Tyler, 2012; Bellesoeur et al., 2017; Zarrabi et al., 2017). The recommended starting dose is 5 mg twice a day (bis in die, BID), which can be further increased up to 10 mg BID, based on individual patient response and tolerability (van Geel et al., 2012). The main inhibitory activity of this RTKI is against VEGFR-1/2/3, with IC_{50} values ranging from 0.06 to 0.3 nM while showing a ~10-fold lower potency for the inhibition of PDGFR-β and KIT (Hu-Lowe et al., 2008; Bukowski, 2012). Axitinib-induced blockage of VEGFRs phosphorylation, including the inhibition of downstream elements such as Akt and eNOS signalling pathways, results in a diminished ECs proliferation and migration, reduced sprouting and lumen formation and consequent decrease of tumour permeability and vascularisation (Agency, 2012). Safety pharmacology screenings did not reveal any notable functional effect of axitinib on central nervous, respiratory and gastrointestinal systems (Agency, 2012). In terms of cardiovascular safety studies, axitinib was not associated with remarkable alterations of QT interval and ECG (Agency, 2012). Secondary pharmacology studies investigated the binding activity of axitinib against almost 40 receptors and ion channels, revealing weak binding activity for adenosine A_{2A}, muscarinic M_2 and neuropeptide Y_2 receptors, which was not however associated with functional antagonism for the screened targets (Inlyta., 24 May 2012; Agency, 2012).

Following oral administration in humans in the fed state, axitinib achieves peak plasma levels withing 2-6 hours, depending on the dose given, which decline with a terminal plasma half-life ranging from 2 and 5 hours (Rugo et al., 2005; van Geel et al., 2012; Chen et al., 2013). This RTKI shows linear pharmacokinetics with a steady state reached withing 15 days (Rugo et al., 2005). It has an apparent volume of distribution of 129-263 l, with a plasma clearance between 20 and 113 $l.h^{-1}$ (Rugo et al., 2005; van Geel et al., 2012). The binding of axitinib to

human plasma proteins is >99% and it preferentially binds albumin, although discrete binding occurs also on α1-acid glycoprotein (Chen et al., 2013). The major pathway of axitinib metabolism is via CYP3A4, followed by CYP2C19 and CYP1A2, with additional metabolism via uridine diphosphate glucuronosyltransferase-mediated glucuronidation (Rugo et al., 2005; van Geel et al., 2012). The N-glucuronide and sulfoxide are the predominant metabolites of axitinib and are both inactive (Rugo et al., 2005; van Geel et al., 2012). The plasma elimination half-life is between 2 and 5 hours, with faecal elimination via hepatobiliary excretion being the major elimination pathway, with renal elimination accounting for around 20% (Rugo et al., 2005; van Geel et al., 2012). Being predominantly metabolised by CYP3A4, coadministration of axitinib and compounds that induce or inhibit this subfamily of drug-metabolising enzymes is not recommended (Rugo et al., 2005; van Geel et al., 2012).

The most reported adverse effects associated with axitinib include hypertension, diarrhoea, fatigue, nausea, weight loss, dysphonia, proteinuria and hypothyroidism (Inlyta., 24 May 2012; Agency, 2012; Geller et al., 2018). Hypertension is one of the most common complications reported in cancer patients treated with axitinib (40.4%), with 15.3% developing severe (grade 3 or higher) hypertension, defined as systolic BP (SBP) $\geq$ 180 mmHg and/or diastolic BP (DBP) $\geq$ 120 mmHg (Rini et al., 2011; Abdel-Rahman & Fouad, 2014; Rini et al., 2015; Kadowaki et al., 2021). Among those patients, hypertension led to treatment interruption (12%), dose reduction (5%) and discontinuation (<1%) (Rini et al., 2015). The median time to onset for grade 1-2 and grade ≥ 3 hypertension associated with axitinib is 16 days and 24 days, respectively, although increased DBP was already occurring after 4 day of treatment (Agency, 2012; Rini et al., 2015; Geller et al., 2018).

1.4.1.3 LENVATINIB

Lenvatinib (E 7080), sold under the brand name Lenvima®, is a small molecule tyrosine kinase inhibitor developed by Eisai (Agency, 2021a). It is an orally active multi-kinase inhibitor that targets VEGFR-1/2/3, FGFR-1/2/3/4, PDGFR-α and proto-oncogenes RET and KIT (Tohyama et al., 2014; Hussein et al., 2017; Goel & Singla, 2021). With a recommended daily dose of 24 mg, lenvatinib was first approved by FDA and EMA in 2015 for the treatment of radioiodine-refractory differentiated thyroid cancer (DTC), before its use being subsequently extended to metastatic renal cell carcinoma (mRCC) (2016), unresectable or advanced hepatocellular carcinoma (2018) and advanced, recurrent or metastatic endometrial carcinoma (2019) (Killock, 2015; Ikeda et al., 2016; Hussein et al., 2017; Goel & Singla, 2021; Makker et al., 2022).

Lenvatinib primarily binds to VEGFR-1/2/3 with IC_{50} values of 4.7, 3.0, 3.3 nM, respectively; in addition, it also binds with different potencies at RET (IC_{50} = 6.4 nM), FGFR-1 (IC_{50} = 61 nM), FGFR-2 (IC_{50} = 27 nM) FGFR3 (IC_{50} = 52 nM), FGFR4 (IC_{50} = 43 nM), PDGFR-α (IC_{50} = 29 nM) and KIT (IC_{50} = 85 nM) (Hussein et al., 2017).

The binding activity of lenvatinib (10 $\mu mol.L^{-1}$) against a panel of 50 non-kinase receptors was assessed as part of secondary pharmacology studies, revealing no significant binding to any receptor, with the exception for the 5-hydroxytryptamine receptor 1B (5-HT1B), which mediates coronary artery vasoconstriction, and NET (norepinephrine transporter), responsible for the reuptake of extracellular norepinephrine (Kaumann & Levy, 2006; Mandela & Ordway, 2006; Agency, 2021a). Considering the total C_{max} at the therapeutic dose of 24 $mg.day^{-1}$ (573 $ng.ml^{-1}$) and protein binding (>98%), free C_{max} reaches 7.9 $ng.ml^{-1}$, therefore no secondary pharmacodynamic effects on these targets were expected (Agency, 2021a). Safety pharmacology studies did not reveal significant alterations of QT interval, indicating a lack of potential QT prolongation at clinically relevant doses (Agency, 2021a).

After oral administration in humans, lenvatinib reaches peak plasma concentration within 1-4 hours, with a complex absorption described as mixed and simultaneous first- and zero-order kinetics (Hussein et al., 2017; Goel & Singla, 2021). With a protein binding range of 98%-99%, lenvatinib is extensively bound to human plasma proteins, primarily to albumin (Gupta et al., 2016; Hussein et al., 2017). The apparent volume of distribution of lenvatinib varies from 50.5 to 163 l, with a plasma clearance ranging between 4.2 and 7.1 $l.h^{-1}$, while its terminal half-life is 28 hours (Gupta et al., 2016; Hussein et al., 2017). Lenvatinib mainly undergoes a CYP3A-mediated metabolism, but a non-enzymatic metabolism via aldehyde oxidase also occurs (Gupta et al., 2016; Hussein et al., 2017; Goel & Singla, 2021). The biliary route, accounting for ~64%, is the main excretion mechanism, while ~25% of the drug is eliminated through renal excretion (Gupta et al., 2016; Hussein et al., 2017; Goel & Singla, 2021). The main metabolites of lenvatinib derives from decyclopropylation, demethylation, N-oxidation and O-dearylation (Hussein et al., 2017).

The most common adverse effects reported with lenvatinib include hypertension, fatigue, diarrhoea, nausea, decreased appetite, proteinuria, liver events and hypocalcaemia, hyperbilirubinemia and palmar-plantar erythrodysesthesia syndrome (Ikeda et al., 2016).

Hypertension is the most reported toxicity reported in cancer patients treated with lenvatinib (72.8%), with 44.4% of them reaching grade 3 or higher, leading to dose interruption, reduction and premature discontinuation in 13%, 13.4% and 1.1% of the cases, respectively (Agency, 2021a). The median time to onset for this cardiovascular adverse effect was 16 days

(Agency, 2021a). In addition, 7% and 2% of thyroid cancer patients receiving lenvatinib experienced cardiac dysfunction and severe (grade 3 or higher) cardiac dysfunction, respectively (Killock, 2015).

1.4.2 Cardiovascular toxicity associated with VEGFR-2 inhibitors

According to a recent meta-analysis, RTKIs targeting VEGFR-2 considerably increased the risk of hypertension with an odds ratio (OR; a measure of association between exposure and an event) of 5.28 and a number needed to harm (NNH; defined as number of individuals that must be treated in order for one individual to experience an adverse outcome accountable to the treatment) of 6, severe hypertension (OR 5.59; NNH 22), arterial thromboembolism (OR 1.52; NNH 140) and cardiac dysfunction (OR 1.35; NNH 139) (Abdel-Qadir et al., 2017). Even if from clinical practice it is clear that VEGF inhibition strongly affects the haemodynamic balance in patients treated with RTKIs (Bair et al., 2013), the molecular mechanisms behind these cardiovascular toxicities are still unknown. Many hypotheses, including the role of NO and endothelin system, have been proposed but we are still far from clearly understanding the cardiovascular biology of VEGF and the mechanisms by which its inhibition impairs cardiovascular function (Small et al., 2014; Dobbin et al., 2021; Camarda et al., 2022). This uncertainty about the mechanism of action makes it difficult to find an adequate therapeutic scheme (Bair et al., 2013; Dobbin et al., 2018). Therefore, it is fundamental to define the pathophysiology of RTKIs-induced cardiovascular toxicities, especially hypertension, in order to get a more effective therapeutic management of these adverse effects (Copur & Obermiller, 2011; Camarda et al., 2022). Identifying the specific mechanisms of VEGFIs-related cardiovascular complications can strongly contribute to develop new targeted cancer therapies which do not alter the signalling pathway responsible for the cardiotoxicity (Dobbin et al., 2018). Moreover, considering the multiplicity of molecular targets of these antiangiogenic drugs (Fabian et al., 2005; Force et al., 2007), it is essential to discriminate the “on-target” and “off-target” cardiovascular effects associated with their clinical use (Bellinger et al., 2015; Dobbin et al., 2021). The “on-target” toxicity derives from the expression of targeted kinases both in cardiovascular structures and tumour environment (Cheng & Force, 2010; Brown et al., 2020). Nevertheless, the promiscuity of VEGFR-TKIs may also be responsible for “off-target” toxicity due to the alteration of unintended pathways (e.g., PDGFRs), which have a crucial role in cardiovascular function (Moslehi, 2016; Dobbin et al., 2021). Given the considerable impact that these targeted therapies have on the prognosis and survival of cancer patients (Yeh & Bickford, 2009;

Vasudev & Reynolds, 2014; Iacovelli et al., 2015), cardiovascular safety of VEGFR inhibitors represents an emerging challenge in oncology. The severity of cardiovascular events associated with these therapeutics often requires dose adjustments or treatment interruption (Abdel-Qadir et al., 2017; Parmar & Bjarnason, 2019). Along with the detrimental impact of dose reduction on cancer patient outcomes, the clinically relevant increase in the risk of cardiovascular events (i.e., hypertension, severe hypertension, cardiac dysfunction and thromboembolism) requires a better understanding of the mechanisms driving such complications to improve both the cardiovascular and the cancer outcomes within this patients population (Abdel-Qadir et al., 2017; Camarda et al., 2022). Additionally, establishing preclinical models able to recapitulate key characteristics of anticancer treatment-associated cardiovascular toxicities in patients will be crucial for a better prediction, early detection and improved translatability of such cardiovascular complications observed with the current drug safety testing paradigms (Savoji et al., 2019; Asnani et al., 2021).

1.4.2.1 VEGFR-2 INHIBITORS AND LEFT VENTRICULAR DYSFUNCTION

The clinical spectrum of VEGFR inhibitor-induced cardiac toxicities ranges from asymptomatic LVD to symptomatic heart failure and cardiogenic shock (Force et al., 2007; Bair et al., 2013; Ghatalia et al., 2015; Dobbin et al., 2021). The pathophysiological events driving such cardiotoxic manifestations in response to antiangiogenic therapies are still scarcely identified, as well as is not yet clear if these complications are the direct result of their impact on the heart or they are secondary to alterations in the peripheral or coronary circulation (Chen et al., 2008; Dobbin et al., 2021). Moreover, as VEGF has a crucial role in maintaining myocardial capillary density in response to pressure overload, VEGFR inhibitors-induced cardiotoxicity is suggested to be the result of on-target effects of such compounds (Izumiya et al., 2006; Dobbin et al., 2021). Indeed, inhibition of VEGFR signalling pathway may lead to reduced myocardial capillarisation and impaired contractility, therefore accelerating the shift from compensated cardiac hypertrophy to heart failure (Izumiya et al., 2006; Rhian M. Touyz et al., 2017). However, due to the limited selectivity of these antiangiogenic therapies, off-targets mechanisms have also been proposed to explain the cardiac impairment observed with these compounds (Touyz & Herrmann, 2018; Dobbin et al., 2021). VEGFRIs-mediated downregulation of adenosine monophosphate-activated protein kinase (AMPK), with consequent disruption of cardiac energy production, is one of the off-target mechanisms of cardiotoxicity attributed to RTKIs targeting VEGFRs (Rhian M. Touyz et al.,

2017; Dobbin et al., 2021). In this regard, sunitinib-induced alteration of cardiac function has been associated with the inhibition of AMPK pathway, resulting in ATP depletion and alteration of cardiac homeostasis (Kerkela et al., 2009; Yang et al., 2019). An underexplored mechanism underlying cardiotoxicity associated with the use of targeted antiangiogenic drugs is represented by the interaction of these compound with adenosine receptors (Mellor et al., 2011). Under hypoxic conditions and cardiac ischemia, the increased levels of adenosine and the activation of adenosine A_1 and A_3 receptors have shown to exert a cardioprotective effect (Parsons et al., 2000), leading to investigate the activation of A_3 receptors as a strategy to prevent RTKI-induced cardiac impairment (Sandhu et al., 2017).

The off-target inhibition of the pro-survival factor Raf-1 (rapidly accelerated fibrosarcoma 1) has also been implicated in the development of cardiac dysfunction following antiangiogenic treatment (Cheng et al., 2011; Dobbin et al., 2021). Indeed, sorafenib has shown to inhibit Raf-1 signalling pathway, whose activity is associated with cardiomyocyte survival and the prevention of cardiac hypertrophy (Harris et al., 2004; Cheng et al., 2011; Franczyk et al., 2023). Additional preclinical and clinical investigations are required to fully elucidate the pathophysiological events underlying RTKI-induced cardiac toxicity. Indeed, although the cardiotoxic manifestations associated with these drugs appear to be at least partially reversible with dose adjustment and conventional heart failure therapies (Chu et al., 2007; Narayan et al., 2017), a considerable gap in the mechanistic understanding of such complications still remains, therefore limiting the implementation of preventive strategies and treatment (Dobbin et al., 2021). The unintended targets of antiangiogenic therapies must be better identified to design more selective compounds with limited off-target effects, while a comprehensive insight of the cardiovascular role of the intended kinases will assist in predicting and managing those cardiac complications associated with on-target effects (Chen et al., 2008; Dobbin et al., 2021).

1.4.2.2 VEGFR-2 INHIBITORS AND ARTERIAL THROMBOEMBOLISM

As reported from a recent meta-analysis and systematic review, cancer patients treated with VEGFRs inhibitors showed a significantly increased risk of arterial thromboembolic events (Choueiri et al., 2010; Qi et al., 2014; D. Zhang et al., 2016; Abdel-Qadir et al., 2017). Such cardiovascular complications have been associated with the alteration of endothelium integrity due to the inhibition of VEGF pathway with RKIs, whose use may further exacerbate the hypercoagulable state of tumour microenvironment (Albini et al., 2010; Dobbin et al.,

2021). In this context, promoting platelet activation and the coagulation cascade (Albini et al., 2010; Carmeliet & Jain, 2011), the downregulation of adhesion molecules, as well as the disruption of EC connections may be implicated in thrombotic complications (Bair et al., 2013). Indeed, suppressing the role of VEGF in promoting vascular integrity and EC survival (Ferrara et al., 2003), RTK inhibitors may predispose to the exposure of procoagulant factors (i.e., von Willebrand factor and tissue factor), in turn responsible for such impaired thrombotic status (Kamba & McDonald, 2007). In addition, the reduced levels of NO and prostaglandin I2 (PGI_2), potent inhibitors of platelet aggregation, may have a role in thromboembolic complications associated with VEGFR-TK inhibitors (Kamba & McDonald, 2007). Although all these hypotheses try to explain the mechanisms by which RTK inhibitors evoke the activation of a prothrombotic status, the real causes of such complication are not yet fully clear (Bair et al., 2013).

1.4.2.3 VEGFR-2 INHIBITORS AND HYPERTENSION

Hypertension, being observed in up to 80% of cancer patients treated with anti-VEGF RTKIs, is the prevalent cardiovascular adverse effect evoked by these novel targeted therapeutics, (Bair et al., 2013; Small et al., 2014; Abdel-Qadir et al., 2017; Dobbin et al., 2021). Both functional and structural alterations of the endothelium seem to have a role in the VEGFR-2 inhibitor-induced hypertension (Lankhorst, Saleh, et al., 2015b). In particular, due to the role of VEGF in increasing the expression of eNOS, one of the first hypotheses to explain the hypertension observed with targeted antiangiogenic treatments involved an impairment of NO bioavailability and consequent suppression of the NO-dependent vasodilator tone (Lankhorst, Kappers, van Esch, Danser, et al., 2014; Camarda et al., 2022). In a rodent model, the hypertensive response to sunitinib treatment was associated with reduced urinary excretion of NO metabolites (M. H. Kappers et al., 2011; Camarda et al., 2022). In addition, a polymorphism in the eNOS gene, resulting in functional changes in eNOS activity and reduced NO production, was associated with an increased risk of severe hypertension (grade 3) in sunitinib-treated patients (Eechoute et al., 2012). Although these studies corroborate the involvement of an impaired NO production pathway in RTKIs-induced hypertension, additional experimental and clinical investigations have produced conflicting results, making the role of NO in the development of antiangiogenic drug-induced hypertension controversial and not well-established (Lankhorst, Kappers, van Esch, Danser, et al., 2014; Lankhorst, Saleh, et al., 2015a). In particular, patients receiving vandetanib showed an

increased, rather than a decreased, flow-mediated vasodilation, a measure of NO-mediated vascular function (Mayer et al., 2011). In another study, despite a decrease in flow-mediated vasodilation observed after administration of telatinib, the vasodilatory response to nitroglycerine, an NO-independent vasodilator, was similarly affected (Steeghs et al., 2008; Lankhorst, Saleh, et al., 2015a). Similarly, in the Langendorff isolated rat heart model, sunitinib altered the coronary flow responses both to bradykinin (an endothelium-dependent vasodilator) and to sodium nitroprusside (an endothelium-independent vasodilator) (Kappers et al., 2010), hence implying a wider microvascular dysfunction rather than an exclusive endothelial dysfunction induced by sunitinib. Moreover, the co-treatment with sunitinib and sildenafil (a phosphodiesterase type 5 inhibitor) was not able to show a reduction of BP in rats (Lankhorst, Kappers, et al., 2014a). Altogether, there is currently insufficient evidence to conclude that RTKI-induced hypertension primarily results from a dysregulation of NO pathway (Neves et al., 2020; Camarda et al., 2022).

A reduction in the density of microvessels (also known as capillary rarefaction), by altering peripheral vascular resistance, has been proposed as a plausible mechanism leading to antiangiogenic drugs-induced hypertension (van der Veldt et al., 2010; Dobbin et al., 2021; Camarda et al., 2022; Noble et al., 2023), although this hypothesis is not consistent with the rapid rise in BP observed with these compounds (Lankhorst, Saleh, et al., 2015b). In a clinical study involving cancer patients treated with telatinib, the hypertensive response was accompanied by functional and structural microvascular rarefaction after 5 weeks of treatment (Steeghs et al., 2008). In a first phase, a functional reduction in microvessel density may be the result of the profound vasoconstrictive responses associated with these therapeutics, although a structural rarefaction of capillaries may develop at a later stage as a consequence of the apoptotic effect of RTKIs on ECs and smooth muscle cells, further aggravated by the prolonged vasoconstriction (Neves et al., 2020; Dobbin et al., 2021; Camarda et al., 2022). VEGF controls EC survival, migration and reorganization, therefore its inhibition may contribute to EC apoptosis and remodelling of microvascular beds (Gerber, 2008; van der Veldt et al., 2010). In this contest, a reduced skin capillary density has been observed in clinical studies in patients treated with VEGFIs (van der Veldt et al., 2010; Mourad & Levy, 2011). However, whether microvascular rarefaction is a cause, or a long-term consequence, of RTKI-induced hypertension remains to be clarified (Versmissen et al., 2019; Camarda et al., 2022).

Meanwhile, the ET-1 axis has emerged as an important mediator of the hypertensive effect consequent to the administration of RTKIs targeting VEGFR-2 (Kappers et al., 2010; Neves et al., 2020; Camarda et al., 2022). According to a preclinical study carried out by Kappers and colleagues, the hypertensive response due to the administration of RTKIs targeting VEGF signalling is associated with increased plasma levels of ET-1 (Kappers et al., 2010). ET-1 is a potent vasoconstrictor peptide, whose biological activity is mediated by its binding with two G protein-coupled receptors, ET_A (endothelin receptor type A) and ET_B (endothelin receptor type B), both expressed on vascular smooth muscle cells. ET_B receptors are also expressed on ECs, where the interaction with ET-1 promotes NO synthesis and prostacyclin production (Kohan et al., 2011). Clinical studies revealed that cancer patients treated with sunitinib show a significant increase in circulating levels of ET-1 (Kappers et al., 2010; Markó et al., 2022), therefore reinforcing the hypothesis that the activation of the endothelin axis and the upregulation of ET-1 may have a prominent role in the pathogenesis of RTKI-induced hypertensive response. To investigate the involvement of ET-1 in the BP rise during the treatment with VEGFR-TKIs, the efficacy of dual ET_A and ET_B receptor antagonists and selective ET_A receptor antagonists in preventing such complication was tested in several preclinical studies. In conscious telemetry-instrumented rats pre-treatment with atrasentan, a selective ET_A receptor antagonist, was able to abolish the hypertensive response due to the administration of linifanib (Banfor et al., 2009). Likewise, radiotelemetry studies in rats exposed to sunitinib showed that macitentan, a non-selective ET_A and ET_B receptor blocker, attenuated the rise in BP induced by RTK inhibition (Lankhorst, Kappers, et al., 2014a). However, it should be taken into account that macitentan exhibits a 50-fold selectivity for the ET_A receptor (Iglarz et al., 2008). Moreover, in chronically instrumented awake swine, the administration of tezosentan, a dual ET_A and ET_B receptor antagonist, suppressed the sunitinib-induced hypertensive response, without lowering baseline BP (Kappers et al., 2012), reinforcing the hypothesis that the upregulation of the endothelin system mediates the vasoconstrictive response involved in RTKIs-induced hypertension (Kappers et al., 2012). However, the agents which antagonise the ET system range from those with a dual $ET_{A/B}$ antagonism (e.g., bosentan) to those with a selective ET_A blockade (e.g., sitaxentan) (MacIntyre et al., 2010; Kohan et al., 2011; Enevoldsen et al., 2020). Their difference in terms of receptor selectivity should be carefully considered when it comes to their ability to prevent RTKI-induced hypertension. In this context, bosentan, an agent with combined ET_A and ET_B receptor blockade, did not prevent cediranib-induced rise in BP in conscious freely moving rats (Carter et al., 2017), therefore introducing the hypothesis that hypertensive effects due

to RTKIs may be mainly mediated by ET_A receptor rather than ET_B receptor. Even if several mechanisms have been proposed, the events involved in the activation of ET axis due to the antiangiogenic therapies are still unclear. VEGF promotes the expression of preproET-1 mRNA in ECs via VEGFR-2, as well as enhancing the secretion of ET-1 (Matsuura et al., 1998). However, if VEGF determines the production of ET-1 by ECs, a reduction of ET-1 would be expected during the treatment with VEGF-RTK inhibitors. The fact that increased levels of ET-1 have been observed during antiangiogenic treatments led to the hypothesis that the rise in ET-1 is due to the activation of ECs as a result of VEGF signalling inhibition (Lankhorst, Saleh, et al., 2015b; Lankhorst et al., 2016). Considering the role of NO in inhibiting the ET-1 production in ECs (Boulanger & Lüscher, 1990), a reduced bioavailability of NO may also be responsible for the upregulation of ET-1 (Thorin & Webb, 2010).

In addition to NO, VEGFR signalling is involved in promoting the release of another vasoactive molecule, namely PGI_2, which, interacting with prostacyclin (IP) receptors, elicits vasodilation via adenylyl cyclase (AC)-cyclic adenosine monophosphate (cAMP)-protein kinase A (PKA) pathway (Neagoe et al., 2005; Reid & Kinsella, 2015). The vasodilatory activity of PGI_2 is also mediated by inhibition of ET-1 production (Prins et al., 1994; Razandi et al., 1996; Mirabito Colafella et al., 2020). Although the inhibition of VEGFRs is expected to determine a reduction of PGI_2 levels (R. M. Touyz et al., 2017; Touyz et al., 2018), increased urinary and plasma levels of this have been detected in rats treated with sunitinib (Mirabito Colafella et al., 2020). The rise in PGI_2 production following antiangiogenic treatment may be due to the interaction of ET-1 and ET_A receptors, resulting in the stimulation of PGI_2 expression (Kappers et al., 2012; Mirabito Colafella et al., 2020). In support of this hypothesis, co-treatment with sunitinib and a selective ET_A receptor antagonist was associated with a reduction of circulating and urinary levels of PGI_2 (Mirabito Colafella et al., 2020). A possible mechanism proposed to explain the relationship between enhanced release of PGI_2 and VEGFR inhibitors-induced hypertension includes the interaction of prostacyclin with thromboxane A2 (TXA_2) receptor, therefore acting as a vasoconstrictive agent (Mirabito Colafella et al., 2020). Overall, although the few experimental studies available suggest a possible role for PGI_2 in the hypertensive response observed with antiangiogenic therapies, further investigations are needed to clarify the contribution of prostanoids in the pathophysiology of RTKIs-related hypertension (Mirabito Colafella et al., 2020; Camarda et al., 2022).

The renin angiotensin system has also been evaluated for its potential involvement in BP elevation evoked by RTKIs targeting VEGFR-2, but conflicting results have been obtained

(Lankhorst, Kappers, et al., 2014a; Carter et al., 2017). Indeed, in some rodent models RTK inhibition determined increased levels of Ang II, with an improvement after administration of ramipril, an ACE inhibitor (Lankhorst, Kappers, et al., 2014a). Whereas, studying the effect of RTKIs on haemodynamic parameters of conscious rats and the impact of antihypertensive drugs on these values, it has been shown that losartan (an angiotensin II type 1 receptor blocker) was not able to blunt the hypertensive and vasoconstrictive responses to cediranib (Carter et al., 2017). In line with these data, clinical studies have not reported the activation of the renin angiotensin system as a potential cause of hypertension induced by RTKIs (Kappers et al., 2010).

1.5 PROJECT AIMS

This thesis aimed to investigate the cardiovascular safety liabilities of VEGFR-2 inhibitors, in particular axitinib and lenvatinib. Using *ex vivo* and *in vivo* approaches to study the impact of other therapeutics on the cardiovascular system, this work aimed to characterise the haemodynamic profile of these antiangiogenic agents and to investigate potential mechanisms underlying RTKI-induced cardiovascular alterations.

First, this project aimed to quantify the potency of a panel of RTKIs against VEGFR-2 to then proceed with the characterisation of their haemodynamic profile in animal models. In particular, the project aimed to recapitulate the hypertensive effect of VEGFR-2 inhibitors in conscious and freely moving rats, in addition to evaluating the susceptibility of regional vasculature to the pressor effect associated with these therapeutics (*Chapter 3*). Second, the role of dual versus selective endothelin receptor antagonism in the development of the haemodynamic changes induced by VEGFR-2 inhibitors was interrogated (*Chapter 4*). Finally, this project explored the effect of these anticancer agents on vascular reactivity and remodelling, as well as their impact on cardiac performance, by combining isolated tissue bath approaches with echocardiography and pressure-volume loops analysis (*Chapter 5*). The work described in the following chapters aimed to:

- *Aim 1.* Quantify the potency of a variety of RTKIs against VEGFR-2 (axitinib, erlotinib, linifanib, vatalanib, SU-14813 and lenvatinib) by using a nuclear factor of activated T-cell (NFAT) luciferase reporter gene assay in HEK293 cells expressing the human VEGFR-2 and a firefly luciferase reporter gene regulated by NFAT response elements.

- *Aim 2.* Investigate the effect of axitinib and lenvatinib on chronotropism, arterial pressure and regional vascular conductance in unanaesthetised rats by using the pulsed Doppler flowmetry model.
- *Aim 3.* Elucidate the role of endothelin receptor antagonism in preventing the haemodynamic changes associated with axitinib and lenvatinib.
- *Aim 4.* Assess the effect of axitinib and lenvatinib on endothelial function and vascular reactivity, while also defining their impact on arterial stiffness, on isolated mouse aortic segments by combining two different tissue bath approaches.
- *Aim 5.* Investigate morphological and functional cardiac changes in response to axitinib and lenvatinib using transthoracic echocardiography in mice.
- *Aim 6.* When echocardiographic alterations are present, assess the effect of VEGFR-2 inhibitors on cardiac mechanics, contractility and haemodynamic via pressure-volume loop analysis.

2 Materials & Methods

2.1 MATERIALS & METHODS: IN VITRO

2.1.1 NFAT luciferase reporter gene assay in RE-luc2P VEGFR-2 HEK293 cells

The NFAT reporter gene assay was used to evaluate the potency of selected RTKIs targeting VEGFR-2. The binding between VEGFR-2 and its ligands initiates several intracellular signalling cascades, such as the phosphorylation of PLCγ with the subsequent increase of intracellular calcium (via DAG and inositol-1,4,5-trisphosphate (IP_3)) and the activation of calcineurin. Activated calcineurin dephosphorylates NFAT, thus triggering its translocation to the nucleus where it promotes the transcription of pro-angiogenic and pro-inflammatory genes (M. Simons et al., 2016). By using cells transfected with the firefly luciferase reporter gene under the control of a NFAT response element, the NFAT reporter gene assay permits the quantification of the VEGFR-2 transcriptional activity through the measurement of the luminescent signal due to the NFAT-luciferase response (Hill et al., 2001; Carter et al., 2015). Indeed, the mono-oxygenation of 5'-fluoroluciferin catalysed by firefly luciferase results in the emission of a yellow-green light (550-570 nm) used to quantify the extent of VEGFR-2-mediated Ca^{2+}-calcineurin-NFAT signalling activation. Here, the NFAT reporter gene assay has been used to quantitatively determine the potency of RTKIs targeting VEGFR-2. The inhibition of VEGFR-2 signalling elicited by these drugs results in a reduction of the NFAT-luciferase activity, thus producing a decrease of luminescence (Figure 9).

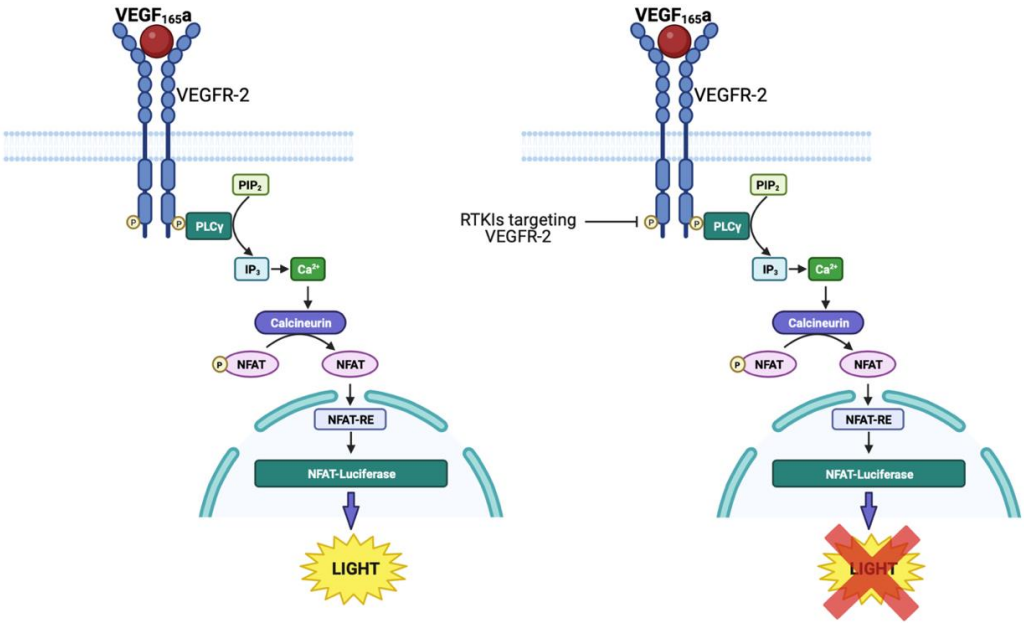

Figure 9. *Schematic illustration of the NFAT reporter gene assay used to evaluate the potency of RTKIs targeting VEGFR-2. VEGF binding to VEGFR-2 causes the autophosphorylation of specific*

tyrosine residues in the kinase domain. Phosphorylated VEGFR-2 initiates the Ca^{2+}/PLCγ cascade, resulting in the activation of calcineurin which, dephosphorylating NFAT, promotes its nuclear translocation and the consequent transcription of firefly luciferase, whose enzymatic activity can be quantified, providing a quantitative measure of the receptor activation. Upon VEGFR-2 inhibition due to RTKIs, the consequent blockage of receptor autophosphorylation results in a reduction of the NFAT-luciferase activity, therefore producing a decrease of luminescence. Figure created with BioRender.com

2.1.1.1 MATERIALS

HEK293 (Human Embryonic Kidney 293) cells were chosen for this functional assay since they have proved to be a reliable cell line for the production of recombinant proteins of interest due to their ease of transfection, high efficiency of protein expression and robust cell growth (Tan et al., 2021). The NFAT-RE-luc2P HEK293 cell line, a clonal derivative of HEK293 cells expressing the firefly luciferase reporter gene (luc2P) under the control of NFAT response elements (NFAT-REs) and stably transfected with the expression vector containing the *KDR* gene (human gene encoding for VEGFR-2) (Promega pGL4.30, E8481), were purchased from Promega Corporation (Madison, USA), and are referred as VEGFR-2/NFAT-ReLuc2P HEK293 cells hereafter. Dulbecco's Modified Eagle's Media (DMEM), Dulbecco's phosphate buffered saline (PBS), foetal calf serum (FCS), dimethyl sulfoxide (DMSO), trypsin (0.25% w/v in EDTA solution) and poly-D-lysine (PDL) hydrobromide were purchased from Sigma-Aldrich (Gillingham, UK).

Axitinib, erlotinib, lenvatinib, linifanib, SU-14813 and vatalanib were purchased from Stratech Scientific Ltd (UK). ONE-Glo™ Luciferase Assay System was purchased from Promega Corporation (Madison, USA). $VEGF_{165}$a was provided by R&D (Abingdon, UK). Other tissue culture reagents were purchased from Sigma-Aldrich (Gillingham, UK). Unless otherwise stated, cell culture reagents, laboratory equipment and chemical stocks were supplied by Sigma-Aldrich (Gillingham, UK). Cell culture consumables were purchased from Fischer Scientific (Loughborough, UK).

2.1.1.2 CELL LINE

The VEGFR-2/NFAT-RE-luc2P HEK293 cell line, allowing a rapid and convenient analysis of any cellular response resulting in a modulation of the NFAT transcriptional activity, was used for the *in vitro* experiments presented in *Chapter 3* of this thesis. Derived from human embryonic kidney cells, HEK293 cells express adenovirus genes (Ad5 E1A and E1B) which, interfering

with cell cycle control pathways, prevent apoptosis, as well as allowing for high-level expression of recombinant proteins (Graham et al., 1977; Louis et al., 1997). In addition, HEK293 cells are characterised by an easy reproduction and maintenance, making them a versatile and robust cell line with several applications in molecular biology (Thomas & Smart, 2005).

2.1.1.3 CELL CULTURE

VEGFR-2/NFAT-RE-luc2P cells were grown in DMEM (supplemented with 10% FCS to provide additional nutrients) and maintained in T75 flasks within a humidified 5% CO_2 atmosphere in incubators at 37°C. All media were stored at 4°C and warmed to room temperature before use so as not to create excessive stress to the cells. All sterile cell culture techniques were performed in a class II Microbiological Safety Cabinet (TriMAT; Contained Air Solutions, UK) to prevent contamination.

2.1.1.4 PASSAGING

Cell were checked daily to monitor culture health and degree of confluency using an inverted microscope (Primovert, Zeiss) fit with a Pan Apochromat 10X objective. The VEGFR-2/NFAT-RE-luc2 cell line was used as an adherent monolayer for the experiments reported in this thesis. Cell passaging was performed when cells reached 80-90% confluency to maintain log phase growth and maximum viability. In order to passage the cells, medium was removed from the T75 flask and 3-4 ml of PBS were added to rinse cell monolayer and remove traces of old medium and any non-adherent cells. Subsequently, adherent cells were detached from the flask surface by 5-min incubation at room temperature with 1 ml of 1x trypsin-EDTA solution (diluted from a 10x solution using PBS). Trypsin, as proteolytic enzyme, digests adhesion molecules and detaches cells, allowing easy resuspension of the cells. Since trypsin is inactivated by the bivalent ions (Ca^{2+} or Mg^{2+}) present in culture media, the chelating agent EDTA was added to weaken cell-cell adhesion, thus improving the enzymatic activity of trypsin. Detached cells were then washed off into 10 ml growth medium and the resulting cell suspension was then transferred into a 25 ml universal tube and centrifuged at 1000 rpm for 5 min. After discarding the supernatant, the pellet was resuspended in 10 ml of growth medium, and the appropriate volume of cell suspension to achieve the desired split ratio (typically 1:5, 1:10 or 1:20) was then added into a new T75 flask containing 20 ml of growth medium.

2.1.1.5 FREEZING

Multiple passages of VEGFR-2/NFAT-RE-luc2 HEK293 cell line were stored at -80°C or in liquid nitrogen dewars for long-term storage (Isothermal V3000- EHAB/C, Custom Biogenic System, USA). To allow good cell recovery after the freeze-thaw process, cells were frozen in FCS containing 10% of the cryoprotectant DMSO to prevent cell lysis upon freezing. Before use, the cryopreservation medium was sterilised by filtration using a 0.22 µm filter to remove potential contaminants. Cells were passaged as described in *2.1.1.4* until the centrifugation step, after which cell pellet weas resuspended in cryopreservation medium and aliquoted into cryogenic storage vials. A constant cooling rate of -1°C.min^{-1} is crucial to maximise cell viability and integrity. For this reason, cell-containing cryovials were placed in a Mr Frosty™ freezing container (Nalgene, Thermo Fisher Scientific, UK) and placed at -80°C for 24 h, before being transferred to the liquid nitrogen vapour phase for long-term storage.

To recover cryopreserved cells, a previously frozen cell-containing cryovial was removed from liquid nitrogen storage and rapidly thawed. Once defrosted, the aliquot was suspended in 10 ml growth medium, centrifuged at 1000 rpm for 5 min and the resulting pellet was resuspended in 1 ml of growth medium and seeded into a T75 flask. After 24 h, the medium was replaced with 10 ml of fresh growth medium to remove dead cells and any remaining traces of DMSO.

2.1.1.6 LIGAND STOCKS

Axitinib, erlotinib, lenvatinib, linifanib, SU-14813 and vatalanib stock solutions of 10^{-2} M were prepared by dissolving each individual compound, provided as powder, in DMSO, then aliquoted onto Eppendorf tubes and stored at -20°C until use. Recombinant human VEGF-A_{165}a stock solutions of 10^{-6} M were prepared by resuspending the protein in PBS with 0.1% protease-free bovine serum albumin (BSA) (as per the manufacturer's instructions to prevent interactions with the plasticware), aliquoted into Eppendorf tubes and stored at -20°C until use.

2.1.1.7 EXPERIMENTAL PROTOCOL

Prior to seeding cells, white 96-well plates were coated with PDL, a chemically synthesised extracellular matrix used to facilitate cell adhesion to plastic surfaces, therefore allowing removal of medium during the assay without dislodging the cells. PDL hydrobromide was diluted with PBS to make 5 mg.ml^{-1} aliquot stocks (40 µl), which were stored at -20°C. On the day of use, a PDL aliquot was diluted in 20 ml PBS to a final concentration of 10 µg.ml^{-1} and

filter sterilised using a sterile syringe filter (0.22 µm pore size). 50 µl of 10 µg.ml^{-1} PDL was added to each well of the plate and incubated at room temperature for 30 min to allow adherence to the bottom of the wells, before being aspirated off.

VEGFR-2/NFAT-RE-luc2 cells were grown in a T75 flask until approximately 80% confluent before being washed, detached from the flask, resuspended, and centrifuged as described previously (*Methods 2.1.1.4*). The resulting pellet was resuspended in 10 ml cell culture medium. To ensure experiments used cells at optimal confluency, the cell density was determined using the average cell count calculated with a haemocytometer (BRAND® counting chamber, BLAUBRAND® Neubauer improved, BR717805, Sigma-Aldrich, UK). Cells were diluted in culture medium and seeded 100 µl/well at the required density (20,000 cells/well) in the white 96-well pre-treated with PDL. Cells were left to grow for 24 h at 37°C/5% CO_2. After that time, growth medium was replaced with FCS-free medium to prevent growth factors in the serum from interfering with the assay and cell were incubated at 37°C/5% CO_2 for a further 24 h.

2.1.1.7.1 VEGF$_{165}$a CONCENTRATION-RESPONSE CURVE

For the VEGF$_{165}$a concentration-response curve, on the day of the assay, medium was removed and 90µl/well serum-free DMEM/0.1% protease-free BSA was added. Increasing concentrations of VEGF$_{165}$a (final concentrations: 10^{-12} M - 10^{-8} M) were added in 10 µl to the appropriate wells in triplicate replicates and cells were then incubated for 5 h at 37°C/5% CO_2. After the incubation period has lapsed, assay medium was removed and replaced with 50 µl/well serum-free DMEM and 50 µl/well ONE-Glo™ Luciferase reagent, containing luciferin as a substrate for the luciferase (Promega Corporation, USA). A white plate back seal was applied, and luminescence was measured by a TopCount plate reader (Perkin Elmer, Llantrisant, UK) with a 5-min delay to allow reagent to react with transcribed luciferase and to allow the attenuation of background luminescence.

2.1.1.7.2 INHIBITION OF VEGF$_{165}$a RESPONSE USING RTKIS

For the competition assay, on the day of the experiment FCS-free medium was removed and 80µl/well serum-free DMEM/0.1% protease-free BSA was added. Vehicle (serum-free DMEM/0.1% protease-free BSA) was added in 10 µl to the control wells. Then 10 µl of increasing concentrations of RTKIs (final concentrations: 10^{-11} M - $3x10^{-7}$ M for erlotinib,

axitinib and SU-1483; $3x10^{-11}$ M - 10^{-6} M for vatalanib and linifanib) were added to the appropriate wells in triplicate replicates and cells were then incubated for 1 h at 37°C/5% CO_2 prior to addition of $VEGF_{165}a$. $VEGF_{165}a$ (1 nM) was added to each well and cells were then incubated for 5 h at 37°C/5% CO_2. After the incubation period lapsed, assay medium was removed and replaced with 50µl/well serum-free DMEM and 50µl/well ONE-Glo™ Luciferase reagent (Promega Corporation, USA). A white plate back seal was applied, and luminescence was measured by a TopCount plate reader (Perkin Elmer, Llantrisant, UK) with a 5-min delay to allow reagent to react with transcribed luciferase and to allow the attenuation of background luminescence.

2.1.1.8 DATA ANALYSIS

All data are presented as mean ± S.E.M. and were analysed using non-linear regression in Prism 10 (GraphPad Software, San Diego, CA, USA). The n in the text refers to the number of independent experiments. Statistical analysis was determined by unpaired t-test and $p<0.05$ was considered statistically significant.

2.1.1.8.1 $VEGF_{165}a$ CONCENTRATION-RESPONSE CURVE

The $VEGF_{165}a$ concentration-response curve was fitted with a non-linear regression (variable slope) using the following equation:

$$Response = \frac{E_{max} \times [A]^n}{[A]^n + EC_{50}}$$

Where [A] is the $VEGF_{165}a$ concentration, E_{max} is the maximal response of an agonist, n is the Hill coefficient and EC_{50} is the molar concentration of the agonist required to induce 50 % of the E_{max}.

2.1.1.8.2 INHIBITION OF $VEGF_{165}a$ RESPONSE USING RTKIs

All data obtained from NFAT luciferase reporter gene assays were normalised to responses to 1nM $VEGF_{165}a$, then fitted with a non-linear regression (variable slope) using the following equation:

$$\%\ Inhibition\ of\ the\ response\ to\ VEGF_{165}a = \frac{100 \times IC_{50}}{[I] + IC_{50}}$$

Where IC_{50} is the molar concentration of RTKI required to inhibit 50 % of the response to VEGF and [I] is the concentration of RTKI.

2.2 MATERIALS & METHODS: *IN VIVO*

2.2.1 Pulsed Doppler flowmetry

The Doppler Flowmetry model has been used in this project to assess the haemodynamic effects of selected RTKIs (i.e., axitinib and lenvatinib) in conscious and freely moving rats. This approach allows measurement of the effects of therapeutics on arterial BP, as well as the changes in the haemodynamic responses in different vascular beds, in unanaesthetised animals, providing an effective way to study physiological parameters without the interference of anaesthetic agents (Gardiner & Bennett, 1988; S.M. Gardiner et al., 1990). Indeed, general anaesthesia can alter animal's physiology, affecting in particular BP, oxygen saturation, cerebral metabolism and other electrophysiological signals (Claassen, 2013). In addition, the use of this *in vivo* model provides an exquisite way to evaluate drug-induced responses in the presence of intact autoregulatory systems, thus maintaining physiological neurohormonal interactions and autonomic nervous system responses (i.e., baroreceptor reflex). In this regard, to ensure that the drug-induced cardiovascular effects are not modified or biased by anaesthetics and to have a better comprehension of integrated cardiovascular effects *in vivo*, the use of conscious and freely moving animals is fundamental.

In order to investigate the regional haemodynamic impact of antiangiogenic therapies with this model, the Doppler effect (*2.2.1.1*) was applied to derive blood flow velocity by chronically implanting ultrasonic pulsed Doppler flow probes (*2.2.1.5.1*) in rats. Essentially, the implantation of miniaturised pulsed Doppler flow probes around the vessels of interest allowed for measurement of the frequency difference (in Hz) between the transmitted and received sound waves (Doppler shift), thus enabling calculation of blood flow velocity, as described in greater detail in the section below (*2.2.1.1).* In addition, rats were implanted with intraarterial catheters to derive BP and heart rate (HR) measurements and intravenous catheters to minimise animal discomfort during drug administration by using intravenous route. This is discussed in more details in *2.2.1.5.1* and *2.2.1.5.2.*

2.2.1.1 THE PULSED DOPPLER FLOWMETRY METHOD

First developed for the measurements of blood flow in dogs, the pulsed Doppler approach revealed its main advantage in the adoption of a single ultrasonic crystal compared to the

previously-used bulky electromagnetic or continuous wave Doppler probes (Hartley & Cole, 1974). It was in 1981 that this model was applied in rats, to be then further improved by the Haemodynamics group of Gardiner and Bennett at the University of Nottingham, which was able to reduce signal "aliasing" by using a modified high pulse repetition frequency (PRF) mainframe (Haywood et al., 1981; S.M. Gardiner et al., 1990; S. M. Gardiner et al., 1990). Indeed, the PRF must be twice the frequency of the expected maximum Doppler shift ($2f$D) in order to avoid aliasing of the real signal. The condition when PRF equals to $2f$D is also known as Nyquist limit (S. M. Gardiner et al., 1990). If sampling rate is over the Nyquist limit, the sampling will be adequate, while if the sampling rate is below this limit, the resultant frequency is an artefact (Figure 11).

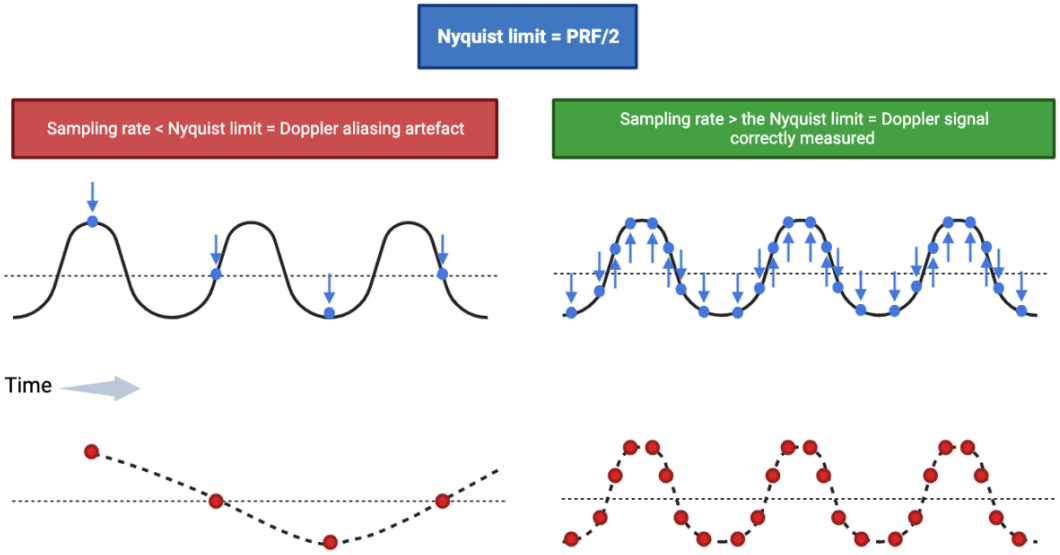

Figure 11. *Aliasing is the major artifact of the Doppler method and occurs when PRF is less than twice the maximum Doppler shift. Two sine waves and the relative samplings at different sampling rate are represented. The arrows indicate the sampling time, while the dotted red lines are the resultant of the sampling. On the left side, the PRF is below the Nyquist limit, resulting in aliasing of the signal. On the right, the sampling rate is over the Nyquist limit, resulting in a sampling representative of the real signal. PRF = pulse repetition frequency. Figure created with BioRender.com*

When connected to a flowmeter, the piezoelectric crystal embedded in a probe (details of probe construction are reported in *section 2.2.1.2*) emits short pulses of ultrasonic energy (20 MHz). When this ultrasonic energy comes into contact with a moving element (i.e., an erythrocyte) it is reflected back towards the crystal, time-delayed and with a slightly different frequency than the one emitted (Figure 12). This change in frequency, also known as Doppler frequency shift (DFS or Δ_f), equals the difference between the transmitted and received

frequencies and is directly related to the velocity of the moving element (Hartley & Cole, 1974). The DFS (MHz) depends on blood flow velocity (V, m/s), transmitted frequency (f_t, MHz), speed of sound in blood (c, m/s) and the angle between the crystal and the direction of blood flow (θ, constant at 45°):

$$\Delta_f = \frac{2 \times f_t \times V}{c} \times \cos\theta$$

In the probe, the angle of the crystal (θ) remains constant at 45°. The frequency of the transmitted signal (f_t) and velocity of sound in the blood (c) are also constants, therefore the Doppler frequency shift (Δ_f) is directly proportional to blood flow velocity.

The time between probe implantation and catheterisation allowed a fibrous capsule to grow around the cuff and the vessel, preventing vessel diameter changes beneath the probe. Therefore, as the vessel diameter remains constant, blood flow velocity is directly proportional to blood flow and a change in the Doppler shift is an index of changes in blood flow in the vascular bed downstream of the probe (Hartley & Cole, 1974; Haywood et al., 1981).

The measurement of Doppler shift in conjunction with mean arterial pressure (detailed in *2.2.1.3*) allows vascular conductance (VC) to be derived (S. M. Gardiner et al., 1990):

$$\%\,\Delta \text{ Vascular Conductance } = \%\,\Delta\, \frac{\text{Doppler shift}}{\text{Mean arterial pressure}}$$

An increase in vascular conductance indicates vasodilation in the vascular bed downstream of the probe, while a decrease is representative of vasoconstriction.

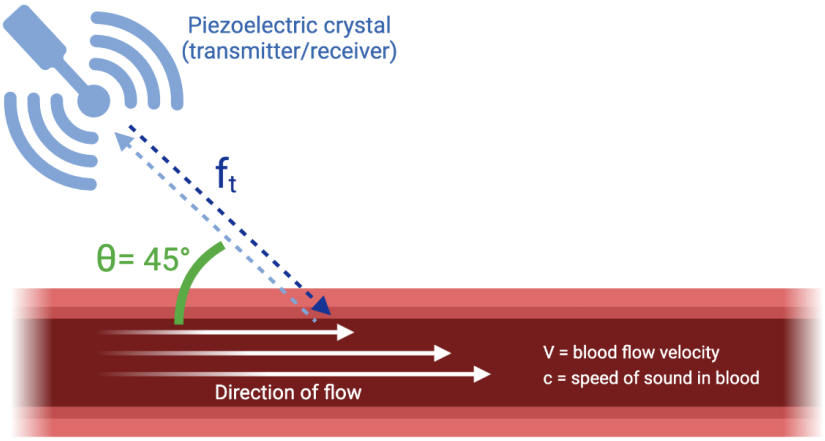

Figure 12. *Schematic representation of the Doppler flowmetry principle. Figure created with BioRender.com*

2.2.1.2 CONSTRUCTION OF DOPPLER FLOW PROBES

Pulsed Doppler flow probes were constructed according to the method described by Haywood *et al* (Figure 13) (Haywood et al., 1981). Piezoelectric crystals (1 mm in diameter) attached to insulated silver-plated copper wires were purchased from Crystal Biotech Inc (USA). The crystal was placed into a medical grade silicon tubing (3-4 mm in length), one side of which was then cut at a 45° angle to allow the piezoelectric crystal, when implanted, to have the correct orientation to the vessel. The paired probe wires of the crystal were then pulled through the other side of the silicon tubing, ensuring that the crystal was facing the angled side of the tubing. At that point, the crystal was stabilised with sticky dental wax, before being permanently fixed. Polystyrene foam, which was used as an acoustic baffle to prevent the detection of flow from surrounding areas, was spread with a needle over the silicon tubing and left to set for 24 h. To create the lumen space where the blood vessel will be placed, the resulting subunit was then mounted onto a needle, appropriate in size to the diameter of the vessels of interest (Table 2), by melting the dental wax on the crystal and then surrounded by a cuff created with soft Silastic material, which will be sutured around the vessel. The probe was then left overnight to allow the soft silastic cuff to settle. Finally, the encapsulate probe was removed from the needle by cutting the cuff parallel to the needle in the opposite side of the crystal. Silk sutures (6/0) were then put in place at the top of the resulting two flaps, to allow the probe to be secured around the vessel at the stage of the surgical implantation. Refinements have been made in the construction of the probes, with the result of smaller and lighter units. This allowed not only to implant multiple probes in a

single animal, but also to minimise tissue damage during and after the implantation procedures.

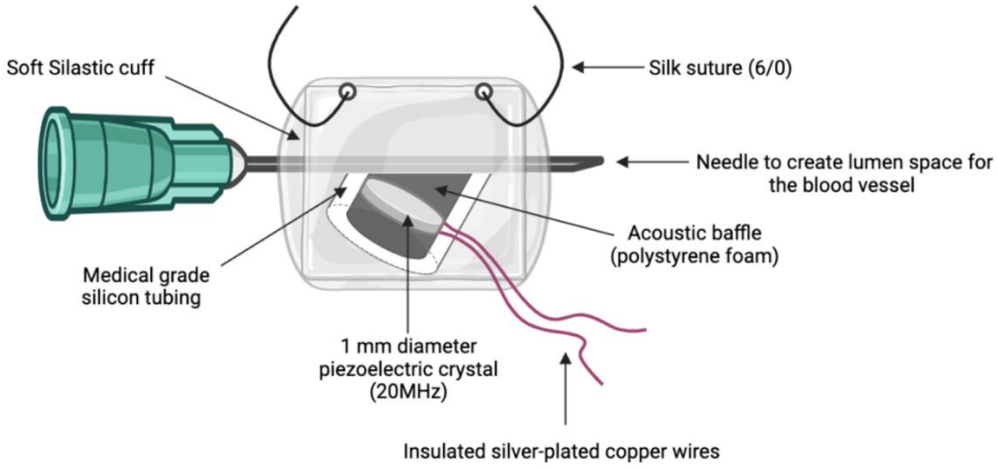

Figure 13. *Representation of the in-house made miniaturised pulsed Doppler flow probe. Figure created with BioRender.com*

Blood vessel	Approximate size	Lumen diameter
Left renal artery	3 mm x 4 mm	1 mm
Superior mesenteric artery	3 mm x 4 mm	1.2 mm
Descending aorta	3 mm x 5 mm	1.7 mm

Table 2. *Approximate size and lumen diameter of the vessels of interest. These values were used as a reference for the construction of the pulsed Doppler flow probes.*

2.2.1.3 MEASURING BLOOD PRESSURE

While monitoring regional blood flow, this model allows the simultaneous measurement of BP by using a fluid-filled arterial catheter connected to a pressure transducer (Figure 14). The arterial catheter, also known as PE_{50}/PE_{10} catheter, was made up of two tubing (Braintree Scientific), which differed in terms of size and material (S. M. Gardiner et al., 1990). The portion of the arterial catheter that was inserted into the distal abdominal aorta via the ventral caudal artery consisted of a short (approximately 7.0 cm), flexible and small-diameter polyethylene tubing (PE_{10}) (internal diameter: 0.28 mm), which was welded to a longer (100 cm), wider (internal diameter: 0.58 mm) and thicker nylon tubing (PE_{50}). Catheter design has a substantial influence on its performance and dynamic response, in particular influencing catheter natural frequency and damping ratio (Gardiner et al., 1980; Schenk et al., 1992). The

appropriate damping ratio is crucial to correct pressure measurements obtained with a low natural frequency catheter (Schenk et al., 1992). Damping (or internal impedance) is inversely proportional to catheter diameter. Therefore, the combination of different internal diameter obtained with PE_{50}/PE_{10} catheter, compared to a catheter exclusively made from PE_{50}, results in an increased damping ratio and consequent attenuation of pressure signal to an acceptable level (Schenk et al., 1992). To have a reliable measure of BP, a catheter exclusively made from PE_{10} is also not ideal, since the excessively small diameter can lead to a reduced dynamic sensitivity of the pressure measurements and the signal would be drastically dampened (Van Vliet et al., 2000). As a result, the PE_{50}/PE_{10} catheter has been demonstrated to have the natural frequency and damping characteristics necessary for the accurate acquisition of BP (Schenk et al., 1992). This catheter system has been tested and verified to accurately measure pressure at the frequencies of the signal generated by a rat heart (around 6 Hz at rest, 360 beats per minute (bpm)) (Gardiner et al., 1980).

The arterial catheter was connected to a pressure transducer via a stainless-steel needle and a 3-way tap. The pressure transducer system consisted of a Bell and Howell type 4-42 pressure transducer incorporated into a displacement dome filled with degassed double-distilled water. The whole system was connected to a transducer amplifier (model 13-4615-50; Gould, Cleveland, Ohio, USA), which was associated to a computer running customised software (Instrument Development Engineering Evaluation, IdeeQ version 2.5; Maastricht Instruments, Maastricht, The Netherlands). The 3-way tap allowed enabled temporarily disconnection of the transducer in order to flush the arterial line with heparinised saline (40 Industrial Units (IU).ml^{-1}, ~0.2 ml). This step was essential to maintain arterial catheter patency, preventing the formation of blood clots. When no pressure measurement was performed, the arterial catheter was connected to a fluid-filled swivel (Figure 15), made in-house as described in Brown et al (Brown et al., 1976), which was in turn connected to a pump providing constant infusion of heparinised saline (20 IU.ml^{-1}, 0.4 ml.hr^{-1}).

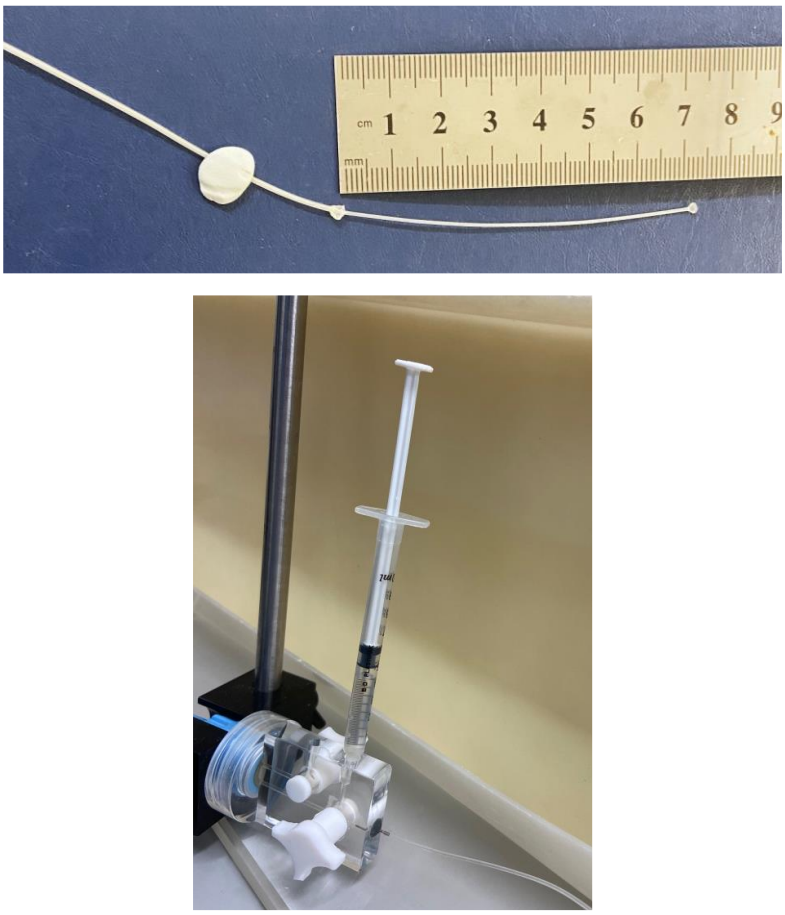

Figure 14. *Photograph of the intraarterial catheter and pressure-transducer.*

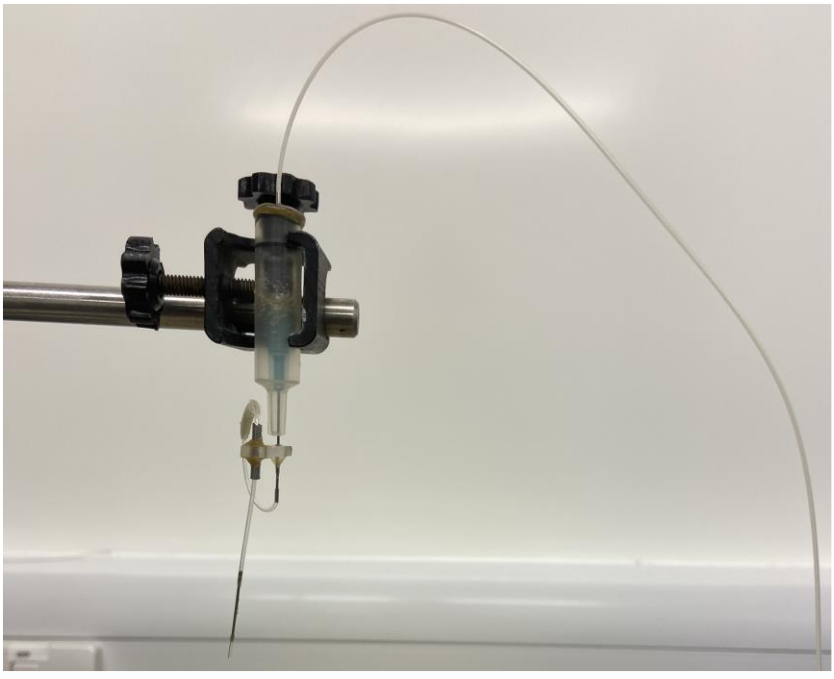

Figure 15. *Photograph of the in-house made fluid-filled swivel.*

2.2.1.4 ANIMALS

Adult male Sprague-Dawley rats (Charles River Laboratories and Envigo, UK) weighing between 350 and 500 g were used to perform the pulsed Doppler flowmetry studies described in *Chapter 3* and *Chapter 4* of this thesis. Animals arrived at the animal house at least 7 days before any surgical procedure and were housed in a temperature-controlled (21-23°C) room with a 12 h light/dark cycle (lights on at 6:00 am) and *ad libitum* access to food (18% Protein Rodent Diet; Envigo, Madison WI, USA) and drinking water. Rats were housed in pairs prior to the surgical implantation of the Doppler flow probes, at which point they were singularly housed overnight and housed in pairs again the following day till the surgical implantation of intraarterial and intravenous catheters. Post-catheterisation, animals were individually housed in the experimental room with free access to food and drinking water.

All surgical and experimental procedures were conducted with approval of the University of Nottingham Animal Welfare and Ethical Review Board (establishment license: X653228F4) and performed in conformity with the Animals (Scientific Procedures) Act (1986), under UK Home Office approved Project Licence (PF0F2A6EC) and Personal License (PIL) authority (I95023042).

For the studies mentioned in this thesis, 96 rats were used, and all animal experiments are reported in compliance with the ARRIVE guidelines and the editorial on reporting animal studies (Kilkenny et al., 2010; McGrath & Lilley, 2015).

Animals were subjected to two rounds of surgeries: the first surgery consisted of the implantation of the Doppler flow probes, while the second procedure was carried out to insert intraarterial and intravenous catheters. Pharmacological agents used during the surgical procedures and the relative doses were chosen according to the recommendations described in the fourth edition of Laboratory Animal Anaesthesia (Flecknell, 2015).

The surgical success rates and humane endpoints were in keeping with the Home Office licence.

2.2.1.5 SURGICAL PROCEDURES

2.2.1.5.1 IMPLANTATION OF DOPPLER FLOW PROBES

Rats were initially anaesthetised with intraperitoneal injection of 300 µg.kg^{-1} fentanyl citrate (synthetic opioid acting as full agonist of µ opioid receptors; Jansen-Cilac Ltd) mixed with 300 µg.kg^{-1} Domitor (medetomidine, selective α_2-adrenergic agonist; Pfizer). Prior to starting the surgery, animals also received 1 mg.kg^{-1} meloxicam (injected subcutaneously) as supplementary analgesia. If required, supplementary anaesthesia was provided throughout the surgery to maintain appropriate anaesthetic depth. Once animals were fully anaesthetised (toe pinch was used for anaesthetic depth assessment), weight was recorded and the abdominal midline, cervical region and left flank above the hind limb were shaved. After cleaning the shaved areas, paws and tail with Clinell skin wipes (2% chlorhexidine in 70% isopropyl alcohol; Gama Healthcare Ltd.), the rat was wrapped in a clear surgical drape (cling film; Glad, USA) and then placed on a heated surgical table (37°C) in the supine position. A 5-inch midline laparotomy incision was made down the middle of the abdomen along the *linea alba*. The contents of the abdomen were then wrapped in sterile, saline-saturated tissue and held on one side, allowing the exposure of the vasculature underneath. Using a microscope, the vessels of interest were identified and cleared of adipose and connective tissue using blunt dissection techniques. A suitable pulsed Doppler probe, with an internal diameter equivalent to the diameter of the vessel of interest, was selected for each vessel and was then connected to a Doppler flowmeter to check if the signal detection was appropriate, before being sutured and secured around the vessel (Haywood et al., 1981; S. M. Gardiner et al., 1990).

Probe wires were secured to the left abdominal wall with 3/0 Mersilk suture (Ethicon, UK) and tunnelled via the left flank to the posterior of the neck, where a second verification of the signals was performed. The extra wire length was coiled and anchored subcutaneously at the left flank. Wire ends were then secured with Mersilk suture and sterile tape to the nape of the neck, leaving their ends (about 0.5 cm long) protruding from the skin. The abdominal contents were carefully repositioned, the abdominal wall was reapproximated using 2/0 Vicryl (Ethicon, UK) and then the skin was closed with subcuticular sutures using 4/0 Vicryl (Ethicon, UK). An absorbent and antibacterial powder (Battle, Hayward and Bower Ltd, UK) was applied over the wounds for optimum healing. 5 ml of warmed saline were administered subcutaneously to provide postoperative hydration. 0.02 mg.kg^{-1} Vetergesic (buprenorphine, opioid partial agonist; Alstoe Animal Health, UK) and 1 mg.kg^{-1} Antisedan (atipamezole hydrochloride, α_2-adrenergic antagonist; Pfizer) were provided as

postoperative analgesia and reversal agent, respectively. Supplementary analgesia (Meloxicam, 1 $mg.kg^{-1}.day^{-1}$, s.c) was given for 3 days after surgery. Animals, individually housed, were closely monitored post-surgery, with welfare checks carried out every 15 min. After a minimum of 3 h of observations, on confirmation that the rats had fully recovered, the animals were taken to the holding room and housed in pairs the following day. As part of animal welfare assessment, rats were checked daily in the period between Doppler flow probes implantation and the surgery to implant intravenous and intraarterial catheters.

2.2.1.5.2 IMPLANTATION OF INTRAVENOUS AND INTRAARTERIAL CATHETERS

A second surgical procedure, performed at least 10 days after probe implantation and after an appropriate welfare check from the Named Veterinary Surgeon, was conducted to implant catheters into the right jugular vein (for drug administration) and into the distal abdominal aorta, via the caudal artery (to record BP and HR).

Venous catheters consisted of polyethylene tubing (150 cm in length with internal diameter of 0.28 mm and outer diameter of 0.61 mm, total lumen dead-space 0.1 ml; Braintree Scientific). The arterial line consisted of polyethylene tubing (6 cm in length with internal diameter of 0.28 mm and outer diameter of 0.61 mm; Braintree Scientific) heat-sealed to nylon tubing (85 cm in length with internal diameter of 0.58 mm and outer diameter of 1.02 mm; Portex, Sims, UK). All catheters were packed and sterilised with ethylene oxide prior to their surgical implantation. In addition, before surgery all catheters were flushed and prefilled with 20 $IU.ml^{-1}$ heparinised saline (Wockhardt UK Ltd, UK)

Local anaesthetic (lidocaine hydrochloride, 2% stock solution; Hameln Pharma Ltd, UK) was applied dropwise to all vessels exposed during the procedures described in this section.

After being anaesthetised (as previously described in *2.2.1.5.1),* rats were weighed and the anterior of the neck (between the larynx and sternum) and right flank were shaved and cleaned with Clinell skin wipes.

Before starting the catheterisation, the Doppler probe wires were released from the skin at the back of the neck and stripped of insulation to check the signals before soldering them into a 6-way miniature plug (Omnetic Connector Corporation, USA). Animals were then wrapped in a clear surgical drape (cling film; Glad, USA) and placed on the operating table in the supine position.

2.2.1.5.2.1 Intravenous catheters

An incision, approximately 1 cm in length, was made on the anterior of the neck and the incision was deepened using blunt dissection, taking care to preserve the surrounding structures. Before isolating the vein and proceeding with catheterisation, the catheters were tunnelled subcutaneously to the back of the neck. Afterwards, the right jugular vein was isolated and its rostral end ligated, before a small incision was made into the vessel. At that stage, two venous catheters were inserted (approximately 1.5 cm) through the jugular vein and secured to the vessel using 3/0 Mersilk suture, flushed with heparinised saline (20 $IU.ml^{-1}$) and sealed with a wire spigot. The incision on the neck was then sutured using 4/0 Vicryl (Ethicon, UK) and absorbent and antibacterial powder (Battle, Hayward and Bower Ltd, UK) was applied over the wound.

2.2.1.5.2.2 Intraarterial catheters

A 2 cm incision was made on the ventral side of the tail, beginning approximately 1.5 cm from its base, and the ventral caudal artery was then exposed. Using closed forceps beneath the artery, the vessel was elevated until flow was obstructed before being ligated. A small incision was made into the vessel and arterial catheter was then inserted 6 cm into the distal aorta and secured to the vessel using 3/0 Mersilk suture. The catheter was then flushed with heparinised saline (20 $IU.ml^{-1}$) and sealed with a wire spigot before being tunnelled subcutaneously via the dorsal end of the tail to the nape of the neck, where the probe wires and venous catheters exited. The tail incision was then sutured using 4/0 Vicryl (Ethicon, UK).

2.2.1.6 PULSED DOPPLER FLOWMETRY: EXPERIMENTAL SET-UP

Upon completion of the surgical implantation of the intraarterial and intravenous catheters, rats were transferred in the experimental room where they were prepared for the following day's experimental procedure, before being individually housed. Firstly, they were fitted with a custom-designed harness (Figure 16) and catheters were passed through a protective spring secured to the harness and attached to a counterbalance. A miniature 6-way plug (Omnetic connector corporation, USA) soldered to the probe wires was also mounted on the harness, before being plugged into the connector to check the Doppler flow signals. Any exposed wires were protected with tape. The arterial catheter was then connected to a fluid-filled swivel, which was in turn connected to a pump infusing heparinised saline (20 $IU.ml^{-1}$, 0.4 $ml.h^{-1}$) throughout the day and overnight to preserve patency (as described above

in *2.2.1.3*). Animals were free to move within the cage and had free access to food and water. Wooden chew blocks and cardboard tubes were also placed into the cage as enrichment items.

Figure 16. *Photographs of the custom-designed harness and 6-way plug connector.*

A satisfactory welfare check was carried out every 15 min to monitor the animals and ensure their adequate recovery. Approximately 4.5 h after the surgery, an additional dose of analgesia was administered (buprenorphine, 15 µg.kg^{-1}, s.c.).

Experiments began 24 h after the catheter implantation, following an appropriate check by the Named Animal Care and Welfare Officer (NACWO).

2.2.1.7 PULSED DOPPLER FLOWMETRY: CARDIOVASCULAR RECORDINGS

HR, BP, renal, mesenteric and hindquarters Doppler shifts, which are an index of blood flow downstream of the implanted probe, were measured by a transducer amplifier (13-4615-50; Gould, Cleveland, OH, USA), a Doppler flowmeter (Crystal Biotech, Holliston, MA, USA), and a VF-1 mainframe (pulse repetition frequency 125 kHz) fitted with high-velocity (HVPD-20) modules. Raw data were recorded and sampled by a customised computer software (IdeeQ; Maastricht Instruments, Maastricht, The Netherlands) every 2 ms, averaged, and stored to disc every cardiac cycle. Changes in vascular conductance (VC) in the renal (RVC), mesenteric (MVC), and hindquarter (HVC) vascular beds, respectively, were derived from the changes in mean arterial pressure (MAP) and Doppler shift. Pulse pressure (PP) was also derived as the difference between SBP and DBP (Homan et al., 2022). At the end of each experiment,

animals were euthanised by an Animals (Scientific Procedure) Act 1986 Schedule one procedure, with Dolethal overdose (200 $mg.ml^{-1}$) and exsanguination.

2.2.1.8 EXPERIMENTAL PROTOCOLS

Hydroxypropyl β-cyclodextrin (HPβCD) and ET-1 were acquired from Sigma-Aldrich (Gillingham, UK). Axitinib and lenvatinib were obtained from Stratech (Ely, UK).

2.2.1.8.1 SERIES 1

This series of experiments was run for 4 days; the contemporaneous control group was administered vehicle (40% HPβCD in sterile saline). Experiments were run with treatment groups of 8 to 10 rats.

Two groups of rats were used to assess the cardiovascular responses to axitinib. On day 1 of the experiment, after a period of baseline recordings, rats were dosed with axitinib (3 (low) $mg.kg^{-1}$ or 6 (high) $mg.kg^{-1}$) as an intravenous bolus (0.2 ml administered over 10 s) followed by a 1-h intravenous infusion (0.4 $ml.h^{-1}$) at the same dose (3 or 6 $mg.kg^{-1}.h^{-1}$) (Carter et al., 2017).

Three groups of rats were used to evaluate the cardiovascular changes induced by lenvatinib. On day 1 of the experiment, after a period of baseline recordings, rats were dosed with lenvatinib (1 (low) $mg.kg^{-1}$, 3 (mid) $mg.kg^{-1}$ or 6 (high) $mg.kg^{-1}$) as an intravenous bolus (0.2 ml administered over 10 s) followed by a 1-h intravenous infusion (0.4 $ml.h^{-1}$) at the same dose (1, 3 or 6 $mg.kg^{-1}.h^{-1}$).

Contemporaneous control group received vehicle as an intravenous bolus (0.2 ml administered over 10 s) followed by a 1-h intravenous infusion (0.4 $ml.h^{-1}$).

The intravenous bolus followed by intravenous infusion dosing regimen allowed to rapidly achieve and maintain plasma concentration plateau.

Haemodynamic recordings were continued for a further 5 h after completion of the axitinib, lenvatinib or vehicle intravenous infusion period. The same treatment regimen was followed on days 2-4 after a baseline recording period on each day.

2.2.1.8.2 SERIES 2

This series of experiments was run for 2 days. Experiments were run with treatment groups of 7 to 8 rats. Three groups of rats were used for each RTKI, namely axitinib and lenvatinib, to assess the role of endothelin antagonism in the prevention of the cardiovascular responses

associated with these agents. Rats were randomly assigned to one of three treatment groups: axitinib or lenvatinib in the presence of vehicle (40% HPβCD in sterile saline), axitinib or lenvatinib in the presence of a dual ET_A and ET_B receptor antagonist (bosentan), axitinib or lenvatinib in the presence of a selective ET_A receptor antagonist (sitaxentan). On day 1 of the experiment, after a period of baseline recordings, rats were dosed with bosentan (15 $mg.kg^{-1}$) or sitaxentan (5 $mg.kg^{-1}$) as an intravenous bolus (0.2 ml administered over 10 s) followed by a 5-h (for axitinib groups) or 6-h (for lenvatinib groups) intravenous infusion (0.4 $ml.h^{-1}$) at the same dose (15 $mg.kg^{-1}.h^{-1}$ for bosentan and 5 $mg.kg^{-1}.h^{-1}$ for sitaxentan). The contemporaneous control group received vehicle (40% HPβCD in sterile saline) as an intravenous bolus (0.2 ml administered over 10 s) followed by a 5-h (for axitinib groups) or 6-h (for lenvatinib groups) intravenous infusion (0.4 $ml.h^{-1}$).

After 1-h infusion of the endothelin antagonists or vehicle, axitinib (3 $mg.kg^{-1}$) or lenvatinib (1 $mg.kg^{-1}$) was administered to all animals as an intravenous bolus (0.2 ml administered over 10 s) followed by a 1-h intravenous infusion (0.4 $ml.h^{-1}$) at the same dose (3 $mg.kg^{-1}.h^{-1}$ for axitinib and 1 $mg.kg^{-1}.h^{-1}$ for lenvatinib) (Carter et al., 2017). The same treatment regimen was followed on day 2 after a baseline recording period. The intravenous bolus followed by intravenous infusion dosing regimen allowed to rapidly achieve and maintain plasma concentration plateau. At the end of day 2, all groups received ET-1 (administered as 0.1 ml bolus in 1% bovine serum albumin/saline) at the following concentrations: 0.1 μM, 0.3 μM and 1 μM, 3 min per concentration.

To explain the different infusion time between axitinib and lenvatinib groups, the occurrence of neck swelling during experiments with axitinib-treated animals required the shortening of the infusion time to be sure that the swelling was not caused by the prolonged infusion. This adjustment for animal welfare was supported by licence approval.

2.2.1.9 STATISTICAL ANALYSIS

Power calculations were carried out by Professor Jeanette Woolard (the PPL holder) to estimate the sample size required to measure clinically relevant changes in BP (>10 mmHg) and in regional blood flows (>10%) (80%, p = 0.05, effect size of 10 mmHg, SD=8.48, paired *t*-test), as well as to minimise the number of animals used. Combining previous experience from the Haemodynamics group with the results of the NC3R's Experimental Design Assistant tool, eight animals per group were found to be appropriate.

In some cases, one or two Doppler probe signals were lost during the experiment. This was either due to direct damage to the probe or its wires, or to positional changes relative to the blood vessel. For each group, a minimum of 5 signals for each vascular bed measured was required. As a result of this requirement and attrition due to the nature of the research, each experiment had an n number per group varying from 7 to 10.

All data were analysed offline using IdeeQ software (Maastricht Instruments, Maastricht University, NL). For all experiments, time-averaged data are shown as changes from baseline [HR (beats.min^{-1}); MAP (mmHg); VC (%); SBP (mmHg); DBP (mmHg); PP (mmHg)]. Nonparametric tests were performed for all the *in vivo* data reported in *Chapter 3* and *Chapter 4* since they did not satisfy the assumption of normality, which means that the sample means of these data cannot be assumed to be normally distributed (Nahm, 2016; Gosselin, 2019). Statistical comparisons between groups of animals were performed on the integrated changes over specified time periods. A Friedman's test, which is a nonparametric, repeated-measures analysis of variance was used for within-group comparisons to baseline; this data analysis was performed on the first 2 days of the experimental period due to changes in sample size (n) after day 2. A Mann-Whitney U test for integrated area under or above curve analysis was used for comparisons between groups. A Mann-Whitney U test was also performed for comparisons between groups at a specific time point. Vascular conductances were calculated from the MAP and Doppler shift (flow) data. PP was calculated from SBP and DBP. A value of $p<0.05$ was considered significant.

2.2.2 Echocardiography

Echocardiography in animal models is a valuable non-invasive approach to visualise cardiovascular structures in order to quantitatively and qualitatively assess cardiac function. In this context, although telemetry is extensively used in rodent and non-rodent studies as a sensitive and accurate method to evaluate drug-induced alterations of haemodynamic parameters, it provides limited information related to cardiac function (Chui et al., 2009; Bhatt et al., 2019).

Although the use of echocardiographic evaluation in preclinical safety assessment has been limited by a lack of sufficient background studies from a regulatory perspective, several basic science studies on various animal species demonstrated that echocardiography is a reliable and sensitive approach to detect RTKI-induced cardiac dysfunction (Chui et al., 2009; French

et al., 2010; Klaeboe & Edvardsen, 2019; Smiseth et al., 2023). Indeed, mild to moderate LV dysfunction was observed in monkeys following treatment with sunitinib (FDA, 2006), as well as sorafenib-receiving rats showed abnormal echocardiographic parameters when compared to animals treated with sunitinib or pazopanib (French et al., 2010). As a result, echocardiography may represent a routine tool to screen and evaluate these novel anticancer therapeutics for their potential effects on cardiac function. All the echocardiographic parameters evaluated in this thesis are described in more details in *section 2.2.2.4*.

2.2.2.1 MATERIALS

Echocardiography was performed using a Vevo 2100 ultrasound system (FUJIFILM VisualSonics, Amsterdam, the Netherlands). The linear UHF 57 transducer used had a frequency between of 57 MHz and an imaging depth of 18 mm. Images were taken at a frame rate ranging between 50 and 300 frames per sec (fps).

Aquasonic ultrasound gel was purchased from Van Houdt Medical (Antwerp, Belgium). Isofluorane was supplied by IsoFlo (Zavantem, Belgium). Everflow Oxygen generator was purchased by Phillips (Belgium). HPβCD was acquired from Sigma-Aldrich (Belgium). Axitinib and lenvatinib were obtained from Stratech (Ely, UK).

2.2.2.2 ANIMALS AND EXPERIMENTAL PROTOCOL

Male 10-week-old C57BL/6J mice (Charles River Laboratories, France) weighing between 25 and 30 g were used to perform the experiments. Animals were housed in standard cages in the animal facility at the University of Antwerp, with a 12 h light/dark cycle and *ad libitum* access to food (ssniff® Complete feed for rats & mice, Germany) and water.

Three groups of mice were used to assess the structural and functional impact of axitinib and lenvatinib on the cardiovascular system. Animals were dosed with axitinib (12 $mg.kg^{-1}$) or lenvatinib (4 $mg.kg^{-1}$) as an intravenous injection for 4 consecutive days; contemporaneous control group was administered vehicle (40% HPβCD in sterile saline). On day 2 of the treatment period, echocardiography was performed on all the groups (details reported in *Methods 2.2.2.3* and *2.2.2.4*).

On day 4 animals were randomly divided into two clusters: cardiac function was assessed in anaesthetised animals via PV-loop experiments (described in *2.2.3*), whereas vascular reactivity was investigated *ex vivo* using isolated tissue baths (described in *2.3.4* and *2.3.5*).

All surgical and experimental procedures were conducted with approval of the Ethical Committee for Animal Testing of the University of Antwerp (Code 2022-40, date of approval: 08-07-2022) and all experiments were performed in accordance with Directive 2010/63/EU, the ARRIVE guidelines (Kilkenny et al., 2010) and the *Guide for the Care and Use of Laboratory Animals* published by the US National Institutes of Health (National Research Council Committee for the Update of the Guide for the & Use of Laboratory, 2011).

All the work described in *Methods 2.2.2*, *2.2.3*, *2.3* and *Chapter 5* was part of a 6-month secondment at the University of Antwerp.

2.2.2.3 ANIMAL PREPARATION

Mice were anesthetised in an induction chamber with isoflurane at a concentration of 3-5% v/v combined with O_2 generated by Everflow Oxygen generator (Phillips, Belgium). To verify the appropriate depth of anaesthesia, the loss of the righting reflex was checked by gently rolling the induction chamber until the mouse was placed on its back. Upon confirmation that the righting reflex was absent, the mouse was positioned in a supine position on a heating table (FUJIFILM VisualSonics, Amsterdam, Netherlands) to maintain the body temperature at 37°C for the whole procedure. The head of the mouse was positioned inside a cylindric mask, suppling isoflurane (1-3 % v/v for maintenance). The paws were taped on four electrocardiography leads to allow ECG recording to monitor HR and respiratory rate (RR). By adjusting the anaesthetic concentration, the HR and RR were maintained for the whole imaging period between 400-500 bpm and 60-120 breaths per minute, respectively. Hair remover lotion was used to shave the chest of the animal and subsequently removed by wiping the area with a water-moistened cotton bud. Ultrasound gel was applied on the shaved chest of the mouse and the heart was then imaged with a linear transducer.

Two-dimensional (2D) imaging (also called B-mode) and one-dimensional (1D) imaging (also known as M-mode) of the LV parasternal long-axis (PLAX) was obtained by placing the transducer with an angle of 80° to the head-tail axis of the mouse, before rotating the transducer clockwise by 90° to obtain parasternal short-axis (PSAX) view of the LV. The schematic representation of the positions and directions of the transducer for B-mode and

M-mode imaging views is shown in Figure 17. Maintaining the short-axis rotation of the transducer and placing it below the diaphragm oriented toward the right shoulder of the mouse, the apical four-chamber view was obtained to measure competency and pressure gradients across the mitral valve (MV) using colour Doppler imaging. Details about the echocardiographic measurements are described in the section below (*2.2.2.4*). Upon completion of the imaging acquisition, the residual ultrasound gel was removed and the animal was returned to the cage for recovery.

To obtain consistent and reliable echocardiographic data, animal body temperature was maintained between the interval specified above. In addition, since cardiac function is dependent on HR, this parameter was monitored and maintained within a similar range for all the animals, with a variation of ± 100 bpm considered acceptable in this study. Finally, the timing of echocardiographic measurements after anaesthesia was kept constant among the animals to minimise the effect of different anaesthetic.

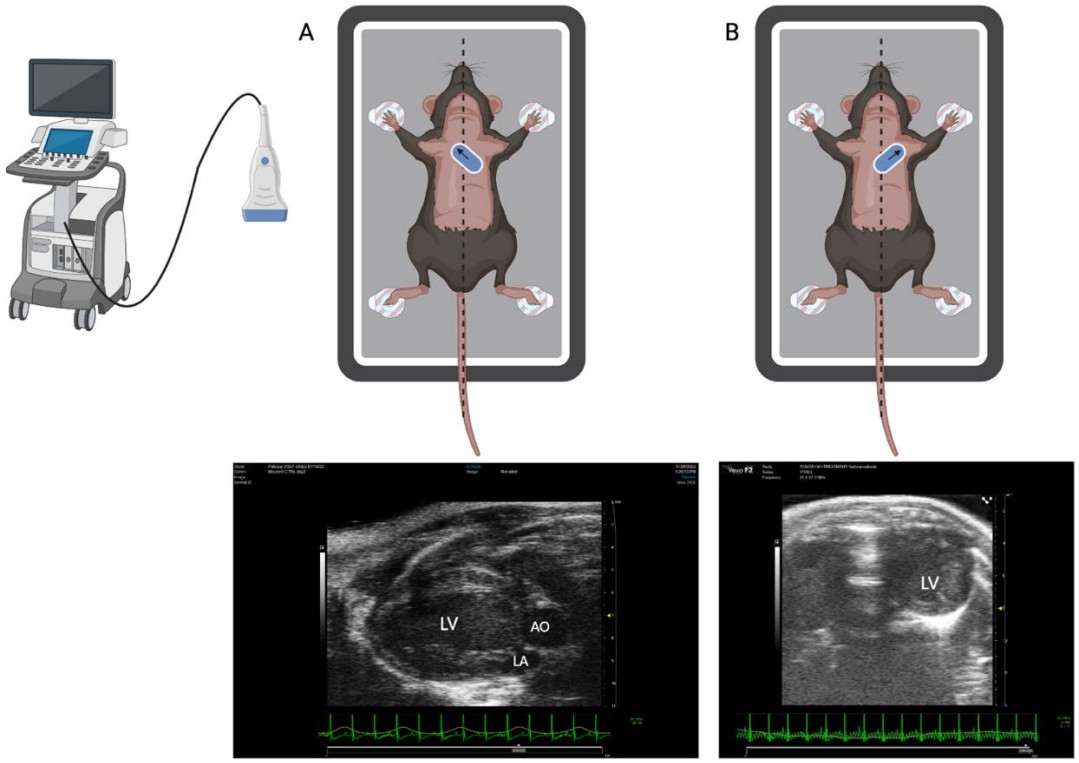

Figure 17. *Schematic representation showing position and direction of the ultrasound transducer to capture LV parasternal long-axis projection (PLAX) (Panel A) and short-axis projection (PSAX) (Panel B). AO= aorta; LA = left atrium; LV = left ventricle. Figure created with BioRender.com*

2.2.2.4 ECHOCARDIOGRAPHIC MEASUREMENTS

For echocardiographic measurements, 2D (B-Mode) images of the heart were acquired in parasternal long-axis and short-axis projections, as well as 1D (M-mode) images were taken in the mid-ventricular region, at the level of the posteromedial papillary muscle in both PLAX and PSAX views. Apical four-chamber view was also obtained to visualise the LV with an accurate angle for the colour Doppler imaging of the MV. Image depth, width and gain settings were used to optimise image quality.

All the echocardiographic parameters were measured during at least three heart beats and averaged.

2.2.2.4.1 B-MODE IMAGING

B-mode (brightness mode) was used to acquire 2D images of the heart, both in PLAX and PSAX views, allowing for visualisation of cardiac anatomical structures (i.e., papillary muscles and cardiac valves) and for evaluation of cardiac chambers dimension and cardiac physiology. This imaging mode also served as an orientation guideline to further assess cardiac structures with other imaging modes, such as M-mode and colour Doppler mode.

2.2.2.4.2 M-MODE IMAGING

M-mode (motion mode) was used to obtain 1D images of the heart, both in PLAX and PSAX views, in real time. Indeed, by placing the ultrasound line along the cardiac structures of interest identified with the B-mode view, the M-mode provided a succession of images along that line over time, allowing to quantify the mobility of those structures (i.e., contractility during systole and diastole), as well as their thickness and internal diameter. Parameters such as LV anterior wall thickness in diastole and systole (LVAWd, LVAWs), LV posterior wall thickness in diastole and systole (LVPWd, LVPWs), LV internal diameter in diastole and systole (LVIDd, LVIDs) were measured from PSAX images acquired with M-mode (Figure 18).

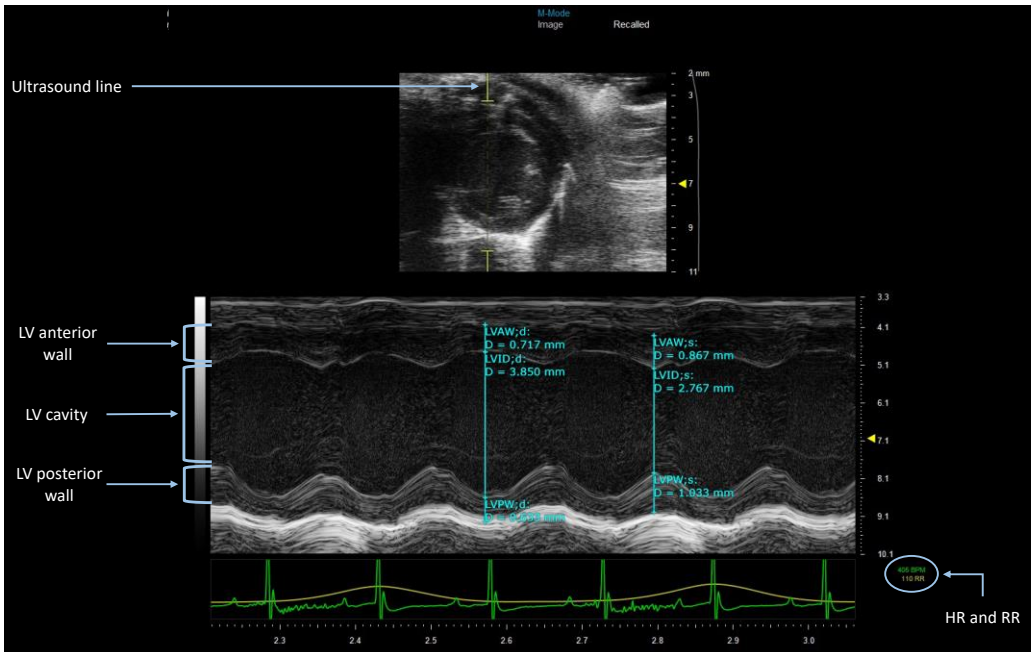

Figure 18. *Echocardiographic measurements for assessment of LV function from M-mode imaging. LVAW = left ventricular anterior wall; LVPW = left ventricular posterior wall; LVID = left ventricular internal diameter; HR = heart rate; RR = respiratory rate.*

2.2.2.4.3 PULSED WAVED (PW) DOPPLER IMAGING

This imaging mode applies the Doppler shift principle (previously described in *2.2.1.1*) to determine blood flow velocity and direction (PW colour Doppler M-mode) and the velocity of myocardial tissue motion (PW tissue Doppler M-mode). In the colour Doppler, the moving target is represented by blood cells (moving parallel to the ultrasound beam), while in the tissue Doppler the moving target is the myocardium. Blood flow velocities across the MV were assessed via the four-chamber view. Colour Doppler M-mode uses a colour-coded representation of blood flow velocity superimposed onto a 2D image. Blood flowing toward the ultrasound transduces is depicted in red (increased frequency), while blood flowing away is represented in blue (decreased frequency).

The Doppler imaging mode is particularly useful to assess diastolic function, as it allows to measure mitral E-wave and A-wave, both representative of transmitral blood flow velocities (Figure 19). In particular, MV E-wave is an index of peak mitral inflow velocity during early diastole (also known as early diastolic filling velocity) and reflects passive blood flow from the left atrium to the left ventricle (Mottram & Marwick, 2005). A pressure gradient between these two structures is generated by the closure of aortic valve and the start of diastole. As a consequence of LV relaxation, ventricular pressure drops rapidly. When LV pressure falls

below the atrial pressure, the resultant is the opening of MV to allow blood to flow from the atrium into the ventricle. The left atrium-to-left ventricle pressure gradient and LV compliance are the main determinant of E-wave velocity. MV A-wave represents the blood flow actively generated by atrial contraction and its amplitude is determined by both LV compliance and atrial contractility. E'-wave (early diastolic mitral annulus velocity) and A'-wave (mitral annulus velocity during active atrial contraction) can also be derived by the Doppler imaging mode and reflect the same event described for E-wave but related to mitral annulus rather than mitral valve.

2.2.2.5 LEFT VENTRICULAR SYSTOLIC FUNCTION

LV systolic function was assessed by measuring LVEF and FS. If LV geometry is maintained and no regional abnormalities in LV contractile function are present (e.g., in case of ischaemic heart disease), LVEF and FS are strongly correlated (Rottman et al., 2007).

FS was obtained by measuring the percentage change in LV diameter during systole in PSAX view using M-mode imaging to derive left ventricular internal diameter during systole (LVIDs) and left ventricular internal diameter during diastole (LVIDd). LVEF, represented by the percentage change in LV volume ejected during systole and LV volume at the end of diastole, was derived by measuring left ventricular volume during systole (LVVs) and left ventricular volume during diastole (LVVd) in PLAX view using M-mode imaging:

$$\text{Fractional shortening (\%)} = \frac{\text{LVIDd - LVIDs}}{\text{LVIDd}} \times 100$$

$$\text{Ejection fraction (\%)} = \frac{LVVd \; - \; LVVs}{LVVd} \times 100$$

2.2.2.6 LEFT VENTRICULAR DIASTOLIC FUNCTION

Echocardiographic assessment of diastolic function is more complex than the evaluation of systolic function (Gaasch & Little, 2007; Rottman et al., 2007). In this context, due to the ease and unambiguousness in the interpretation of the ejection fraction values, the percentage change in the volumetric fraction of blood ejected by the LV with each heartbeat is recognised as well-validated echocardiographic measure for the clinical evaluation of systolic function (Gaasch & Little, 2007). A clinical ejection fraction (EF) range between 50% and 70%

is classified as normal, while any values below 50% are representative of mild (EF 40-49%), moderate (EF 30-39%) or severe (EF ≤ 30%) LV systolic dysfunction (Kosaraju et al., 2023). The lack of an analogous easy-to-interpret clinical standard for diastolic dysfunction makes the diagnosis and evaluation of such event less straightforward (Gaasch & Little, 2007). However, transmitral blood flow velocities and mitral annular blood flow velocities obtained via Doppler mode are indicative of diastolic function (Nagueh et al., 2016). In particular, measuring the blood flow pattern across the mitral valve by using pulsed wave Doppler, two waves can be identified: one representing passive LV filling (E-wave) and one corresponding to the active LV filling (A-wave) (Figure 19). The ratio of peak mitral inflow velocity during early diastole due to LV relaxation to peak mitral inflow velocity during late diastole due to atrial contraction, also known as E/A ratio, is used as a marker of diastolic dysfunction (Mitter et al., 2017). In healthy conditions, E-wave velocity is greater than A-wave velocity (Panesar & Burch, 2017). In case of impaired LV relaxation and consequent reduction of passive LV filling (decreased E-wave velocity), a larger volume of blood is left in the atrium to be ejected during atrial contraction (increased A-wave velocity), resulting in a reduced E/A ratio, representative of diastolic dysfunction (Mottram & Marwick, 2005).

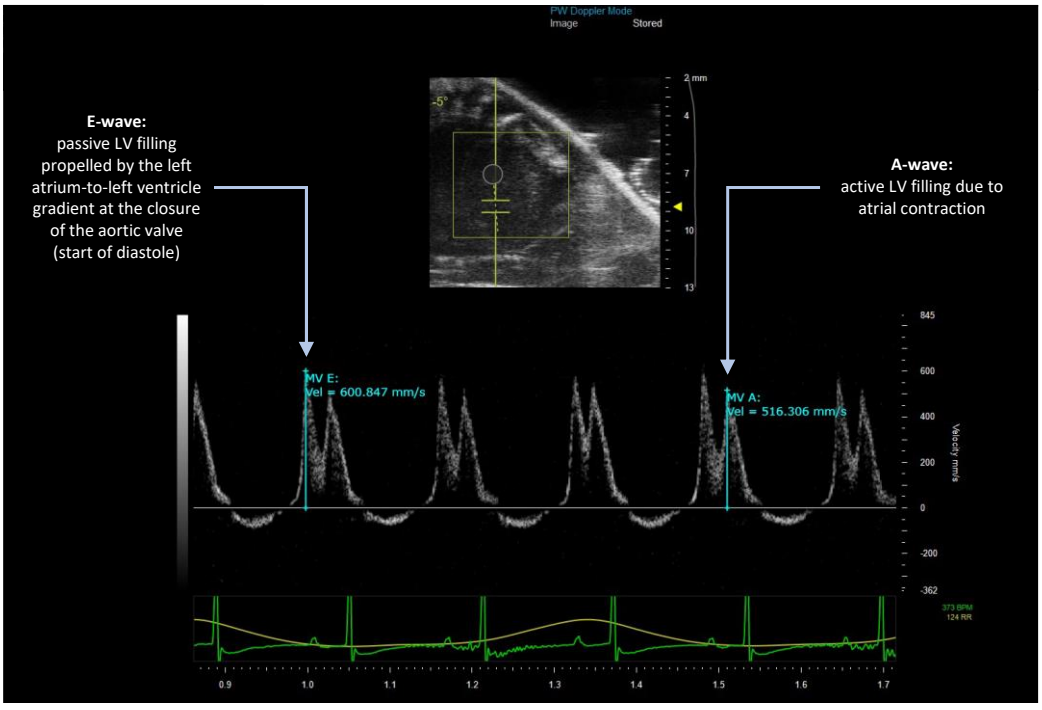

Figure 19. *Echocardiographic measurements of Doppler mode waveform of mitral valve inflow for assessment of diastolic function by measuring E-wave and A-wave from four-chamber view. Measuring blood flow from the left atrium to the left ventricle through mitral valve (so directed toward the ultrasound transducer), the pulsed wave Doppler signal is recorded as upward deflection.*

In addition to E/A ratio, dividing peak E-wave velocity by peak E'-wave velocity provides an indicator of LV end-diastolic pressure (LVEDP). Indeed, measuring the mitral annulus motion during diastole by using pulsed wave tissue Doppler, two waves can be identified: one representing mitral annulus movement during passive LV filling (E'-wave) and one corresponding to the mitral annulus movement during active LV filling (A'-wave) (Figure 20). The resultant E/E' ratio is also used as an index to estimate LV filling pressure (M. K. Kim et al., 2013). With diastolic dysfunction, impaired LV relaxation results in a reduced E'-wave velocity. In contrast, progressive impairment of LV relaxation leads to elevated filling pressure which is associated with an increased E-wave velocity. As a result, an increased E/E' ratio is observed in the case of diastolic dysfunction (Mottram & Marwick, 2005).

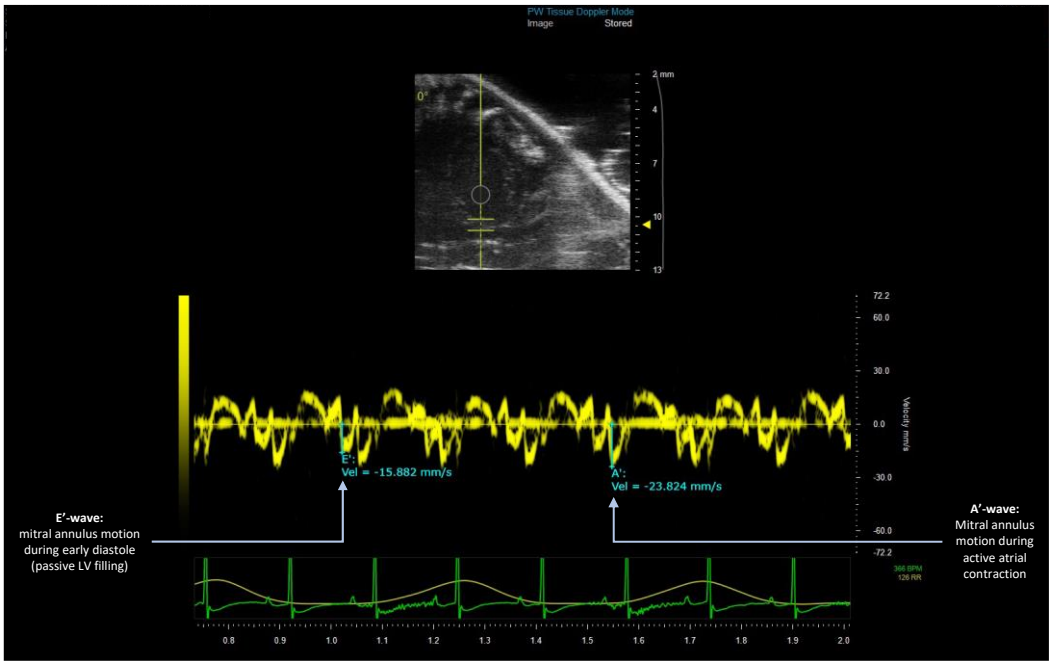

Figure 20. *Echocardiographic measurements of pulsed wave tissue Doppler mode waveform of mitral annulus motion from four-chamber view. Measuring mitral annulus movement, the pulsed wave tissue Doppler signal results in a downward deflection, as during diastole the mitral annulus is directed away from the ultrasound transducer due to its expansion to allow blood to fill the left ventricle.*

Progressive diastolic dysfunction results both in an impaired LV relaxation and increased atrial and end-diastolic pressures (Mottram & Marwick, 2005). This leads to opposing effects on E-wave velocity. If at the early stage of diastolic dysfunction, impaired relaxation and LV compliance lead to a reduced E-wave-velocity, progressive diastolic dysfunction causes

elevated filling pressures, which in turn result in an increased E-wave velocity. Therefore, increasing filling pressures trying to compensate and overcompensate the effect of diastolic function on E-wave velocity result in a non-linear association between this index and the progression of diastolic dysfunction (Mottram & Marwick, 2005).

2.2.2.7 LEFT VENTRICULAR REGIONAL FUNCTION

LV wall thickness is used as a basic index of regional systolic and diastolic function (Grossman et al., 1974; Dong et al., 1994). Regional function in terms of systolic and diastolic wall thickening was evaluated by measuring LV anterior wall and posterior wall both during systole and diastole.

2.2.2.8 DATA ANALYSIS

The acquired digital images of the areas of interest were manually analysed off-line using the Vevo 2100 workstation software.

The first echocardiographic evaluation (n=8 per group) was performed to assess the impact of axitinib and lenvatinib on cardiac function and structure. Due to the absence of axitinib-induced changes in the echocardiographic parameters, the pressure-volume loops analysis was only performed on vehicle- and lenvatinib-treated animals. As a result, the echocardiographic evaluation for the pressure-volume loop cohort of animals was only carried out on vehicle and lenvatinib.

All data were analysed using Prism 10 (GraphPad Software, La Jolla, CA, USA) and expressed as mean ± SEM, with *n* representing the number of mice used. Statistical comparisons of echocardiographic parameters between three groups (vehicle, axitinib and lenvatinib) were made using ordinary one-way ANOVA with Tukey's multiple comparisons test. Statistical comparisons of echocardiographic parameters between two groups (vehicle and lenvatinib) were made using unpaired *t*-test with Welch's correction. Statistical significance was defined as *p<0.05, **p<0.01, ***p<0.001 and ****p<0.0001.

2.2.3 Pressure-volume loops

Firstly described for the assessment of ventricular function in a canine model (Kass et al., 1986) and subsequently improved for its application in rodents (Georgakopoulos et al., 1998),

simultaneous measurements of pressure and volume signals is the gold standard approach to quantify cardiac function (Pacher et al., 2008).

The insertion of a pressure and conductance catheter along the long axis of the ventricle allows real-time acquisitions of both volume and pressure (Pacher et al., 2008). To derive ventricular volume from changes in conductance detected by the PV catheter, the Ohm's law was applied:

$$Voltage\ (V)\ =\ Current\ (I)\ \times\ Resistance\ (R)$$

Since conductance (G) is the reciprocal of resistance, Ohm's law can be also expressed as:

$$Voltage\ (V)\ =\ \frac{Current\ (I)}{Conductance\ (G)}$$

The catheter has four equidistant conductance electrodes with a pressure sensor in the middle of the electrode array (Figure 21). A high-frequency constant-amplitude alternating current passes through the outer pair of electrodes (E1 and E4), also known as excitation electrodes, generating an electrical field in the ventricle from the aortic valve to the apex. Voltage changes (proportional to changes in resistance) are then measured by the inner pair of electrodes (E2 and E3), also called recording electrodes. The potential difference between the excitation and recording electrodes is inversely proportional to the amount of conductive material in the ventricle, allowing for the derivation of ventricular blood volume. Although blood is the main conductor, the conductivity of myocardium must be taken into account to derive the absolute ventricular volume, as described in detail in *section 2.2.3.4.*

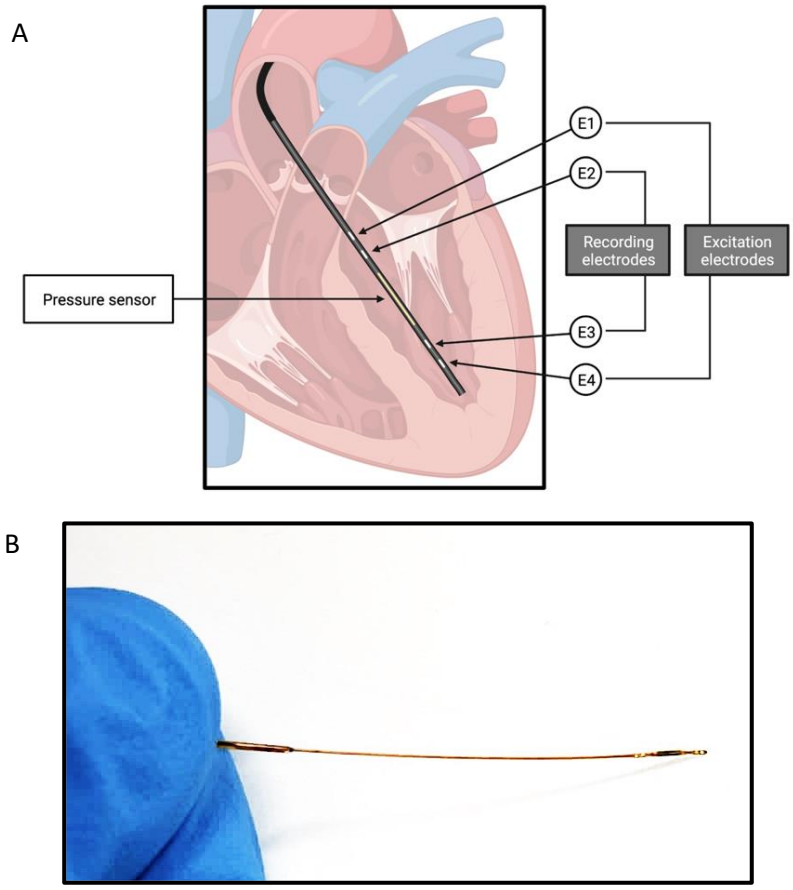

Figure 21. *Illustration (A) and photograph (B) of the Millar SPR-839 mouse pressure-volume catheter's tip, combining four electrodes (E1-4) for conductance (volume) recordings with a central sensor for pressure measurements. Top figure (A) created with BioRender.com*

The pressure-volume (PV) loops method was used in this project to assess the functional impact of lenvatinib on ventricular performance independently from loading conditions. Such methodology allows to derive a loop, representative of one cardiac cycle, defined by LV pressure on the y axis and LV volume on the x axis, providing a powerful approach to characterise the effect of RTKIs on cardiac mechanics, contractility and haemodynamics.

Each PV loop is defined by four segments, corresponding to the four phases of the cardiac cycle: passive ventricular filling during diastole (Phase I), isovolumetric contraction (Phase II), ventricular ejection (Phase III) and isovolumetric relaxation (Phase IV) (Figure 22) (King et al., 2019). Phase I is characterised by mitral valve opening and consequent large increase in ventricular volume due to passive ventricular filling with only a small increase in pressure. The closure of mitral valve defines the Phase II, where systole begins and a rapid increase in pressure is observed. No changes in ventricular volume occur at this stage since both mitral

and aortic valve are closed. When the aortic valve opens (Phase III), ejection causes a rapid drop in ventricular volume, while ventricular pressure continues to increase. The closure of the aortic valve determines the Phase IV of the cardiac cycle, represented by rapid fall in ventricular pressure with no changes in volume (isovolumetric relaxation).

A unique advantage of pressure-volume loop technique is the possibility to measure load-independent parameters of ventricular contractility, derived by end-systolic pressure-volume relationship (ESPVR) and end-diastolic pressure-volume relationship (EDPVR). Preload, also known as LVEDP, is a measure of the degree of ventricular stretch at the end of diastole, just prior to the systolic contraction (King & Lowery, 2023). Representing the end-diastolic length of sarcomeres, preload determines the force of contraction and is usually derived by measuring ventricular pressure and volume just before isovolumetric contraction. By varying loading conditions via obstruction of venous return (as detailed in *2.2.3.5*) and the consequent derivation of ESPVR and EDPVR, PV loop approach allows to quantify haemodynamic changes in response to different loading conditions.

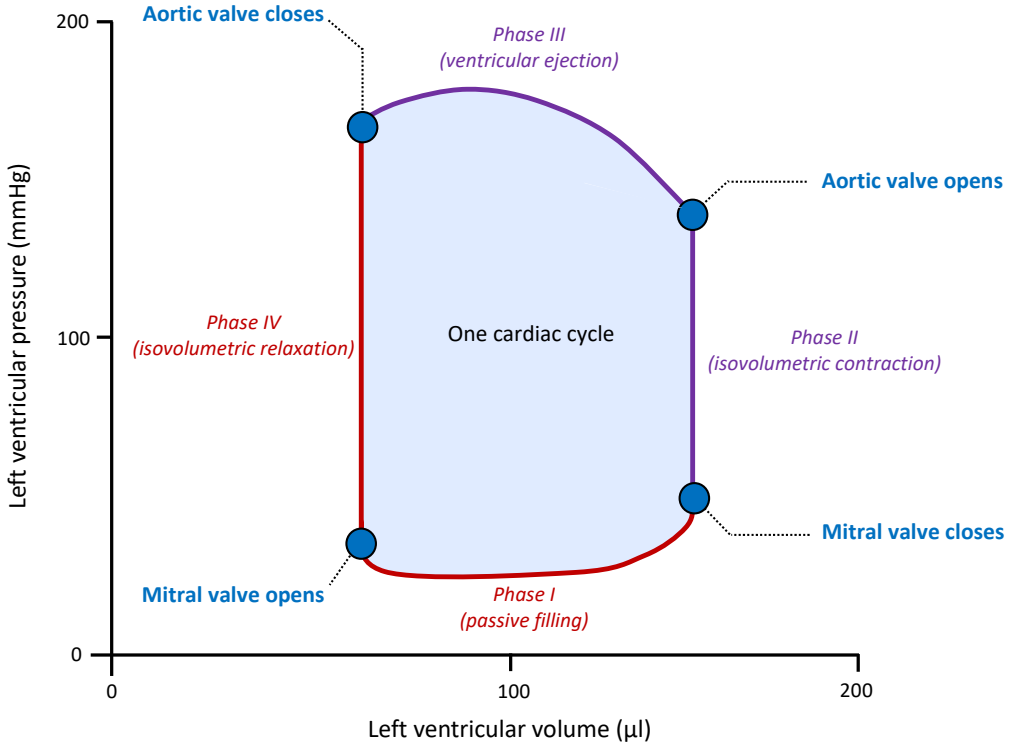

Figure 22. *Representation of pressure-volume loop for one cardiac cycle and description of its phases. The red line describes the diastole, while the purple line represents the systolic component. Adapted from (Bastos et al., 2020). Figure created with BioRender.com*

2.2.3.1 MATERIALS

Left ventricular PV loops were recorded using Millar 1.4 F SPR-839 miniaturised mouse pressure-volume catheter (Millar, Huston, USA). The tip of the catheter consists of two proximal and two distal conductance electrodes and a central pressure sensor to record real-time measurement of volume and pressure, respectively. The catheter was connected to a PV extension cable (Ventri-Cath to MPVS Ultra) (ADInstruments, Oxford, UK), which was associated with a PowerLab 4/35 analog-to-digital converter (sampling data 2 kHz) (ADInstruments, Oxford, UK), suitable for the downstream software (LabChart 8, ADInstruments, Oxford, UK). The anaesthetic agent sevoflurane was purchased from (Abbive, Belgium).

2.2.3.2 ANIMALS

All the details about animals used for assessing cardiac performance via PV loop were described in *section 2.2.2.2.*

2.2.3.3 SURGICAL PROCEDURES

2.2.3.3.1 INDUCTION AND SURGICAL PREPARATION

Mice were placed in an induction chamber and anesthetised by inhalation of sevoflurane at a concentration of 8% v/v combined with O_2 generated by Everflow Oxygen generator (Phillips, Belgium). To confirm the appropriate level of anaesthetic induction, loss of the righting reflex was assessed by gently rolling the induction chamber until the mouse was placed in a dorsal position. Once the righting reflex was lost, the animal was positioned in a supine position on a heating platform (Kent Scientific, CT, USA) to maintain the appropriate body temperature (37°C) and its paws were fixed to the heating table with surgical tape. The head of the mouse was positioned inside a cylindric mask, suppling sevoflurane (4-5 % v/v for maintenance). A piece of yarn was positioned around the upper incisors and its extremities taped down to the operating table to pull the head back slightly in order to allow maximal extension of the neck and facilitate the surgical procedures. A stereoscopic microscope was used for the whole surgical procedure. Following a suprasternal notch incision, skin was pulled away from surrounding tissues and underlying muscular structures. To expose the trachea, parotid, sublingual and submandibular salivary glands were gently pulled apart with forceps. The carotid artery was identified to the right of the trachea, while the external jugular vein was identified further lateral to the right, below the right salivary

gland (Figure 23). Oral intubation was performed by inserting an endotracheal tube (20-gauge catheter) into the trachea. Upon insertion, ventilatory excursions were evident, confirming the correct positioning of the tube and appropriate ventilation settings (Penlon Sigma Delta, Massachusetts, USA). Specifically, tidal volume (VT, ml) and RR (min^{-1}) were calculated from the weight of the mice (M, kg) according to the following formulae:

$$\text{Tidal volume (ml)} = 6.2 \times \text{M}^{1.01}$$
$$\text{Respiratory rate } (\text{min}^{-1}) = 53.5 \times \text{M}^{-0.26}$$

The adequate VT and RR for a 30-g mouse were 179.6 µl and 122 min^{-1}, respectively.
Once oral intubation was completed and the depth of anaesthesia checked, the venous catheter and the pressure-volume catheter were surgically placed in the jugular vein and in the LV, respectively, as described in sections below (*2.2.3.3.2* and *2.2.3.3.3*).

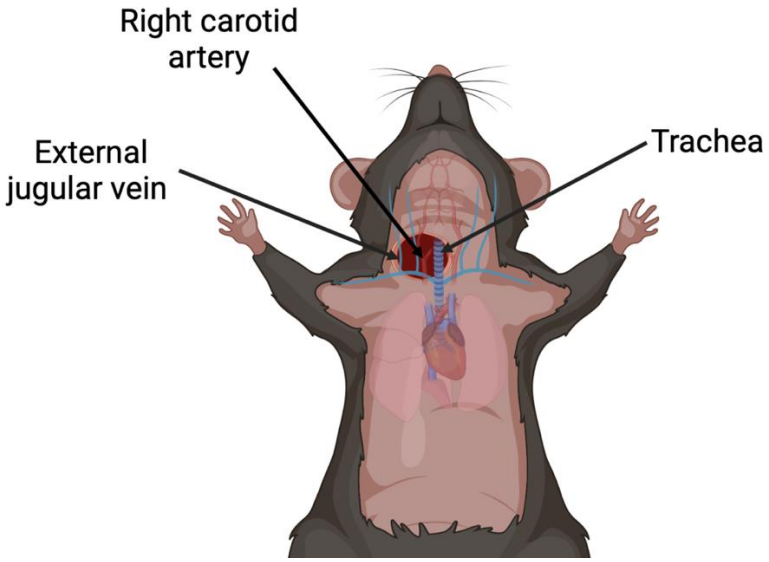

Figure 23. *Illustration of the surgical incision to expose the trachea, the right carotid artery (for PV catheter insertion) and the external jugular vein (for venous catheter insertion). Figure created with BioRender.com*

2.2.3.3.2 PLACEMENT OF THE CATHETER IN THE JUGULAR VEIN

A venous catheter (2FR, 0.69 mm outer diameter) connected to a microliter syringe (C20PU-MJV1301, INSTECH, Leipzig, Germany) was inserted into the jugular vein to allow the administration of hypertonic saline (15% NaCl). Hypertonic saline bolus injections were performed during the experimental procedure for calculation of parallel conductance (or

parallel volume, V_p) and consequent estimation of the absolute ventricular volume (detailed in *2.2.3.4*).

The external jugular vein was separated by the surrounding sternomastoid muscle with blunt dissection, before the cranial end of the vessel was ligated with a 6/0 silk suture to occlude blow flow. An additional 6/0 silk loose suture was placed around the caudal section of the external jugular vein and a small incision was made to introduce the venous catheter by using a bent hypodermic needle to facilitate the insertion. Once properly positioned, the catheter was secured by tightening the loose knot at the caudal site of the vein.

During the whole procedure, warm saline (37°C) was regularly applied to the wound to prevent fluid loss.

2.2.3.3.3 PLACEMENT OF PRESSURE-VOLUME CATHETER IN THE LEFT VENTRICLE

The pressure-volume catheter was inserted into the LV via the right carotid artery, using a closed-chest approach. Once identified, the carotid artery was separated from the parallel vagus nerve via blunt dissection and the cranial end of the artery was ligated to occlude blood flow. Another loose piece of yarn was placed around the caudal area of the vessel. A clamp was used to occlude the carotid artery caudally to ensure that this section of the vessel is not perfused. An incision was made, and the pressure-volume catheter (pre-soaked into warm physiological saline solution) was introduced into the artery by lifting the incision with a bent hypodermic needle. After securing the catheter into the carotid with the caudal yarn, the clamp was then removed, and the catheter was advanced into the aorta and subsequently into the left ventricle. The optimal placement of the PV catheter was monitored via the recorded pressure signal. Figure 24 shows typical aortic and left ventricular pressure recordings during the placement of the pressure-volume catheter. Once the catheter was placed and its position secured, cardiac pressure and volume were electronically calibrated by recording pre-set pressure and volume tracings. Tracings of 0 mmHg and 100 mmHg were recorded, and voltages were assigned to all the pressure tracings. Similarly for the volume, to convert conductance to relative value units (RVUs), volume tracings of 5 RVU and 50 RVU were recorded and voltages were assigned.

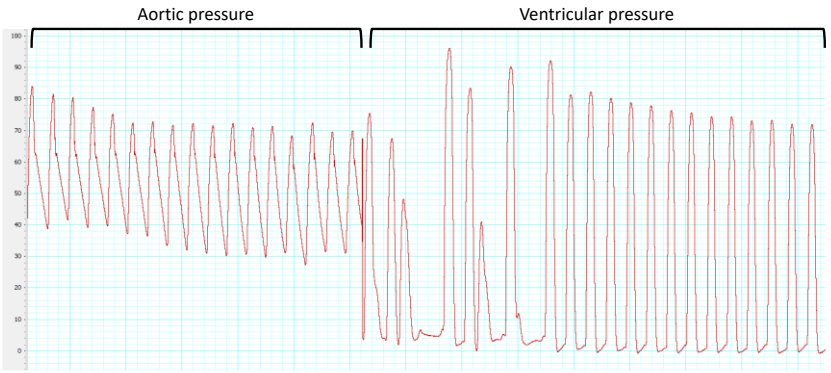

Figure 24. *Transition from aortic to ventricular pressure recordings, confirming the proper placement of the PV catheter in the ventricle during the surgical insertion.*

During the whole procedure, warm saline (37°C) was regularly applied to the wound to prevent fluid loss.

After stabilisation of pressure and volume signals, baseline measurements of cardiac function were performed both at a steady state and at varying preload conditions.

2.2.3.4 SALINE CALIBRATION

LV pressure-volume recordings are derived from a pressure transducer and the use of blood conductance to measure LV volume (Pacher et al., 2008). To obtain LV volume, blood conductance is converted to volume using Baan's equation:

$$Vol = \frac{1}{\alpha} \rho L^2 (G_x - G_p)$$

Where α (alpha factor) represents Baan's stroke volume (SV) correction factor (SV conductance/SV reference) and is assumed to be 1 in mice (Porterfield et al., 2009), ρ is the specific resistance of blood, L is the distance between the recording electrodes, G_x represents measured total conductance value and G_p is the Baan's parallel conductance (also known as V_p). G_x results from two components: blood conductance (G_b) and parallel conductance (G_p) (Figure 25).

As is evident from this formula, the measured total conductance derives from blood conductance and parallel conductance.

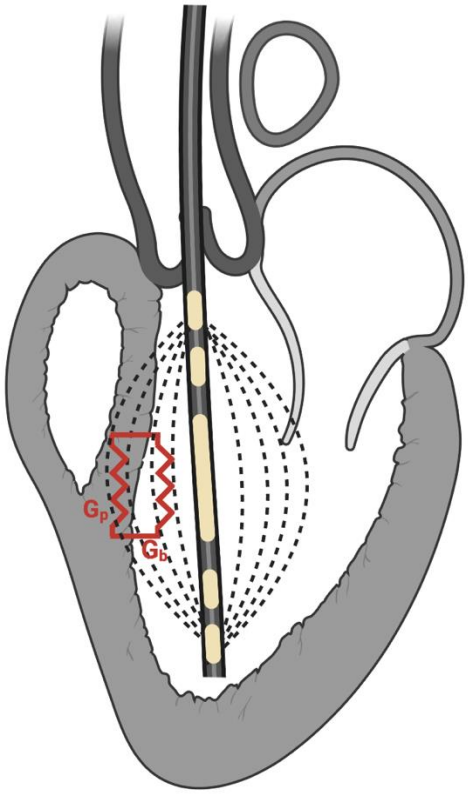

Figure 25. *Representation of the blood conductance (G_b) and parallel conductance (G_p) as the two components describing the total conductance measured via PV catheter. Figure created with BioRender.com*

Conductance is inversely related to voltage, which is measured by four electrodes placed at the tip of the catheter. The LV volume is derived by changes in the electric field generated and detected by these electrodes. In particular, the two excitation electrodes of the PV catheter create an electric field inside the LV, specifically from the aortic valve to the LV apex, whose voltage or conductance changes (proportional to change in resistance) are then measured by the two recording electrodes (Pacher et al., 2008).

Although the conduction though blood constitutes the primary contributor to the conductance signal measured by the catheter, this signal derives also from a second component, represented by the conduction through and along the ventricular wall. This second component, also called parallel conductance (G_p) or parallel volume (V_p), may result in an overestimation of the LV volume, and therefore must be removed in order to obtain the absolute ventricular volume (Pacher et al., 2008; Abraham & Mao, 2015). Given that parallel conductance remains essentially constant (Georgakopoulos & Kass, 2000), changes in conductance signal are associated with time-varying changes in ventricular volume (Pacher et al., 2008; Bastos et al., 2020).

To measure the parallel conductance and subsequently correct the absolute ventricular volume, the injection of hypertonic saline (15% NaCl), also known as saline calibration, was performed. Indeed, this bolus injection transiently changes blood conductance, while the conductivity of the ventricular wall remains unchanged, allowing for the measurement of the conductance signal effectively deriving from the blood (G_b) or from the ventricular wall (G_p) (Abraham & Mao, 2015). In particular, 10 µl of hypertonic saline solution were administered through bolus injection using the venous catheter placed in the jugular vein and a visible rightward shift of the PV loops (representative of change in blood conductance) was observed, with no significant alterations of the pressure signal. During this procedure, ventilation was paused. Due to possible variability, saline calibration was performed three times, allowing the stabilisation of the volume signal after each injection before repeating the next one (Abraham & Mao, 2015; Townsend, 2016).
The value at the intersection of the saline calibration line and the $V_{ed} = V_{es}$ line, derived by solving a system of linear equations (Pacher et al., 2008), represented the parallel volume and was calculated by the PV analysis program in PowerLab.

2.2.3.5 VARYING PRELOAD USING TRANSIENT INFERIOR VENA CAVA OCCLUSION (IVCO)

To determine load-independent parameters of cardiac contractility, transient alterations in the cardiac loading conditions (i.e., reduction in preload) were performed by obstructing the venous return to the heart via inferior vena cava occlusions (IVCOs). In particular, a midline incision was made below the xiphoid process to access inferior vena cava. The occlusion was performed by compressing the vessel with a forceps (no more than 2-3 sec), resulting in a leftward shift of the PV loops (Pacher et al., 2008). During these measurements, ventilation was paused to reduce haemodynamic artefacts due to respiratory dependent alterations of LV preload (i.e., reduced preload due to positive pressure ventilation). This procedure was repeated until three optimal recordings (at least six PV loops and a steady decrease in LVEDP) were obtained.

The ESPVR, characterised by its slope (E_{es}) and volume axis intercept (V_0), was derived by performing a linear regression from the end systolic PV points that were modulated by reduced preload from IVCOs (detailed description of the ESPVR is reported in *2.2.3.8.1*).

2.2.3.6 CUVETTE CALIBRATION

To convert volume signal from RVUs to units of true volume (µl), volume signal was calibrated at the end of the experimental procedure by using an insulator-type calibration cuvette (P/N 910-1049, Millar, Huston, USA) of known diameters filled with blood. Specifically, after removing the PV catheter, blood was aspirated with a syringe containing EDTA and placed into cuvette wells of known volumes. PV catheter was then dipped into each cuvette well with all the four electrodes submerged into the blood and hold in that position for 10-20 sec. Cuvette conductance outputs were recorded in RVUs. Each cuvette well conductance and its respective known volume were then entered into the PV analysis program in PowerLab, which generated a calibration equation to convert RVUs into µl.

Upon completion of the experimental protocol, the animal was euthanised by exsanguination following transection of the vena cava.

2.2.3.7 LOAD-DEPENDENT MEASURES OF CARDIAC FUNCTION

Arterial elastance (E_a), an index of LV afterload (Kelly et al., 1992), was derived as the ratio between left ventricular end-systolic pressure (P_{es}) and SV, where SV is defined as the difference between end-diastolic volume (EDV or V_{ed}) and end-systolic volume (ESV or V_{es}) (Figure 26):

$$SV = EDV - ESV$$

$$E_a = \frac{P_{es}}{SV}$$

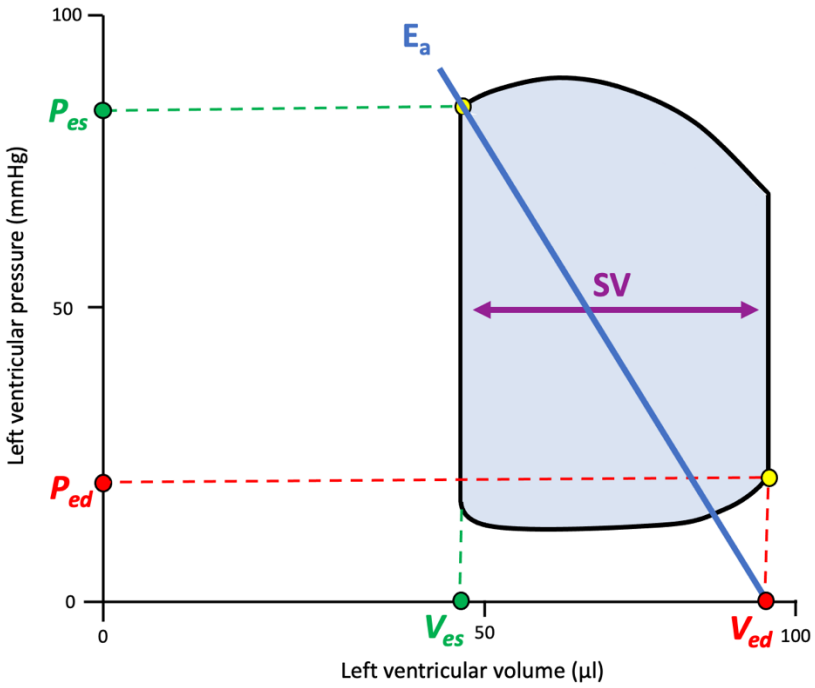

Figure 26. *Arterial elastance (E_a) and stroke volume (SV) derived from pressure-volume loops analysis. E_a is represented by the slope of the line that intercepts the volume axis at the end-diastolic volume and goes through the end-systolic pressure-volume point on the loop. Stroke volume, as the difference between end-diastolic volume and end-systolic volume is the width of the pressure-volume loop. P_{ed} = end-diastolic pressure; P_{es} = end-systolic pressure; V_{ed} = end-diastolic volume; V_{es} = end-systolic volume. Figure created with BioRender.com*

Another load-dependent measure of cardiac function derived from pressure-volume loops analysis is the isovolumic relaxation constant (Tau) (Pacher et al., 2008). This parameter represents the decay of LV pressure between the closure of the aortic valve and the opening of the mitral valve, providing information about active relaxation of the ventricle and, therefore, diastolic function (Pacher et al., 2008). The minimum derivative of change in diastolic pressure during isovolumic relaxation (dP/dt_{min}) was also derived to evaluate diastolic function (Pacher et al., 2008). In terms of systolic function, the maximum derivative of change in systolic pressure during isovolumic contraction (dP/dt_{max}) was used as index of ventricular contractility.

2.2.3.8 LOAD-INDEPENDENT MEASURES OF CARDIAC FUNCTION

2.2.3.8.1 END-SYSTOLIC PRESSURE-VOLUME RELATIONSHIP

End-systolic pressure volume relationship, a reliable index of LV contractility, is defined as the maximal pressure that LV can develop at any ventricular volume. This linear relationship (Figure 27) is described by a slope, also known as end-systolic ventricular elastance (E_{es}), and a volume axis intercept (V_0), which are derived experimentally by performing IVCOs, so that:

$$P_{es} = E_{es} \times (V_{es} - V_0)$$

Where P_{es} and V_{es} represent end-systolic pressures and volumes, respectively.

An increased E_{es} slope, resulting in an upward shift of the ESPVR, is representative of increased contractility of the left ventricle, whereas a decreased E_{es} slope reflects a reduced ventricular inotropic response.

2.2.3.8.2 END-DIASTOLIC PRESSURE-VOLUME RELATIONSHIP

Contrary to the ESPVR, the EDPVR is a curvilinear relationship derived from downward shift of PV loops during preload reduction via IVCOs (Figure 27). The EDPVR describes the compliance of the ventricle. As a result, a rightward shift of EDPVR is representative of ventricular remodelling, while a leftward shift of EDPVR, describing a decreased compliance, reflects ventricular stiffness and diastolic dysfunction.

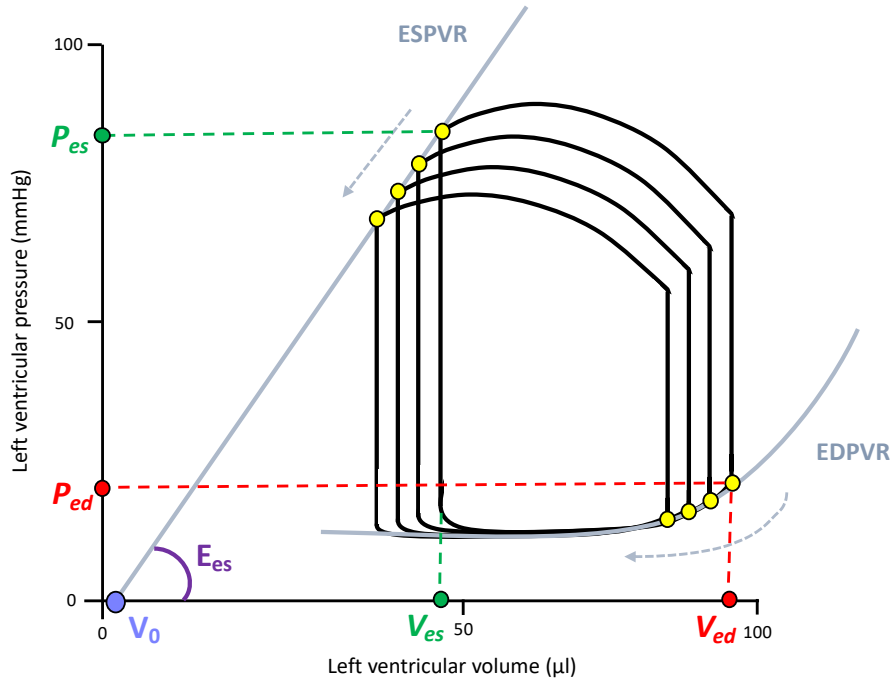

Figure 27. *Left ventricular pressure-volume relationships and rightward shift of pressure-volume loop during inferior vena cava occlusions. EDPVR = end-diastolic pressure-volume relationship; E_{es} = end-systolic elastance; ESPVR = end-systolic pressure-volume relationship; P_{ed} = end-diastolic pressure; P_{es} = end-systolic pressure; V_0 = volume at P_{es} of 0 mmHg; V_{ed} = end-diastolic volume; V_{es} = end-systolic volume. Figure created with BioRender.com*

2.2.3.9 STATISTICAL ANALYSIS

All data were analysed using Prism 10 (GraphPad Software, La Jolla, CA, USA) and expressed as mean ± SEM, with *n* representing the number of mice. Statistical comparisons of cardiac functional parameters between groups were made using unpaired *t*-test with Welch's correction. Statistical significance was defined as *p<0.05, **p<0.01, ***p<0.001 and ****p<0.0001.

2.3 MATERIALS & METHODS: *EX VIVO*

Isolated tissue bath systems have been extensively used as a valuable approach in pharmacology research to investigate contractile and relaxation processes in a variety of contractile tissues in response to physiological and pharmacological stimuli (Jespersen et al., 2015). The main advantage of isolated tissue baths is to quantify concentration-dependent changes during isometric contraction. Evaluating tissue behaviour in a controlled environment, without the systemic influences of the intact animal, allows for a better

comprehension of the effect of a therapeutic specifically on tissue function; at the same time, maintaining the integrity of the tissue, it allows for a more complete understanding of the physiological outcome (contraction or relaxation) than a cellular setting (Jespersen et al., 2015). This project, combining the use of isometric tissue bath and the ROTSAC, aimed to define the effect of selected RTKIs on vascular reactivity, as well as investigating the role of arterial stiffness in the haemodynamic responses associated with these therapeutics.

2.3.1 Animals

All the details about animals used for isolated tissue bath experiments were described in *section 2.2.2.2.*

At the end of day 4, animals used for isolated tissue bath assays were euthanised with overdose of anaesthesia via intraperitoneal injection of 200 $mg.kg^{-1}$ Dolethal (sodium pentobarbital, VetCompendium, Brussels, Belgium).

2.3.2 System preparation and set-up

Water-jacketed reservoirs (250 ml capacity) and 10-ml bath chambers of both isometric and ROTSAC set-up were preheated at 37°C with recirculating heating water (Pura Water Baths, Julabo, Germany).

Both systems were connected to a 95% O_2 / 5% CO_2 medical grade gas cylinder (Air Liquide Belbe NV, Belgium) to ensure constant solution aeration and the motion of the compounds that were added in the tissue bath.

Krebs-Ringer solution, a physiological salt solution containing (in mM): NaCl 118, KCl 4.7, $CaCl_2$ 2.5, KH_2PO_4 1.2, $MgSO_4$ 1.2, $NaHCO_3$ 25, CaEDTA 0.025, and glucose 11.1 (Sigma-Aldrich, Belgium), was prepared and used to fill reservoirs and bath chambers, where it was continuously aerated with a 95% O_2/5% CO_2 gas mixture and maintained at a temperature of 37°C, resulting in the optimal physiological pH value of 7.4.

After launching data acquisition software (PowerLab 8/30 and LabChart 8, ADInstruments, Oxford, UK), force transducers were calibrated prior to tissue placement.

To establish cumulative concentration-response curves for the isometric tissue bath experiments, increasing concentrations of each agonist (20 µl) were added into the bath (10 ml) (1:500 dilution factor) taking into account the concentration of agonist already present in the bath. Distilled water was the solvent used to prepare dilutions of ACh, phenylephrine (PE) and ATP; NaOH was the solvent used to prepare dilutions of diethylamine NONOate (DEANO).

2.3.3 Tissue preparation and mounting

After euthanising the mice, an incision was made along the diaphragm at the bottom of the rib cage, then proceeding to the sternum to bisect the animal. After placing aside the abdominal and thoracic organs situated above the spinal cord, the aorta was exposed. The thoracic and infrarenal aorta was excised and placed in a dissection dish containing Krebs-Ringer solution, where it was cleaned of perivascular fat and tissue before being cut into segments of 2 mm length. The resulting segments were placed in a dish containing Krebs-Ringer solution to maintain their function in between their preparation and their mounting on the system.

The aortic rings were mounted on the upper hook by using forceps to gently slide the segment onto the hook. Once the upper part of the segment was in place, the second hook was also inserted into the ring. After completing the mounting, the rod and the mounted aortic segments were placed into the tissue bath chamber filled with Krebs-Ringer solution (Figure 28).

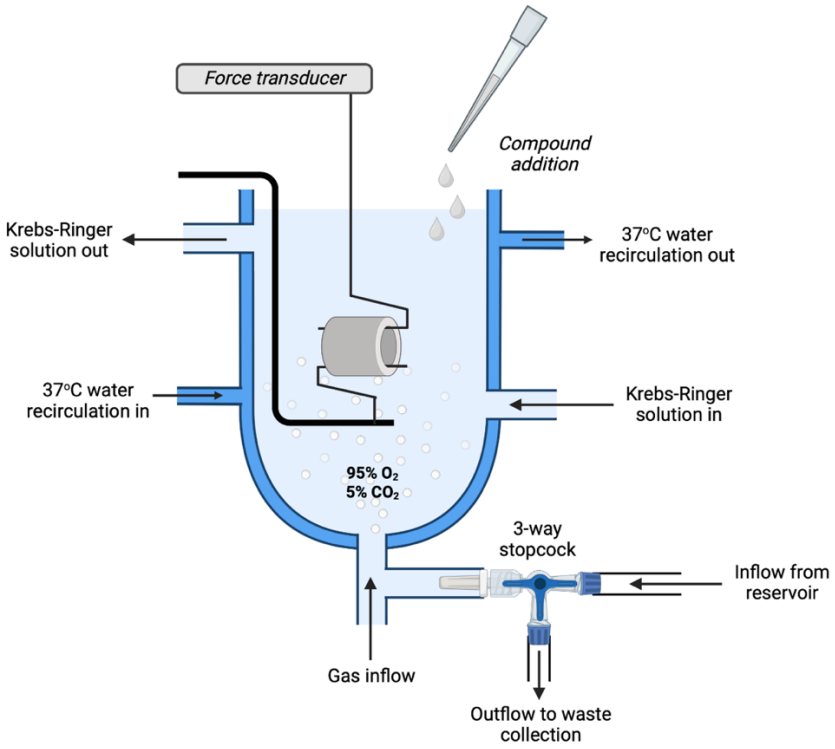

Figure 28. *Schematic representation of tissue bath. The tissue segment was placed between two hooks and submerged with physiological solution in a double-wall water-jacketed bath. Inflow from reservoir and outflow to waste collection were regulated by a 3-way stopcock on the base of the chamber. Figure created with BioRender.com*

2.3.4 Rodent Oscillatory Set-up to Study Arterial Compliance (ROTSAC)

The Rodent Oscillatory Set-up to Study Arterial Compliance (ROTSAC) tissue bath developed by Leloup *et al.* (Leloup et al., 2016) was used to evaluate the effect of axitinib and lenvatinib on aortic stiffness.

Stiffening of aorta is the leading cause of increased PP, which, in turn, has been associated with an increased risk for cardiovascular events (Benetos et al., 1998; Homan et al., 2022). A compliant aorta, buffering arterial pulsatility due to intermittent LV ejection, exerts a crucial cushioning function, therefore limiting detrimental fluctuations in BP and flow and preventing microvascular complications (Chirinos et al., 2019). Arterial compliance (C_A), derived as the ratio of SV to PP (Homan et al., 2022), can be quantified from the relationship between lumen area (A) and arterial pressure (P) and defined as the slope to the pressure-lumen area curve (Figure 29):

$$C_A = \frac{\Delta_A}{\Delta_P}$$

Where Δ_A defines the lumen area change, while Δ_P represents change in arterial pressure. Arterial compliance can be calculated at any pressure levels, with the derived pressure-lumen area curve showing a nonlinear pressure-dependent behaviour, where maximal arterial compliance is observed in the low-pressure range to then rapidly decrease at high-pressure range (Chirinos et al., 2019). This nonlinear relationship is due to the composition of arterial wall, with elastin accommodating the load changes at low pressures and collagen fibres being recruited at high pressures, therefore resulting in a stiffer aorta and reduced arterial compliance (Chirinos et al., 2019). Although structural components, such as elastin and collagen, have a crucial role in defining arterial compliance, dynamic elements (i.e., VSMCs and endothelium-released factors) are also important contributors to arterial stiffness (Wilkinson & McEniery, 2004).

Despite isolated tissue bath approaches allow for the evaluation of vascular reactivity, the lack of cyclic stretch does not reflect the *in vivo* situation and may interfere with eNOS activity and the release of endothelium-derived factors (Peng et al., 2003; Leloup et al., 2016). In addition, HR being an important determinant of arterial stiffness (Tan et al., 2018), it should be taken into account in the evaluation of vascular behaviour. Stretching aortic segments at physiological frequencies and amplitudes (Leloup et al., 2016), the ROTSAC set-up represents a powerful tool to study arterial stiffness. In this study, this set-up was used to assess arterial stiffness at the same pressure levels and to evaluate the pressure sensitivity of arterial stiffness in response to axitinib and lenvatinib.

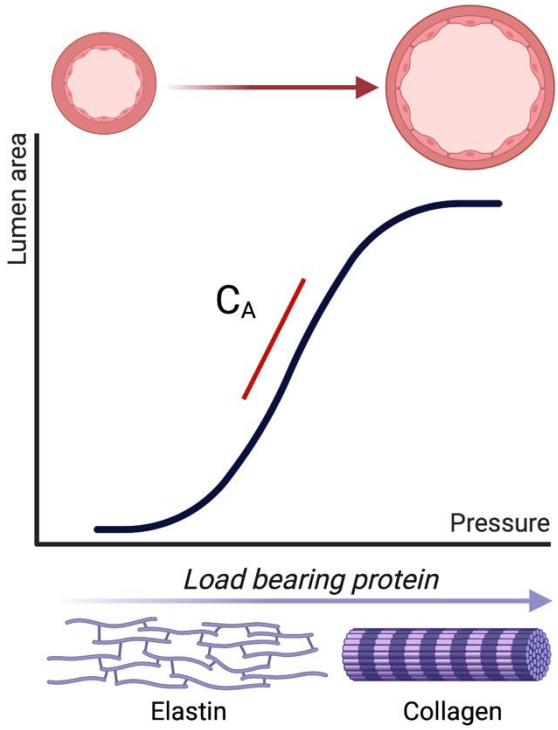

Figure 29. *Arterial compliance described by the relationship between arterial pressure and lumen area. Arterial compliance (C_A) (red line) is tangent to the pressure-area relationship and can be calculated at any pressure level. Figure created with BioRender.com*

2.3.4.1 AORTIC SEGMENTS SET-UP AND CALIBRATION

Thoracic and infrarenal aortic segments were mounted between two parallel wire hooks in 10-ml tissue baths. Force and displacement of the upper hooks were acquired at 1 kHz by a force length transduced connected to a PowerLab 8/30 analog-to-digital converter (ADInstruments, Oxford, UK), suitable for the downstream software (LabChart 8, ADInstruments, Oxford, UK) (Figure 30).

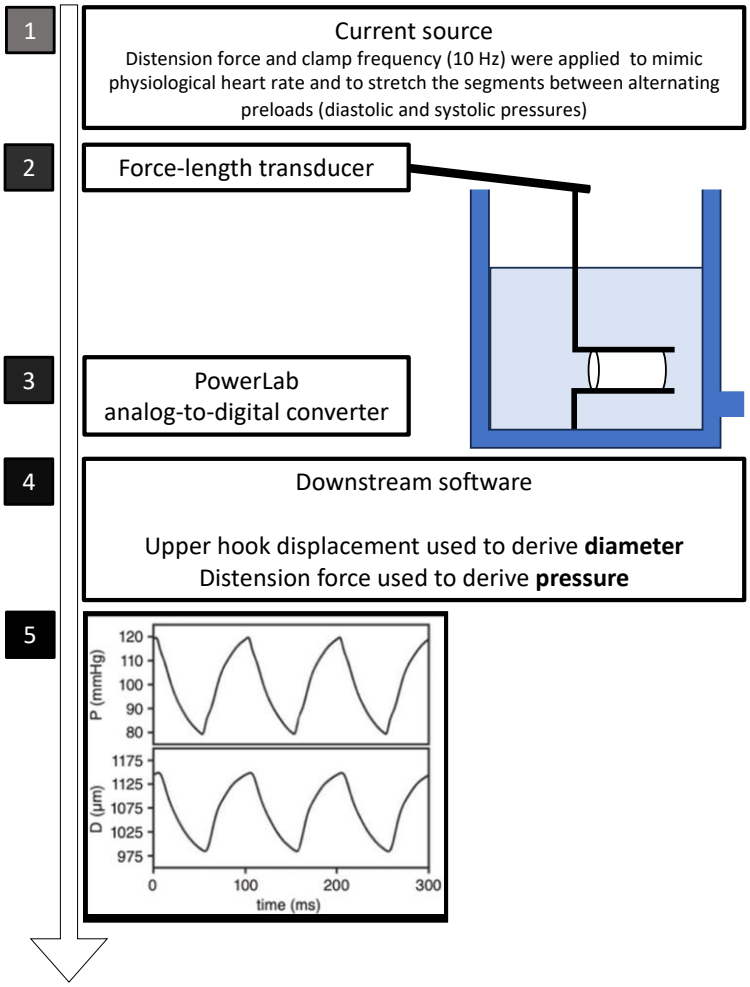

Figure 30. *Schematic representation of ROTSAC set-up. To mimic HR of mice (600 bpm), aortic segments were mounted between two parallel hooks. The upper hook was connected to the aluminium lever, whose displacement was measured by a photo-electric system (Brutsaert et al., 1971), associated to a force-length transducer (Brutsaert et al., 1971), whose distension force and clamp frequency (10 Hz) were controlled by a current source. The transducer was connected to PowerLab 8/30 analog-to-digital converter, suitable for the downstream software. Figure created with BioRender.com*

Using a 10 Hz frequency to mimic the physiological HR of mice (600 bpm), segments were continuously stretched between alternating preloads, representing diastolic and systolic pressures. To estimate the transmural pressure at a given distension force and dimensions, the following formula was used:

$$P = \frac{F}{l \times D}$$

Where F is the distension force (preload), l the length and D the diameter of the segment derived from the displacement of the upper hook.

Prior to starting the experimental procedure, width (w) and length (l) of the segments were measured at six different preloads (10, 20, 30, 40, 50, and 60 millinewton (mN)) (Figure 31), using a stereomicroscope and calibrated image software. Being w the outer distance between the two hooks, it was used to approximate the inner circumference of the vessel. Indeed, since the aortic segments were stretched between the two hooks, the diameter of the segment (D) at a given preload was derived from the displacement of the upper hook, which is directly proportional to the inner circumference:

$$D = 2 \times \frac{w}{\pi}$$

At any given pressure, a stretch amplitude of 40 mmHg was chosen to derive the Peterson's elastic modulus (Ep), with D_0 being the minimal ("diastolic") diameter, ΔP being the pressure difference (kept constant at 40 mmHg) and ΔD being the difference between systolic and diastolic diameter:

$$Peterson's\ elastic\ modulus\ (Ep) = D_0 \times \frac{\Delta P}{\Delta D}$$

2.3.4.2 EXPERIMENTAL PROTOCOL

Arterial stiffness was evaluated in isobaric conditions, both under increasing and decreasing pressures, also defined as "loading" and "unloading" conditions, respectively. In particular, the Peterson's elastic modulus, as a measure of arterial stiffness, was evaluated at different pressures (i.e., 60–100 mmHg until 180–220 mmHg with 20 mmHg incremental intervals) and performed under physiological conditions (Krebs-Ringer solution), as well as following contraction with α_1-adrenergic receptor agonist PE (Sigma-Aldrich, Belgium) and relaxation with DEANO (Sigma-Aldrich, Belgium) (Figure 31). The α_1-adrenergic receptor agonist PE was used to maximally stimulate VSMCs in order to evaluate their contribution (and the contribution of the active components that modulate VSMCs) to the mechanical response of aorta (Leloup et al., 2016; Mozafari et al., 2019). Using DEANO as exogenous donor of NO, the purpose was to maximally relax VSMCs in order to assess the role of passive components (collagen and elastin) in the mechanical response of aorta (De Munck et al., 2020).

Aortic segments were subjected to increasing and decreasing pressures under physiological conditions (Krebs-Ringer solution). After loading/unloading pressure steps under physiological condition, aortic segments were then treated with L$^{\omega}$-Nitro-L-arginine methyl ester hydrochloride (L-NAME) (300 µM) to inhibit eNOS and remove the influence of NO. Thereafter, 2 µM PE was added to the tissue bath and the loading/unloading pressure steps where repeated. 3 washes were then performed before treatment with DEANO (2 µM) and subsequent increase and decrease of pressure conditions.

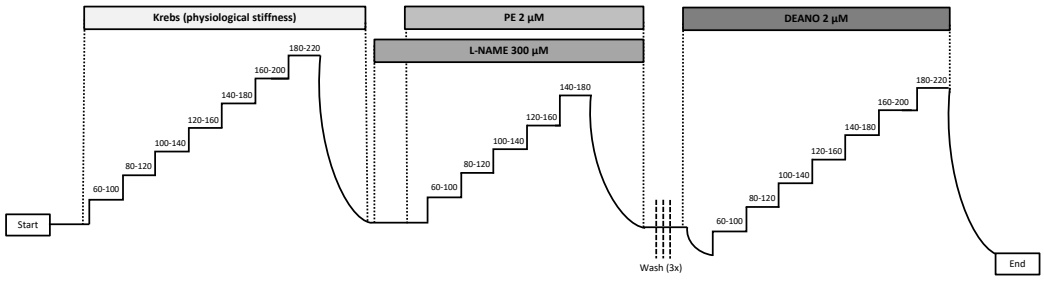

Figure 31. *Schematic representation of the experimental protocol used for the role of axitinib and lenvatinib on arterial stiffness. Different pressure steps per each condition were shown. DEANO = diethylamine NONOate; L-NAME = L$^{\omega}$-Nitro-L-arginine methyl ester hydrochloride; PE = phenylephrine. Figure created with BioRender.com*

2.3.4.3 STATISTICAL ANALYSIS

All data were analysed using Prism 10 (GraphPad Software, La Jolla, CA, USA) and expressed as mean ± SEM, with *n* representing the number of mice. Two-way ANOVA with Dunnett's *post-hoc* test was used for comparison of arterial stiffness between control and treated groups. Statistical significance was defined as $p<0.05$.

2.3.5 Isometric organ bath

At the end of the 4-day treatment period, vascular function was assessed under isometric conditions in response to the vasodilators ACh (Sigma-Aldrich, Belgium), DEANO and ATP (Sigma-Aldrich, Belgium) or to the vasoconstrictor PE in isolated thoracic artery segments as described in more details in *2.3.5.2*.

Passive tension was measured isometrically with a Statham UC2 force transducer (Gould, Cleveland, OH), and the data were captured by an analog-to-digital converter (Powerlab 8/30, ADInstruments, Oxford, UK). A suitable software (LabChart 8, ADInstruments, Oxford, UK) was then used to visualise and analyse the recordings. Isometric force was expressed in mN.

2.3.5.1 SETTING PASSIVE TENSION AND EQUILIBRATION

Vascular smooth muscle cells (VSMCs) function at their best when at their optimal length for tension development (L_0), also known as resting length, where actin-myosin interactions are maximal, resulting in maximum force development (Wilson, 2011). If the resting length of sarcomere falls below L_0, filaments overlap with each other, reducing cross-bridge formation and leading to reduced tension. Conversely, when VSMCs are stretch beyond their optimal resting length, the excessive overlapping of actin-myosin filaments also results in their inability to maintain or generate maximum force (Wilson, 2011). Preliminary experiments determined the optimal preload for mice thoracic aortic segments, which provides the maximal contraction by both non-receptor and receptor-mediated stimulation (De Moudt et al., 2017). As a result, a constant preload of 20 mN was applied to all the aortic segments. This caused an initial plateau of the tension, followed by a drop in the passive tension as the segment relaxed due to stretch-induced hyperpolarization. Passive tension was then adjusted till all the aortic rings reached a stable plateau, corresponding to 20 mN. After applying passive tension, aortic segments were allowed to equilibrate for 60 min prior to starting the experimental protocol to minimize the effect of NO in a time-dependent manner and to ensure optimal stabilisation of the segments. During the equilibration phase, tissues were washed once with Krebs-Ringer solution flowing from temperature-controlled reservoirs to remove any residual debris from the dissection.

2.3.5.2 EXPERIMENTAL PROTOCOL

After 60-min equilibration period, segments were randomly assigned into two groups:

Protocol A

L-NAME was administered to abolish the influence of NO (Figure 32). Cumulative concentrations of PE ($3x10^{-9}$ M till $3x10^{-6}$ M) were added to assess vascular smooth muscle cells contraction in all the segments. Afterwards, endothelium-independent relaxation was

evaluated by adding cumulative concentrations of DEANO ($3x10^{-10}$ M till 10^{-5} M). At the end of the relaxation curve, all segments should have a passive tension of 20 mN. After washing 3 times with warm Krebs-Ringer solution, a Ca^{2+}-free environment ($0Ca^{2+}$) was prepared by using a Ca^{2+}-free Krebs-Ringer solution and adding ethylene glycol-O, O'-bis(2-aminoethyl)-N,N,N',N'-tetraacetic acid (EGTA) (Alfa Aesar) as a Ca^{2+}-chelating agent. Subsequently, phasic contraction was determined by α_1-adrenergic receptor stimulation with PE (2 µM), before restoring normal conditions by adding 1.75 nM $CaCl_2$ to induce tonic contraction in response to PE.

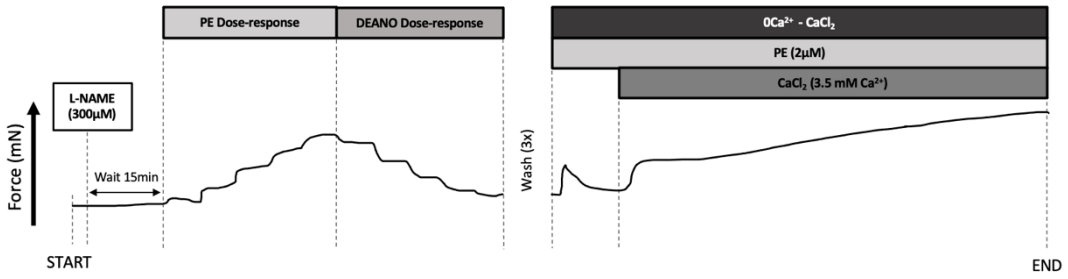

Figure 32. *Schematic representation of the experimental protocol used for group 1. Vascular reactivity was investigated in presence of eNOS inhibition by adding L-NAME at the beginning of the experimental protocol and endothelium-independent relaxation was assessed by adding cumulative concentrations of DEANO. DEANO = diethylamine NONOate; L-NAME = L$^{\omega}$-Nitro-L-arginine methyl ester hydrochloride; PE = phenylephrine. Figure created with BioRender.com*

Protocol B

In this group of segments, cumulative concentrations of PE ($3x10^{-9}$ M till $3x10^{-6}$ M; 20 µl added for each concentration) were added to assess VSMCs contraction (Figure 33). After that, endothelium-dependent relaxation responses were assessed by adding cumulative concentrations of the muscarinic receptor agonist ACh ($3x10^{-9}$ M till 10^{-5} M; 20 µl added for each concentration). Following 3 washes with warm Krebs-Ringer solution and maximum contraction due to addition of 20 µl PE (2 µM), endothelium-dependent relaxation responses were also assessed by adding cumulative concentrations of ATP (10^{-8} M till 10^{-4} M; 20 µl added for each concentration), a purinergic receptor agonist.

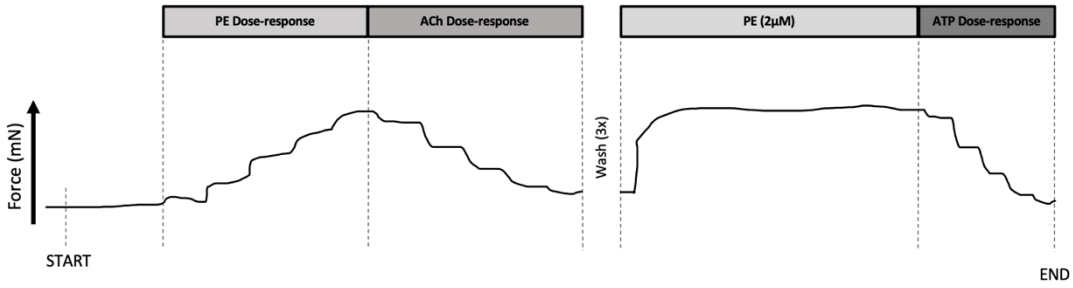

Figure 33. *Schematic representation of the experimental protocol used for group 2. Vascular reactivity was investigated in absence of eNOS inhibition and endothelium-dependent relaxation was investigated both in response to ACh and to ATP. ACh = acetylcholine; ATP = adenosine triphosphate; PE = phenylephrine. Figure created with BioRender.com*

2.3.5.3 STATISTICAL ANALYSIS

All data were analysed using Prism 10 (GraphPad Software, La Jolla, CA, USA) and expressed as mean ± SEM, with *n* representing the number of mice used. Two-way ANOVA with Dunnett's *post-hoc* test was used for comparison of vascular reactivity between control and treated groups. Statistical significance was defined as $p<0.05$.

2.3.6 Histology

After dissection, aortic and cardiac tissues were cleaned in Krebs-Ringer solution, immediately submerged in buffered 4% formaldehyde (Merck, Overijse, Belgium) and stored at room temperature for 24 h, after which both tissues were transferred in 60 % isopropanol and stored at 4°C for 24 h. Subsequently, the tissues were embedded in paraffin (Leica Biosystems, Diegem, Belgium) and transversely cut in 5 µm segments. Sirius red staining was used to determine total collagen content, while immunohistochemical staining using with primary antibody against laminin (1:1000; lmNB300-144 Novus Biologicals, Abingdon, UK) was used to quantify cardiomyocyte hypertrophy. In this case, following visualization using a goat anti-rabbit biotinylated secondary antibody (1:200; Vector Laboratories, Burlingame, USA), cardiac tissues were stained with 3,3'-diaminobenzidine tetrahydrochloride hydrate solution (Sigma-Aldrich, Overijse, Belgium).

The Olympus BX40 microscope and Universal Graph 6.1 software were used to acquire images, which were quantified using the ImageJ software.

2.3.7 Vascular mRNA expression (qRT-PCR)

Real-time quantitative polymerase chain reaction (qRT-PCR) was performed to determine vascular mRNA expression of thrombospondin-1 (TSP-1), $P2Y_2$ and $P2Y_6$ purinergic receptors using TaqMan™ probes (Thermo Fisher Scientific) and the TaqMan™ Fast Advanced Master Mix (Applied Biosystems™, Thermo Fisher Scientific). RNA was extracted from thoracic aortic segments by using the ISOLATE II RNA Micro Kit (Bioline) in accordance with the manufacturer's instructions and reverse transcribed into cDNA using an AMV cDNA synthesis kit (TaqMan™ Reverse Transcription Reagents, Invitrogen, Thermo Fisher Scientific). In particular, the reaction Master Mix was prepared first according to the manufacturer's manual for a total volume of 20 µl per reaction. The concentration for one reaction included: 10 µL TaqMan™ Fast Advance Master Mix (2x), 1 µL of the TaqMan™ assay (20x) and 7 µL nuclease free water (total volume 18 µL). This mixture was multiplied by the samples needed for the reaction. 18 µl of Master Mix was then added to each well of a 96 well plate, before adding 2 µL of cDNA per well. Afterwards, the reaction plate was sealed with an optical adhesive film and gently centrifuged for 5 sec. To start the reaction, the plate was placed in the real time PCR-system (QuantStudio™ 3, Applied Biosystems™) and the program was initiated. To activate the polymerase the plate was heated to 95°C for 20 sec. The PCR was performed for 40 cycles. One cycle consists of 1 sec denaturation (95°C), followed by 20 sec annealing (60°C). Each cDNA samples was run in duplicates and a no template control (NTC) consisting of nuclease free water was run for every assay. From the extracted data, the relative mRNA expression (target gene/β-actin reference gene) of thrombospondin, $P2Y_2$ and $P2Y_6$ was reported as fold-change calculated using the ΔΔCT method.

Thrombospondin-1 is a matricellular protein that inhibits NO-mediated activation of soluble guanylate cyclase (sGC), thereby limiting NO-mediated relaxation of VSMCs (Isenberg et al., 2009; N. M. Rogers et al., 2014). By altering the VSMCs responses to NO, increased vascular levels of TSP-1 may indicate an impaired NO signalling (Isenberg et al., 2009; Roberts et al., 2012). As a result, the assessment of aortic expression of this protein aimed to define if elevated vascular levels of TSP-1 were contributing to the haemodynamic responses observed with axitinib and lenvatinib.

$P2Y_2$ and $P2Y_6$ purinergic receptors have a crucial role in the control of VSMCs function and vascular reactivity (Martin-Aragon Baudel et al., 2020). Indeed, $P2Y_2R$ modulates vascular tone in response to shear stress, while both $P2Y_2R$ and $P2Y_6R$ promote the release of pro-

inflammatory cytokines (Wu et al., 2023). In this context, their overexpression has been associated with EC dysfunction (Wu et al., 2023). For this reason, the vascular expression of these purinergic receptors was also studied, in order to integrate the *ex vivo* investigation of the vascular responses observed after treatment with axitinib and lenvatinib.

3 Chapter 3. Characterisation of the haemodynamic profile of VEGFR-2 inhibitors axitinib and lenvatinib

3.1 INTRODUCTION

The development of a tumour vascular network (neoangiogenesis) is a fundamental event in the process of cancer progression and metastatic spread (*Introduction 1.3.2*) (Folkman, 1995, 2002; Ferrara, 2004a). VEGFR-2 has been shown to be the dominant mediator of VEGF-A-induced cellular responses involved in the complex formation of new vasculature to support cancer growth, therefore providing an important therapeutic target in oncology (*Introduction 1.3.2.1*) (Lee et al., 2018). Indeed, dysfunctional VEGF/VEGFR-2 signalling pathway results in uncontrolled pro-angiogenic stimuli, impaired ECs proliferation, hyperpermeability and abnormal blood flow (Viallard & Larrivee, 2017). The first antiangiogenic agent to be approved from FDA (2004) and EMA (2005) was bevacizumab, a human monoclonal antibody that, by binding to circulating VEGF, prevents the interaction with its cell surface receptors (Yang et al., 2003; Agency, 2023). The complexity of the VEGF signalling, with multiple isoforms of VEGF (*Introduction 1.2.1*) and three variants of VEGFR (*Introduction 1.2.2*), has led to the development of small molecule inhibitors that competitively bind to the ATP binding site of VEGFRs and block the functional activity of this protein (Bhullar et al., 2018; Lee et al., 2018). Considering the genetic stability and quiescence of mature ECs, these therapeutics, targeting the immature phenotype of tumour ECs, were expected not to be associated with major toxicities (Verheul & Pinedo, 2007; Liang et al., 2021). Nevertheless, the clinical use of these agents revealed acute and long-term cardiovascular sequalae that were not anticipated based on the current preclinical safety testing and which still remain a leading cause of morbidity and mortality among cancer survivors (Mellor et al., 2011; Yang & Papoian, 2012; Barac et al., 2015; Guha et al., 2019). The severity of RTKI-induced cardiovascular complications, especially hypertension, often necessitates a dose reduction, temporary discontinuation or permanent interruption of potentially lifesaving therapy (Copur & Obermiller, 2011; Small et al., 2014; Cohen et al., 2023). Although the clinical cardiovascular manifestations of antiangiogenic therapies in cancer patients are now well-defined (Albini et al., 2010; Li et al., 2015), the pathophysiological mechanisms by which these therapeutics impair cardiovascular system are still largely unknown (Small et al., 2014; Camarda et al., 2022), thus making it difficult to find an effective therapeutic approach to manage cancer patients who develop such complications (Copur & Obermiller, 2011; Dobbin et al., 2018). As a result, characterising the RTKI-induced cardiovascular consequences and their underlying mechanisms in preclinical models, as well as improving the predictive and

translational value of the current preclinical methodologies, is crucial in order to adequately assess and limit cardiovascular safety liabilities of these therapeutics (Laverty et al., 2011).

Even though hypertension is the most common cardiovascular toxicity associated with antiangiogenic drugs targeting VEGFR-2, its incidence varies considerably amongst different VEGFR-2 inhibitors (Versmissen et al., 2019). In addition, the incidence of RTKI-induced hypertension observed in clinical studies appears to be related to the potency of these agents against VEGFR-2 (Bhargava, 2009; Dirix, 2010). RTKIs with higher potency against this subtype of VEGFR have been associated with a higher incidence of hypertension (Bhargava, 2009). For this reason, the *in vitro* quantification of the potency of a variety of RTKIs targeting VEGFR-2 is important to better understand the mechanism behind such cardiovascular complication and to proceed with the *in vivo* characterisation of their cardiovascular profile.

Recent studies have demonstrated that the hypertensive effect of RTKIs targeting the VEGF pathway can also be confirmed in animal models (Kappers et al., 2010; Blasi et al., 2012; Carter et al., 2017). However, the majority of these investigations were carried out by using telemetry or *ex vivo* methods, providing information about the impact of angiogenic inhibitors on HR, BP, as well as cardiac function and structure (Kappers et al., 2010; M. H. Kappers et al., 2011; Blasi et al., 2012; Collins et al., 2018), without any or little insight about the consequences of these drugs on systemic vasculature and its role in eliciting the hypertensive response. For this reason, there is still a knowledge gap related to the susceptibility of peripheral vasculature to VEGFR inhibitors and its relationship with the alteration of arterial BP observed with these drugs. The Doppler flowmetry model, measuring VC in different vascular beds while also deriving BP and HR, has proven to be an exquisite approach to explore drug-induged changes on regional and systemic haemodynamics (Haywood et al., 1981; S. M. Gardiner et al., 1990; Carter et al., 2017; Cooper et al., 2022; Wragg et al., 2022). Using this model for the haemodynamic assessment of axitinib and lenvatinib, the purpose of this study was to investigate not only their consequences in terms of HR and BP, but also their impact in regional vasculature and whether the onset of the pressor effect induced by these drugs coincides with alteration of vascular tone in specific vascular beds. Simultaneously measuring arterial pressure and blood flow to kidney, mesentery and hindquarters for a 4-d period of time, we characterised whether certain vascular beds were more vulnerable to BP changes, in addition to defining the time course of hypertension and/or alterations in regional VC after the treatment with the selected RTKIs.

Among the currently approved VEGFR-2 inhibitors (*Introduction 1.4.1, Table 1*), the pharmacological and cardiovascular profile of sorafenib, pazopanib and vandetanib has been previously investigated (Carter et al., 2015; Carter et al., 2017). As a result, the choice to characterise the haemodynamic impact of axitinib and lenvatinib *in vivo* was informed not only by the *in vitro* quantification of the potency of a spectrum of RTKIs against VEGFR-2, but also by the incidence of hypertension reported in cancer patients for the most recently approved VEGFR-2 inhibitors. Indeed, lenvatinib and axitinib have been associated with the highest incidence of overall hypertension (67.8% and 40.1%, respectively) (Rini et al., 2011; Abdel-Rahman & Fouad, 2014; Rini et al., 2015; Agency, 2021a; Kadowaki et al., 2021), compared to the other recent VEGFR-2 inhibitors (regorafenib 36.8%, cabozantinib 27.8% and nintedanib 15.4%) (X. Zhang et al., 2016; Bronte et al., 2017; Chen & Wang, 2018).

3.2 AIMS

The work described in *Chapter 3* aimed to:

1. Determine the potency of selected RTKIs against VEGFR-2 by using an NFAT luciferase reporter gene assay in HEK293 cells.
2. Characterise the pressure effects induced by axitinib and lenvatinib, while simultaneously evaluating their effect on distinct vascular beds, in conscious and freely moving rats using the Doppler flowmetry model.

3.3 METHODS

3.3.1 In vitro: NFAT luciferase reporter gene assay in RE-luc2P VEGFR-2 HEK293 cells

The NFAT reporter gene assay (*Methods 2.1.1)* was used as a cell-based approach to quantify the $VEGF_{165}$a-stimulated NFAT-luciferase response (*Methods 2.1.1.7.1*) and to subsequently determine the potency of a spectrum of RTKIs against VEGFR-2 (*Methods 2.1.1.7.2*).

In brief, VEGFR-2/NFAT-RE-luc2 cells were plated into 96-well plates at the required density (20,000 cells/well) and left to grow for 24 h. After that time, growth medium was replaced with FCS-free medium cell were incubated for a further 24 h (*Methods 2.1.1.7).* For the $VEGF_{165}$a concentration-response curve (*Methods 2.1.1.7.1)*, medium was replaced with serum-free DMEM/0.1% protease-free BSA. Increasing concentrations of $VEGF_{165}$a were added to the appropriate wells and, after the incubation period has lapsed, assay medium was replaced with serum-free DMEM and ONE-Glo™ Luciferase reagent, containing luciferin

as a substrate for the luciferase. Luminescence was then measured by a TopCount plate reader with a 5-min delay to allow reagent to react with transcribed luciferase and to allow the attenuation of background luminescence (*Methods 2.1.1.7.1).*

For the competition assay (*Methods 2.1.1.7.2*), medium was replaced with serum-free DMEM/0.1% protease-free BSA. Vehicle (serum-free DMEM/0.1% protease-free BSA) was added to the control wells. Increasing concentrations of RTKIs (final concentrations: 10^{-11} M - $3x10^{-7}$ M for erlotinib, axitinib and SU-1483; $3x10^{-11}$ M - 10^{-6} M for vatalanib and linifanib) were added to the appropriate wells and cells were then incubated for 1 h prior to addition of $VEGF_{165}a$. $VEGF_{165}a$ (1 nM) was added to each well and cells were then incubated. After a 5-h incubation period, assay medium was replaced with serum-free DMEM and ONE-Glo™ Luciferase reagent. Luminescence was measured by a TopCount plate reader with a 5-min delay to allow reagent to react with transcribed luciferase and to allow the attenuation of background luminescence (*Methods 2.1.1.7.2*).

3.3.2 In vivo: Pulsed Doppler flowmetry in conscious and freely moving rats

3.3.2.1 ANIMALS AND SURGICAL PROCEDURES

All surgical and experimental procedures were conducted with approval from the UK Home Office and the University of Nottingham, as previously described (*Methods 2.2.1.4*).

Adult male Sprague-Dawley rats weighing between 350 and 500 g were used to perform the pulsed Doppler flowmetry studies described in this chapter (*Methods 2.2.1.4*). Animals were subjected to two rounds of surgeries (*Methods 2.2.1.5)*: the first surgery consisted of the implantation of the Doppler flow probes (*Methods 2.2.1.5.1*), while the second procedure was carried out to insert intraarterial and intravenous catheters (*Methods 2.2.1.5.2*).

3.3.2.2 CARDIOVASCULAR RECORDING

Detailed information on the cardiovascular recordings and statistical analysis can be found in the general methodology (*Methods 2.2.1.7, 2.2.1.9).*

Briefly, rats were indirectly connected to the data acquisition programme (IdeeQ) during the monitoring periods via a tether system *(Methods 2.2.1.7)*. HR, BP, renal, mesenteric and hindquarters Doppler shifts were measured and changes in VC in the renal, mesenteric, and hindquarter vascular beds were derived from the changes in MAP and Doppler shift (*Methods 2.2.1.7)*. PP was also derived as the difference between SBP and DBP (*Methods 2.2.1.7).*

For all experiments, time-averaged data are shown as changes from baseline [HR (beats.min^{-1}); MAP (mmHg); VC (%); SBP (mmHg); DBP (mmHg); PP (mmHg)] (*Methods 2.2.1.9)*. A Friedman's test was used for within-group comparisons to baseline; this data analysis was performed on the first 2 days of the experimental period due to changes in sample size (n) after day 2 (*Methods 2.2.1.9)*. The reduction in sample size over the 4 days was due either to the loss of all Doppler probe signals, blockage of intravenous catheters or in case adverse effects were observed that could not be controlled within the severity limit. A Mann-Whitney U test for integrated area under or above curve analysis was used for comparisons between groups (*Methods 2.2.1.9)*. A Mann-Whitney U test was also performed for comparisons between groups at a specific time point. A value of $p<0.05$ was considered significant (*Methods 2.2.1.9).*

3.3.2.3 EXPERIMENTAL PROTOCOL

This series of experiments was run for 4 days. Experiments were run with treatment groups of 8 to 10 rats (*Methods 2.2.1.8.1).*

Two groups of rats were used to assess the cardiovascular responses to axitinib. On day 1 of the experiment, after a period of baseline recordings, rats were dosed with axitinib (3 (low) mg.kg^{-1} or 6 (high) mg.kg^{-1}) as an intravenous bolus followed by a 1-h intravenous infusion at the same dose (*Methods 2.2.1.8.1).*

Three groups of rats were used to evaluate the cardiovascular changes induced by lenvatinib. On day 1 of the experiment, after a period of baseline recordings, rats were dosed with lenvatinib (1 (low) mg.kg^{-1}, 3 (mid) mg.kg^{-1} or 6 (high) mg.kg^{-1}) as an intravenous bolus followed by a 1-h intravenous infusion at the same dose (*Methods 2.2.1.8.1)*.

Contemporaneous control group received vehicle (40% HPβCD in sterile saline) as an intravenous bolus followed by a 1-h intravenous infusion (*Methods 2.2.1.8.1)*.

Haemodynamic recordings were continued for a further 5 h after completion of the axitinib, lenvatinib or vehicle intravenous infusion period. The same treatment regimen was followed on days 2-4 after a baseline recording period on each day (*Methods 2.2.1.8.1)*.

3.4 RESULTS

3.4.1 In vitro: Quantitative analysis of the effect of selected RTKIs on VEGF$_{165}$a-stimulated NFAT-luciferase response

3.4.1.1 CHARACTERISATION OF THE VEGF$_{165}$a-STIMULATED NFAT-LUCIFERASE RESPONSE

In HEK293 cells stably expressing VEGFR-2 and NFAT-RE-luc2P, VEGF$_{165}$a produced a concentration-dependent increase (pEC$_{50}$ 9.73 ± 0.11, *n* = 5) in NFAT-luciferase production (Figure 34). The pEC$_{50}$ obtained was in close agreement with that reported from previous work (Carter et al., 2015).

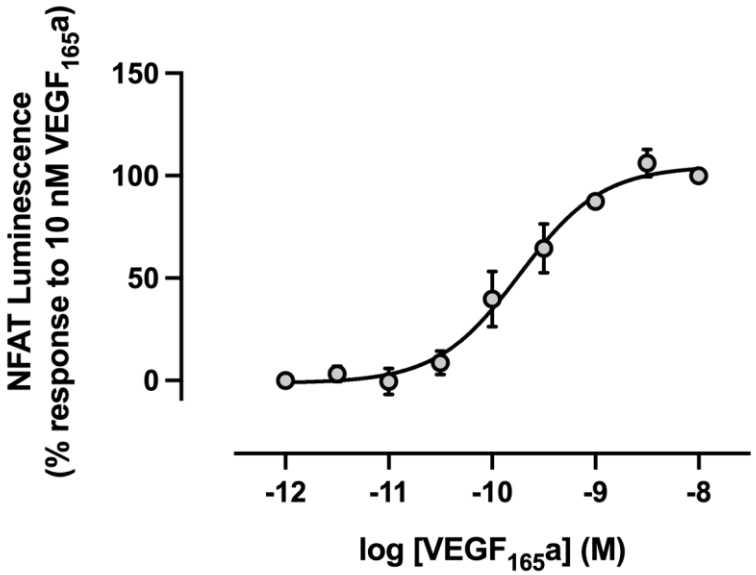

Figure 34. *The effect of VEGF$_{165}$a on NFAT-mediated gene transcription in VEGFR-2/NFAT-ReLuc2P HEK293 cells. Normalised data from five independent experiments expressed as a percentage (mean ± SEM) of the response to 10 nM VEGF$_{165}$a (100%). Each individual experiment was performed in triplicate.*

3.4.1.2 INHIBITION OF VEGF$_{165}$a-STIMULATED NFAT-LUCIFERASE RESPONSE BY RTKIs

Previous studies used the NFAT luciferase reporter gene assay to evaluate the effect of several RTKIs (e.g., cediranib, sorafenib, pazopanib, vandetanib, sunitinib and motesanib) on

$VEGF_{165}$a-stimulated NFAT-luciferase response (Carter et al., 2015; Van Daele et al., 2023). To extend this investigation to a wider range of RTKIs and to better inform the choice of VEGFR-2 inhibitors to be used for the further characterisation of their cardiovascular profile in animal models, the inhibition of the response to 1 nM $VEGF_{165}$a was tested for six different RTKIs, namely axitinib, erlotinib, linifanib, vatalanib, SU-14813 and lenvatinib (Figure 35 and 36).

In HEK293 cells stably expressing VEGFR-2 and NFAT-RE-luc2P, a concentration-dependent reduction in $VEGF_{165}$a-stimulated NFAT-luciferase production was observed in response to all of the RTKIs tested, with the exception of erlotinib (Figure 35 and 36). Indeed, this drug targets EGFR, showing a marginal affinity for VEGFR-2 (pKd 5.24) (Davis et al., 2011). The pIC_{50} values obtained from all the other RTKIs were consistent with those reported in previous studies (Table 3). It is worth noting that no inhibition below basal levels was recorded even at the highest concentration used (Figure 35A-F), suggesting that the potential interactions between these RTKIs and other kinases did not significantly affect the responses observed. In addition, even though SU-14813 was shown to be one of the least potent inhibitors of VEGFR-2 (pIC_{50} 8.00 ± 0.23) among those tested, its inhibition curve reached a plateau above baseline values (Figure 35E). This observation is consistent with its affinity for VEGFR-2 (pKd 8.64) (Davis et al., 2011), that is one of the highest among those reported for the studied RTKIs (Table 3) (Davis et al., 2011; Okamoto et al., 2014).

RTKIs	**pIC_{50} for inhibition of $VEGF_{165}$a-induced NFAT response**	***n***	**Reported pIC_{50} from literature**	**pKd for VEGFR-2**
Axitinib	9.28 ± 0.13	5	9.6 (Lee et al., 2010)	8.22 (Davis et al., 2011)
Lenvatinib	8.88 ± 0.13	4	8.4 (Musumeci et al., 2012)	8.68 (Okamoto et al., 2014)
Linifanib	8.34 ± 0.19	5	8.4 (Albert et al., 2006)	8.09 (Davis et al., 2011)
SU-14813	8.00 ± 0.23	5	7.3 (Patyna et al., 2006)	8.64 (Davis et al., 2011)
Vatalanib	7.36 ± 0.26	6	7.7 (Kiselyov et al., 2006)	7.21 (Davis et al., 2011)
Erlotinib	NI	6	NI	5.24 (Davis et al., 2011)

Table 3. *pIC_{50} values obtained from the inhibition of 1 nM $VEGF_{165}$a-stimulated NFAT-luciferase activity due to selected RTKIs. pIC_{50} values are mean ± SEM of n independent experiments performed in triplicate. pIC_{50} and pKd values for VEGFR-2 from previous studies are also reported. NI = no inhibition at the highest concentrations used ($3x10^{-7}$ M).*

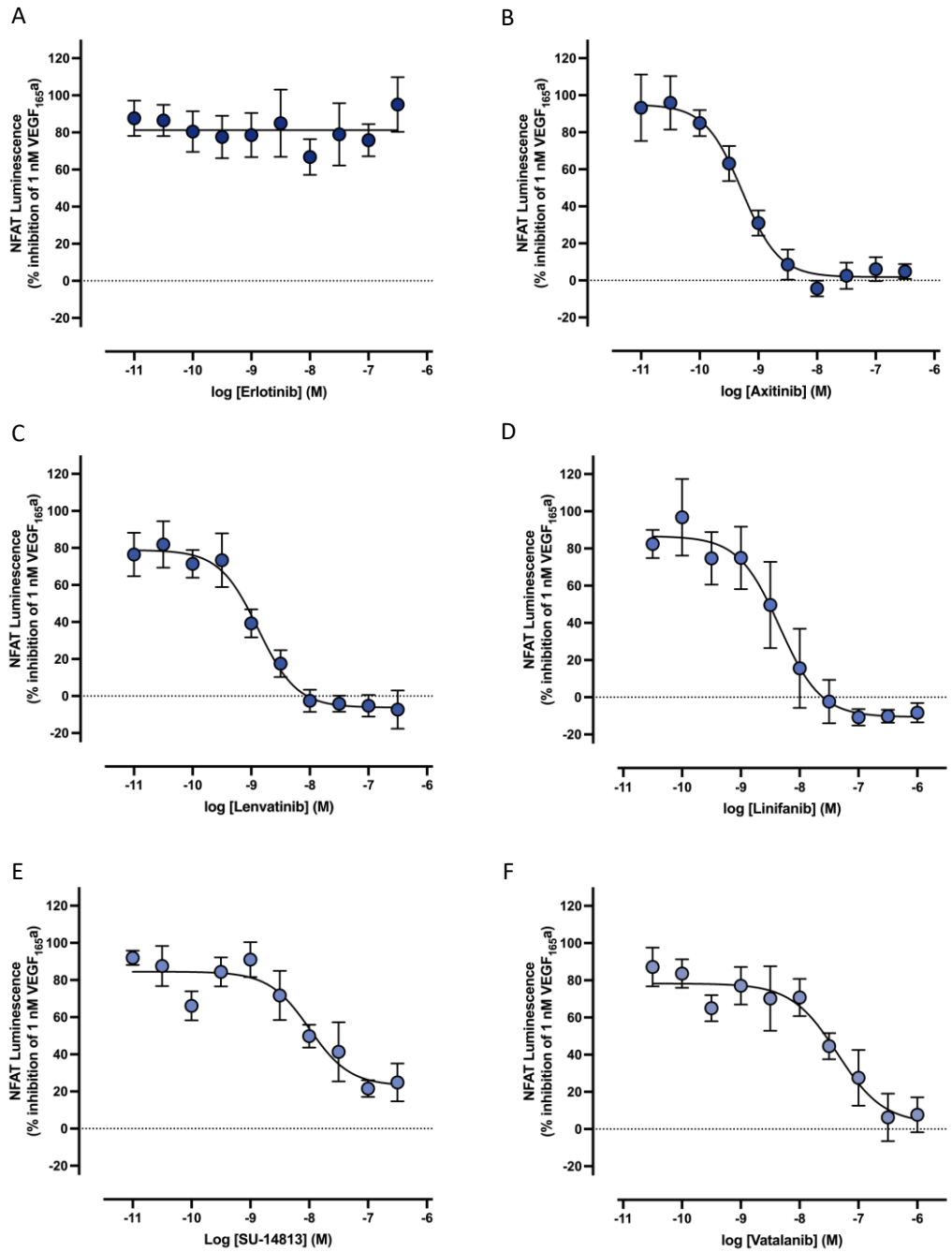

Figure 35. *Inhibition of VEGF165a-induced (1nM) NFAT reporter gene transcription in HEK293 cells expressing VEGFR-2/NFAT-ReLuc2P by erlotinib (A), axitinib (B), lenvatinib (C), linifanib (D), SU-14813 (E) and vatalanib (F). Data were normalised as a percentage of the response to 1nM $VEGF_{165}a$ (100%), with basal levels set at 0%. Data are shown as mean ± SEM of n independent experiments (Table 3). Each experiment was performed using triplicate wells.*

Figure 36. *Schematic representation of tested RTKIs based on their potency in inhibiting VEGFR-2. The potency of the compounds decreases from left to right.*

3.4.2 In vivo: Assessment of the haemodynamic profile of axitinib and lenvatinib

To comprehensively characterise the haemodynamic impact of axitinib and lenvatinib, the pulsed Doppler flowmetry was used in conscious and freely moving rats, allowing the simultaneous evaluation of their effects on chronotropism, arterial pressure and regional VC. The doses of axitinib and lenvatinib were chosen based on previous experimental results on other RTKIs (Carter et al., 2015; Carter et al., 2017). In particular, the evaluation of the potency of cediranib against VEGFR-2 showed that this agent inhibits $VEGF_{165}$a-stimulated NFAT-luciferase response with a similar potency to axitinib and lenvatinib (pIC_{50} cediranib: 9.13; pIC_{50} axitinib: 9.28; pIC_{50} lenvatinib: 8.88). The same compound was then investigated *in vivo,* where a low dose of 3 $mg.kg^{-1}$ and an high dose of 6 $mg.kg^{-1}$ showed a sustained hypertensive effect over the experimental period, while also being well-tolerated (Carter et al., 2015; Carter et al., 2017). As a result, 3 $mg.kg^{-1}$ and 6 $mg.kg^{-1}$ were selected for the assessment of axitinib- and lenvatinib-induced haemodynamic changes in this study. As to lenvatinib, the introduction of a lower dose was needed to characterise its submaximal effects on haemodynamics (*Chapter 3, section 3.5*).

Baseline cardiovascular parameters taken before the administration of axitinib, lenvatinib or vehicle control are shown in Table 4.

	Vehicle		**Axitinib 3 mg.kg^{-1}**		**Axitinib 6 mg.kg^{-1}**		**Lenvatinib 1 mg.kg^{-1}**		**Lenvatinib 3 mg.kg^{-1}**		**Lenvatinib 6 mg.kg^{-1}**	
	Mean ± SEM	*n*	*Mean ± SEM*	*n*	*Mean ± SEM*	*n*	*Mean ± SEM*	*n*	*Mean ± SEM*	*n*	*Mean ± SEM*	*n*
HR (beats.min^{-1})	344 ± 9	9	346 ± 8	10	357 ± 13	8	342 ± 12	8	340 ± 14	9	343 ± 10	8
MAP (mmHg)	103 ± 3	9	101 ± 4	10	99 ± 6	8	98 ± 3	8	96 ± 3	9	95 ± 3	8
DBP (mmHg)	84 ± 3	9	84 ± 3	10	82 ± 5	8	83 ± 3	8	79 ± 2	9	79 ± 3	8
SBP (mmHg)	142 ± 4	9	136 ± 6	10	135 ± 8	8	135 ± 4	8	136 ± 4	9	130 ± 4	8
RVC (U)	92 ± 6	7	94± 5	10	67 ± 5	8	97 ± 7	8	74 ± 12	8	85 ± 6	7
MVC (U)	98 ± 9	9	84 ± 10	10	109 ± 11	8	85 ± 7	8	104 ± 11	8	104 ± 9	8
HVC (U)	55 ± 4	9	51 ± 10	10	52 ± 7	8	53 ± 8	8	59 ± 8	8	50 ± 3	8

***Table 4**. Baseline cardiovascular variables prior to administration of vehicle or RTKIs. Values are mean ± SEM. Units of vascular conductance (VC) are kHz. mmHg^{-1} x 10^{3}. U, units.*

3.4.2.1 ASSESSMENT OF AXITINIB-INDUCED HAEMODYNAMIC CHANGES

Administration of vehicle did not elicit significant cardiovascular effects, despite some sporadic reduction in MVC and HVC at the end of day 2 (#p<0.05, Friedman's test; Figure 37 and 38). Axitinib, at both 3 $mg.kg^{-1}$ and 6 $mg.kg^{-1}$, evoked a consistent increase of MAP, which was evident from day 1 of the experimental period (#p<0.05, Friedman's test; Figure 37 and 38), with no corresponding alteration in HR. Treatment with low or high dose of axitinib led to maximal increases in MAP on day 4 of 29% and 37%, respectively (Figure 37 and 38). Such hypertensive response was associated with a significant vasoconstriction in the mesenteric and hindquarters vasculature at both doses used (#p<0.05, Friedman's test; Figure 37 and 38). In particular, a maximal reduction of 50% and 62% in MVC occurred on day 4 of treatment with low or high dose of the drug, respectively (Figure 37 and 38). HVC was maximally reduced on day 4 by 61% (following the administration of low-dose axitinib) and 69% (following the administration of high-dose axitinib) (Figure 37 and 38). However, a sustained renal vasoconstriction was only observed with the low and the high dose of axitinib on day 2. This was more marked in the group receiving the 6 $mg.kg^{-1}$ dose (Figure 38). DBP and SBP were significantly increased (#p<0.05, Friedman's test) after the administration of axitinib 3 $mg.kg^{-1}$ and 6 $mg.kg^{-1}$, whereas no appreciable alteration was detected in PP (Figure 37 and 38).

Considerable differences in BP and vascular responses were observed between the axitinib-receiving groups and vehicle group over the 4-day recording period (θp<0.05, Mann-Whitney U test, integrated area under curve, 0–78 h; Figure 37 and 38). An additional Mann-Whitney test was conducted between treated and control groups at each time point to determine the time of onset of the cardiovascular effects (*p<0.05, Mann-Whitney U test; Figure 37 and 38). In both the low dose- and high dose-treated groups, the pressor effect and the vascular changes, particularly in the mesentery and hindquarters, showed a striking difference from the vehicle group for almost all points of analysis (*p<0.05, Mann-Whitney U test; Figure 37 and 38). Although the renal integrated responses to both doses of axitinib over the 78-h recording period were significantly different from the vehicle (θp<0.05, Mann-Whitney U test, integrated area under curve, 0–78 h; Figure 37 and 38), only specific time points on day 2 in the group receiving high dose of axitinib showed a significant difference in the reduction of RVC (*p<0.05, Mann-Whitney U test; Figure 38). When compared to vehicle, low dose of axitinib induced a sporadic increase of PP throughout the experimental period, while a consistent increase of PP was observed on day 4 in response to the high dose of the drug

(*$p<0.05$, Mann-Whitney U test; Figure 37 and 38). Comparing the differential impact of axitinib on SBP and DBP, this agent appeared to significantly increase and equally affect the two components of BP (Figure 39A-B). In this context, a maximal increase of 24% in DBP was observed on day 3 of treatment with the low dose of axitinib, while systolic pressure peaked on day 4 (31%) (Figure 39A). On day 4 of treatment with the high dose of the drug, the increase in DBP and SBP reached a maximum of 37% and 42%, respectively (Figure 39B).

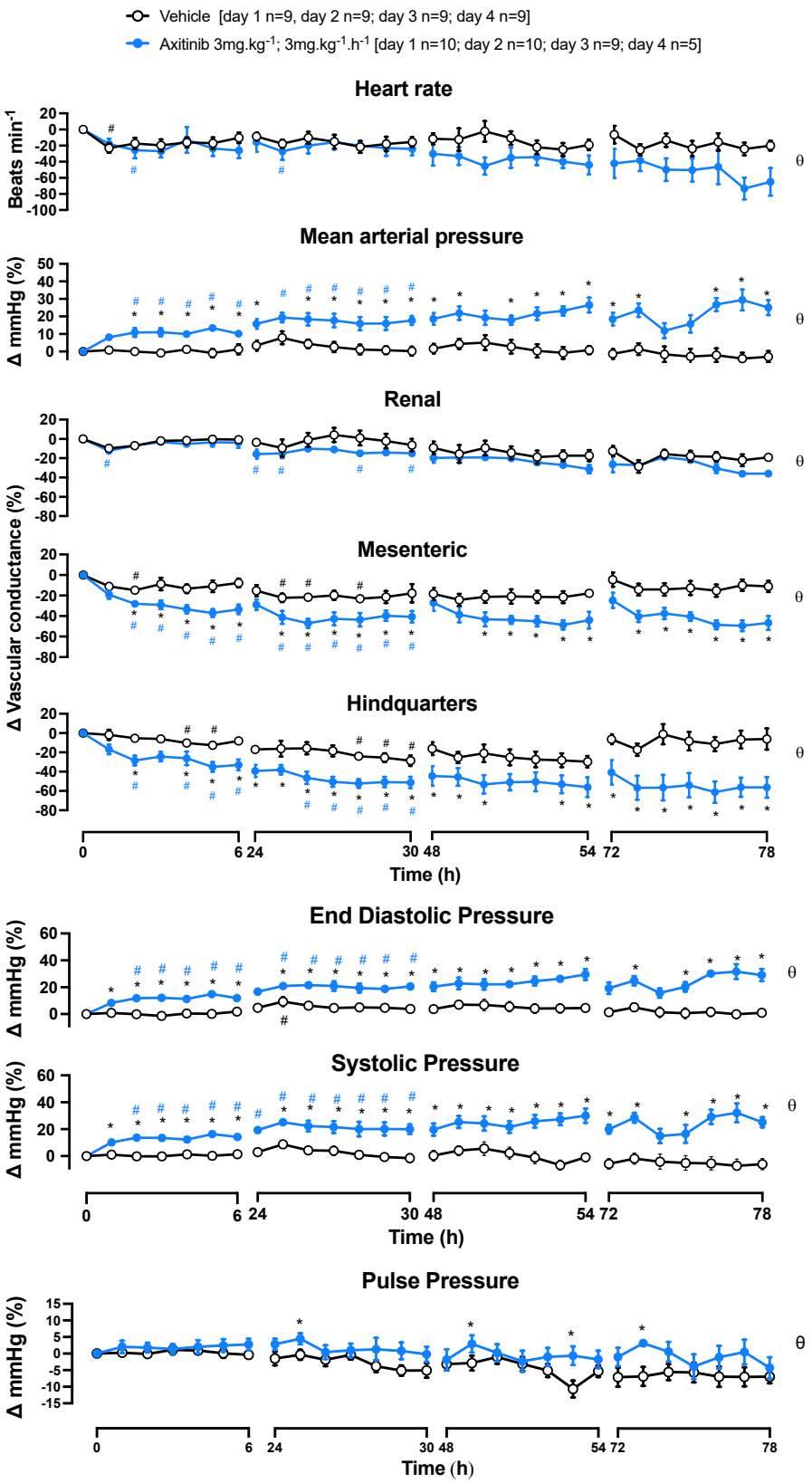

Figure 37. *Cardiovascular responses to axitinib in conscious, freely moving rats. Animals were dosed with 3 mg.kg^{-1}, intravenously (initial bolus followed by 3 mg.kg^{-1}.h^{-1}, intravenous infusion for 1 h). Vehicle controls were administered 40% HPβCD in sterile saline as described in Methods 2.2.1.8.1. The same dose regimen was repeated on day 2,3 and 4. Data points are means; vertical bars*

*represent SEM. Friedman's test was performed on the first 2 days of the experimental period (#p<0.05 vs. baseline). Mann-Whitney U test was conducted between treated and vehicle control groups for a comparison of area under/over the curve (θp<0.05, 0–78 h) and to determine differences at each time point (*p<0.05, Mann-Whitney U test).*

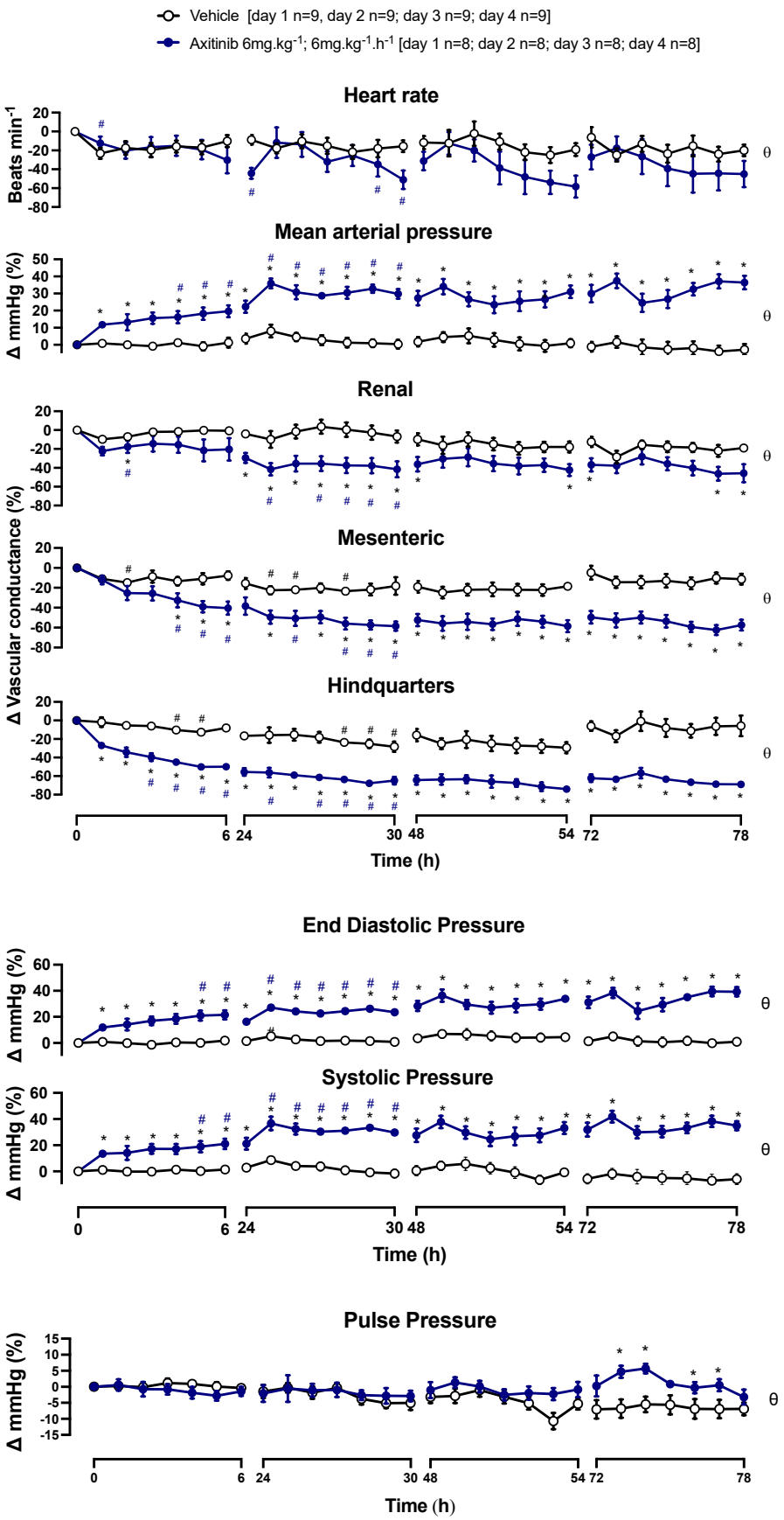

Figure 38. *Cardiovascular responses to axitinib in conscious, freely moving rats. Animals were dosed with 6 mg.kg^{-1}, intravenously (initial bolus followed by 6 mg.kg^{-1}.h^{-1}, intravenous infusion for 1 h).*

*Vehicle controls were administered 40% HPβCD in sterile saline as described in Methods 2.2.1.8.1. Same dose regimen was repeated on day 2,3 and 4. Data points are means; vertical bars represent SEM. Friedman's test was performed on the first 2 days of the experimental period (#p<0.05 vs. baseline). Mann-Whitney U test was conducted between treated and vehicle control groups for a comparison of area under/over the curve (θp< 0.05, 0–78 h) and to determine differences at each time point (*p<0.05, Mann-Whitney U test).*

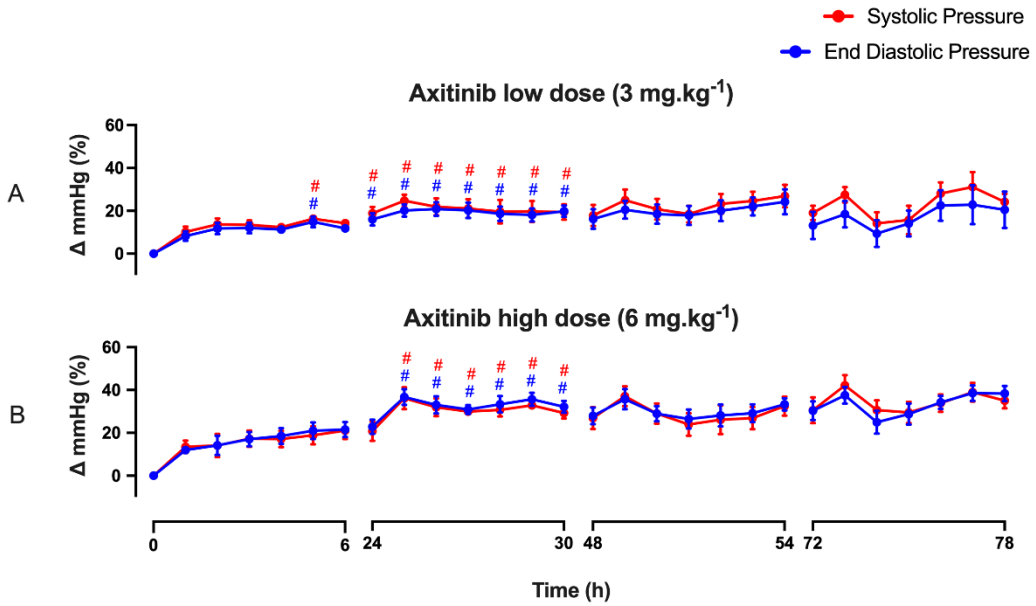

Figure 40. *Axitinib-induced changes in SBP and DBP in conscious, freely moving rats. Animals were dosed with either 3 mg.kg^{-1}, intravenously (initial bolus followed by 3 mg.kg^{-1}.h^{-1}, intravenous infusion for 1 h) (A) or 6 mg.kg^{-1}, intravenously (initial bolus followed by 6 mg.kg^{-1}.h^{-1}, intravenous infusion for 1 h) (B) of axitinib. Same dose regimen was repeated on day 2,3 and 4. Data points are means; vertical bars represent SEM. Friedman's test was performed on the first 2 days of the experimental period (#p<0.05 vs. baseline). A Mann-Whitney U test was conducted between groups for a comparison of area under/over the curve (θp<0.05, 0–78 h) and to determine differences at each time point (*p<0.05, Mann-Whitney U test).*

3.4.2.2 ASSESSMENT OF LENVATINIB-INDUCED HAEMODYNAMIC CHANGES

Lenvatinib, at 1 mg.kg^{-1}, 3 mg.kg^{-1} and 6 mg.kg^{-1}, significantly increased MAP when compared to baseline values (#p<0.05, Friedman's test; Figure 41, 42 and 43), without consistently affecting HR. Low dose and high dose of lenvatinib were associated with maximal increases in MAP of 32% and 55 % on day 4 (Figure 41 and 43), while mid dose of the drug determined a peak in MAP on day 3, with a rise of 38% when compared to baseline (Figure 42). The lenvatinib-induced hypertensive effect was accompanied by significant reductions in MVC

and HVC, which were observed with all doses of the compound (#p<0.05, Friedman's test; Figure 41, 42 and 43). MVC was maximally reduced by 59% (on day 3 of low-dose lenvatinib), 69% (on day 4 of mid-dose lenvatinib) and 77% (on day 3 of high-dose lenvatinib) (Figure 41, 42 and 43). A sustained elevation of SBP and DBP was also detected (#p<0.05, Friedman's test) in all lenvatinib-treated groups; however, neither dose of lenvatinib produced a notable change in PP over the first 2 days (Figure 41, 42 and 43).

Comparing the integrated responses over the 78-h recording period, the pressor effects and the vascular responses observed in lenvatinib-receiving animals were significantly different from vehicle group (θp<0.05, Mann-Whitney U test, integrated area under curve, 0–78 h; Figure 41, 42 and 43). Comparison of each time point showed a significant difference in MAP, MVC, HVC, SBP and DBP between the lenvatinib-treated groups and vehicle-receiving group for almost all time points of the analysis (*p<0.05, Mann-Whitney U test; Figure 41, 42 and 43). However, the vasoconstrictive response in renal vasculature was sustained only in the groups receiving the mid and the high dose of lenvatinib and was mainly evident on day 2 (*p<0.05, Mann-Whitney U test; Figure 42 and 43). The integrated increase in PP was detected in the groups treated with the low and the high dose of lenvatinib (θp<0.05, Mann-Whitney U test, integrated area under curve, 0–78 h; Figure 41 and 43), reaching statistical significance for almost all time points after 72 hours (*p<0.05, Mann-Whitney U test; Figure 41 and 43). There was no marked difference between the effects in SBP and DBP evoked by all doses of lenvatinib (Mann-Whitney U test; Figure 44A-C). In particular, with the low dose of the drug, SBP and DBP increased to a maximum of 40% and 35%, respectively, on day 4 of the experimental period (Figure 44A). The mid dose was associated with a maximal increase of 40% in DBP and 35% in SBP on day 3 (Figure 44B). The high dose led to a maximal increase in DBP of 54% and SBP of 63% on day 4 (Figure 44C).

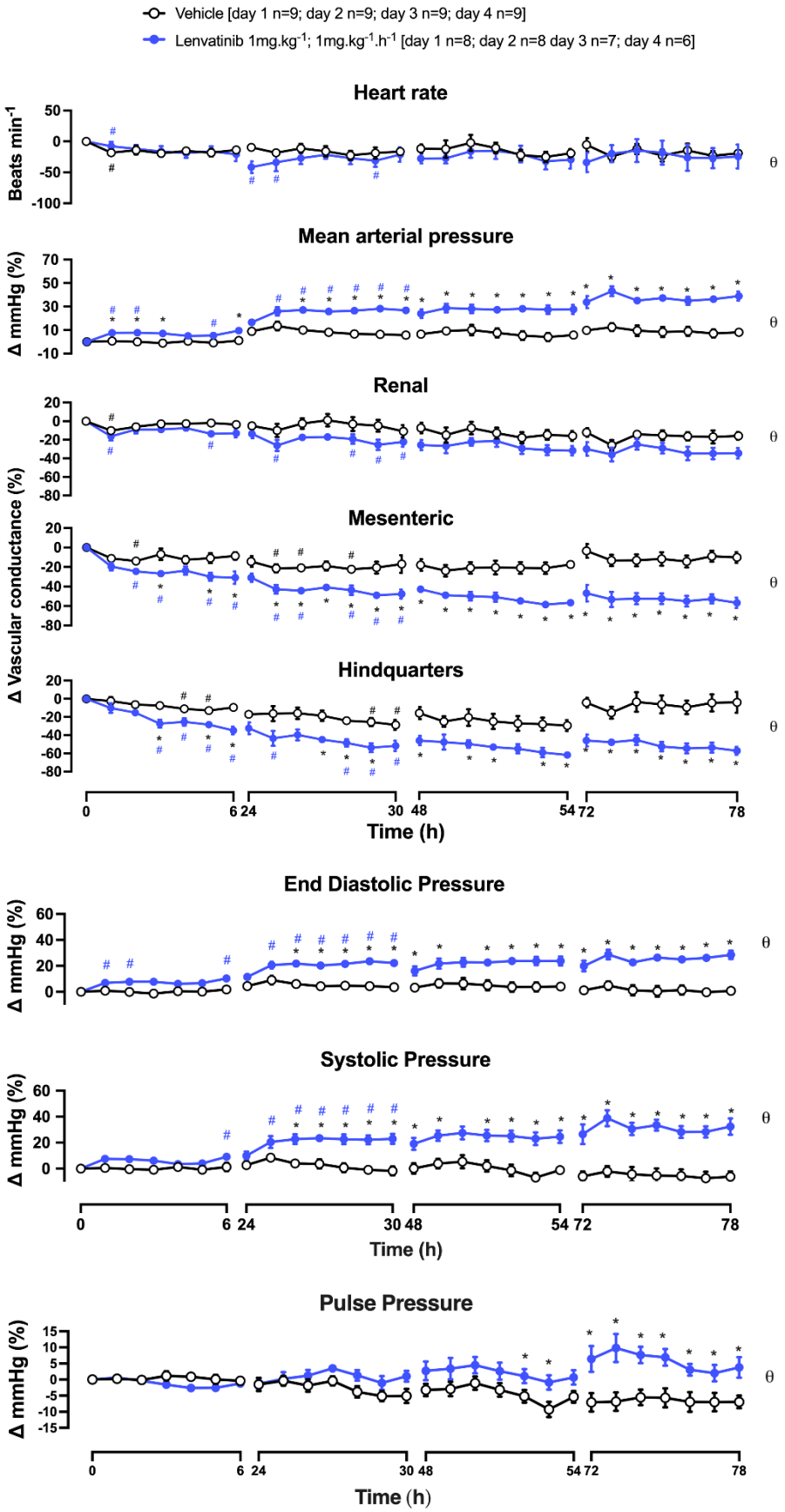

Figure 41. *Cardiovascular responses to lenvatinib in conscious, freely moving rats. Animals were dosed with 1 mg.kg^{-1}, intravenously (initial bolus followed by 1 mg.kg^{-1}.h^{-1}, intravenous infusion for 1*

*h). Vehicle controls were administered 40% HPβCD in sterile saline as described in Methods 2.2.1.8.1. Same dose regimen was repeated on day 2,3 and 4. Data points are means; vertical bars represent SEM. Friedman's test was performed on the first 2 days of the experimental period (#p<0.05 vs. baseline). Mann-Whitney U test was conducted between treated and vehicle control groups for a comparison of area under/over the curve (θp<0.05, 0–78 h) and to determine differences at each time point (*p<0.05, Mann-Whitney U test).*

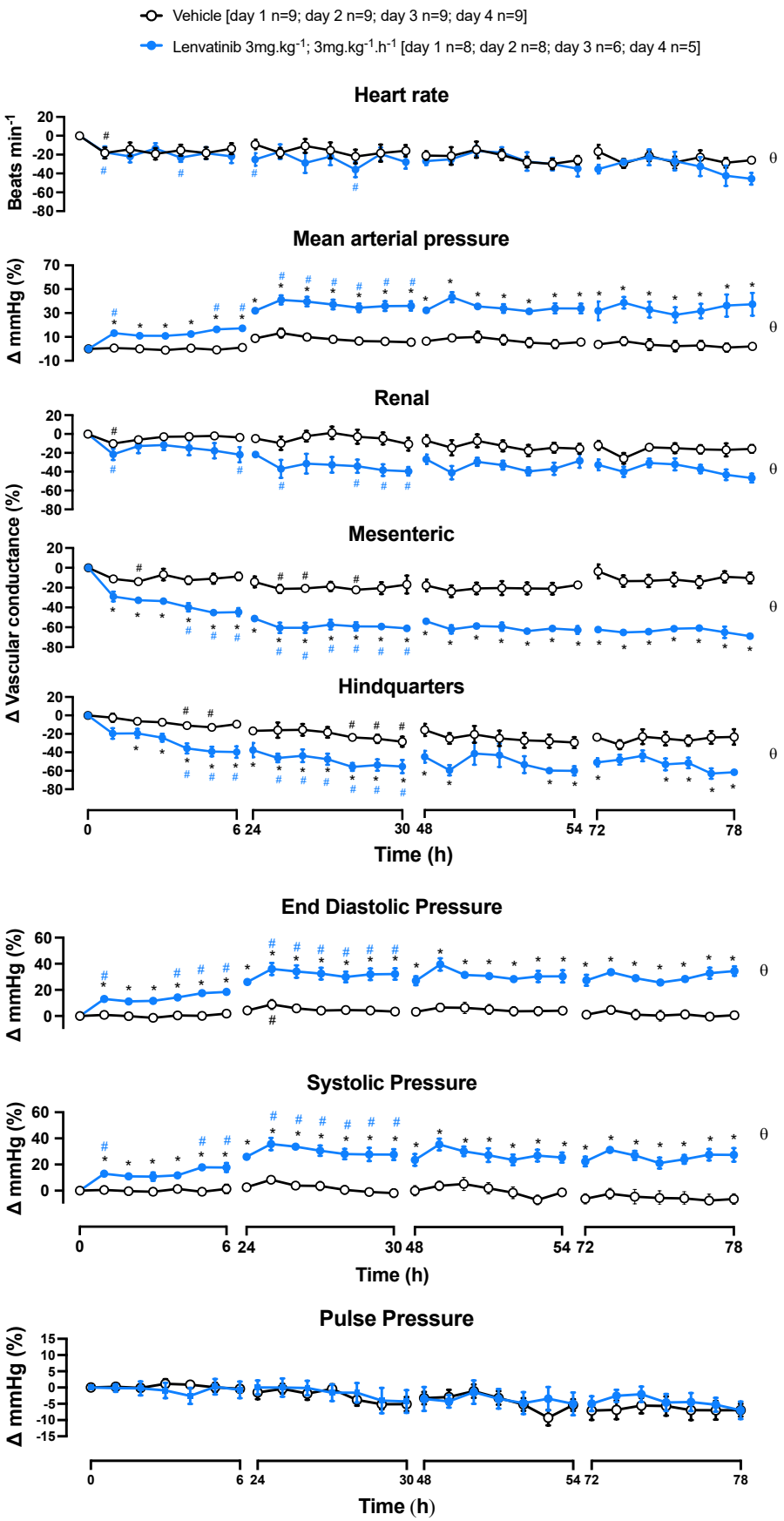

Figure 42. *Cardiovascular responses to lenvatinib in conscious, freely moving rats. Animals were dosed with 3 mg.kg^{-1}, intravenously (initial bolus followed by 3 mg.kg^{-1}.h^{-1}, intravenous infusion for 1*

*h). Vehicle controls were administered 40% HPβCD in sterile saline as described in Methods 2.2.1.8.1. Same dose regimen was repeated on day 2,3 and 4. Data points are means; vertical bars represent SEM. Friedman's test was performed on the first 2 days of the experimental period (#p<0.05 vs. baseline). Mann-Whitney U test was conducted between treated and vehicle control groups for a comparison of area under/over the curve (θp<0.05, 0–78 h) and to determine differences at each time point (*p<0.05, Mann-Whitney U test).*

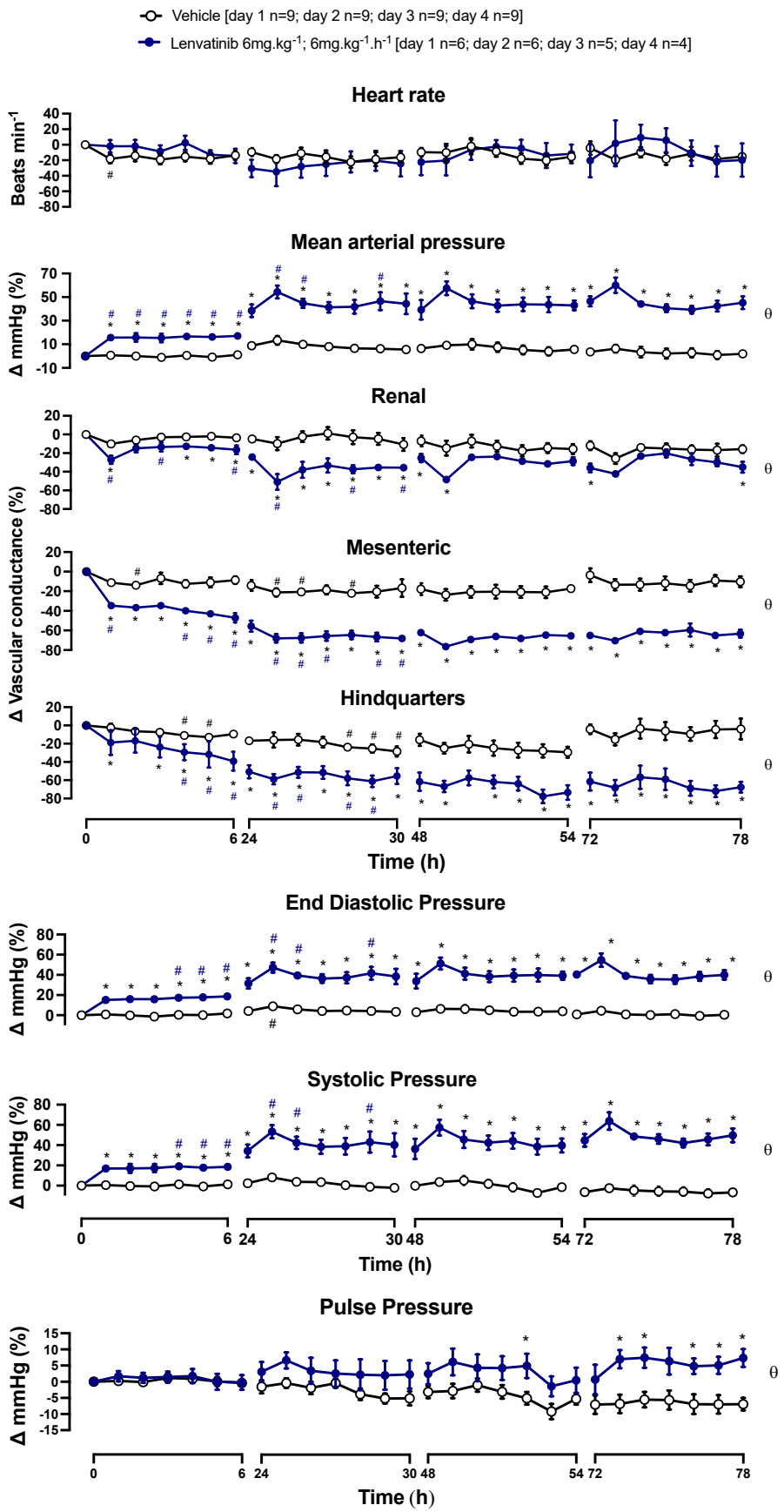

Figure 43. *Cardiovascular responses to lenvatinib in conscious, freely moving rats. Animals were dosed with 6 mg.kg^{-1}, intravenously (initial bolus followed by 6 mg.kg^{-1}.h^{-1}, intravenous infusion for 1*

*h). Vehicle controls were administered 40% HPβCD in sterile saline as described in Methods 2.2.1.8.1. Same dose regimen was repeated on day 2,3 and 4. Data points are means; vertical bars represent SEM. Friedman's test was performed on the first 2 days of the experimental period (#p<0.05 vs. baseline). Mann-Whitney U test was conducted between treated and vehicle control groups for a comparison of area under/over the curve (θp<0.05, 0–78 h) and to determine differences at each time point (*p<0.05, Mann-Whitney U test).*

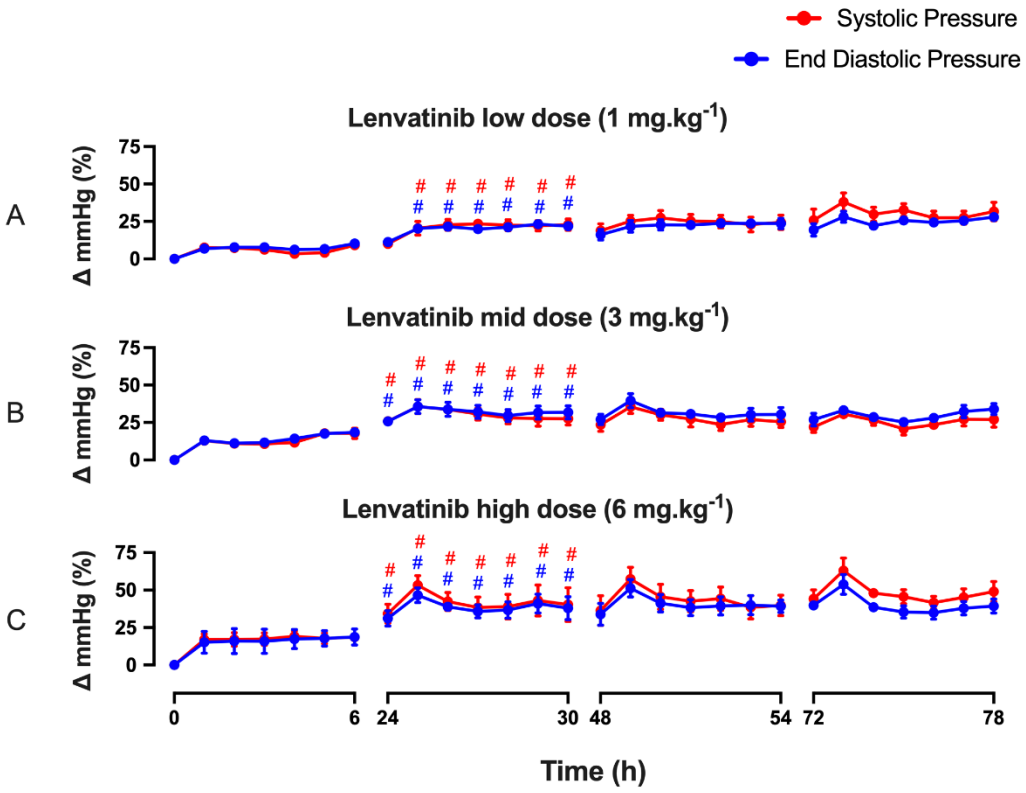

Figure 44. *Lenvatinib-induced changes in SBP and DBP in conscious, freely moving rats. Animals were dosed with either 1 mg.kg^{-1}, intravenously (initial bolus followed by 1 mg.kg^{-1}.h^{-1}, intravenous infusion for 1 h) (A), 3 mg.kg^{-1}, intravenously (initial bolus followed by 3 mg.kg^{-1}.h^{-1}, intravenous infusion for 1 h) (B) or 6 mg.kg^{-1}, intravenously (initial bolus followed by 6 mg.kg^{-1}.h^{-1}, intravenous infusion for 1 h) lenvatinib (C). Same dose regimen was repeated on day 2,3 and 4. Data points are means; vertical bars represent SEM. Friedman's test was performed on the first 2 days of the experimental period (#p<0.05 vs. baseline). A Mann-Whitney U test was conducted between groups for a comparison of area under/over the curve (θp<0.05, 0–78 h) and to determine differences at each time point (*p<0.05, Mann-Whitney U test).*

3.5 DISCUSSION

The NFAT reporter gene assay was used to define the effect of selected RTKIs on $VEGF_{165}$a-stimulated NFAT-luciferase response in HEK293T cells. VEGF signalling is a crucial target for anticancer therapies. As a result, the development and approval of RTKIs targeting VEGFR-2 have provided an important therapeutic strategy in the oncology field. However, new onset or worsening all-grade hypertension has been described in 17-80% of RTKI-treated patients (Small et al., 2014; Chung et al., 2020; Mohammed, Singh, et al., 2021), representing a major challenge for the overall prognosis of these patients and for their therapeutic management, especially since it is not yet clear whether such adverse effect is the result of an "on-target" activity of these agents on the intended kinase target or "off-target" interaction with other kinases. Considering that the incidence of hypertension appears to be correlated to the potency of these agents against VEGFR-2, an NFAT reporter gene assay was used to monitor the inhibitory effects of a spectrum of RTKIs on VEGFR-2 mediated responses. The resulting pIC_{50} values provided information about their potency, which were essential for the subsequent *in vivo* characterisation of the cardiovascular consequences of these drugs. Indeed, RTKIs that inhibit VEGFR-2 with a higher potency have been associated with a higher incidence of hypertension in clinical studies (Bhargava, 2009; Dirix, 2010). In addition, although the main hypothesis is that the cardiovascular toxicities associated with VEGFR-2 inhibitors are the result of an "on-target" effect, an "off-target" toxicity may also contribute to the altered cardiovascular function observed with these antiangiogenic therapeutics (Schiller et al., 2009; Cabanillas & Habra, 2016; Matsuki et al., 2018; Lamore et al., 2020). For this reason, understanding the effect of RTKIs on $VEGF_{165}$a-stimulated NFAT response informed about the choice of the compounds to be characterised *in vivo*. It is worth noting that all the RTKIs evaluated, with the exception of erlotinib (used as a negative control, given its negligible affinity for VEGFR-2), did not show inhibition of the $VEGF_{165}$a-stimulated NFAT response below basal levels, which may indicate the absence of interactions with other tyrosine kinases even at the highest concentrations required to inhibit VEGFR-2 with these RTKIs. The pIC_{50} values obtained were similar to the pKd values reported from previous binding studies (Davis et al., 2011; Okamoto et al., 2014). The 5 RTKIs targeting VEGFR-2 tested here (axitinib, linifanib, vatalanib, SU-14813 and lenvatinib) showed a potent VEGFR-2 inhibitory activity with IC_{50} values in nanomolar range. Among the RTKIs evaluated, axitinib and lenvatinib showed the highest relative potency for VEGFR-2. Based on this data, and considering that, among the most recently developed RTKIs, axitinib and lenvatinib exhibit

the highest rates of hypertension in cancer patients (Rini et al., 2011; Abdel-Rahman & Fouad, 2014; Rini et al., 2015; Agency, 2021a; Kadowaki et al., 2021), these two agents were selected to be characterised *in vivo*. Combining the VEGFR-2 inhibitory activity of axitinib and lenvatinib *in vitro* with their haemodynamic profile in animal models allowed to further explore the role of VEGFR-2 signalling in the hypertensive response associated with these agents.

In the present study, we have demonstrated that both axitinib and lenvatinib cause a hypertensive response in conscious rats. In addition, the rise in BP induced by these antiangiogenic agents coincided with regionally selective changes in vasculature. The hypertensive response was indeed mainly associated with a reduction in HVC and MVC, representative of an increased vascular tone in such vascular beds. For both RTKIs, renal vascular flow was least compromised, and mainly affected at the highest doses with a more marked vasoconstriction on the second day of treatment. These findings are consistent with the hypertensive and vascular effects previously observed with the same model for other RTKIs targeting VEGFR-2 (Carter et al., 2017). Indeed, cediranib, sorafenib, pazopanib and vandetanib showed a hypertensive effect that occurred concurrently with the hindquarters vasoconstriction (Carter et al., 2017). Similarly to our results, the renal vasculature exhibited the least susceptibility to treatment with these RTKIs (Carter et al., 2017). However, a greater variability was reported for their effects on mesenteric vascular bed, where cediranib and pazopanib were able to produce a sustained vasoconstriction, which was less marked in response to sorafenib and vandetanib (Carter et al., 2017). Interestingly, cediranib elicited the most marked vasoconstriction in this vascular bed when compared to pazopanib, sorafenib and vandetanib. This is in accordance with the effect observed for axitinib and lenvatinib. Considering that cediranib showed a potency against VEGFR-2 similar to axitinib and lenvatinib (pIC_{50} cediranib: 9.13; pIC_{50} axitinib: 9.28; pIC_{50} lenvatinib: 8.88), this may suggest that not only the hypertensive effect but also the vascular responses may be dependent on the potency of RTKIs for VEGFR-2.

Axitinib and lenvatinib produced a striking elevation in BP within 24 hours of experimental period, which became even more marked on the second day of treatment, when the pressure values essentially reached a plateau. A similar trend was also reported for cediranib, sorafenib, pazopanib and vandetanib, indicating a similar timeline for the onset of hypertension following treatment with RTKIs (Carter et al., 2017). As to lenvatinib, the

introduction of a lower dose was needed to characterise its submaximal effects on haemodynamics since the two doses chosen at the beginning (3 $mg.kg^{-1}$ and 6 $mg.kg^{-1}$) were shown to elicit a severe vasoconstriction, particularly in the mesenteric artery, in addition to determining a drastic increase in MAP of 55mmHg versus baseline values, compared with the 37mmHg-increase observed with the high dose of axitinib. It is worthy of note that the median time to onset of all-grade hypertension in axitinib-treated patients was within one month from the first dose, with hypertensive episodes observed already after 4 days of treatment (Agency, 2012; Rini et al., 2015); in cancer patients receiving lenvatinib, the median interval from the first dose to the development of hypertension was 16 days (Agency, 2021a). Given the onset time for RTKI-induced hypertension in the animal model used (24-48 hours), this *in vivo* approach has proven to be a sensitive and translational model for the prediction and early detection of haemodynamic effects of these novel anticancer therapies.

Angiogenetic pathways have a crucial role in the pathogenesis of RCC (Zarrabi et al., 2017), where the loss of tumour suppressor function of von Hippel-Lindau protein promotes a hypoxic status and the consequent overexpression of VEGF, resulting in uncontrolled angiogenesis, tumour progression and metastatic dissemination (Folkman, 1995; Zarrabi et al., 2017). As a result, RTKIs blocking the activity of VEGFR-2 have positively redefined the therapeutic approach in patients with mRCC, for which both axitinib and lenvatinib represent the recommended second-line treatment options (Choueiri & Motzer, 2017; McKay et al., 2018). Despite an overall improvement of clinical outcomes, safety concerns have arisen from the use of these drugs, particularly in terms of the hypertensive response associated with these agents (Bair et al., 2013; Small et al., 2014). The characterisation of the haemodynamic profile of these two RTKIs allowed us to concomitantly evaluate their effect on BP and provided important insights into the vascular beds mainly affected by these drugs. Interestingly, for both axitinib and lenvatinib, the major vascular changes were observed in the hindquarters and mesenteric arteries, whose vasoconstrictive responses generally occurred over the same time course as the elevation in MAP, with the only difference in the magnitude of the vasoconstriction among the diverse doses of the two RTKIs. These findings indicate the changes in these vascular beds as major causal factors in the development of hypertension observed with these agents. However, further investigations are needed to evaluate whether these regionally specific changes in the vascular tone are primary causative factors or rather secondary adaptive responses put in place to compensate the reduction in renal blood flow in the context of RTKI-induced hypertension.

Moreover, both axitinib and lenvatinib have shown a less consistent effect on renal vascular bed, whose vasoconstriction was only evident with the high doses of the compounds and at a specific time point, precisely on day 2, of the recording period. This may indicate a compensatory adaptation of renal vasculature in response to hypertensive conditions, in addition to suggesting that renal vasoconstrictive response is minimal even in case of severe increase in BP due to axitinib and lenvatinib. Considering the role of these drugs in the treatment of mRCC, constricted renal arteries and consequent disruption of blood flow in this vasculature might limit the delivery of these therapeutics to the kidney, therefore restraining their efficacy. The absence of a major vasoconstriction of renal vasculature observed in this study is consistent with their maintained optimum efficacy in clinical management of patients with mRCC, also of those patients who develop hypertension (Rini et al., 2015; Liu et al., 2019), suggesting that the onset of hypertension and the associated vascular changes in response to these drugs do not alter their ability to reach the target organ.

Even though RTKIs are designed to block the functional activity of a particular kinase, they have been shown to bind additional targets, the inhibition of which may be associated with unintended cardiovascular toxicities (Ellis & Hicklin, 2008; Mellor et al., 2011). With regard to the antiangiogenic drugs evaluated in this study, they do not only interfere with VEGFRs signalling (Schiller et al., 2009; Matsuki et al., 2018). Indeed, axitinib extends its activity to platelet-derived growth factor receptor-β, KIT and polo-like kinase 4 (Schiller et al., 2009), while lenvatinib shows a significant interaction with fibroblast growth factor receptor 1–4, platelet-derived growth factor receptor-α, RET and KIT (Matsuki et al., 2018) (Table 5). However, although the drugs used are multi-kinase inhibitors, the similarity of the haemodynamic profiles observed with this study, along with the results from the *in vitro* evaluation of their VEGFR-2 inhibitory activity, where no inhibition of NFAT activity below basal levels was observed, suggest that the cardiovascular sequelae induced by these drugs are mainly the result of their “on-target” activity on VEGFR-2 rather than the consequence of their “off-target” interactions with other kinases, which are different for axitinib and lenvatinib (Schiller et al., 2009; Cabanillas & Habra, 2016; Matsuki et al., 2018). The similar haemodynamic profile of cediranib, sorafenib, pazopanib and vandetanib reported in a previous study further reinforces the hypothesis that the haemodynamic effects of RTKIs are primarily related to their “on-target” activity on VEGFR-2 (Carter et al., 2017). Identifying the

main kinase(s) associated with cardiovascular complications induced by these therapeutics is crucial not only to prevent such toxicities but also to better understand the mechanisms by which its inhibition impairs cardiovascular system.

RTKI	Targets	Reference
Axitinib	VEGFR-1/2/3, PDGFR-β, KIT, PLK4	(Schiller et al., 2009; Rini et al., 2011)
Lenvatinib	VEGFR-2/3, PDGFR-α, FGFR-1/2/3/4, RET, KIT	(Cabanillas & Habra, 2016; Matsuki et al., 2018)

Table 5. *Summary of kinases targeted by axitinib and lenvatinib.*

In addition to monitoring the impact of antiangiogenic drugs on the steady component of blood pressure, specifically MAP, we also investigated the implications of these agents on the dynamic component, namely PP. Despite MAP being a good predictor of overall cardiovascular risk, PP has a better predictive value for coronary heart disease, atrial fibrillation and congestive heart failure (Vlachopoulos & O'Rourke, 2000; Safar & Laurent, 2003; Homan et al., 2022). This study has demonstrated that both axitinib and lenvatinib were associated with an increase in PP on day 4 of experimental period when compared to the vehicle group. Considering PP is the result of SV divided by arterial compliance (Homan et al., 2022), the raised PP observed in this study may be due either to an increased arterial stiffness or to an augmented SV over the 4-day period of treatment. Understanding the differential impact of these RTKIs on DBP and SBP is also crucial to define which form of hypertension is mainly associated with these drugs and, consequently, the pathophysiological responses underlying such condition. Hypertension is defined as a combined elevation of SBP (≥ 140 mmHg) and DBP (≥ 90 mmHg), while isolated systolic hypertension is characterised by a rise of SBP with normal or low DBP values (Williams et al., 2018). The first form of hypertension is the result of augmented systemic vascular resistance, arterial stiffening and increased SV, while isolated systolic hypertension is mainly due to reduced arterial compliance (Vlachopoulos & O'Rourke, 2000). In addition, alterations of vascular resistance are generally associated with changes in DBP (Vlachopoulos & O'Rourke, 2000). This study has shown that axitinib and lenvatinib strongly influence both SBP and DBP, which were actually affected to the same extent, suggesting a combination of augmented peripheral vascular resistance, arterial stiffness and increased SV as mechanisms potentially involved in the RTKIs-induced hypertensive response. Further investigations are needed to

clarify the prevalent mechanisms underlying the changes in the pulsatile component of BP in response to these antiangiogenic drugs, as well as their effects on SBP and DBP.

In summary, the quantification of the inhibitory activity of a spectrum of RTKIs for VEGFR-2 allowed to define the most potent agents for this receptor, informing about the choice of which compounds to further investigate *in vivo.* This study has demonstrated that the pulsed Doppler flowmetry model represents an outstanding and effective *in vivo* approach to predict and evaluate the hypertensive response induced by RTKIs, also providing crucial information about the regionally selective vasoconstrictive effects associated with such condition. Indeed, as previously demonstrated, therapeutics can determine a distinct, regionally selective and sometimes opposing effect in different vascular beds (Woolard, Bennett, et al., 2004; Carter et al., 2017). Characterising the correlation between hypertension and specific changes in vascular flow due to these drugs has also a key role in the identification of the most affected vascular beds, with important implications for the ability of these anticancer therapeutics to reach the target site. Finally, the haemodynamic profile of RTKIs obtained from this study is crucial for the future investigation of the complex mechanisms behind the haemodynamic effects induced by these antiangiogenic agents.

4 Chapter 4. Selective ET_A receptor antagonism in the prevention of axitinib- and lenvatinib-induced hypertension in conscious, freely moving rats

4.1 INTRODUCTION

Hypertension, affecting up to 80% of cancer patients treated with VEGFR-2 inhibitors, represents the predominant cardiovascular toxicity associated with these therapeutics (Abdel-Qadir et al., 2017; Dobbin et al., 2021; Cohen et al., 2023). Due to the severity of the hypertensive response evoked by RTKIs, reduction or early discontinuation of treatment are often required, with detrimental impact on cancer patient survival (Cohen et al., 2023). The exact molecular events contributing to RTKI-induced hypertension are still not clear, compromising the prevention and proper management of such complication (Yeh & Bickford, 2009; Steingart et al., 2012). Among the various hypotheses, the activation of the ET-1 axis seems to play a key role in the development of hypertension associated with antiangiogenic therapies (Kappers et al., 2012; Lankhorst, Kappers, van Esch, Danser, et al., 2014; Camarda et al., 2022). ET-1 is a potent endogenous vasoconstrictive peptide which, when released by ECs, predominantly stimulates VSMCs in a paracrine manner by binding ET_A and ET_B receptors (Schiffrin, 1999; Thorin & Webb, 2010). This interaction mediates vasoconstrictive and hypertrophic responses (Schiffrin, 1999; Schneider et al., 2007). In addition, ET-1 also acts in an autocrine loop by interacting with endothelial ET_B receptors, resulting in a vasorelaxant action via the production of NO and PGI_2 (Schiffrin, 1999; Thorin & Webb, 2010). Treatment with VEGFR-2 inhibitors has been associated with increased circulating ET-1 levels in cancer patients and animal models (Kappers et al., 2010; Markó et al., 2022). Such increase in plasma ET-1 is dose-dependent, consistently with the elevation of blood pressure (Lankhorst, Baelde, et al., 2015; Versmissen et al., 2019). Previous preclinical studies explored the possible involvement of ET-1 in RTKI-induced hypertension by investigating the role of ET-1 receptor antagonism in preventing such side effect. In particular, the linifanib-mediated hypertensive response was abolished by atrasentan, a selective ET_A receptor antagonist, in telemetered rats (Banfor et al., 2009). However, the dual ET_A/ET_B receptor antagonist bosentan did not prevent the hypertensive response to cediranib in conscious freely moving rats (Carter et al., 2017). Macitentan, a non-selective ET_A/ET_B receptor blocker, hampered the rise in BP in sunitinib-treated rats (Lankhorst, Kappers, et al., 2014a). In this context, it should be noted that macitentan is 50-fold more selective for ET_A receptors than for ET_B receptors (Iglarz et al., 2008). Indeed, endothelin receptor antagonists have a spectrum of selectivity ranging from those with a dual ET_A/ET_B receptor antagonism (bosentan, macitentan and tezosentan) to those with a selective ET_A blockade (ambrisentan, atrasentan, avosentan, clazosentan, darusentan, and sitaxsentan) (Table 6) (Battistini et al., 2006; MacIntyre et al., 2010; Kohan

et al., 2011). Their difference in terms of receptor selectivity should be carefully considered when it comes to their ability to prevent RTKI-induced hypertension. In this regard, the different results obtained with antagonists having distinct selectivity for ET_A and ET_B receptors suggest that the hypertensive effects associated with VEGFR-2 inhibitors may be primarily due to ET_A receptor rather than ET_B receptor (Banfor et al., 2009; Lankhorst, Kappers, et al., 2014a; Carter et al., 2017; Mirabito Colafella et al., 2020).

	Drug	Approval status	ET_A:ET_B blockade ratio	pA_2		References
				ET_AR	ET_BR	
Dual ET_A/ET_BR antagonists	Bosentan	Approved	20:1	7.2	6.0	(Clozel et al., 1994; Battistini et al., 2006)
	Macitentan	Approved	50:1	7.6	5.9	(Iglarz et al., 2008)
	Tezosentan	Investigational	30:1	9.5	7.7	(Merkus et al., 2003)
Selective ET_AR antagonists	Ambrisentan	Approved	4000:1	7.7[b]	5.9[b]	(Bolli et al., 2004; Martínez-Díaz et al., 2023)
	Atrasentan	Phase 3	1200:1	10.5[a]	6.9[a]	(Winn et al., 1996)
	Avosentan	Phase 1	300:1	7.3[b]		(Davenport et al., 2016)
	Clazosentan	Approved	1300:1	9.5	6.4	(Kirkby et al., 2008)
	Darusentan	Investigational	1000:1	8.2[a]	6[a]	(Kirkby et al., 2008)
	Sitaxentan	Withdrawn	6500:1	8.9[b]	5.0[b]	(Kirkby et al., 2008)

Table 6. *List of ET receptor antagonists in clinical use or clinical development. [a] denotes pK_i rather than pA_2; [b] denotes pIC_{50}.*

Understanding the pathophysiological events contributing to RTKIs-induced hypertension is crucial for the development of appropriate mechanism-based treatment options and for the prevention of such cardiovascular complication. As a result, this study aimed to investigate the efficacy of dual ET_A/ET_B receptor antagonism and selective ET_A receptor antagonism in the prevention of the hypertensive response mediated by two VEGFR-2 inhibitors (i.e., axitinib and lenvatinib). In order to clarify the involvement of ET_A and/or ET_B receptors in the development of RTKI-induced hypertension, the choice of bosentan and sitaxentan in this study was based on the selectivity of these agents for endothelin receptors. Indeed, bosentan, firstly approved in 2001 for the treatment of pulmonary arterial hypertension, represents the dual ET_A/ET_B receptor antagonist with the lowest selectivity for ET_A (20:1 ET_A/ET_B selectivity ratio), while sitaxentan, with a 6500:1 ET_A/ET_B selectivity ratio, is the most selective ET_A receptor antagonist available (although it was withdrawn from clinical use in 2010 due to liver toxicity) (Battistini et al., 2006; Maguire & Davenport, 2015). In particular, the use of the Doppler flowmetry model allowed for the study of the impact of dual and selective endothelin receptor antagonists on the pressor effect associated with RTKIs, as well as to simultaneously evaluate the role of this antagonism in preventing the RTKI-mediated alterations of vascular tone in regional vascular beds previously reported (*Chapter 3*).

4.2 AIMS

The work described in *Chapter 4* aimed to:

1. Define whether the activation of endothelin axis has a role in axitinib- and lenvatinib-induced hypertension and the contribution of dual ET_A/ET_B receptor antagonism and selective ET_A receptor antagonism in preventing such response in conscious and freely moving rats.
2. Investigate the efficacy of non-selective ET_A/ET_B receptor blockade and selective ET_A receptor blockade in preventing the changes in regional vascular conductance associated with axitinib and lenvatinib.

4.3 METHODS

4.3.1 In vivo: Pulsed Doppler flowmetry in conscious and freely moving rats

4.3.1.1 ANIMALS AND SURGICAL PROCEDURES

All surgical and experimental procedures were conducted with approval from the UK Home Office and the University of Nottingham, as previously described (*Methods 2.2.1.4*).

Adult male Sprague-Dawley rats weighing between 350 and 500 g were used to perform the pulsed Doppler flowmetry studies described in this chapter (*Methods 2.2.1.4*). Animals were subjected to two rounds of surgeries (*Methods 2.2.1.5)*: the first surgery consisted of the implantation of the Doppler flow probes (*Methods 2.2.1.5.1*), while the second procedure was carried out to insert intraarterial and intravenous catheters (*Methods 2.2.1.5.2*).

4.3.1.2 CARDIOVASCULAR RECORDING

Detailed information on the cardiovascular recordings and statistical analysis can be found in the general methodology (*Methods 2.2.1.7, 2.2.1.9).*

Briefly, rats were indirectly connected to the data acquisition programme (IdeeQ) during the monitoring periods via a tether system *(Methods 2.2.1.7).* HR, BP, renal, mesenteric and hindquarters Doppler shifts were measured and changes in VC in the renal, mesenteric, and hindquarter vascular beds were derived from the changes in MAP and Doppler shift (*Methods 2.2.1.7)*. PP was also derived as the difference between SBP and DBP (*Methods 2.2.1.7).*

For all experiments, time-averaged data are shown as changes from baseline [HR ($beats.min^{-1}$); MAP (mmHg); VC (%); SBP (mmHg); DBP (mmHg); PP (mmHg)] (*Methods 2.2.1.9)*. A Friedman's test was used for within-group comparisons to baseline; this data analysis was performed on the first 2 days of the experimental period due to changes in sample size (n) after day 2 (*Methods 2.2.1.9)*. A Mann-Whitney U test for integrated area under or above curve analysis was used for comparisons between groups (*Methods 2.2.1.9)*. A Mann-Whitney U test was also performed for comparisons between groups at a specific time point. A value of $p<0.05$ was considered significant (*Methods 2.2.1.9).*

4.3.1.3 EXPERIMENTAL PROTOCOL

This series of experiments was run for 2 days. Experiments were run with treatment groups of 7 to 8 rats (*Methods 2.2.1.8.2).*

Three groups of rats were used for each RTKI, namely axitinib and lenvatinib, to assess the role of endothelin antagonism in the prevention of the cardiovascular responses associated with these agents. Rats were randomly assigned to one of three treatment groups: axitinib or lenvatinib in the presence of vehicle (40% HPβCD in sterile saline), axitinib or lenvatinib in the presence of a dual ET_A and ET_B receptor antagonist (bosentan), axitinib or lenvatinib in

the presence of a selective ET_A receptor antagonist (sitaxentan). On day 1 of the experiment, after a period of baseline recordings, rats were dosed with bosentan (15 $mg.kg^{-1}$) or sitaxentan (5 $mg.kg^{-1}$) as an intravenous bolus followed by a 5-h intravenous infusion (for axitinib groups) or a 6-h infusion (for lenvatinib groups) at the same dose (*Methods 2.2.1.8.2)*. The contemporaneous control group received vehicle (40% HPβCD in sterile saline) as an intravenous bolus followed by a 5-h (for axitinib groups) or 6-h (for lenvatinib groups) intravenous infusion at the same dose (*Methods 2.2.1.8.2)*.

After 1-h infusion of the endothelin antagonists or vehicle, axitinib (3 $mg.kg^{-1}$) or lenvatinib (1 $mg.kg^{-1}$) was administered to all animals as an intravenous bolus followed by a 1-h intravenous infusion at the same dose (*Methods 2.2.1.8.2).* The same treatment regimen was followed on day 2 after a baseline recording period. At the end of day 2, all groups received ET-1 (administered as bolus) at the following concentrations: 0.1 μM, 0.3 μM and 1 μM (3 min per concentration) (*Methods 2.2.1.8.2).*

4.4 RESULTS

To investigate the role of dual ET_A/ET_B or selective ET_A receptor blockade in the prevention of axitinib- and lenvatinib-induced haemodynamic changes, the pulsed Doppler flowmetry model was used in conscious and freely moving rats.

Baseline cardiovascular parameters taken before the administration of vehicle, dual ET_A and ET_B receptor antagonist (bosentan) or selective ET_A receptor antagonist (sitaxentan) are shown in Table 7 (axitinib-treated animals) and Table 8 (lenvatinib-treated animals).

	Vehicle		Bosentan		Sitaxentan	
	Mean ± SEM	*n*	*Mean ± SEM*	*n*	*Mean ± SEM*	*n*
HR (beats.min^{-1})	358 ± 15	8	364 ± 17	7	372 ± 12	7
MAP (mmHg)	112 ± 5	8	116 ± 5	7	109 ± 6	7
DBP (mmHg)	98 ± 4	8	98 ± 4	7	92 ± 5	7
SBP (mmHg)	146 ± 7	8	149 ± 6	7	146 ± 9	7
RVC (U)	66 ± 14	8	43 ± 5	7	77 ± 14	6
MVC (U)	67 ± 8	8	61 ± 8	7	65 ± 4	7
HVC (U)	44 ± 6	5	35 ± 4	7	39 ± 6	7

Table 7. *Baseline cardiovascular variables prior to administration of vehicle or dual ET_A and ET_B receptor antagonist (bosentan) or selective ET_A receptor antagonist (sitaxentan) in axitinib-treated rats. Values are mean ± SEM. Units of vascular conductance (VC) are kHz. mmHg^{-1} x 10^3. U, units.*

	Vehicle		Bosentan		Sitaxentan	
	Mean ± SEM	*n*	*Mean ± SEM*	*n*	*Mean ± SEM*	*n*
HR (beats.min^{-1})	353 ± 8	8	353 ± 17	7	355 ± 14	7
MAP (mmHg)	106 ± 2	8	99 ± 5	7	97 ± 5	7
DBP (mmHg)	90 ± 2	8	85 ± 5	7	83 ± 4	7
SBP (mmHg)	139 ± 3	8	129 ± 6	7	127 ± 6	7
RVC (U)	63 ± 8	6	81± 14	6	76 ± 13	7
MVC (U)	74 ± 11	8	94 ± 16	7	92 ± 14	7
HVC (U)	42 ± 8	5	45 ± 8	7	47 ± 7	7

Table 8. *Baseline cardiovascular variables prior to administration of vehicle or dual ET_A and ET_B receptor antagonist (bosentan) or selective ET_A receptor antagonist (sitaxentan) in lenvatinib-*

receiving rats. Values are mean ± SEM. Units of vascular conductance (VC) are kHz. $mmHg^{-1}$ x 10^3. U, units.

4.4.1 Role of dual versus selective endothelin receptor antagonists in the prevention of axitinib-induced haemodynamic changes

Administration of axitinib in animals pre-treated with vehicle caused a significant rise in MAP, resulting in a maximal increase of 23% on day 2 (#p<0.05, Friedman's test; Figure 45B and 47A). Such a pressor effect was not accompanied by corresponding changes in HR (Figure 45A and 47A). The axitinib-induced hypertensive response in vehicle-treated animals was associated with a consistent reduction in MVC (#p<0.05, Friedman's test; Figure 45D and 47D), while no significant alterations in RVC and HVC were observed during the experimental protocol (Figure 45C-E and 47C-E). Specifically, a maximal reduction of 37% and 35% in MVC was reached on day 1 and day 2, respectively (Figure 45D and 47D). Axitinib treatment also increased DBP and SBP, which reached significance on day 2, where also a rise of PP was observed (#p<0.05, Friedman's test; Figure 46A-C and 48A-C).

The co-treatment with bosentan (dual ET_A and ET_B receptor antagonist) completely prevented the axitinib-induced increase in MAP (θp<0.05, Mann-Whitney U test, integrated area under curve, 0–28 h; *p<0.05, Mann-Whitney U test to determine differences at each time point; Figure 45B). In addition, the axitinib-induced mesenteric vasoconstrictive response was consistently abolished by the co-treatment with the dual ET_A and ET_B receptor antagonist (*p<0.05, Mann-Whitney U test to determine differences at each time point; Figure 45D). Bosentan counteracted the effect of axitinib on HVC on day 1, yet this reached statistical significance only at the 3-h time point post treatment with this RTKI (*p<0.05, Mann-Whitney U test to determine differences at each time point; Figure 45E). However, the dual antagonism did not elicit any notable effect on RVC (Figure 45C). The axitinib-induced rise in DBP and SBP was abolished by bosentan, while no alteration of PP was detected with this agent (*p<0.05, Mann-Whitney U test to determine differences at each time point; Figure 46A-C).

In an attempt to confirm that endothelial ET_B receptors were blocked by bosentan and not by sitaxentan, ET-1 was administered by intravenous infusion at the end of day 2 at 0.1 μM, 0.3 μM and 1 μM. In vehicle-receiving animals, the low dose of ET-1 (0.1 μM) did not cause alteration of MAP, HR or vascular conductances (Figure 45). The mid dose of ET-1 (0.3 μM)

was associated with a small initial and transient depressor effect on BP and tachycardia, although both did not reach significance (Figure 45A-B and 47A-B). These responses were accompanied by a significant increase in HVC (within 1 min) and a reduction of MVC (at 3-min time point), with no alterations in the renal vasculature (#p<0.05, Friedman's test; Figure 45C-E and 47C-E). The high dose of ET-1 (1 µM) elicited an initial and transient (within 1 min) drop in MAP and a tachycardic effect, accompanied by an increase in HVC at the same time point (#p<0.05, Friedman's test; Figure 45A-B-E and 47A-B-E). Reductions in RVC and MVC also occurred in response to high dose of ET-1 (#p<0.05, Friedman's test; Figure 45C-D and 47C-D).

The pressor and tachycardic effects of ET-1 were abolished in the group co-treated with bosentan, for which an increase in MAP was only observed at the last time point of the high dose of ET-1 (#p<0.05, Friedman's test; Figure 45A-B). In presence of bosentan, the mesenteric vasoconstriction was inhibited both in response to the low and mid dose of ET-1 (*p<0.05, Mann-Whitney U test to determine differences at each time point; Figure 45D), although a significant reduction of MVC was still observed at the high dose of ET-1 (#p<0.05, Friedman's test; Figure 45D). The co-treatment with bosentan, fully prevented the effect of ET-1 on DBP and SBP, although no alterations were observed on PP (*p<0.05, Mann-Whitney U test to determine differences at each time point; Figure 46A-B).

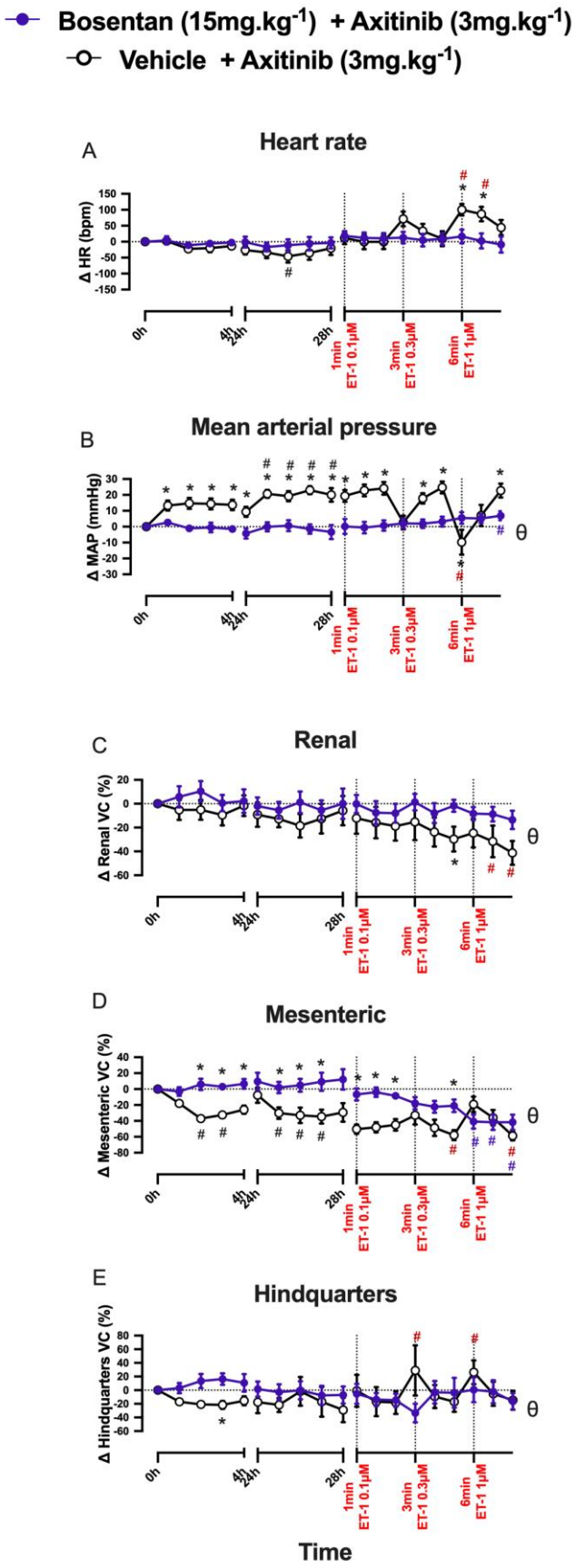

Figure 45. *Role of dual ET_A and ET_B receptor antagonist (bosentan) in axitinib-induced cardiovascular responses in conscious, freely moving rats. Animals were dosed with bosentan (15 mg.kg^{-1}) or vehicle*

*as an intravenous bolus followed by a 5-h intravenous infusion. One hour after commencement of the endothelin receptor antagonist or vehicle infusion, axitinib (3 mg.kg^{-1}) was administered to all animals as an intravenous bolus followed by a 1-h intravenous infusion. Same dose regimen was repeated on day 2, at the end of which ET-1 was administered as bolus at increasing concentrations Details of the experimental protocol are described in Methods 2.2.1.8.2. Data points are means; vertical bars represent SEM. Friedman's test was performed for within-group comparisons to baseline (0h time point was used as a baseline for the entire 28h period prior to the administration of ET-1, while 28h time point was used as a baseline for ET-1 dose-response (#p<0.05 vs. baseline). Mann-Whitney U test was conducted between treated and vehicle control groups for a comparison of area under/over the curve (θp< 0.05) and to determine differences at each time point (*p<0.05, Mann-Whitney U test).*

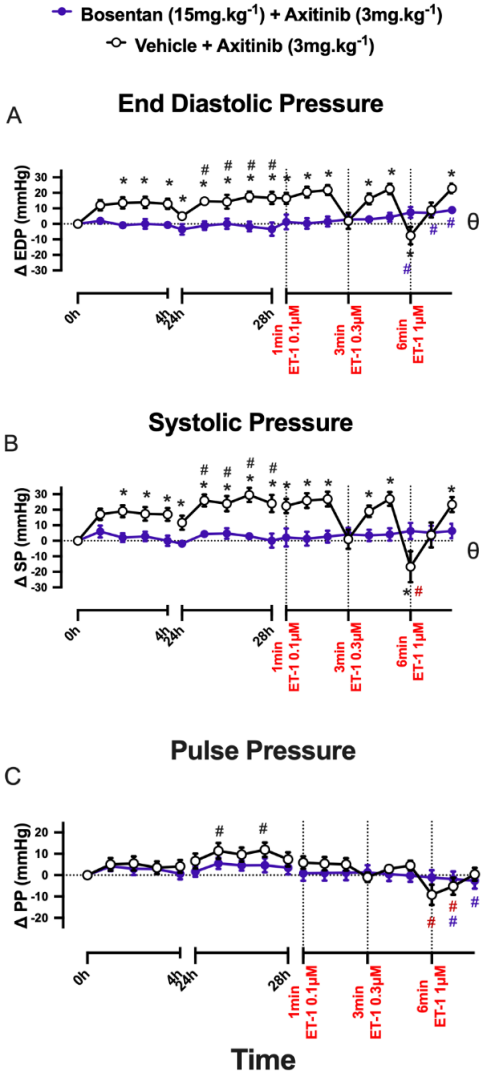

Figure 46. *Role of dual ET_A and ET_B receptor antagonist (bosentan) in axitinib-induced changes in DBP, SBP and PP in conscious, freely moving rats. Animals were dosed with bosentan (15 mg.kg^{-1}) or vehicle as an intravenous bolus followed by a 5-h intravenous infusion. One hour after*

*commencement of the endothelin receptor antagonist or vehicle infusion, axitinib (3 mg.kg^{-1}) was administered to all animals as an intravenous bolus followed by a 1-h intravenous infusion. Same dose regimen was repeated on day 2, at the end of which ET-1 was administered as bolus at increasing concentrations Details of the experimental protocol are described in Methods 2.2.1.8.2. Data points are means; vertical bars represent SEM. Friedman's test was performed for within-group comparisons to baseline (0h time point was used as a baseline for the entire 28h period prior to the administration of ET-1, while 28h time point was used as a baseline for ET-1 dose-response (#p<0.05 vs. baseline). Mann-Whitney U test was conducted between treated and vehicle control groups for a comparison of area under/over the curve (θp< 0.05) and to determine differences at each time point (*p<0.05, Mann-Whitney U test).*

The co-treatment with sitaxentan (selective ET_A receptor antagonist) fully abolished the axitinib-induced increase in MAP (θp<0.05, Mann-Whitney U test, integrated area under curve, 0–28 h; *p<0.05, Mann-Whitney U test to determine differences at each time point; Figure 47B). The selective ET_A receptor antagonism also attenuated axitinib-induced mesenteric vasoconstrictive response (*p<0.05, Mann-Whitney U test to determine differences at each time point; Figure 47D). No significant effects were observed on RVC in response to sitaxentan in axitinib-treated animals, while HVC was significantly improved by selective ET_A receptor antagonism exclusively on day 1 and at a specific time point (3h) (Figure 47C-E). The selective ET_A receptor antagonist completely abolished the RTKI-induced rise in DBP and SBP, while also preventing the effect of axitinib on PP (*p<0.05, Mann-Whitney U test to determine differences at each time point; Figure 48A-C).

The cardiovascular changes following ET-1 administration in vehicle-treated animals have been described above. In keeping with its better selectivity for ET_A receptors, the co-treatment with sitaxentan did not prevent the vascular changes induced by ET-1 when compared to the vehicle group (Figure 47A-E and 48A-C).

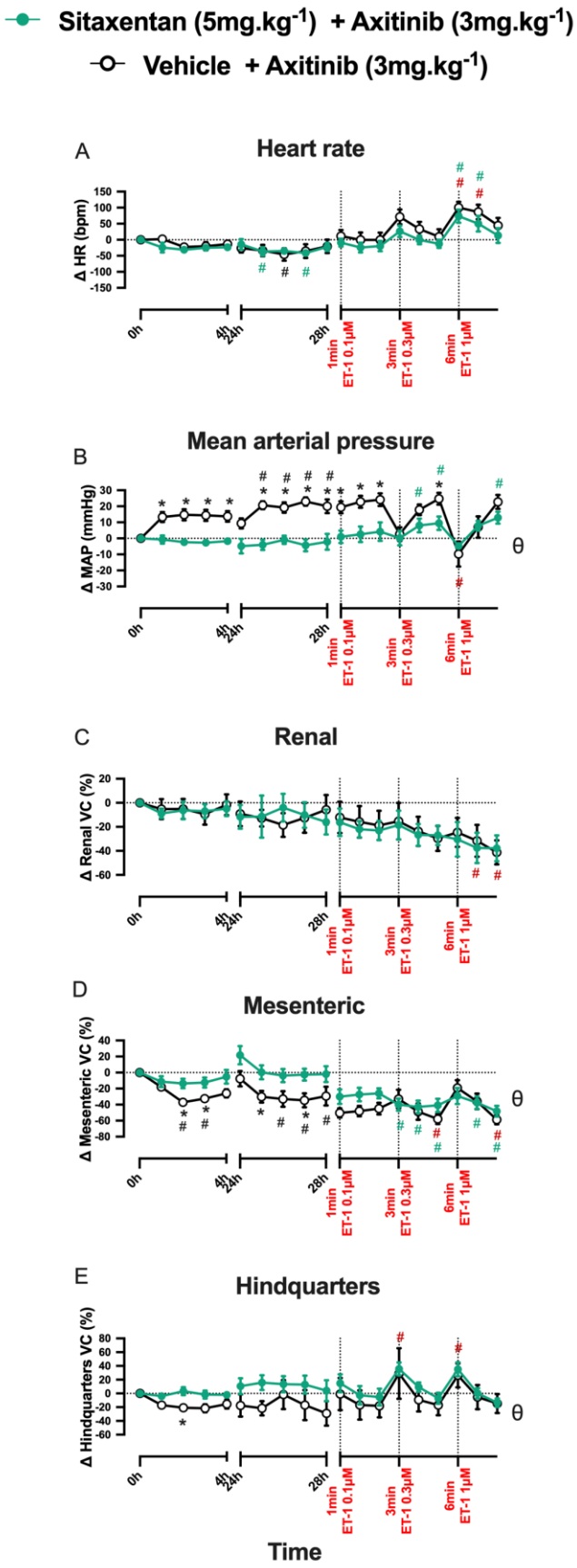

Figure 47. *Role of selective ET_A receptor antagonist (sitaxentan) in axitinib-induced cardiovascular responses in conscious, freely moving rats. Animals were dosed with sitaxentan (5 mg.kg^{-1}) or vehicle*

*as an intravenous bolus followed by a 5-h intravenous infusion. One hour after commencement of the endothelin receptor antagonist or vehicle infusion, axitinib (3 mg.kg^{-1}) was administered to all animals as an intravenous bolus followed by a 1-h intravenous infusion. Same dose regimen was repeated on day 2, at the end of which ET-1 was administered as bolus at increasing concentrations Details of the experimental protocol are described in Methods 2.2.1.8.2. Data points are means; vertical bars represent SEM. Friedman's test was performed for within-group comparisons to baseline (0h time point was used as a baseline for the entire 28h period prior to the administration of ET-1, while 28h time point was used as a baseline for ET-1 dose-response (#p<0.05 vs. baseline). Mann-Whitney U test was conducted between treated and vehicle control groups for a comparison of area under/over the curve (θp< 0.05) and to determine differences at each time point (*p<0.05, Mann-Whitney U test).*

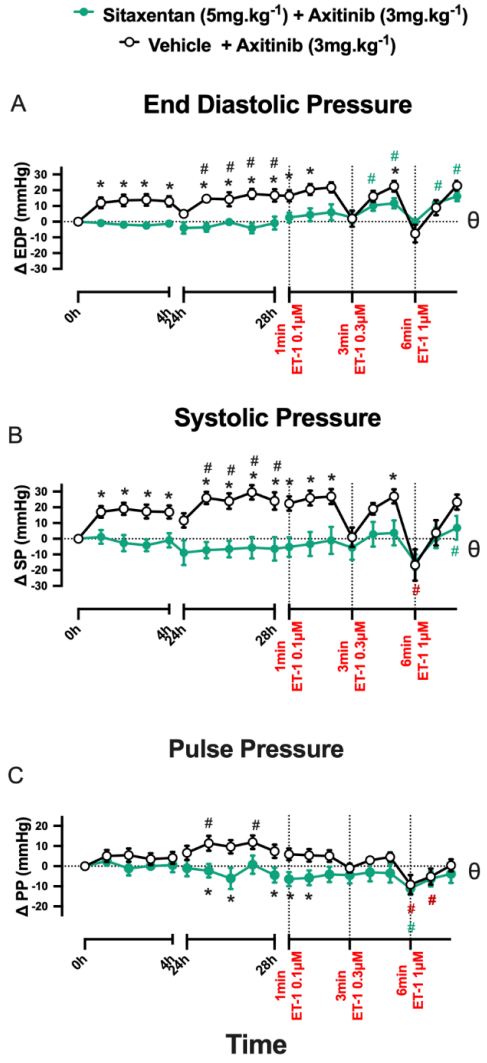

Figure 48. *Role of selective ET_A receptor antagonist (sitaxentan) in axitinib-induced changes in DBP, SBP and PP in conscious, freely moving rats. Animals were dosed with sitaxentan (5 mg.kg^{-1}) or vehicle as an intravenous bolus followed by a 5-h intravenous infusion. One hour after*

*commencement of the endothelin receptor antagonist or vehicle infusion, axitinib (3 mg.kg^{-1}) was administered to all animals as an intravenous bolus followed by a 1-h intravenous infusion. Same dose regimen was repeated on day 2, at the end of which ET-1 was administered as bolus at increasing concentrations Details of the experimental protocol are described in Methods 2.2.1.8.2. Data points are means; vertical bars represent SEM. Friedman's test was performed for within-group comparisons to baseline (0h time point was used as a baseline for the entire 28h period prior to the administration of ET-1, while 28h time point was used as a baseline for ET-1 dose-response (#p<0.05 vs. baseline). Mann-Whitney U test was conducted between treated and vehicle control groups for a comparison of area under/over the curve (θp< 0.05) and to determine differences at each time point (*p<0.05, Mann-Whitney U test).*

4.4.2 Role of dual versus selective endothelin receptor antagonists in the prevention of lenvatinib-induced haemodynamic changes

In presence of vehicle, lenvatinib evoked a significant elevation in MAP on day 2, where a maximal increase of 24% was observed (#p<0.05, Friedman's test; Figure 49B and 51B), without notable alteration of HR (Figure 49A and 51A). In vehicle-treated animals lenvatinib caused a significant reduction in MVC (#p<0.05, Friedman's test; Figure 49D and 51D). In particular a maximal reduction of 36% and 42% in MVC was reached on day 1 and day 2, respectively (Figure 49D and 51D). Except a reduced HVC at 27h time point, no other marked alterations of RVC and HVC were reported during the experimental protocol (Figure 49C-E and 51C-E). Lenvatinib caused a rise of both DBP and SBP, reaching a statistical significance on day 2 (#p<0.05, Friedman's test; Figure 50A-B and 52A-B). No alteration of PP was detected in response to this RTKI during the experimental period (Figure 50C and 52C).

The co-treatment with bosentan did not prevent the lenvatinib-induced hypertensive effect, except a significant reduction of MAP at 4h time point (θp<0.05, Mann-Whitney U test, integrated area under curve, 0–29 h; *p<0.05, Mann-Whitney U test to determine differences at each time point; Figure 49A-B). Nevertheless, the dual ET_A and ET_B receptor antagonist bosentan was able to ameliorate the effect of lenvatinib on MVC, particularly on day 1 (θp<0.05, Mann-Whitney U test, integrated area under curve, 0–29 h; *p<0.05, Mann-Whitney U test to determine differences at each time point; Figure 49D). The dual antagonism did not evoke any notable effect on RVC and HVC in lenvatinib-treated rats when compared to control group (Figure 49C-E). Bosentan did not show any significant role in preventing lenvatinib-induced increase in DBP, SBP and PP (Figure 50A-C).

As before, we evaluated whether endothelial ET_B receptors were adequately blocked by bosentan and not by sitaxentan by administering ET-1 by intravenous infusion at the end of the experimental period. Thus, ET-1 was administered at the end of d 2 at 0.1 µM, 0.3 µM and 1 µM (3 min per concentration). In animals co-treated with vehicle and lenvatinib, the effect of ET-1 were comparable to those already reported for vehicle and axitinib co-treated rats. The only difference was in a more sustained reduction of RVC in response to both mid and high dose of the peptide (#p<0.05, Friedman's test; Figure 49C and 51C).

In the presence of bosentan, low dose of ET-1 did not elicit any effect on MAP, while the mid dose (at 3-min time point) and the high dose of ET-1 were associated with a significant pressor effect (#p<0.05, Friedman's test; Figure 49A-B). However, the effects of ET-1 on MAP observed in the vehicle group were still prevented in presence of bosentan at specific time points (*p<0.05, Friedman's test; Figure 49B). The tachycardic response to high dose of ET-1 observed in the vehicle group was also prevented in the bosentan-treated rats (#p<0.05, Friedman's test; Figure 49A). In addition, co-treatment with bosentan improved MVC, mainly at the low and mid dose of ET-1, while also preventing the increased HVC associated with high dose of ET-1 (*p<0.05, Friedman's test; Figure 49C-E). The co-treatment with bosentan abolished the effect of ET-1 on DBP and SBP only at specific time points and no alterations were observed on PP (*p<0.05, Mann-Whitney U test to determine differences at each time point; Figure 50A-C).

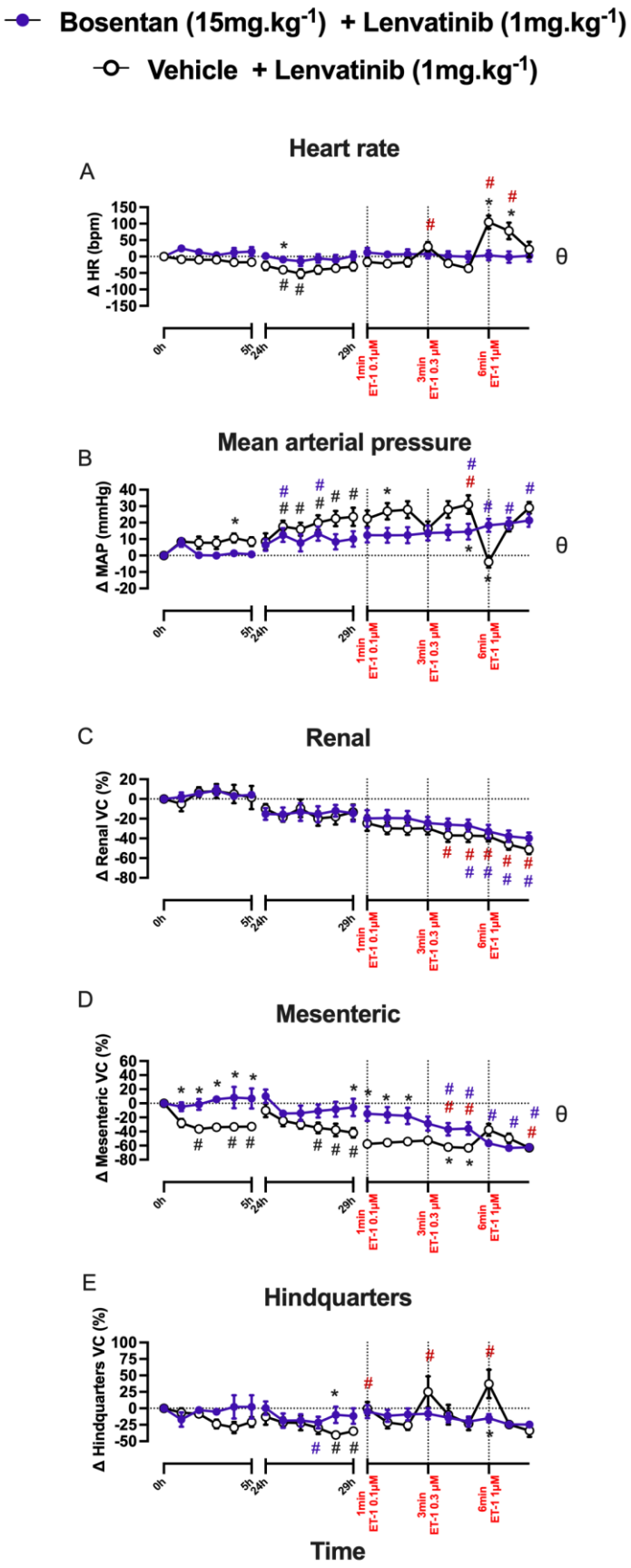

Figure 49. *Role of dual ET_A and ET_B receptor antagonist (bosentan) in lenvatinib-induced cardiovascular responses in conscious, freely moving rats. Animals were dosed with bosentan (15*

*mg.kg^{-1}) or vehicle as an intravenous bolus followed by a 6-h intravenous infusion. One hour after commencement of the endothelin receptor antagonist or vehicle infusion, lenvatinib (1 mg.kg^{-1}) was administered to all animals as an intravenous bolus followed by a 1-h intravenous infusion. Same dose regimen was repeated on day 2, at the end of which ET-1 was administered as bolus at increasing concentrations Details of the experimental protocol are described in Methods 2.2.1.8.2. Data points are means; vertical bars represent SEM. Friedman's test was performed for within-group comparisons to baseline (0h time point was used as a baseline for the entire 29h period prior to the administration of ET-1, while 29h time point was used as a baseline for ET-1 dose-response (#p<0.05 vs. baseline). Mann-Whitney U test was conducted between treated and vehicle control groups for a comparison of area under/over the curve (θp< 0.05) and to determine differences at each time point (*p<0.05, Mann-Whitney U test).*

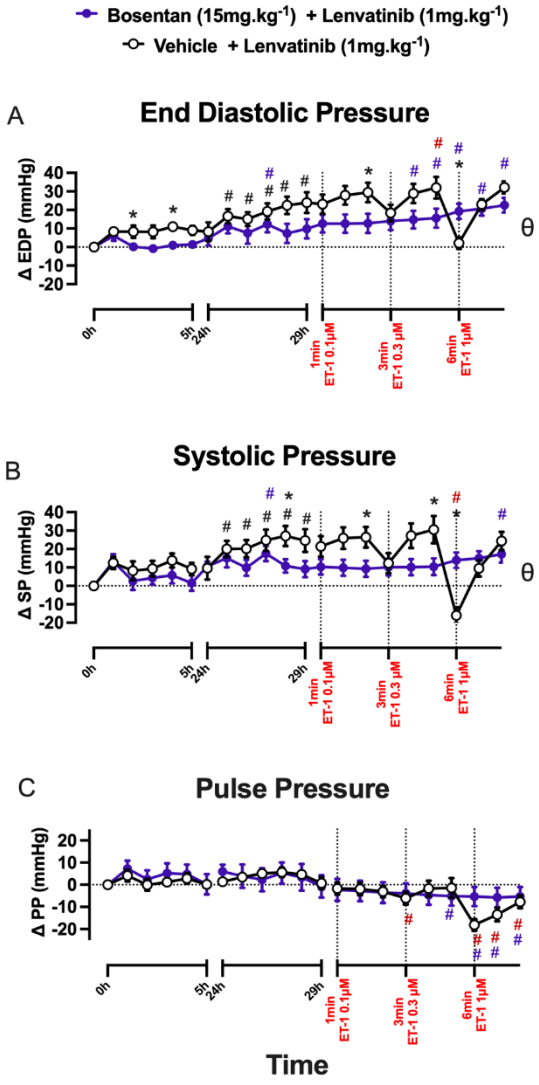

Figure 50. *Role of dual ET_A and ET_B receptor antagonist (bosentan) in lenvatinib-induced changes in DBP, SBP and PP in conscious, freely moving rats. Animals were dosed with bosentan (15 mg.kg^{-1}) or vehicle as an intravenous bolus followed by a 6-h intravenous infusion. One hour after*

*commencement of the endothelin receptor antagonist or vehicle infusion, lenvatinib (1 mg.kg^{-1}) was administered to all animals as an intravenous bolus followed by a 1-h intravenous infusion. Same dose regimen was repeated on day 2, at the end of which ET-1 was administered as bolus at increasing concentrations Details of the experimental protocol are described in Methods 2.2.1.8.2. Data points are means; vertical bars represent SEM. Friedman's test was performed for within-group comparisons to baseline (0h time point was used as a baseline for the entire 29h period prior to the administration of ET-1, while 29h time point was used as a baseline for ET-1 dose-response (#p<0.05 vs. baseline). Mann-Whitney U test was conducted between treated and vehicle control groups for a comparison of area under/over the curve (θp< 0.05) and to determine differences at each time point (*p<0.05, Mann-Whitney U test).*

Sitaxentan completely attenuated the lenvatinib-induced hypertensive effect (θp<0.05, Mann-Whitney U test, integrated area under curve, 0–29 h; *p<0.05, Mann-Whitney U test to determine differences at each time point; Figure 51B). Co-treatment with sitaxentan was also associated with a significant reduction of HR on d2 of experimental period (#p<0.05, Friedman's test; Figure 51A), although no difference was observed when compared to the control group. As observed for axitinib, the selective ET_A receptor antagonist was able to prevent the lenvatinib-induced mesenteric vasoconstriction mainly on day 1, although a significant attenuation was also reported at the last time point on day 2 (θp<0.05, Mann-Whitney U test, integrated area under curve, 0–29 h; *p<0.05, Mann-Whitney U test to determine differences at each time point; Figure 51D). In presence of sitaxentan, no significant effects were observed on RVC in lenvatinib-treated animals, while a significant improvement of HVC was reached exclusively at specific time points, specifically 5h and 28h (Figure 51C-E).

As reported for axitinib, the lenvatinib-induced increase in DBP and SBP was prevented by selective ET_A receptor antagonism (*p<0.05, Figure 52A-B). Similarly, the co-treatment with sitaxentan was also associated with a reduction of PP in response to lenvatinib (θp<0.05, Mann-Whitney U test, integrated area under curve, 0–29 h; *p<0.05, Mann-Whitney U test to determine differences at each time point; Figure 52C).

The haemodynamic effects due to ET-1 administration in vehicle-treated animals have been previously outlined. During the administration of low and mid doses of ET-1, the co-treatment with sitaxentan was still able to attenuate the hypertensive response to lenvatinib, while at the high dose of ET-1 such effect was reduced, except for the 3-min time point

(*$p<0.05$, Mann-Whitney U test to determine differences at each time point; Figure 51B). Consistent with its selectivity for ET_A receptors, sitaxentan did not prevent the ET-1-mediated responses in terms of HR and VCs under any dose of the peptide (Figure 51A-C-D-E).

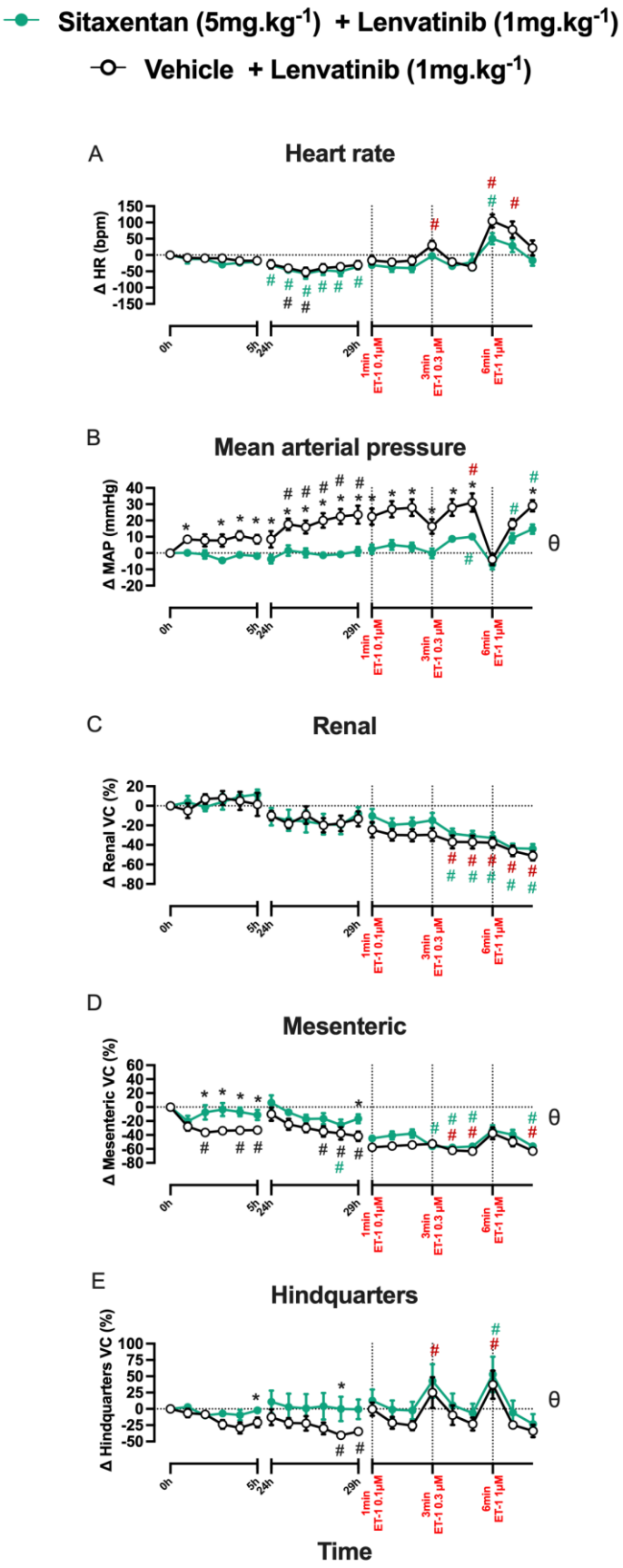

Figure 51. *Role of selective ET_A receptor antagonist (sitaxentan) in lenvatinib-induced cardiovascular responses in conscious, freely moving rats. Animals were dosed with sitaxentan (5 mg.kg^{-1}) or vehicle*

*as an intravenous bolus followed by a 6-h intravenous infusion. One hour after commencement of the endothelin receptor antagonist or vehicle infusion, lenvatinib (1 mg.kg^{-1}) was administered to all animals as an intravenous bolus followed by a 1-h intravenous infusion. Same dose regimen was repeated on day 2, at the end of which ET-1 was administered as bolus at increasing concentrations Details of the experimental protocol are described in Methods 2.2.1.8.2. Data points are means; vertical bars represent SEM. Friedman's test was performed for within-group comparisons to baseline (0h time point was used as a baseline for the entire 29h period prior to the administration of ET-1, while 29h time point was used as a baseline for ET-1 dose-response (#p<0.05 vs. baseline). Mann-Whitney U test was conducted between treated and vehicle control groups for a comparison of area under/over the curve (θp< 0.05) and to determine differences at each time point (*p<0.05, Mann-Whitney U test).*

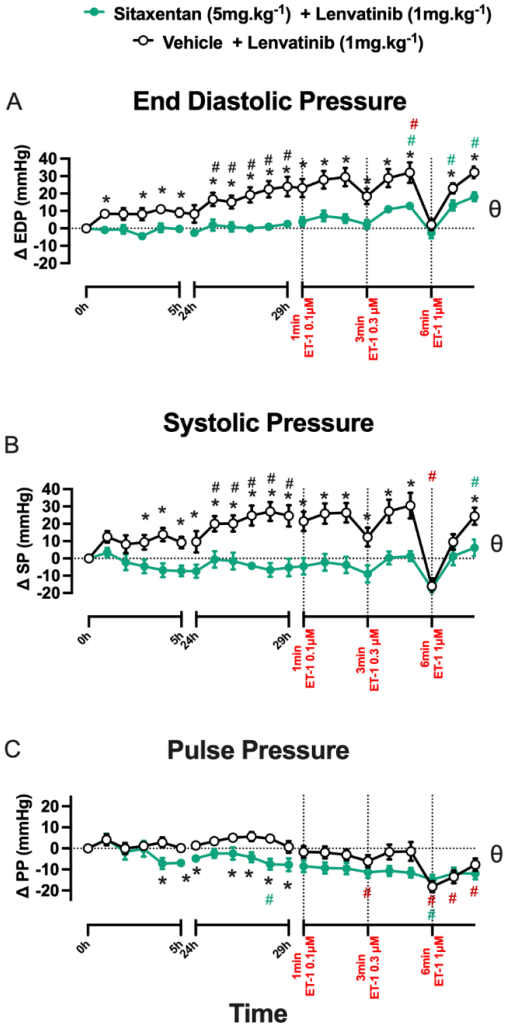

Figure 52. *Role of selective ET_A receptor antagonist (sitaxentan) in lenvatinib-induced changes in DBP, SBP and PP in conscious, freely moving rats. Animals were dosed with sitaxentan (5 mg.kg^{-1}) or vehicle as an intravenous bolus followed by a 6-h intravenous infusion. One hour after commencement of the endothelin receptor antagonist or vehicle infusion, lenvatinib (1 mg.kg^{-1}) was*

*administered to all animals as an intravenous bolus followed by a 1-h intravenous infusion. Same dose regimen was repeated on day 2, at the end of which ET-1 was administered as bolus at increasing concentrations Details of the experimental protocol are described in Methods 2.2.1.8.2. Data points are means; vertical bars represent SEM. Friedman's test was performed for within-group comparisons to baseline (0h time point was used as a baseline for the entire 29h period prior to the administration of ET-1, while 29h time point was used as a baseline for ET-1 dose-response (#p<0.05 vs. baseline). Mann-Whitney U test was conducted between treated and vehicle control groups for a comparison of area under/over the curve (θp< 0.05) and to determine differences at each time point (*p<0.05, Mann-Whitney U test).*

4.5 DISCUSSION

The activation of endothelin axis has been identified as a crucial determinant in the hypertensive effect associated with antiangiogenic therapies (Banfor et al., 2009; Kappers et al., 2010; M. H. Kappers et al., 2011; Kappers et al., 2012; Lankhorst, Kappers, et al., 2014a; Mirabito Colafella et al., 2020). The present study unequivocally established the contribution of ET-1 to RTKIs-induced hypertension. In particular, our results have demonstrated that such increase in BP is purely mediated by ET_A receptors, as axitinib- and lenvatinib-induced hypertension was consistently prevented by the selective ET_A receptor antagonist. Additionally, sitaxentan at a dose of 5 $mg.kg^{-1}$ did not prevent the vascular responses due to the administration of ET-1, suggesting that at the dose at which sitaxentan prevented the axitinib- and lenvatinib-induced hypertensive effect ET_B receptors have not been inhibited.

The detection of elevated ET-1 plasma levels in patients and animals treated with sunitinib, as well as the observation that such increase shows the same dose-dependency as the rise in BP during antiangiogenic treatment, were the first evidence of an implication of the endothelin system in the hypertensive response associated with VEGFR-2 inhibitors (Kappers et al., 2010; Lankhorst, Baelde, et al., 2015). Subsequent studies revealed that linifanib-induced hypertension was suppressed by co-treatment with the selective ET_A receptor antagonist atrasentan in telemetered Sprague-Dawley rats (Banfor et al., 2009). Analogously, dual ET_A/ET_B receptor antagonism with tezosentan prevented the rise in BP in response to sunitinib in chronically instrumented swine (Kappers et al., 2012). In addition, the dual ET_A/ET_B receptor antagonist macitentan abolished the effect of sunitinib on BP in Wistar Kyoto rats (Lankhorst, Kappers, et al., 2014b) suggesting a crucial role of ET-1 in the pathogenesis of hypertension in presence of VEGFR-2 inhibition. However, bosentan, an antagonist with non-selective affinity for ET_A/ET_B receptor, was not associated with a suppression of the hypertensive response to cediranib in conscious and freely moving rats

(Carter et al., 2017). This finding support the hypothesis that the hypertensive effects due to VEGFR-2 inhibitors may be predominantly associated with the activation of ET_A receptor rather than the ET_B subtype (Mirabito Colafella et al., 2020). Although the dual ET_A/ET_B receptor antagonists atrasentan, tezosentan and macitentan attenuated the RTKI-induced hypertension, it is worth noting that they all display an higher selectivity for ET_A receptor than bosentan (Merkus et al., 2003; Battistini et al., 2006; Iglarz et al., 2008; Martínez-Díaz et al., 2023). While bosentan exhibits an ET_A:ET_B blockade ratio of 20:1, atrasentan, tezosentan and macitentan show an ET_A:ET_B blockade ratio of 1200:1, 30:1 and 50:1, respectively (Merkus et al., 2003; Battistini et al., 2006; Iglarz et al., 2008; Martínez-Díaz et al., 2023). As a result, in order to fully characterise the net contribution of ET_A and ET_B receptors in the regulation of BP and regional vascular tone in response to axitinib and lenvatinib in conscious and freely moving animals, the present study used bosentan as a clinically approved ET_A/ET_B receptor antagonist with the lowest selectivity for ET_A receptor and sitaxentan as the most selective ET_A receptor antagonist clinically developed (ET_A:ET_B blockade ratio of 6500:1) (Battistini et al., 2006).

Sitaxentan fully prevented the hypertensive response to axitinib and lenvatinib, while the dual ET_A/ET_B receptor antagonism with bosentan abolished the axitinib-induced hypertension but did not cause any significant reduction in the lenvatinib-induced pressor effect. The same effects described for MAP in response to bosentan and sitaxentan were also observed for DBP and SBP, where both of these components were strongly influenced by axitinib and lenvatinib and their increase was effectively prevented by the selective ET_A receptor antagonism. In addition, the co-treatment with the selective ET_A receptor antagonist significantly reduced the PP in axitinib- and lenvatinib-treated rats. These findings strongly suggest that the hypertensive effect of axitinib and lenvatinib is due to an activation of the ET-1 axis and that such response is exclusively regulated by the activation of ET_A receptors. The effects observed in response to ET-1 seem to confirm this. Indeed, as ET-1 was administered intravenously, it is unlikely that it was able to reach VSMCs and exert its effect on both ET_A and ET_B receptors at this level. More likely, the responses observed following ET-1 administration are rather due to the activation of endothelial ET_B receptors. In this regard, the vascular effects due to the intravenous administration of ET-1 were prevented by the co-treatment with bosentan but not by the co-treatment with sitaxentan, showing that ET_B receptor antagonism was absent during the co-treatment with sitaxentan.

These data suggest that the reduction of MVC is independent of axitinib- and lenvatinib-induced hypertensive effect and it may be mainly mediated by ET_B receptors. Indeed,

although both bosentan and sitaxentan fully attenuated axitinib-induced hypertension, only bosentan was able to consistently abolish the reduction of MVC observed with this RTKI. As for lenvatinib, bosentan was associated with a significant attenuation of its effect on MVC on day 1, which was not accompanied by alteration of BP. At the same time, sitaxentan, although abolishing the lenvatinib-induced pressor effect throughout all the experimental period, was associated with an attenuation of mesenteric vasoconstriction only on day 1, therefore reinforcing the hypothesis that the effect of RTKIs on BP occurs independently from their effect on mesenteric vascular tone. This *in vivo* data, suggesting that mesenteric vascular tone during VEGFR-2 inhibition is mainly mediated by ET_B receptors, is conflicting with previous studies performed *in vitro* or on isolated mesenteric arteries, which were supportive of an ET_A receptor-mediated mesenteric vasoconstriction (D'Orléans-Juste et al., 1993; Deng et al., 1995). On the contrary, a subsequent study from Mickley *et al.* clarified that the dual blockade of both ET_A and ET_B receptor blockade was necessary to fully inhibit the vasoconstrictive effect of ET-1 in rat isolated mesenteric arteries, while the selective ET_A antagonism alone only led to an incomplete inhibition of the ET-1 induced mesenteric vasoconstriction (Mickley et al., 1997). In line with this *ex vivo* observation, the mesenteric vasoconstriction induced by ET-1 was found to be unaffected by ET_A receptor-antagonism both in conscious rats and anaesthetised ganglion-blocked rats (Gardiner et al., 1994; Allcock et al., 1995), thus supporting our findings and a possible ET_B receptor-mediated mesenteric vasoconstriction. This hypothesis may appear in contradiction with the vasodilating role of ET_B receptors. However, it should be noted that this subtype of endothelin receptor is not only present in the endothelium, where it mediates vasodilation by promoting the release of several endothelium-derived relaxing factors, but also on VSMCs, where it evokes a contractile response via different mechanisms, including PKC and MAPK pathways, as well as a rise in intracellular Ca^{2+} concentration (White et al., 1993; Mazzuca & Khalil, 2012). This would explain why bosentan, by simultaneously antagonising ET_B receptors (both on endothelium and VSMCs) and ET_A receptors, resulted in a more marked vasodilation of mesenteric artery than the selective ET_A receptor blockade with sitaxentan. However, to adequately establish the involvement of ET_B receptors in the RTKI-induced mesenteric vasoconstriction, additional studies with an antagonist selective for ET_B receptor would be necessary.

Axitinib and lenvatinib did not elicit any notable effect on RVC over the experimental period. Both the co-treatment with bosentan and sitaxentan did not interfere with such response. Although no renal vasoconstriction was observed with the two RTKIs tested, a vasodilatory

effect in the renal vascular bed in response to sitaxentan was expected (Gardiner et al., 1994). Indeed, although ET_A receptors are the prevalent subtype in the medial smooth muscle layer of all vessels, ET_B receptors are more abundant than ET_A receptors in endothelium-cell rich organs such as kidney, lungs and liver (Maguire & Davenport, 2015). In addition, ET_B receptors act also as clearance receptors for circulating ET-1, especially in the pulmonary, splanchnic and renal circulation (Fukuroda et al., 1994; Lüscher & Barton, 2000). As a result, a selective blockade of ET_A receptors with sitaxentan was expected to determine a vasodilatory response potentially due to a predominant activity of endothelial ET_B receptors and increased ET-1 clearance. A downregulation of endothelial ET_B receptors has been observed in a rat model of preeclampsia (Mazzuca et al., 2014), suggesting that a loss of ET_B receptor-mediated vasodilation may occur under pathological conditions such as hypertension. Whether this is also the case for the hypertensive status occurring during treatment with RTKIs needs to be clarified and further investigations in this direction are required.

In this study, the reduction of HVC in response to axitinib and lenvatinib was mild and not significant. This is in contrast with the results from *Chapter 4*, where axitinib and lenvatinib showed a significant vasoconstriction in the hindquarters vascular bed. The variability of the response of this vascular bed to the hypertensive condition associated with axitinib and lenvatinib may suggest that the rise in BP associated with these agents is independent of the changes on HVC. Although the dual ET_A/ET_B receptor antagonism showed a modest improvement of the hindquarters vascular tone on day 1 of treatment with axitinib, this does not seem to correlate with the pressor effect associated with this agent. This may also suggest that the reduction of hindquarters vascular tone may be mainly associated with ET_B receptors. However, the attenuation of the reduction in HVC in response to bosentan was not observed in lenvatinib-treated rats, making it difficult to formulate such hypothesis. The absence of an effect on HVC under the co-treatment with the selective ET_A receptor antagonist may support the hypothesis that the hypertensive response to VEGFR-2 inhibitors is independent of the reduction on HVC.

Our data may support the use of endothelin receptor antagonists, in particular those selective for ET_A subtype, as effective approach based on pathophysiology to prevent and manage the hypertensive response to RTKIs. Although ET_A receptor appears as promising target, none of the selective antagonists for this receptor are currently approved for the treatment of hypertension. Among the selective ET_A receptor antagonists developed, only ambrisentan and clazosentan have been approved for use in pulmonary arterial hypertension

and aneurysmal subarachnoid haemorrhage-induced vasospasm, respectively (Rivera-Lebron & Risbano, 2017; Lee, 2022). Sitaxentan was firstly approved for pulmonary arterial hypertension, but the association with hepatic injury led to its withdrawal in 2010 (Galiè et al., 2011). Interestingly, targeting the endothelin system may also be beneficial in terms of cancer treatment. Indeed ET-1 has been identified as pro-angiogenic mediator, which supports tumour angiogenesis directly via an effect on endothelial and perivascular cells and indirectly by stimulating the release of VEGF (Bagnato & Spinella, 2003; Knowles et al., 2005; Russignan et al., 2020; Tocci et al., 2021). In this regard, the use of endothelin antagonists may be supportive of the antiangiogenic effect of RTKIs, while preventing the hypertensive response associated with these therapeutics.

5 Chapter 5. Influence of axitinib and lenvatinib on vascular reactivity, arterial stiffness and cardiac performance

5.1 INTRODUCTION

VEGFR-2 inhibitor-induced hypertension appears to be mediated by both structural and functional changes of the vascular endothelium (Lankhorst, Saleh, et al., 2015a). Considering the role of VEGFR-2 in controlling BP via regulation of NO synthase expression (Facemire et al., 2009), a reduction in the endothelium-dependent vasodilation, primarily via impairment of NO availability, was initially hypothesised as the principal event involved in the hypertensive effect observed with RTKIs (Lankhorst, Kappers, van Esch, Danser, et al., 2014; Camarda et al., 2022). Although several investigations, both in animal models and in patients, corroborate the implication of endothelial dysfunction and reduced NO production in such cardiovascular complication (*Introduction 1.4.2.3*) (M. H. Kappers et al., 2011; Eechoute et al., 2012; Camarda et al., 2022), further experimental and clinical studies have shown conflicting results, demonstrating that the role of NO and endothelial dysfunction in the development of RTKI-induced hypertension is still controversial (*Introduction 1.4.2.3*) (Steeghs et al., 2008; Kappers et al., 2010; Mayer et al., 2011; Lankhorst, Kappers, van Esch, Danser, et al., 2014; Lankhorst, Saleh, et al., 2015b). As a result, the aim of this study was to assess the contribution of axitinib and lenvatinib to endothelial dysfunction and whether the hypertensive effect observed with these agents reflects an alteration in vascular reactivity.

Secondly, the results from *Chapter 3* demonstrated that both axitinib and lenvatinib, two RTKIs strongly associated with hypertension (Agency, 2012; Rini et al., 2015; Shah & Morganroth, 2015b; Agency, 2021a), also resulted in an increased PP (defined as the ratio of SV to arterial compliance). This evidence, coupled with a comparable effect in terms of rise of SBP and DBP observed with these two agents, suggested that RTKI-induced hypertension may be the result of augmented peripheral vascular resistance, arterial stiffness and increased SV (*Chapter 3*). Arterial stiffness, defined as a reduced distensibility of the arterial wall and an impaired capacity of the aorta to buffer the cardiac pulsatile fluctuation generated by LV contraction, has a major role in the increase of PP (Benetos et al., 1998; Chirinos, 2012; Homan et al., 2022). The haemodynamic consequences of increased arterial stiffness include not only an augmented PP in the large arteries, but also an hyperpulsatility in the small peripheral arteries, resulting in organ damage (Chirinos, 2012; Laurent & Boutouyrie, 2020). As a result, this work investigated the possible contribution of arterial stiffness to the PP alterations observed in response to axitinib and lenvatinib.

In addition, although the regulation of BP is the product of a fine interaction between the vasculature and the heart (Mayet & Hughes, 2003), whether the development of hypertension associated with VEGFR-2 inhibitors derives primarily from vascular changes or cardiac alterations is not yet clear. Although cardiac dysfunction is considered to be secondary to the detrimental impact of RTKIs on vasculature (Maurea et al., 2016; Mihalcea et al., 2023), a direct cardiotoxic effect of these therapeutics may not be excluded (Dobbin et al., 2018). Cardiomyocytes not only express VEGFR-1 and VEGFR-2 but are a source of the angiogenic factor VEGF-A, which acts as a paracrine and autocrine effector (Giordano et al., 2001; Zentilin et al., 2010). Cardiomyocyte-specific deletion of VEGF-A in mice resulted in ventricular wall thinning and depression of contractile function (Giordano et al., 2001; Hsieh et al., 2006), highlighting the importance of VEGF-A/VEGFR signalling in cardiac function (Giordano et al., 2001; Braile et al., 2020). VEGF-A also delays progression to hypertrophy and decline in ventricular function (Friehs et al., 2006; Dobbin et al., 2021). In this regard, RTKIs targeting VEGFR-2 have been associated with cardiac decompensation and hypertrophy (Izumiya et al., 2006; Dobbin et al., 2018; Mihalcea et al., 2023). Four of the clinically available VEGFR-2 inhibitors, specifically sorafenib, sunitinib, pazopanib and lenvatinib, have been shown to cause cardiac dysfunction (Jin et al., 2020). Among them, lenvatinib has been reported to induce cardiac dysfunction in 7% of patients, with 2% experiencing grade 3 or higher LVD (Costa et al., 2016; Agency, 2021a). Although the clinical profile of the cardiotoxic events due to these agents is well defined (Jin et al., 2020), there is a lack of investigations concerning the cardiac consequences of VEGFR-2 inhibitors in preclinical models. As a result, this Chapter aimed to comprehensively characterise the impact of axitinib and lenvatinib on cardiac function in mice, combining the use of echocardiography and pressure-volume loops. By using these gold standard techniques for diagnosis of cardiotoxicity, the purpose of this study was also to assess whether these approaches were able to early detect the cardiac sequalae associated with VEGFR-2 inhibitors.

Anti-VEGF monoclonal antibodies or RTKIs targeting VEGFR-2 have been mainly characterised in rat models (Kappers et al., 2010; M. H. W. Kappers et al., 2011; Lankhorst, Kappers, van Esch, Danser, et al., 2014; Lankhorst, Kappers, et al., 2014a; Lankhorst, Saleh, et al., 2015a; Carter et al., 2017). However, some studies have been also performed in mice, revealing similar cardiovascular sequelae as observed in rats and humans (Belcik et al., 2012; Liang et al., 2023). In particular, BP measurements via tail-cuff plethysmograph in conscious

C57BL/6J mice revealed hypertension in response to lenvatinib (Liang et al., 2023). The same study also showed an impaired cardiac function, in particular reduced EF and FS, in mice treated with this RTKI (Liang et al., 2023). Similarly, treatment with anti-VEGF monoclonal antibody was associated with increased BP and echocardiographic alterations (Belcik et al., 2012). As hypertension and cardiac dysfunction have been largely reported in rat models and in cancer patients (Kappers et al., 2010; M. H. Kappers et al., 2011; Abdel-Rahman & Fouad, 2014; Lankhorst, Kappers, van Esch, Danser, et al., 2014; Abdel-Qadir et al., 2017; Baek Moller et al., 2019), these findings suggest that the inhibition of VEGF-A/VEGFR-2 signalling results in similar cardiovascular toxicities in mice as those found in rats and humans, supporting the use of a murine model in the experiments described in this Chapter.

5.2 AIMS

The work described in *Chapter 5* aimed to:

3. Assess axitinib- and lenvatinib-induced changes on echocardiographic parameters.
4. Define the impact of lenvatinib on ventricular mechanics via intracardiac pressure-volume loops analysis.
5. Investigate the effect of axitinib and lenvatinib on vascular reactivity and endothelial function.
6. Determine the role of arterial stiffness in axitinib- and lenvatinib- induced haemodynamic changes.

5.3 METHODS

5.3.1 Animals and experimental protocol

All surgical and experimental procedures were conducted with approval of the Ethical Committee for Animal Testing of the University of Antwerp, as previously described (*Methods 2.2.2.2*).

Male 10-week-old C57BL/6J mice weighing between 25 and 30 g were used to perform the experiments (*Methods 2.2.2.2*). Briefly, three groups of mice were used to assess the structural and functional impact of axitinib and lenvatinib on the cardiovascular system. Animals were dosed with axitinib (12 $mg.kg^{-1}$) or lenvatinib (4 $mg.kg^{-1}$) as an intravenous injection for 4 consecutive days; contemporaneous control group was administered vehicle

(40% HPβCD in sterile saline). On day 2 of the treatment period, echocardiography was performed on all the groups (details reported in *Methods 2.2.2).*

On day 4 animals were randomly divided into two clusters: cardiac function was assessed in anaesthetised animals via PV-loop experiments (described in *Methods 2.2.3,* whereas vascular reactivity was investigated *ex vivo* using isolated tissue baths (described in *Methods 2.3.4* and *2.3.5).*

5.3.1.1 ECHOCARDIOGRAPHY

Detailed information on the echocardiographic measurements can be found in the general methodology (*Methods 2.2.2).*

Briefly, 2D (B-Mode) and 1D (M-mode) images of the heart were acquired to measure markers of systolic function (EF and FS), as well as LVAWd, LVAWs, LVPWd, LVPWs, LVIDd and LVIDs *(Methods 2.2.2.4, 2.2.2.5, 2.2.2.7).* Apical four-chamber view was also obtained for the colour Doppler imaging of the MV and to measure markers of diastolic function (MV E/E' ratio and MV E/A ratio) *(Methods 2.2.2.6).*

Satisfactory echocardiographic images could be captured in all animals and echocardiographic examination time was around 30 min per animal (*Methods 2.2.2.3).*

A first echocardiographic evaluation (n=8 per group) was performed to assess the impact of axitinib and lenvatinib on cardiac function and structure. Due to the absence of axitinib-induced changes in the echocardiographic parameters, the pressure-volume loops analysis was only performed on vehicle- and lenvatinib-treated animals, for which echocardiography was still performed on day 2 of experimental protocol. For this reason, the echocardiographic data of vehicle and lenvatinib are combined data from different studies which have the same condition on day 2, resulting in a greater sample size, specifically n=22 for lenvatinib group and n=23 for vehicle group.

All data were analysed using Prism 10 (GraphPad Software, La Jolla, CA, USA) and expressed as mean ± SEM, with *n* representing the number of mice used. Statistical comparisons of echocardiographic parameters between three groups (vehicle, axitinib and lenvatinib) were made using ordinary one-way ANOVA with Tukey's multiple comparisons test. Statistical

comparisons of echocardiographic parameters between two groups (vehicle and lenvatinib) were made using unpaired *t*-test with Welch's correction. Statistical significance was defined as *p<0.05, **p<0.01, ***p<0.001 and ****p<0.0001.

5.3.1.2 PRESSURE-VOLUME LOOPS

Detailed information on the cardiac measurements and surgical procedures can be found in the general methodology (*Methods 2.2.3).* This series of experiments was run with treatment groups of 9 to 13 mice.

Real-time measurements of volume and pressure were obtained through the insertion of a pressure-volume catheter in the LV of the animal (*Methods 2.2.3*). E_a, Tau, dP/dt_{min} and dP/dt_{max} were derived as load-dependent measures of ventricular function *(Methods 2.2.3.7)*. To determine load-independent parameters of cardiac contractility (i.e., ESPVR and EDPVR), transient alterations in the cardiac loading conditions were performed by obstructing the venous return to the heart via inferior vena cava occlusions *(Methods 2.2.3.8).*

All data were analysed using Prism 10 (GraphPad Software, La Jolla, CA, USA) and expressed as mean ± SEM, with *n* representing the number of mice. Statistical comparisons of cardiac functional parameters between groups were made using ordinary one-way ANOVA, while the exponential function for EDPVR slope and ESPVR slope were analysed using unpaired *t*-test with Welch's correction. Statistical significance was defined as *p<0.05, **p<0.01, ***p<0.001 and ****p<0.0001.

5.3.1.3 ROTSAC

Detailed information on arterial compliance measurement can be found in the general methodology (*Methods 2.3.4).* This series of experiments was run with groups of 7 mice.

Briefly, the Peterson's elastic modulus, as a measure of arterial stiffness, was evaluated at different pressures and performed under physiological conditions (Krebs-Ringer solution), as well as following contraction with α_1-adrenergic receptor agonist PE and relaxation with DEANO) *(Methods 2.3.4.2).*

Infrarenal and thoracic aortic segments were subjected to increasing and decreasing pressures under physiological conditions (Krebs-Ringer solution). After loading/unloading pressure steps under physiological condition, aortic segments were then treated with L-NAME (300 µM) to inhibit eNOS and remove the influence of NO. Thereafter, 2 µM PE was added to the tissue bath and the loading/unloading pressure steps where repeated. 3 washes were then performed before treatment with DEANO (2 µM) and subsequent increase and decrease of pressure conditions.

All data were analysed using Prism 10 (GraphPad Software, La Jolla, CA, USA) and expressed as mean ± SEM, with *n* representing the number of mice. Two-way ANOVA with Dunnett's *post-hoc* test was used for comparison of arterial stiffness between control and treated groups. Statistical significance was defined as $p<0.05$.

5.3.1.4 ISOMETRIC TISSUE BATH

Detailed information on the assessment of vascular function by using isometric tissue bath can be found in the general methodology (*Methods 2.3.5).* This series of experiments was run with groups of 6 mice.

After 60-min equilibration period, thoracic aortic segments were randomly assigned into two groups:

Protocol A

L-NAME was administered to abolish the influence of NO. Cumulative concentrations of PE ($3x10^{-9}$ M till $3x10^{-6}$ M) were added to assess vascular smooth muscle cells contraction in all the segments. Afterwards, endothelium-independent relaxation was evaluated by adding cumulative concentrations of DEANO ($3x10^{-10}$ M till 10^{-5} M). At the end of the relaxation curve, all segments should have a passive tension of 20 mN. After washing 3 times with warm Krebs-Ringer solution, a Ca^{2+}-free environment ($0Ca^{2+}$) was prepared by using a Ca^{2+}-free Krebs-Ringer solution and adding EGTA as a Ca^{2+}-chelating agent. Subsequently, phasic contraction was determined by α_1-adrenergic receptor stimulation with PE (2 µM), before restoring normal conditions by adding 1.75 nM $CaCl_2$ to induce tonic contraction in response to PE.

Protocol B

In this group of segments, cumulative concentrations of PE ($3x10^{-9}$ M till $3x10^{-6}$ M; 20 µl added for each concentration) were added to assess VSMCs contraction. After that, endothelium-dependent relaxation responses were assessed by adding cumulative concentrations of the muscarinic receptor agonist ACh ($3x10^{-9}$ M till 10^{-5} M; 20 µl added for each concentration). Following 3 washes with warm Krebs-Ringer solution and maximum contraction due to addition of 20 µl PE ($3x10^{-6}$ M), endothelium-dependent relaxation responses were also assessed by adding cumulative concentrations of ATP (10^{-8} M till 10^{-4} M; 20 µl added for each concentration), a purinergic receptor agonist.

All data were analysed using Prism 10 (GraphPad Software, La Jolla, CA, USA) and expressed as mean ± SEM, with *n* representing the number of mice used. Two-way ANOVA with Dunnett's *post-hoc* test was used for comparison of vascular reactivity between control and treated groups. Statistical significance was defined as $p<0.05$.

5.3.1.5 HISTOLOGY

Detailed information about the aortic and cardiac tissue sample preparation can be found in the general methodology (*Methods 2.3.6).*

Sirius red staining was used to determine total collagen content, while immunohistochemical staining using primary antibody against laminin was used to quantify cardiomyocyte hypertrophy (*Methods 2.3.6).*

5.3.1.6 VASCULAR mRNA EXPRESSION (qRT-PCT)

qRT-PCR was performed to determine vascular mRNA expression of TSP-1, $P2Y_2$ and $P2Y_6$ purinergic receptors. Detailed information can be found in the general methodology (*Methods 2.3.7).*

5.4 RESULTS

5.4.1 In vivo: Assessment of axitinib- and lenvatinib-induced effects on cardiac function and structure

5.4.1.1 ECHOCARDIOGRAPHIC EVALUATION OF AXITINIB- AND LENVATINIB-INDUCED EFFECTS ON CARDIAC PERFORMANCE

The systolic measurements (LVEF% and FS%) did not show significant changes in the axitinib-treated mice when compared to the vehicle group, while lenvatinib induced a significant loss of systolic function at day 2 of treatment, with a drop of 24% and 28% for LVEF and FS, respectively (***p<0.001, ****p<0.0001, Figure 53A-B, Figure 54A-B and 55). The evaluation of diastolic function by measuring intracardiac flows in Doppler mode (i.e., MV E/A ratio and MV E/E' ratio) did not reveal significant alterations of LV filling pressure among the groups (Figure 53C-D and Figure 54C-D).

The left ventricular internal diameter at diastole and systole (LVIDd and LVIDs) of lenvatinib-treated mice was significantly enlarged when compared to the vehicle-receiving animals (7.3% increase for LVIDd and 18.6% increase for LVIDs) (Figure 53E-F and Figure 54E-F), while no difference was observed in the axitinib group (*p<0.05, **p<0.01, Figure 53E-F). Although no alteration of the thickness of the left ventricular anterior and posterior wall during diastole (LVAWd and LVPWd) was detected both in the vehicle and in the treated groups (Figure 53G-I and 54G-I), the left ventricular anterior and posterior wall systolic (LVAWs and LVPWs) thickness was significantly reduced in the lenvatinib-treated mice, with a reduction of 17.3% for LVAWs and 22.3% for LVPWs (*p<0.05, ***p<0.001, Figure 53H-J and 54H-J). The systolic LVPW was significantly thinner also in the axitinib group, with a decrease in LVPWs thickness accounting for 21.5% when compared to the vehicle (*p<0.05, Figure 53J).

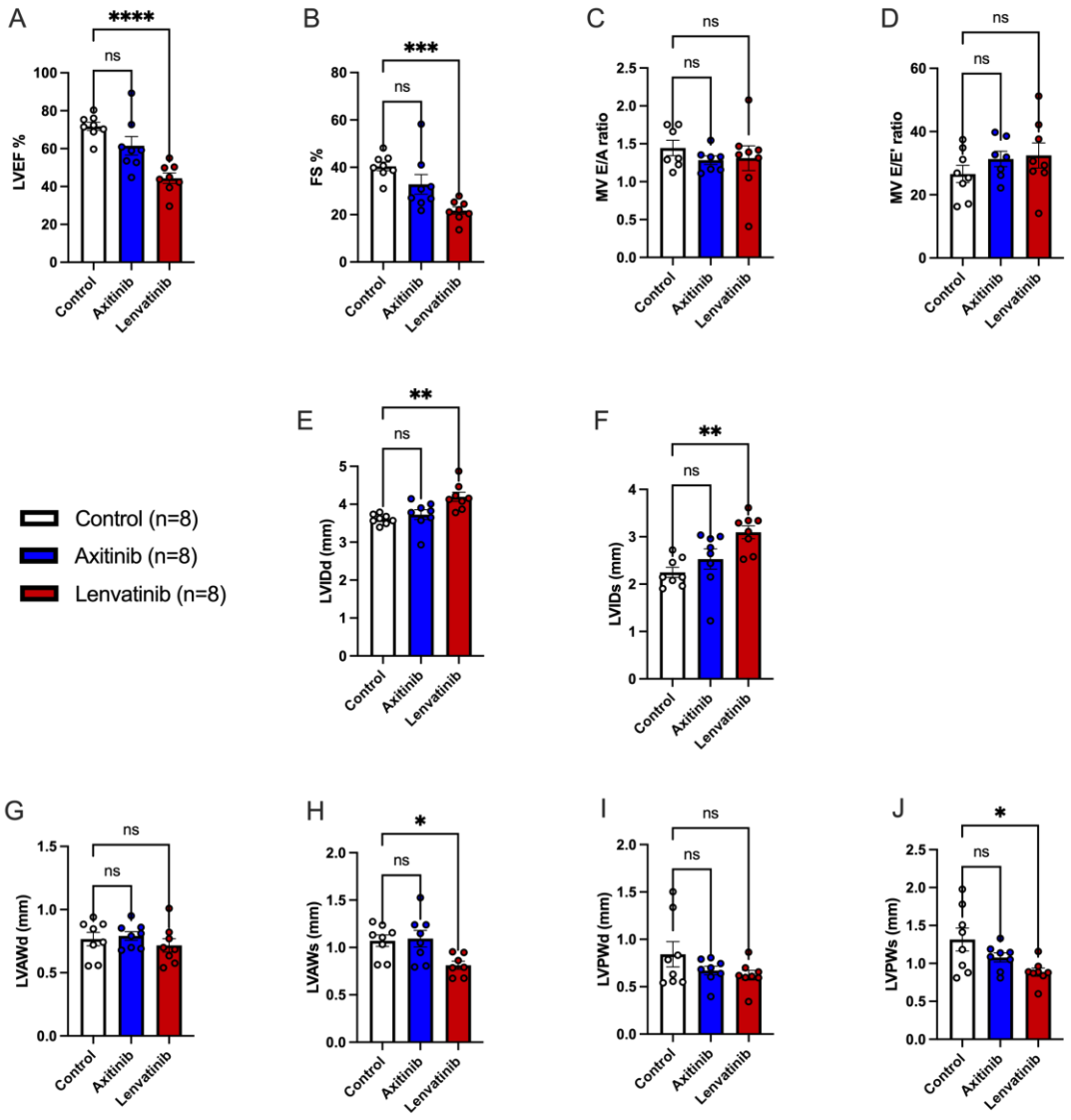

Figure 53. *Echocardiographic changes in mice following 2-day treatment with vehicle (40% HPβCD), axitinib (12 mg.kg^{-1}) and lenvatinib (4 mg.kg^{-1}) as described in Methods 2.2.2.2. (A) LVEF = left ventricular ejection fraction; (B) FS = fractional shortening; (C) MV E/A = mitral valve E/A ratio; (D) MV E/E' = mitral valve E/E' ratio; (E) LVIDd = left ventricular internal diameter during diastole; (F) LVIDs = left ventricular internal diameter during systole; (G) LVAWd = left ventricular anterior wall during diastole; (H) LVAWs = left ventricular anterior wall during systole; (I) LVPWd = left ventricular posterior wall during diastole; (J) LVPWs = left ventricular posterior wall during systole. Data points are means; vertical bars represent SEM. N = 8 per group. Ordinary one-way ANOVA with Tukey's multiple comparisons test was conducted for between-group comparison (*p<0.05, **p<0.01, ***p<0.001, ****p<0.0001).*

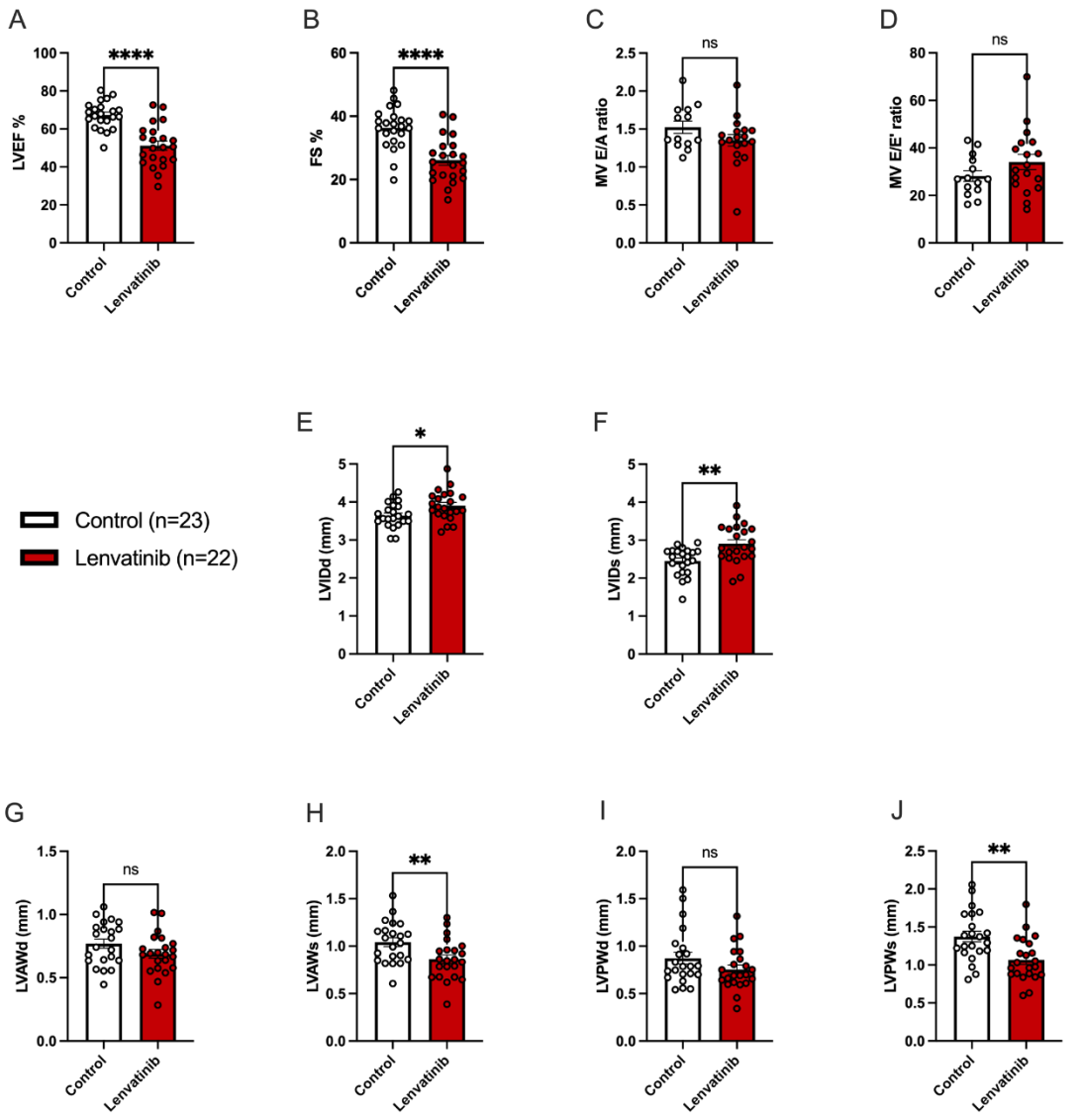

Figure 54. *Echocardiographic changes in mice following 2-day treatment with vehicle (40% HPβCD) and lenvatinib (4 mg.kg^{-1}) as described in Methods 2.2.2.2 (A) LVEF = left ventricular ejection fraction; (B) FS = fractional shortening; (C) MV E/A = mitral valve E/A ratio; (D) MV E/E' = mitral valve E/E' ratio; (E) LVIDd = left ventricular internal diameter during diastole; (F) LVIDs = left ventricular internal diameter during systole; (G) LVAWd = left ventricular anterior wall during diastole; (H) LVAWs = left ventricular anterior wall during systole; (I) LVPWd = left ventricular posterior wall during diastole; (J) LVPWs = left ventricular posterior wall during systole. Data points are means; vertical bars represent SEM. N = 22 for lenvatinib and N = 23 for control. Unpaired t-test with Welch's correction was conducted for between-group comparison (*p<0.05, **p<0.01, ****p<0.0001).*

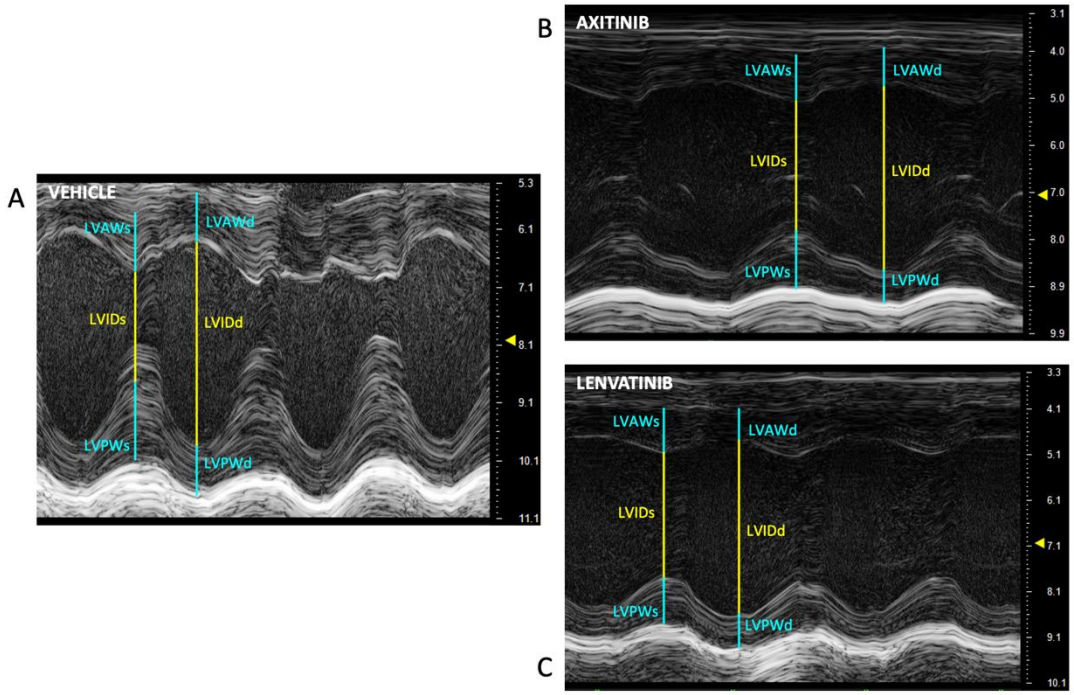

Figure 55. *Representative images of echocardiographic measurements with M-mode to assess LV systolic function in mice receiving (A) vehicle (40% HPβCD), (B) axitinib (12 mg.kg^{-1}) and (C) lenvatinib (4 mg.kg^{-1}) as described in Methods 2.2.2.2. LVIDd = left ventricular internal diameter during diastole; LVIDs = left ventricular internal diameter during systole; LVAWd = left ventricular anterior wall during diastole; LVAWs = left ventricular anterior wall during systole; LVPWd = left ventricular posterior wall during diastole; LVPWs = left ventricular posterior wall during systole.*

5.4.1.2 INVESTIGATING THE EFFECT OF LENVATINIB ON CARDIAC FUNCTION VIA PRESSURE-VOLUME LOOPS

The assessment of lenvatinib-induced effects on haemodynamic parameters via pressure-volume loops did not show a significant difference between vehicle and lenvatinib in terms of end-diastolic pressure (EDP), end-systolic pressure (ESP) and arterial elastance (Ea) (Figure 56A-C). In addition, lenvatinib did not affect ventricular relaxation, as reported by the absence of variations in the time constant of LV isovolumic relaxation (Tau) and on the peak rate of pressure increase (dP/dt_{min}) between the vehicle and the lenvatinib group (Figure 56D-E). LV diastolic function was preserved in both groups, as indicated by the slope of the end-diastolic pressure volume relationship (EDPVR), where no notable difference was detected (Figure 56F-G). Lenvatinib did not significantly alter the maximum rate of increase of left ventricular pressure (dP/dt_{max}), although it was associated with LV systolic dysfunction as indicated by the significant increase in the slope of the end-systolic pressure volume relationship (ESPVR) (**$p<0.01$, Figure 56H-I).

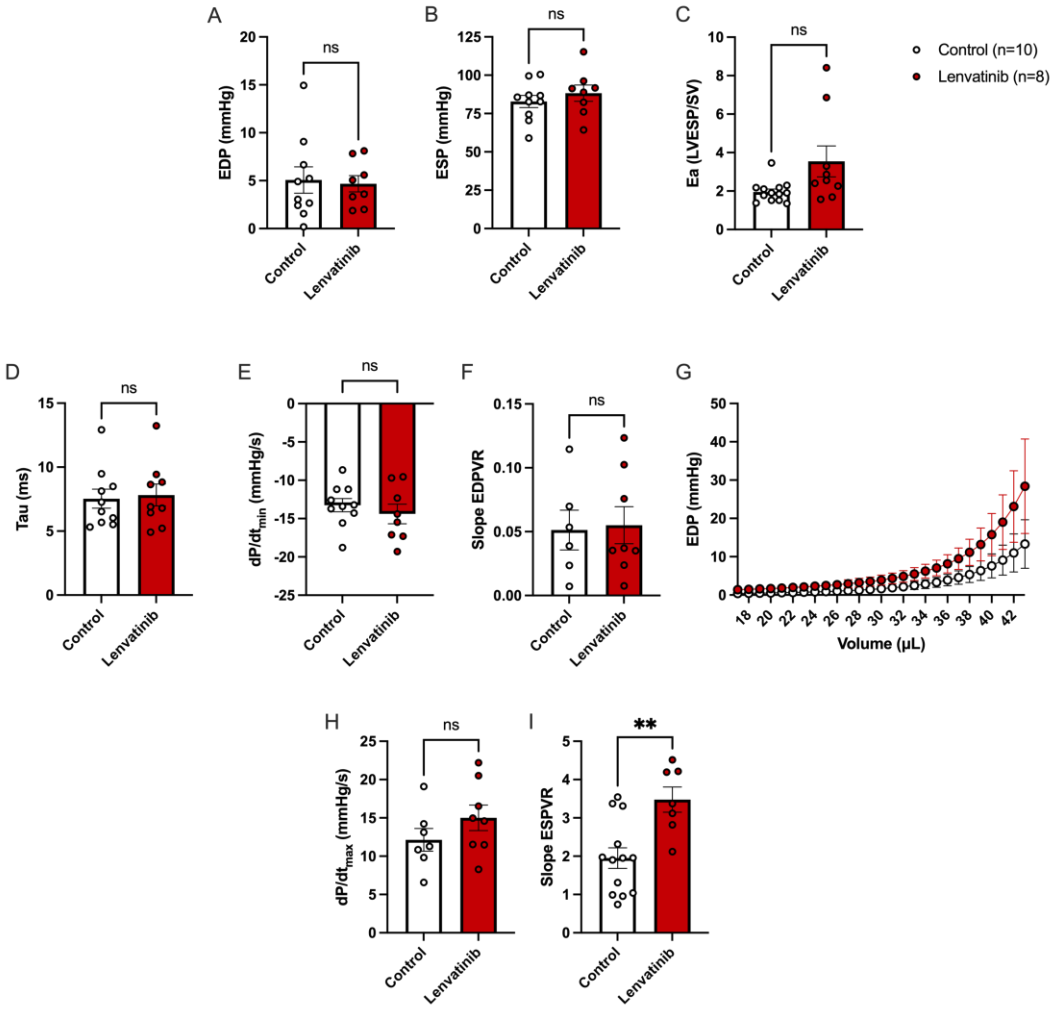

Figure 56. *Haemodynamic parameters (A, B, C) and indices of diastolic (D, E, F, G) and systolic function (E, H, I) derived from PV loops analysis in mice following 4-day treatment with vehicle (40% HPβCD) and lenvatinib (4 mg.kg^{-1}) as described in Methods 2.2.3. EDP = end-diastolic pressure; ESP = end-systolic pressure; Ea = arterial elastance; Tau = isovolumetric relaxation constant; dP/dt$_{min}$ = peak rate of pressure decrease in the ventricle (corrected for HR); dP/dt$_{max}$ = peak rate of pressure rise in the ventricle (corrected for HR); ESPVR = end-systolic pressure-volume relationship; EDPVR = end-diastolic pressure-volume relationship. Data points are means; vertical bars represent SEM. N = 9 for lenvatinib and N = 13 for control. Unpaired t-test with Welch's correction was performed for between-group comparison (**p<0.01).*

5.4.2 Ex vivo: Effect of axitinib and lenvatinib on vascular reactivity and arterial stiffness

5.4.2.1 DEFINING THE IMPACT OF AXITINIB AND LENVATINIB ON VASCULAR REACTIVITY

Vascular reactivity was evaluated *ex vivo* to investigate whether the treatment with axitinib or lenvatinib was associated with endothelial dysfunction. Neither axitinib nor lenvatinib altered the PE-induced contraction, both in the absence and in the presence of L-NAME (Figure 57A-B). Both ACh-induced endothelium-dependent relaxation and DEANO-induced endothelium-independent relaxation were not affected by axitinib and lenvatinib, while the vasodilator response to ATP was significantly increased after treatment with axitinib and lenvatinib (*p<0.05, **p<0.01, ***p<0.001, ****p<0.0001, Figure 57C-E). To specifically evaluate whether the PE-induced phasic contraction phase, caused by intracellular Ca^{2+} release from sarcoplasmic reticulum (SR), was affected by axitinib and lenvatinib, the PE contraction (2 μM) was repeated in the absence of extracellular Ca^{2+} in the groups receiving L-NAME, to prevent the potential influence of NO. The PE-induced phasic contraction phase was not altered in the thoracic aortic segments (Figure 58A-B). and the evaluation of the amplitude (A) and the time course (t) of the PE-mediated phasic contraction did not report significant differences among the groups (Figure 59A-D).

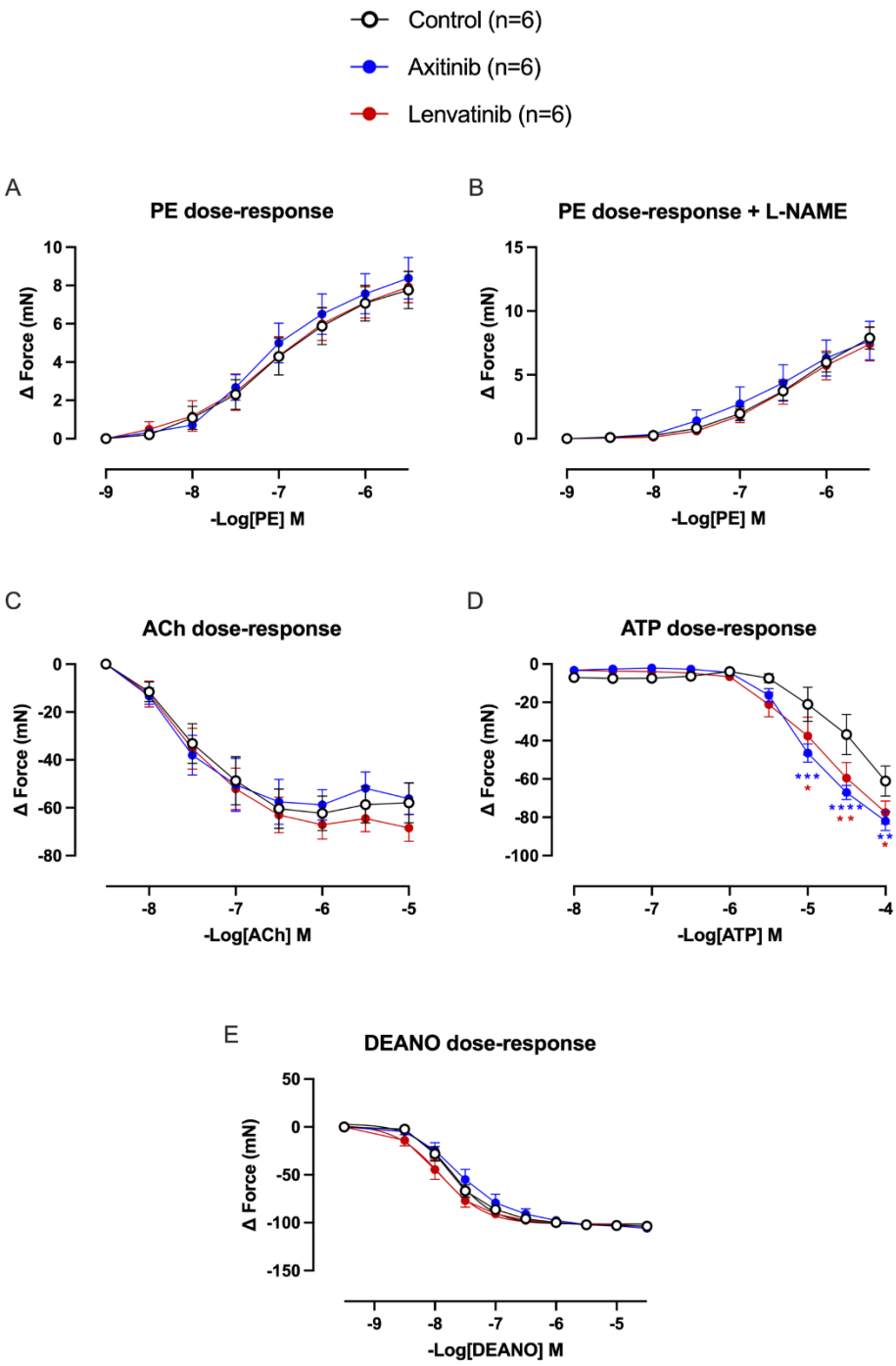

Figure 57. *Contraction and relaxation of thoracic aortic segments of mice following 4-day treatment with vehicle (40% HPβCD), axitinib (12 mg.kg^{-1}) and lenvatinib (4 mg.kg^{-1}) as described in Methods 2.3.5. VSMC contraction elicited by increasing concentrations of PE was evaluated in the absence (A) and in the presence of 300 µM L-NAME (B). Following maximal contraction with PE, VSMC relaxation was assessed in response to increasing concentrations of ACh (C), ATP (D) or DEANO (E). Data points are means; vertical bars represent SEM. N = 6 per group. Two-way ANOVA with Dunnett's post-hoc test was performed (*p<0.05, **p<0.01, ***p<0.001, ****p<0.0001).*

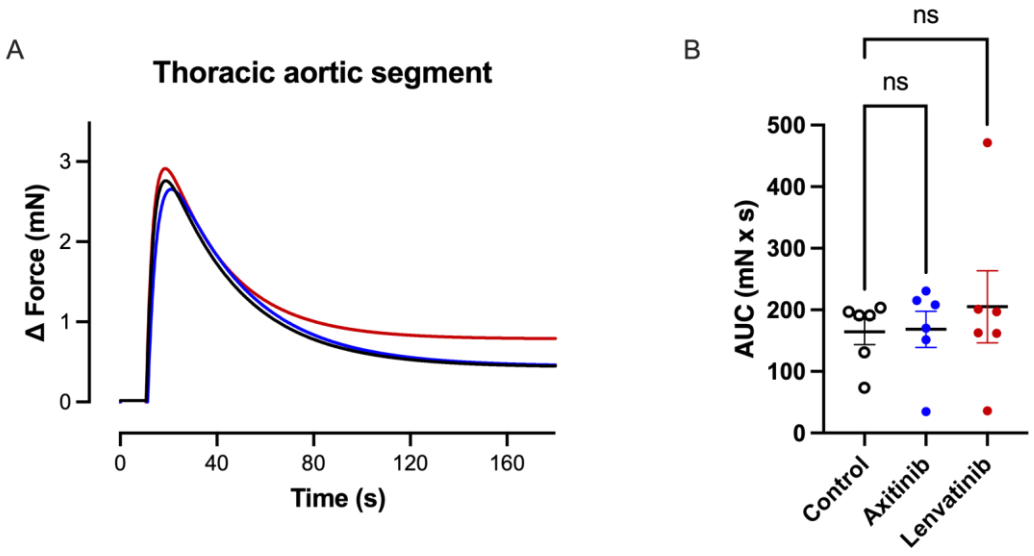

Figure 58. *Isometric contraction by PE (2 µM) in the absence of external Ca^{2+} (A) was assessed in thoracic aortic segments of mice following 4-day treatment with vehicle (40% HPβCD), axitinib (12 $mg.kg^{-1}$) and lenvatinib (4 $mg.kg^{-1}$) as described in Methods 2.3.5. Area under the curve (AUC) for the cumulative change in isometric force in thoracic aortic segments (B). Data points are means; vertical bars represent SEM. N = 6 per group. Two-way ANOVA with Dunnett's post-hoc test was performed.*

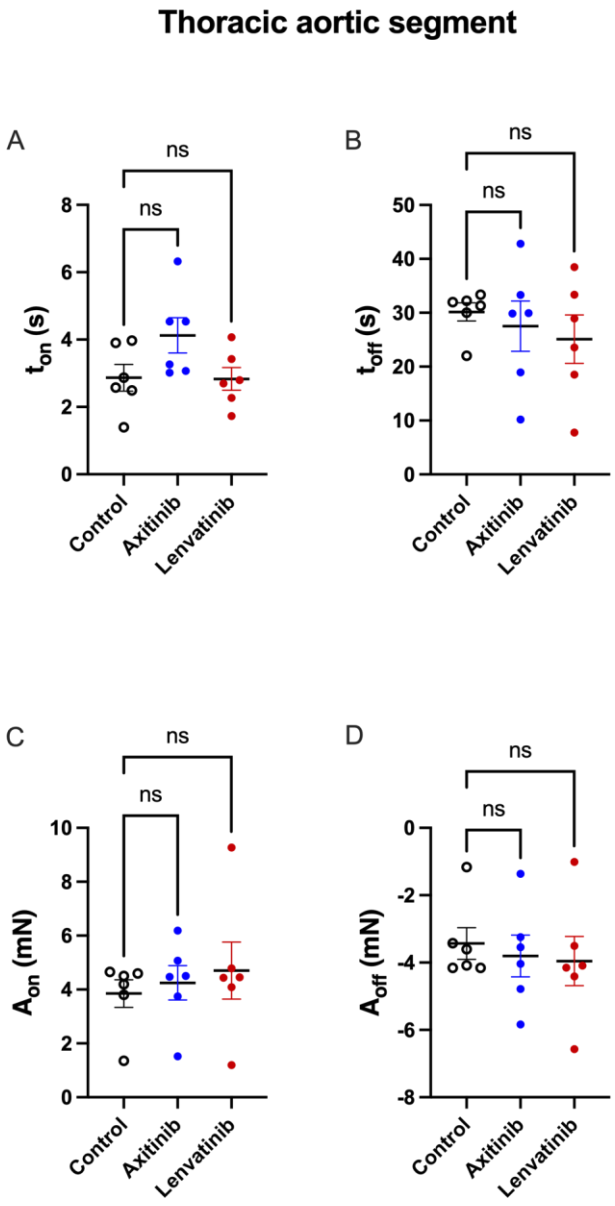

Figure 59. *Kinetic analysis of the isometric contraction induced by PE. The inositol 1,4,5-trisphosphate (IP3)-mediated phasic contraction is characterised by two phases: a first rising phase which represents the release of Ca^{2+} from the sarcoplasmic reticulum and a second phase which corresponds to the active removal of Ca^{2+} from the cytoplasm. Both phases are defined by an amplitude (A_{on} and A_{off}) and a time constant (t_{on} and t_{off}). Effect of axitinib and lenvatinib on the time constant (A, B) and amplitude (C, D) of IP_3-mediated phasic contraction on the thoracic aortic segments. Data points are means; vertical bars represent SEM. N = 6 per group. Two-way ANOVA with Dunnett's post-hoc test was performed.*

5.4.2.2 EVALUATING THE ROLE OF ARTERIAL STIFFNESS IN THE HAEMODYNAMIC RESPONSES ASSOCIATED WITH AXITINIB AND LENVATINIB

The contribution of axitinib and lenvatinib to arterial stiffness was evaluated on thoracic and infrarenal aortic segments under physiological conditions, where neither axitinib and lenvatinib showed alteration of aortic stiffness (Figure 60A and 60D). The contribution of VSMCs to arterial stiffness following treatment with axitinib and lenvatinib was explored after α_1-adrenoreceptor stimulation with PE (2 µM) in the presence of L-NAME (300 µM) to inhibit basal NO release. Even in this case, no difference in active vascular stiffness was observed between the vehicle and the treated animals (Figure 60B and 60E). The assessment of structural arterial stiffness under maximal VSMCs relaxation induced by DEANO (2 µM) did not show changes in the thoracic aortic segment, while a small but significant increase was observed in the lenvatinib-treated group at a mean pressure of 180 mmHg (*p<0.05, Figure 60C and 60F).

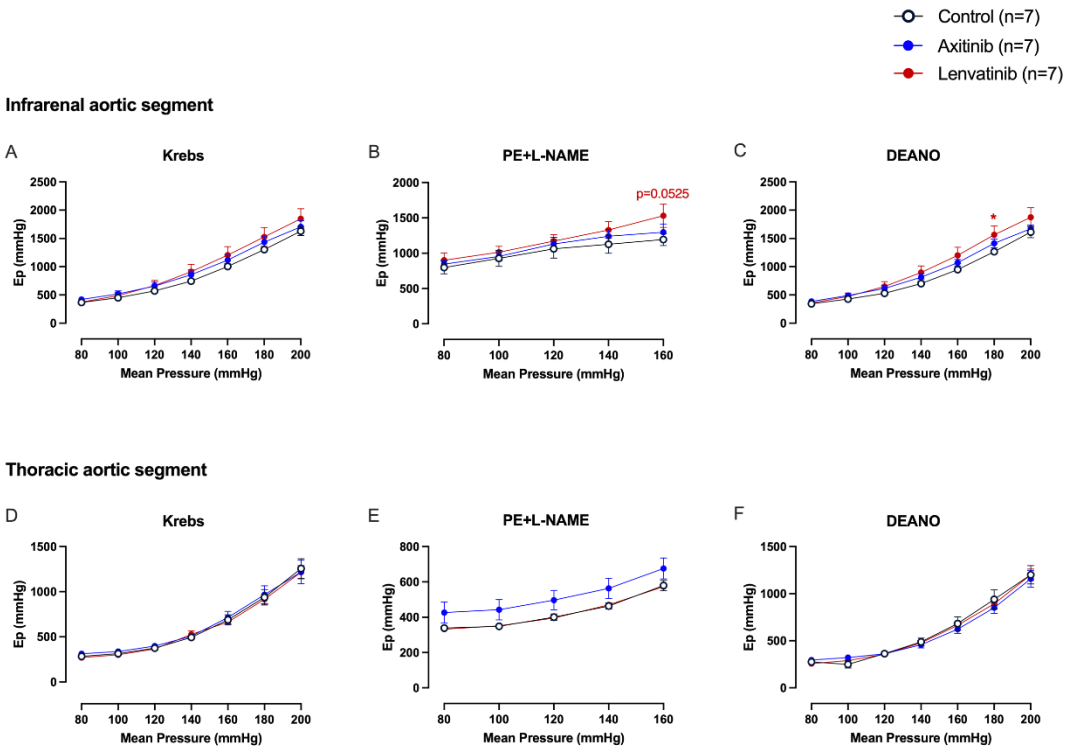

Figure 60. *Peterson's elastic modulus (Ep) as index of arterial stiffness was determined in mouse aortic segments following 4-day treatment with vehicle (40% HPβCD), axitinib (12 mg.kg^{-1}) and lenvatinib (4 mg.kg^{-1}) as described in Methods 2.3.4. Pressure dependency of Peterson's elastic modulus was measured in infrarenal (A, B, C) and thoracic (D, E, F) aortic segments under unstimulated conditions (A, D), after stimulation with 2 µM PE in the presence of 300 µM L-NAME (B, E) or after relaxation with 2 µM DEANO (C, F). Data points are means; vertical bars represent SEM. N = 7 per group. Two-way ANOVA with Dunnett's post-hoc test was performed (*p<0.05).*

5.4.3 Histology

Cardiomyocyte cell size was assessed by staining the heart cross-sections for the ubiquitous non-collagenous connective tissue glycoprotein laminin. Five images from different cross-sectional areas were recorded for each heart. 20 cardiomyocytes were randomly selected from each image and the area of these cell was measured (Figure 61B-G). Both the treatment with axitinib and lenvatinib was associated with cardiomyocyte hypertrophy, with an increase of the cross-sectional cardiomyocyte area of 10.3% for axitinib and 62% for lenvatinib compared to the control group (****$p<0.0001$, Figure 61A).

In addition to cardiomyocyte cell size, the total collagen content and coronary microvessel size were measured in mice cardiac cross-sections stained with Sirius red (Figure 62A-I). For this measurement, between 2 and 4 coronary microvessels per cardiac cross-section were examined. Coronary microvessel wall thickness was analysed by measuring intima-media thickness from four different regions equally distributed around the vessel and the average was then calculated over the four measurements. The treatment with axitinib and lenvatinib was not associated with alterations of the total collagen content (Figure 62A-B). However, an increased lumen size of coronary microvessels was observed in the lenvatinib-treated animals compared to the control group (0.005 μm^2 ±0.0008 vs 0.002 μm^2 ±0.0005, respectively) (**$p<0.01$, Figure 62C). Nevertheless, neither the wall area nor the wall thickness of the coronary microvessels were affected by the treatment (Figure 62D-E).

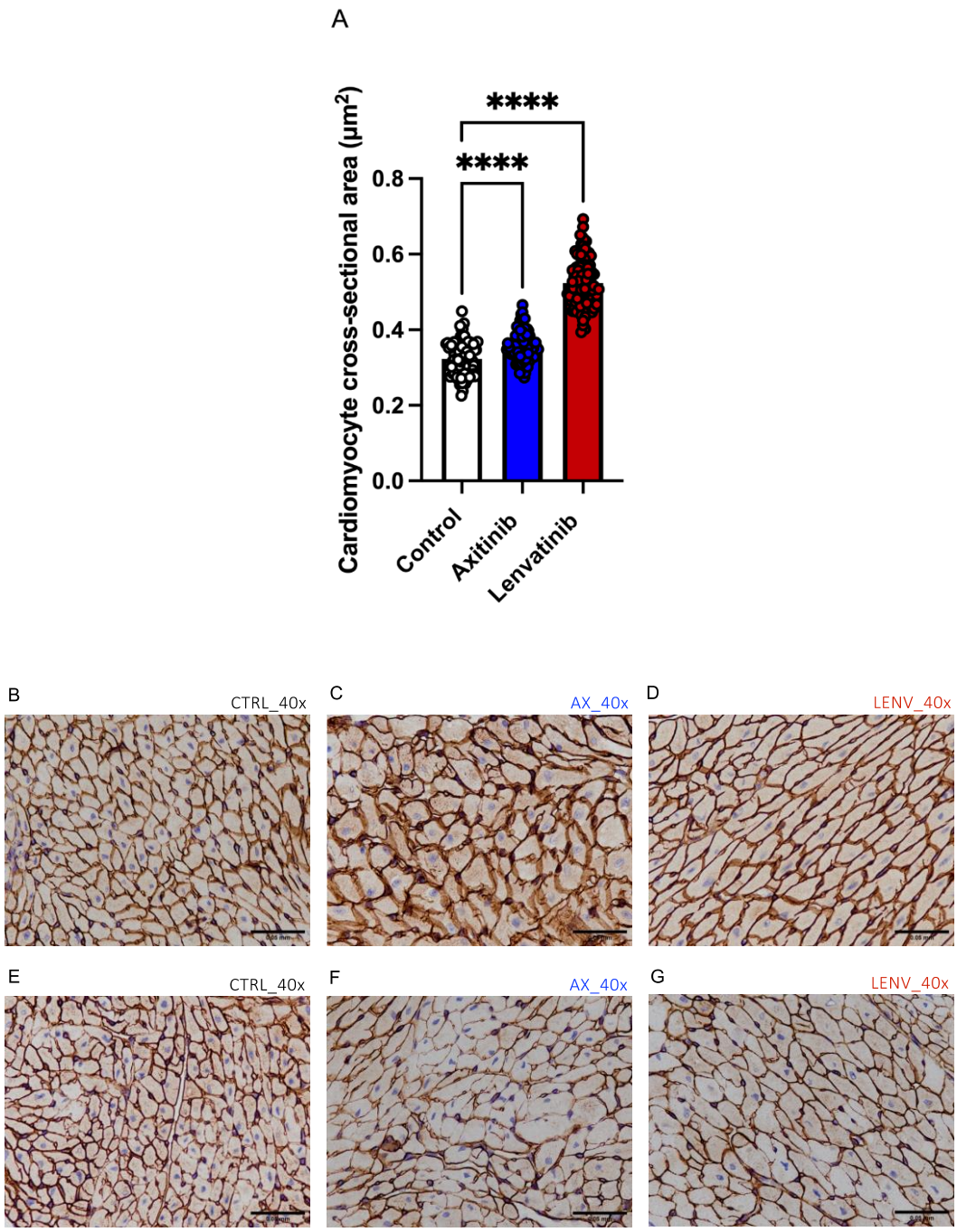

Figure 61. *Laminin immunohistochemical staining of mice hearts to quantify cardiac hypertrophy by evaluation of cardiomyocyte cross-sectional area (A). This measurement was performed by recording five images from different cross-sectional areas of each heart and measuring the cross-sectional area of 20 cardiomyocytes per image (final average of 100 measurements). Representative images of cardiomyocyte cross-sectional area following 4-day treatment with vehicle (40% HPβCD) (B, E), axitinib (12 mg.kg^{-1}) (C, F) and lenvatinib (4 mg.kg^{-1}) (D, G). Scale bar = 0.05 mm. Data points are means; vertical bars represent SEM. Ordinary one-way ANOVA with Dunnett's post-hoc test was performed (****p<0.0001).*

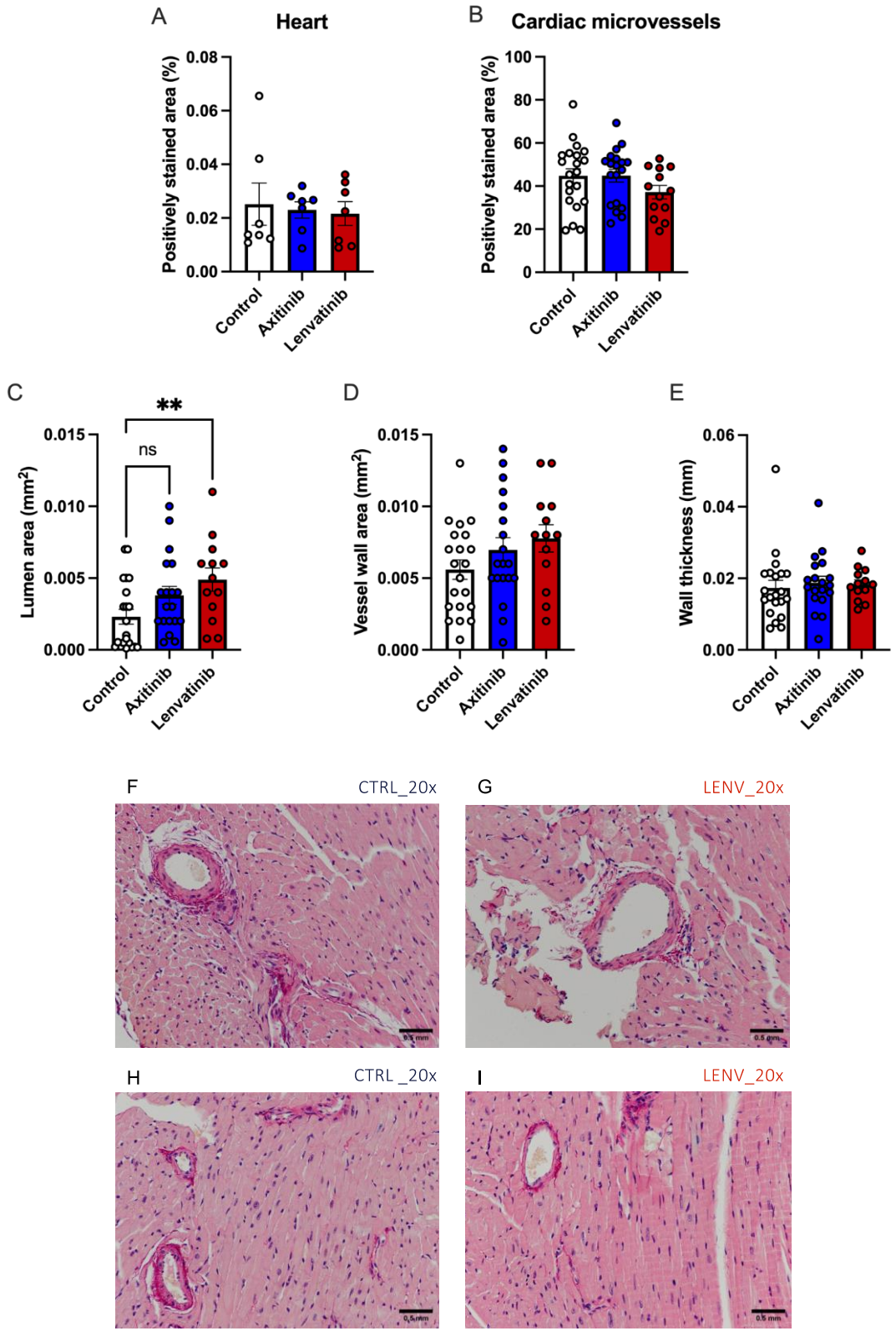

Figure 62. *Sirius red staining of mice cardiac tissue to quantify collagen network alterations in the heart and in the coronary microvessels (A, B). Coronary microvessel lumen area (C), wall area (D) and wall thickness (E) were also analysed. Representative images of cross-sectional areas of mice hearts following 4-day treatment with vehicle (40% HPβCD) (F, H) and lenvatinib (4 mg.kg^{-1}) (G, I) as*

*described in Methods 2.3.6. Scale bar = 0.05 mm. Data points are means; vertical bars represent SEM. Ordinary one-way ANOVA with Dunnett's post-hoc test was performed (**p<0.01).*

5.4.4 Vascular mRNA expression (qPCR)

To integrate the *ex vivo* assessment of the axitinib- and lenvatinib-induced vascular effects, the aortic expression of TSP-1 and $P2Y_2$ and $P2Y_6$ purinergic receptors were also studied. As previously discussed in *section 2.3.7,* increased vascular levels of TSP-1 may describe compromised NO signalling (Isenberg et al., 2009; Roberts et al., 2012). For this reason, measuring the aortic expression of this protein aimed to define its role in the vascular responses associated with axitinib and lenvatinib. As for $P2Y_2$ and $P2Y_6$ receptors, they have a key role in the regulation of vascular tone *(2.3.7)* (Wu et al., 2023). Therefore, assessing whether axitinib and lenvatinib affect the vascular expression of these receptors may help in defining the vascular changes associated with these RTKIs and whether these purinergic receptors may have a role in the vascular effects due to these two RTKIs.

Axitinib and lenvatinib did not alter the vascular mRNA expression of thrombospondin, while the vascular mRNA expression of the genes encoding for $P2Y_2$ and $P2Y_6$ receptors was significantly increased in the lenvatinib-treated group (*p<0.05, Figure 63A-C).

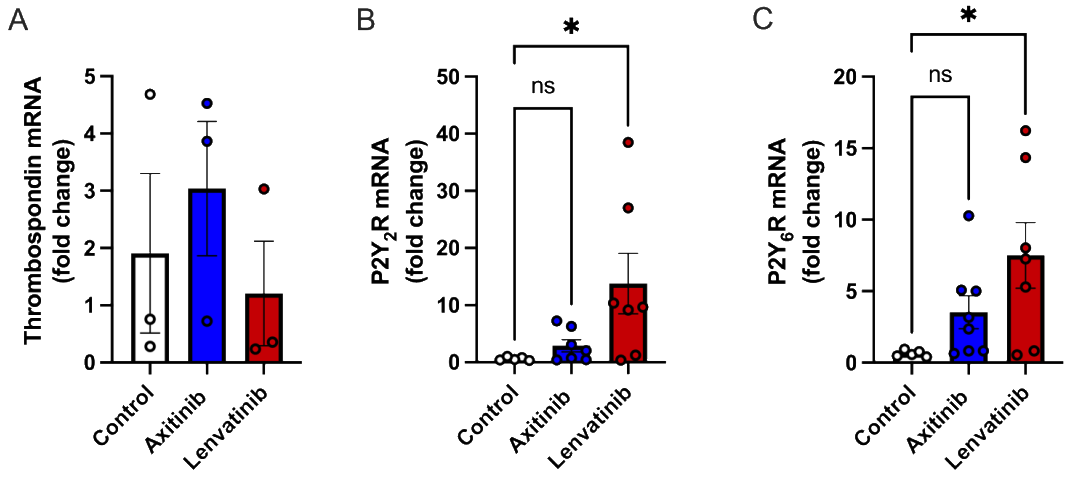

Figure 63. *Aortic mRNA expression of thrombospondin (A), $P2Y_2$ receptor (B), $P2Y_6$ receptor (C) in mice following 4-day treatment with vehicle (40% HPβCD), axitinib (12 mg.kg^{-1}) and lenvatinib (4 mg.kg^{-1}) as described in Methods 2.3.7. Vascular mRNA expression is normalised to the internal reference gene β-actin and is expressed relative to the vehicle-treated group. Data points are means; vertical bars represent SEM. Data were analysed using a Kruskal-Wallis one-way ANOVA (*p<0.05).*

5.5 DISCUSSION

One of the purposes of this Chapter was to define the impact of axitinib and lenvatinib on endothelial function and VSMC reactivity in order to establish the possible contribution of these components in the cardiovascular events associated with VEGF inhibition. The contractile response of thoracic aortic segments to PE following a 4-day period of treatment in C57BL/6J mice did not reveal any differences between the treated groups and the control sample. The same observation applied for the segments pre-treated with L-NAME. The isometric measurements of ACh concentration-response vasodilation in aortic rings pre-contracted with PE, where no difference were reported between control and treated samples, suggest the absence of endothelial dysfunction in response to the treatment. No differences in PE-induced contraction in presence and absence of eNOS inhibitor L-NAME further confirmed this scenario. As the vasodilatory and vasoconstrictive responses are not only influenced by the functional status of endothelium but also by the sensitivity of VSMCs to NO, exogenous NO donor DEANO was used in this study to define whether axitinib and lenvatinib were associated with a decreased responsiveness of VSMCs to NO. Endothelium-independent relaxation in response to DEANO was unaltered for both the RTKIs tested, indicating a preserved reactivity of VSMCs to NO and intact VSMCs function. Several studies associate the development of RTKI-induced hypertension with reduced NO bioavailability and endothelial dysfunction (M. H. Kappers et al., 2011; Eechoute et al., 2012; Neves et al., 2018). In particular, a reduced urinary excretion of NO metabolites was reported in rats treated with sunitinib (M. H. Kappers et al., 2011). In addition, vatalanib showed a reduced production of NO and impaired phosphorylation of eNOS in human aortic ECs (Neves et al., 2018). Although some investigations support the hypothesis that vascular complications in response to RTKIs are mediated by impaired endothelial function and NO deficiency, our findings indicate that the exposure to axitinib and lenvatinib is not associated with alteration of endothelial function or reduced reactivity of VSMCs to NO. This is in agreement with previous studies where sunitinib treatment did not show any alteration of ACh-mediated vasodilation in iliac artery segments of rats (Mirabito Colafella et al., 2020; Mirabito Colafella et al., 2022). Despite vatalanib-receiving patients showing increased levels of plasma NO metabolites, flow-mediated dilation as index of NO bioavailability remained unchanged (Neishi et al., 2005). In this context, the study from Neves et al. described an up-regulated ROS generation concomitantly with the reduced activation of NO pathways (Neves et al., 2018). Considering that NO bioavailability is dependent on oxidative stress (Touyz, 2004; Lubos et al., 2008), the reduction of NO observed in these studies may be secondary to RTKI-

mediated oxidative stress rather than due to a direct toxic effect on the endothelium. Altogether, the current conflicting evidence do not allow us to conclude whether RTKI-induced hypertension primarily derives from endothelial dysfunction. The dissimilarities among these studies may be due to differences in the models used (C57Bl/6 mice in the current study, male Wistar Kyoto rats (M. H. Kappers et al., 2011; Mirabito Colafella et al., 2020), human aortic ECs (Neves et al., 2018)), in the treatment dose and duration of treatment period (4-day treatment with axitinib 12 $mg.kg^{-1}$ and lenvatinib 4 $mg.kg^{-1}$ as an intravenous injection in the present study, 8-day treatment with sunitinib 14 $mg.kg^{-1}.day^{-1}$ (Mirabito Colafella et al., 2020), 8-day treatment with sunitinib 26.7 $mg.kg^{-1}.day^{-1}$ as oral gavage (M. H. Kappers et al., 2011), human aortic ECs stimulated with vatalanib 100 $nmol.L^{-1}$ and mice treated for 2 weeks with vatalanib 100 $mg.kg^{-1}.day^{-1}$ (Neves et al., 2018)), as well as in the RTKIs investigated and their relative cardiovascular risk profile when used in human patients (Abdel-Rahman & Fouad, 2014; Rini et al., 2015; Shah & Morganroth, 2015a; Motzer et al., 2022).

Both lenvatinib and axitinib have shown a concentration-dependent increase in the ATP-mediated relaxation, therefore suggesting a potential role of $P2Y_x$ receptors in the vascular response associated with these RTKIs. Interestingly, Gast et al. showed that ATP and $VEGF_{165}a$ act synergistically on ECs and the resulting complex, leading to a conformational change of the growth factor structure, determines an increased interaction with $P2Y_x$ receptors (Rumjahn et al., 2009; Gast et al., 2011). Although the exact nature of this conformational change is still unknown (Gast et al., 2011), this may explain the augmented ATP-induced relaxation observed in our study. Indeed, the increased $VEGF_{165}a$ levels, due to the VEGFR-2 inhibition by axitinib and lenvatinib, forming a synergistic complex with ATP, would determine a stronger response to the nucleotide via $P2Y_x$ receptor signalling. Moreover, the increased mRNA expression of both $P2Y_2$ and $P2Y_6$ receptors in the aortic segments of lenvatinib-treated mice may support the role of the purinergic signalling in the vascular responses associated with this RTKI.

Additionally, the effect of axitinib and lenvatinib on intracellular Ca^{2+} release was investigated by stimulating aortic rings with α_1-adrenoceptor agonist PE in absence of external Ca^{2+}. Under this condition, PE causes a transient contraction, also known as phasic contraction, while the subsequent reintroduction of Ca^{2+} by adding $CaCl_2$ determines a tonic (permanent) contraction (Fransen et al., 2015). In particular, PE-induced phasic contraction is due to IP_3-mediated Ca^{2+} release from SR (Kim et al., 2014; Fransen et al., 2015). In this context, the PE-

induced phasic contraction is the sum of two phases (Fransen et al., 2015). A first upward phase describes the rapid removal of Ca^{2+} from SR via IP_3 receptor (Gorski et al., 2017), while the second phase (downward) corresponds to the active removal of Ca^{2+} from cytoplasm mainly via plasma membrane Ca^{2+} ATPase (PMCA) and the plasma membrane Na^{+}/Ca^{2+}exchanger (NCX) (Brini & Carafoli, 2011). In this context, axitinib and lenvatinib did not alter the area under the curve (AUC), amplitude of the contraction phase (A_{on}), and time constant of the relaxation phase (τ_{off}) of the SR-mediated contractions, suggesting that intracellular Ca^{2+} storage and SR-mediated phasic contractions are not affected by these RTKIs. Further research would be necessary to fully define the role of Ca^{2+} signalling in RTKI-induced vascular effects.

Hypertension can also be the result of arterial remodelling and stiffness, which have been described as independent predictors of cardiovascular mortality in hypertensive patients (Laurent et al., 2001; Safar et al., 2003). Increased arterial stiffness was observed in sorafenib-treated patients within around 4 weeks of treatment and was still present after 10 months of therapy (Veronese et al., 2006). Similarly, sunitinib has been associated with hypertension and increased arterial stiffness after 3.5 weeks of therapy in patients with mRCC (Catino et al., 2018). These clinical data suggest that vascular stiffness may have a role in VEGFR-2-induced hypertension, although the relationship between the rise in BP and vascular remodelling remains controversial (Veronese et al., 2006). Indeed, despite the fact that arterial stiffness has been speculated to be the result of a hypertensive status, vascular remodelling may actually be the cause instead of the consequence of the pathological changes that occur in the vascular structure in hypertension (Kaess et al., 2012). Mechanisms of arterial stiffness not only include chronic events, such as fibrosis, reduced elastin-collagen ratio, extracellular matrix calcification and VSMC phenotype switching (van Varik et al., 2012), but also acute changes in VSMC contractility or EC stiffness due to increased activity of endothelial sodium channel (Dumor et al., 2018; De Moudt et al., 2021; Camarda et al., 2022). Although the pathophysiological events underlying VEGFR-2-induced arterial stiffness have not been investigated, the rapid onset of vascular stiffness observed in patients suggests an acute component rather than structural remodelling as potential cause of the loss of arterial compliance (Camarda et al., 2022). The present study, comparing the Peterson's elastic modulus as index of arterial stiffness, evaluated arterial compliance in response to axitinib and lenvatinib after 4-day treatment in a rodent model. The assessment of arterial compliance was performed under physiological conditions, as well as following

contraction with α1-adrenergic receptor agonist PE and relaxation with DEANO. Both the infrarenal and thoracic aortic segment did not show any differences among the treated groups and the vehicle, suggesting that these RTKIs and the relative cardiovascular changes are not due to aortic stiffness, at least not in the time period evaluated in this study. In addition, the unaltered mRNA expression of TSP-1 in mice aortic segments observed in this study indicates the absence of alterations on vessel flow dynamic. Indeed, this matricellular protein has been associated with shear-mediated arterial stiffening and its expression level increases under disturbed flow conditions (Natasha M. Rogers et al., 2014; Kim et al., 2017).

Hypertension is not the only cardiovascular event correlated with RTKIs targeting VEGFR-2. Left ventricular dysfunction and cardiomyocyte hypertrophy have been reported in patients receiving these therapeutics (Chu et al., 2007; Shah & Morganroth, 2015a), although their effects on cardiac function is generally inadequately screened during drug development (Force & Kerkelä, 2008). By using echocardiography, this study aimed to comprehensively characterise the cardiac consequences of axitinib and lenvatinib in mice. These RTKIs have both been largely associated with hypertension (Baek Moller et al., 2019), but they differ in terms of their impact on heart (Shah & Morganroth, 2015a). Indeed, although the label for axitinib has been recently revised to incorporate a new association with cardiac events, lenvatinib has been associated with a more significant impact on cardiac function (0.3% vs 7% of patients experiencing cardiac dysfunction with axitinib and lenvatinib, respectively) (Killock, 2015; Agency, 2021b). Echocardiographic evaluation performed in this study revealed a marked systolic dysfunction in response to lenvatinib, as indicated by the significant decline of fractional shortening and ejection fraction. By measuring intracardiac flows, no alterations in the echocardiographic markers of diastolic function were detected, therefore indicating a preserved ventricular filling. These findings were confirmed by pressure-volume loop analysis, where all the diastolic indices (i.e., Tau, dP/dt_{min} and EDPVR) were preserved. In addition to evaluating systolic and diastolic performances, this study also used echocardiography to measure cavity size and ventricular wall thickness, providing further insights about the effect of these RTKIS on cardiac haemodynamic. A significant enlargement of the left ventricle was observed in lenvatinib-treated mice, along with a considerable reduction of systolic ventricular wall thickness. These echocardiographic features are suggestive of lenvatinib-induced dilated cardiomyopathy (Faggiano et al., 2021). Clinical data about lenvatinib-associated cardiomyopathy are rather limited. In this context, Takotsubo cardiomyopathy with severe left ventricular dysfunction has been reported in a

patient receiving lenvatinib for the treatment of thyroid cancer (Chae et al., 2018). Lenvatinib has also been associated with non-ischemic cardiomyopathy in a case report (Matsuo et al., 2020). In order investigate whether these echocardiographic alterations were correlated with changes at a cellular level, histology was performed to quantify both total collagen content and cardiomyocyte hypertrophy. Despite no variations were observed in terms of total collagen content, a larger cardiomyocyte cross-sectional area in lenvatinib-treated animals supports the presence of cardiac hypertrophy. The cardiomyocyte enlargement in response to lenvatinib can be hypothesised as an adaptive response to compensate the reduced ejection fraction by trying to increase wall thickness and preserve systolic function, according to Laplace relationship (Diwan & Gerald W. Dorn, 2007). The resultant hypertrophic remodelling, characterised by an initial reactive increase in wall thickness, may then become maladaptive (Diwan & Gerald W. Dorn, 2007). This progression would ultimately result in ventricular dilation and wall thinning, as indicated by the findings from the echocardiographic measurements. In addition, the pressure-volume loop analysis for lenvatinib revealed an enhanced inotropic state of the ventricle, defined by the increased slope of ESPVR observed in the treated mice. This event may be the result of a compensatory mechanism. Specifically, the Frank-Starling mechanism, along with a potential neurohormonal regulation, could be activated to counterbalance the effects of the reduced ejection fraction and dilated cardiomyopathy by increasing myocardial contractility (Delicce & Makaryus, 2023). The cardiomyocytes hypertrophy observed in axitinib was not correlated with any alteration of the echocardiographic parameters, except for a reduction of the posterior ventricular wall during systole. This suggests an initial stage of cardiac remodelling, where cardiac function is still preserved.

Contrary to expectations, the present study did not show any alteration of BP as shown from pressure-volume loops data. It should be noted that echocardiographic assessment and PV loop analysis were conducted under inhalation anaesthesia. Anaesthetics, both injectable and inhalation, have been associated with vasodilation and increased blood flow, as well as alterations on circulating hormones and metabolic processes (Constantinides et al., 2011). Although isoflurane has been shown to preserve cardiac function better than other anaesthetics, a reduction of mean arterial pressure and heart rate has been associated with this agent (Janssen et al., 2004). As a result, anaesthetic-related vasodilatory effects might explain the absence of hypertension in response to RTKI-treatment observed in this study.

6 Chapter 6. General discussion & future directions

6.1 RESEARCH SUMMARY AND CONCLUDING REMARKS

The cardiovascular safety of VEGFR-2 inhibitors remains a major challenge in oncology, since unanticipated and poorly controlled cardiovascular toxicities induced by these therapeutics often result in a reduction of therapeutic dosage or treatment interruption, therefore influencing cancer management (*Introduction 1.4*). To that end, this project aimed to comprehensively characterise the cardiovascular safety liabilities associated with two VEGFR-2 inhibitors (i.e., axitinib and lenvatinib), as well as investigate the involvement of ET-1 system in the development of RTKI-induced hypertension. Combining diverse *in vitro*, *ex vivo* and *in vivo* approaches, the purpose of this study was also the identification of sensitive approaches to readily detect cardiovascular risk of these novel targeted therapies in preclinical settings.

Although the hypertensive effect of VEGFR-2 inhibitors can be confirmed in animal models, the majority of previous studies was carried out by using telemetry or *ex vivo* methods, investigating the impact of RTKIs on HR, BP, and cardiac function, without any or little insight about the consequences of these agents on systemic vasculature and its role in the development of the associated hypertensive response (*Introduction 1.4.2.3)*. In addition, considering that the incidence of hypertension appears to be correlated to the potency of these agents against VEGFR-2, quantifying the inhibitory effects of six RTKIs (axitinib, erlotinib, linifanib, vatalanib, SU-14813 and lenvatinib) on VEGFR-2 mediated responses would be essential for the subsequent *in vivo* characterisation of the cardiovascular consequences of these drugs.

Chapter 3 aimed to assess the susceptibility of peripheral vasculature to VEGFR-2 inhibitors and its relationship with the alteration of arterial BP observed with these agents. The five RTKIs targeting VEGFR-2 tested in this study showed a potent inhibitory activity on $VEGF_{165}$a-stimulated NFAT response with IC_{50} values in nanomolar range, with axitinib and lenvatinib showing highest relative potency for VEGFR-2 (*3.4.1.2)*. Based on these data and considering the high rates of hypertension reported in clinic for these two RTKIs (*3.1 and 3.5*), axitinib and lenvatinib were selected to be characterised in an animal model. The *in vivo* evaluation showed that both RTKIs cause a striking hypertensive response in conscious rats (*3.4.2.1* and *3.4.2.2)*. Such elevation in BP occurred within 24 hours of the start of the experimental period to then become even more marked on the second day of treatment, when the pressure values essentially reached a plateau (*3.4.2.1* and *3.4.2.2)*. This study also demonstrated a

correlation between axitinib- and lenvatinib-induced hypertension and regionally selective changes in vasculature, which was consistent with previous studies on different VEGFR-2 inhibitors (Carter et al., 2017) (*3.4.2.1* and *3.4.2.2)*. In particular, the elevation of BP was associated with an increased vascular tone in hindquarters and mesenteric arteries. The impairment of renal vascular flow was less consistent, with this vascular bed showing a vasoconstrictive response to both RTKIs only on the second day of treatment and with the highest doses tested (*3.4.2.1* and *3.4.2.2)*. This may suggest a compensatory adaptation of renal vasculature in response to the hypertensive conditions induced by both RTKIs, in addition to demonstrating that renal vasoconstrictive response is minimal even in case of severe rise in BP. Moreover, although the agents used are multi-kinase inhibitors, the similarity of their haemodynamic profiles reported in this study suggest that the cardiovascular alterations induced by these therapeutics are mainly the result of their "on-target" activity on VEGFR-2 rather than the consequence of their "off-target" interactions with other kinases, which are different for axitinib and lenvatinib (*3.5*). This was also supported by the *in vitro* evaluation, where no inhibition of NFAT activity below basal levels was observed, suggesting that no other RTKs with constitutive NFAT activity have been blocked (*3.4.1.2)*. Finally, the median time to onset of all-grade hypertension in patients treated with axitinib (5 to 10 mg twice a day) was within one month from the first dose, with hypertensive episodes observed already after 4 days of treatment (Agency, 2012; Rini et al., 2015), and patients receiving lenvatinib (24 mg per day) showed a median interval from the first dose to the development of hypertension of 16 days (Agency,2021a). Considering these onset times in clinics and the onset time for RTKI-induced hypertension in the animal model used (24-48 hours), this *in vivo* approach has proven to be a sensitive and translational model for the prediction and early detection of haemodynamic effects of these novel anticancer therapies.

Hypertension, reported in up to 80% of cancer patients treated with VEGFR-2 inhibitors, represents the predominant cardiovascular toxicity associated with these agents (*Introduction 1.4.2.3*). The exact pathophysiological events contributing to such complication are still unclear, compromising the prevention and proper management of this adverse effect (*Introduction 1.4.2*). Among the various hypotheses (*Introduction 1.4.2.3)*, the activation of ET-1 axis seems to play a key role in the development of hypertension associated with antiangiogenic therapies (*Introduction 1.4.2.3*). Previous studies supported this scenario, although different results were obtained with antagonists displaying distinct selectivity for

ET_A and ET_B receptors (*Introduction 1.4.2.3)*. This introduces the hypothesis that the hypertensive effects associated with VEGFR-2 inhibitors may be primarily due to ET_A receptor rather than ET_B receptor (*Introduction 1.4.2.3)*. Understanding the pathophysiological events contributing to RTKIs-induced hypertension is crucial for the development of appropriate mechanism-based treatment options and for the prevention of such cardiovascular complication.

Chapter 4 aimed to investigate the efficacy of dual ET_A/ET_B receptor antagonism and selective ET_A receptor antagonism in the prevention of the hypertensive response mediated by VEGFR-2 inhibitors. Sitaxentan, as selective ET_A receptor antagonist, fully prevented the hypertensive response to axitinib and lenvatinib, while the dual ET_A/ET_B receptor antagonist bosentan abolished the axitinib-induced hypertension but did not cause any significant reduction in the lenvatinib-induced pressor effect (*4.4.1* and *4.4.2*). These findings reinforced the hypothesis that the hypertensive effect of VEGFR-2 inhibitors is due to an activation of the ET-1 axis and also indicated that such response is purely regulated by the activation of ET_A receptors (*4.4.1* and *4.4.2*). The simultaneous evaluation of the role of endothelin receptors antagonism in preventing the RTKI-mediated alterations of vascular tone in regional vascular beds revealed that axitinib- and lenvatinib-induced increase in mesenteric vascular tone is independent of their hypertensive effect, and may be mainly mediated by ET_B receptors (*4.4.1* and *4.4.2*).

Due to conflicting results in support of endothelial dysfunction and reduced NO production as mechanism involved in RTKI-induced cardiovascular alterations (*Introduction 1.4.2.3*), the role of NO and endothelial dysfunction in the development of RTKI-induced hypertension is still controversial (*Introduction 1.4.2.3*). In the context of vascular changes in response to antiangiogenic treatment, the contribution of arterial stiffness in the pathogenesis of RTKI-induced haemodynamic changes remains unclear (Veronese et al., 2006) (*5.5*). Hypertension is not the only cardiovascular event correlated with RTKIs targeting VEGFR-2 (*Introduction 1.4.2.1*). Left ventricular dysfunction and cardiomyocyte hypertrophy have been reported in patients receiving these therapeutics (*Introduction 1.4.2.1*), although their effects on cardiac function are generally inadequately screened during drug development (*Introduction 5.1*). Characterising the impact of axitinib and lenvatinib on cardiac function in mice by using diverse existing preclinical approaches (i.e., echocardiography and pressure-volume loops), was important to define whether these models were able to early detect the cardiac sequalae associated with VEGFR-2 inhibitors.

Chapter 5 aimed to assess the contribution of axitinib and lenvatinib to endothelial dysfunction and whether these agents are associated with alterations in vascular reactivity (*5.4.2.1*). The isometric measurements in response to vasoconstrictive agents, as well as endothelium-dependent and endothelium-independent vasodilatory compounds, revealed the absence of endothelial dysfunction and a preserved VSMC reactivity in response to the treatment with axitinib and lenvatinib (*5.4.2.1*). However, a concentration-dependent increase in the ATP-mediated relaxation was observed following treatment with these RTKIs, suggesting a potential role of $P2Y_x$ receptors in the vascular response associated with these agents, further supported by the increased mRNA expression of both $P2Y_2$ and $P2Y_6$ receptors in the aortic segments of lenvatinib-treated mice (*5.4.2.1* and *5.4.4*). This study also evaluated the impact of axitinib and lenvatinib on arterial compliance (*5.4.2.2*). No alterations were observed, suggesting that these RTKIs and the relative cardiovascular changes are not directly due to aortic stiffness (*5.4.2.2*). To define the effect of RTKIs on cardiac function, echocardiographic evaluation and pressure-volume loop analysis were performed (*5.4.1.1* and *5.4.1.2*). A marked systolic dysfunction was observed in response to lenvatinib, while no alterations in the echocardiographic markers of diastolic function indicated a preserved ventricular filling (*5.4.1.1*). A significant enlargement of the left ventricle was observed in lenvatinib-treated mice which, along with a considerable reduction of systolic ventricular wall thickness, were suggestive of lenvatinib-induced dilated cardiomyopathy (*5.4.1.1* and *5.5*). In confirmation of this, cardiomyocyte hypertrophy was also reported in lenvatinib-treated animals (*5.4.3*).

In summary, this thesis highlighted that Doppler flowmetry represents a sensitive and translational model in the early detection of haemodynamic liabilities due to antiangiogenic therapeutics (*Chapter 3)*. In particular, results from this work demonstrated a RTKI-induced hypertensive response which was accompanied by a consistent vasoconstriction in the mesenteric vascular bed (*Chapter 3* and *Chapter 4*). The mechanistic investigation of the role of ET-1 receptors antagonism revealed that such hypertensive effect is primarily mediated by ET_A receptors, while also suggesting that the RTKI-induced hypertension is independent of the regional vasoconstrictive responses observed with these agents (*Chapter 4).* Additionally, experiments in this thesis reported the absence of endothelial dysfunction and arterial stiffness following treatment with axitinib and lenvatinib. However, the *in vivo* investigation of their effect on cardiac performance revealed for the first time in a preclinical model that lenvatinib is associated with systolic impairment, structural remodelling of the LV and

cardiomyocytes enlargement, all suggestive of drug-induced dilated cardiomyopathy (*Chapter 5*). Additional work should be performed to further investigate the underlying signalling events associated with lenvatinib-induced cardiac dysfunction. Finally, future studies could assess the role of selective ET_A receptor antagonists as an effective mechanism-based approach to manage RTKI-induced cardiovascular side effects.

6.2 FUTURE DIRECTIONS

6.2.1 Use the Pulsed Doppler flowmetry to study axitinib and lenvatinib in rat cancer models

In order to fully delineate the cardiovascular profile of RTKIs, the role of tumour microenvironment should be considered in the investigation of the mechanisms underlying the cardiovascular sequalae due to VEGFR-2 inhibition. In this context, the Doppler flowmetry (*Methods 2.2.1, Chapter 3* and *Chapter 4*) could be used to assess the haemodynamic consequences of axitinib and lenvatinib in rat model of renal cell carcinoma, as both of these agents represent a clinical strategy in patients with this malignancy. The most appropriate oncogenic animal models to study the role of tumour environment during VEGFR-2 inhibition in rats are syngeneic models and cell-derived xenograft (CDX) models (Sobczuk et al., 2020). Syngeneic animal models are based on animal-derived tumour cells transplanted into a genetically identical host animal with an intact and functional immune system (Sobczuk et al., 2020). Among syngeneic models, Eker rats (Long-Evans rats bearing the Eker mutation) develop a renal tumour that shows some biological similarities with human renal cancer cells, including overexpression of hypoxia inducible factor 2α (HIF-2α) and upregulation of VEGF (Sobczuk et al., 2020), being therefore one of the most suitable model for the investigation of RTKI-induced cardiovascular toxicity via the Doppler flowmetry approach in a disease model. An alternative option to study cardiovascular toxicity of antiangiogenic therapies in a rat cancer model that better reflects human cancer pathophysiology is represented by CDX models. They are based on the implantation of human tumour cells into immunodeficient animals, thus having the benefit of closely mimicking human carcinogenesis (Sobczuk et al., 2020).

As previously discussed (*Chapter 4*), due to its pro-angiogenic activity, the ET-1 axis is also involved in cancer development (Russignan et al., 2020). As a result, studying the impact of endothelin antagonists in a cancer model would help not only to fully characterise their role

in preventing RTKI-induced haemodynamic toxicities, but also to define the contribution of such antagonism in supporting the antiangiogenic effect of VEGFR-2 inhibitors.

In addition, sex differences influence both pharmacokinetic and pharmacodynamic profiles, resulting in different responses to therapeutics between females and males (Soldin & Mattison, 2009; Gochfeld, 2017). For this reason, the inclusion of female rats would be advisable in order to evaluate possible sex differences in the development of RTKI-induced cardiovascular complications

6.2.2 In vivo investigation of RTKI-induced arterial stiffness

Although our results (*5.4.2.2*) did not show vascular remodelling and arterial stiffness in response to axitinib and lenvatinib in isolated aortic segments, increased arterial stiffness was reported in cancer patients treated with sorafenib and sunitinib (Veronese et al., 2006; Catino et al., 2018). Even if clinical observations suggest that VEGFR-2 inhibition may also result in vascular remodelling and stiffness (*Chapter 5*), the relationship between RTKI-induced hypertension and aortic stiffness remains controversial (Veronese et al., 2006). For this reason, future studies assessing the impact of RTKIs on arterial stiffness *in vivo* would be crucial not only to fully understand the correlation between RTKI and vascular stiffness but also to identify a preclinical model to early detect such drug-induced vascular changes. In this context, pulse wave velocity (PWV), a surrogate marker for arterial stiffness, could be measured non-invasively via applanation tonometry or ultrasound-based pulse wave imaging (PWI) in anesthetised animals treated with RTKIs (Li et al., 2013; Butlin et al., 2020). Also, considering that in cancer patients vascular stiffness increased after a period of about 3-4 weeks, while our measurements of arterial stiffness were performed after a 4-day treatment, future *in vivo* experimental research should consider a longer treatment period.

6.2.3 Characterise the mechanisms underlying lenvatinib-induced cardiac dysfunction

In addition, this work has demonstrated a significant cardiac impairment following treatment with lenvatinib (*5.4.1.1 and 5.4.1.2*). Although this RTKI has been associated with cardiac toxicity in cancer patients, preclinical evidence about lenvatinib-induced cardiac dysfunction is either limited or non-existent (*Chapter 5*). Consequently, management of cancer patients who develop cardiac events in response to lenvatinib is difficult and often inadequate

(*Chapter 5*). The early detection of lenvatinib-induced cardiac dysfunction with this study represents an important step towards a better understanding of the cardiac profile of this agent and laid the foundations for future mechanistic studies. In particular, the reported cardiomyocyte hypertrophy, systolic dysfunction, ventricular dilation and wall thinning are all suggestive of drug-induced dilated cardiomyopathy (*Chapter 5*). However, the mechanisms underlying cardiac toxicity associated with this RTKI are still unknown. For this reason, future work should be performed to clarify the mechanistic events responsible for the detrimental cardiac effect of lenvatinib. *Ex vivo* Langendorff isolated heart, as well as acute and chronic *in vivo* studies, represent potential preclinical approaches that could be used in parallel to achieve a comprehensive overview of RTKI-induced cardiac dysfunction. In this regard, implanted telemetric ECG monitoring could represent an appropriate strategy to investigate the impact of RTKIs on cardiac electrophysiology *in vivo* both acutely and over a prolonged period of time. This work should be supported by the use of isolated retrograde perfused rat heart model to measure the impact of RTKIs on the mechanical activity of the myocardium, left ventricular pressure, end-diastolic pressure, maximal contraction or relaxation velocity (dP/dt_{max} or dP/dt_{min}), atrioventricular conduction time and ECG parameters, in addition to either coronary flow or coronary perfusion pressure. Collecting the perfusate from the heart or the organ itself could also be of help to assess possible lenvatinib-induced changes in protein and/or gene expression. Biomarkers of cardiac injury that could be investigated include cardiac troponin I (TnI) T (TnT), highly specific for myocardial damage, as well as brain natriuretic peptide (BNP), an indicator of increased ventricular wall stretch, haemodynamic overload and cardiac remodelling (Kerkelä et al., 2015). In addition, tumour necrosis factor alpha (TNF-α), interleukin 6 (IL-6), and insulin-like growth factor 1 (IGF-1) have been identified as early biomarkers of load-induced cardiac hypertrophy (Palmieri et al., 2002). As a result, measuring mRNA and protein expression of these cytokines and growth factors in response to lenvatinib in rat heart and heart perfusate would also contribute to further define the relationship between this RTKI and cardiac hypertrophy (*Chapter 5*). Moreover, ET-1 has been found to support hypertrophic remodelling of cardiomyocytes (Larivière et al., 1995; Higazi et al., 2009; Archer et al., 2017). Due to the implications of ET-1 in the haemodynamic changes observed with axitinib and lenvatinib (*Chapter 4*), assessing ET-1 gene expression in the rat heart and perfusate may clarify whether this peptide has also a role in the cardiac consequences of VEGFR-2 inhibition, and specifically in the lenvatinib-induced ventricular hypertrophy.

6.2.4 Define the role of ET-1 axis in the pathogenesis of RTKI-induced hypertension

Results from Chapter 4 highlight the role of ET_A receptors in the hypertensive effect associated with VEGFR-2 inhibitors, in addition to suggesting that such pressor effect is independent of the regional vasoconstriction observed with these agents. However, the vascular implications of ET_A and/or ET_B receptors in the RTKI-induced haemodynamic changes are still not clear. Work investigating the role of ET-1 and its receptors in the cardiovascular liabilities observed with antiangiogenic therapeutics should be continued. In particular, the Doppler flowmetry approach used in this thesis (*Methods 2.2.1, Chapter 3 and Chapter 4*) could be repurposed to investigate the role of selective ET_B antagonism in RTKI-induced vascular changes in conscious rats. This would provide important mechanistic insight about the involvement of ET_B receptors in the vascular responses to VEGFR-2 inhibitors, while also clarifying the relationship between hypertension and regional vasoconstriction during antiangiogenic treatment.

In addition, the downregulation of endothelial cell-specific ET_B receptors reported in a rodent model of preeclampsia leads to the hypothesis that a loss of ET_B receptor-mediated vasodilation may occur also during treatment with RTKIs (*4.5*). Due to the involvement of ET_B receptors in the clearance of ET-1, a deletion of this receptor subtype may further explain the increased circulating levels of ET-1. To establish whether the increased levels of ET-1 are due to an augmented production of the peptide or to an impairment of ET_B receptor-mediated clearance, it would be crucial to quantify the vascular mRNA expression of the genes encoding ET_A and ET_B receptors following treatment with axitinib and lenvatinib.

Future work should combine the quantification of endothelin receptors expression with the investigation of mRNA expression of the genes encoding endothelin converting enzyme-1 (ECE-1) and ET-1 in the vasculature, heart and kidney. Indeed, even if several mechanisms have been proposed, the events involved in the activation of ET axis due to the antiangiogenic therapies are still unclear. VEGF promotes the expression of preproET-1 mRNA via VEGFR-2, as well as enhancing the secretion of ET-1 (Matsuura et al., 1998). However, if VEGF determines the production of ET-1 by ECs, a reduction of ET-1 would be expected during the treatment with VEGFR-2 inhibitors. The fact that increased levels of ET-1 have been observed during antiangiogenic treatments led to the hypothesis that the rise in ET-1 is due to the activation of ECs as a result of VEGF signalling inhibition (Lankhorst, Saleh, et al., 2015b; Lankhorst et al., 2016). In this regard, although vascular endothelium is the main source of

ET-1, this peptide is also produced by VSMCs, macrophages, cardiomyocytes and fibroblasts (Kirkby et al., 2008), which may corroborate the hypothesis of a non-endothelial origin of the ET-1 rise (Kappers et al., 2010). Briefly, ET-1 is produced in a three-step process, starting with the gene encoding for the precursor preproET-1 (Davenport et al., 2016). Once secreted into the cytoplasm, this protein is cleaved by furin to form BigET-1. The final conversion of BigET-1 into ET-1 is then mediated intracellularly by ECE-1. However, some BigET-1 escapes this cleavage within ECs and is then converted to ET-1 by ECE-1 present also on vascular smooth muscle cells (Maguire et al., 1997; Seed et al., 2012; Davenport et al., 2016). Since increased expression and activity of ECE-1 on VSMCs was observed in endothelium-denuded atherosclerotic arteries (Maguire & Davenport, 1998), it would be important to investigate whether non-endothelial ECE-1 may also have a role in RTKI-induced hypertension. This would also define whether the vascular effects of RTKIs are due to enhanced activity of ECE-1 on smooth muscle cells or to an augmented response to ET-1 itself, in addition to clarifying whether the conversion of BigET-1 to ET-1 by smooth muscle ECE-1 has a role in the increased levels of ET-1 observed during treatment with VEGFR-2 inhibitors.

Finally, with its main secretion occurring in the basolateral compartment of ECs, ET-1 is predominantly released abluminally and act in an autocrine and paracrine way on ECs and underlying VSMCs, respectively (Wagner et al., 1992). As a result, circulating levels of this peptide may just be representative of an excess of the locally produced ET-1 and not necessarily being associated with its effect on vascular tone or with pathological relevance (Wagner et al., 1992). For this reason, locally produced ET-1 may be more relevant than the circulating peptide in the pathogenesis of RTKI-induced hypertension. Indeed, VEGFR-2 inhibition may determine a pathological increase in local ET-1 secretion, without being necessarily associated with a considerable rise in its plasma levels. As a result, assays investigating the effect of axitinib and lenvatinib on abluminal ET-1 production in primary human ECs should be conducted to define the pathological relevance of increased abluminal production of ET-1 versus the rise of circulating peptide in the vascular responses to these agents. To support this *in vitro* work, plasma concentrations of immunoreactive ET-1 in rats and immunoreactive ET-1 distribution on vessel sections should be measured to fully define the role of locally produced ET-1 in RTKI-induced haemodynamic changes both *in vitro* and *in vivo.*

6.2.5 Investigate the effect of selective ET_A vs dual $ET_{A/B}$ receptor antagonists on other RTKI-induced cardiovascular toxicities

VEGFR-2 inhibitors have been also associated with nephrotoxicity, in particular proteinuria (Zhang et al., 2014; Meiracker & Danser, 2016). Among the several hypotheses to explain the kidney impairment observed with these agents, an overactivation of the ET-1 system, reflecting an increased renal production of this peptide, has been proposed (Meiracker & Danser, 2016). As a result, investigating the antiproteinuric effect of selective ET_A and dual $ET_{A/B}$ receptor antagonists in presence of VEGFR-2 inhibition would contribute to define whether endothelin antagonism may be the optimal treatment approach to manage both RTKI-induced hypertension and proteinuria in cancer patients. Additionally, axitinib and lenvatinib have some of the highest rates of all-grade proteinuria among RTKIs, with an incidence of 22.7% and 31%, respectively, making them the ideal candidates for future investigations to better understand the relationship between RTKIs and kidney injury and to assess the role of endothelin receptor antagonism in the management of such toxicity (Kuei & Wu, 2013; Zhang et al., 2014).

7 References

Abdel-Qadir, H., Ethier, J. L., Lee, D. S., Thavendiranathan, P., & Amir, E. (2017). Cardiovascular toxicity of angiogenesis inhibitors in treatment of malignancy: A systematic review and meta-analysis. *Cancer Treat Rev, 53*, 120-127. https://doi.org/10.1016/j.ctrv.2016.12.002

Abdel-Rahman, O., & Fouad, M. (2014). Risk of cardiovascular toxicities in patients with solid tumors treated with sunitinib, axitinib, cediranib or regorafenib: an updated systematic review and comparative meta-analysis. *Crit Rev Oncol Hematol, 92*(3), 194-207. https://doi.org/10.1016/j.critrevonc.2014.06.003

Abdeldayem, A., Raouf, Y. S., Constantinescu, S. N., Moriggl, R., & Gunning, P. T. (2020). Advances in covalent kinase inhibitors [10.1039/C9CS00720B]. *Chemical Society Reviews, 49*(9), 2617-2687. https://doi.org/10.1039/C9CS00720B

Abdullah, S. E., & Perez-Soler, R. (2012). Mechanisms of resistance to vascular endothelial growth factor blockade. *Cancer, 118*(14), 3455-3467. https://doi.org/10.1002/cncr.26540

Abraham, D., & Mao, L. (2015). Cardiac Pressure-Volume Loop Analysis Using Conductance Catheters in Mice. *J Vis Exp*(103). https://doi.org/10.3791/52942

Agency, E. M. (2012). EMA/CHMP/453325/2012 - Annual report of the European Medicines Agency https://www.ema.europa.eu/en/documents/assessment-report/inlyta-epar-public-assessment-report_en.pdf

Agency, E. M. (2021a). *EMA/694337/2021 EMEA/H/C/003727 - Annual report of the European Medicines Agency* https://www.ema.europa.eu/en/documents/overview/lenvima-epar-medicine-overview_en.pdf

Agency, E. M. (2021b). EMEA/H/C/002406 - IA/0032 - Inlyta: EPAR - Product Information. ANNEX I SUMMARY OF PRODUCT CHARACTERISTICS. https://www.ema.europa.eu/en/documents/product-information/inlyta-epar-product-information_en.pdf

Agency, E. M. (2023). EMEA/H/C/000582 - N/0130 - Avastin: EPAR - Product Information. https://www.ema.europa.eu/en/documents/product-information/avastin-epar-product-information_en.pdf

Al Kawas, H., Saaid, I., Jank, P., Westhoff, C. C., Denkert, C., Pross, T., Weiler, K. B. S., & Karsten, M. M. (2022). How VEGF-A and its splice variants affect breast cancer development – clinical implications. *Cellular Oncology, 45*(2), 227-239. https://doi.org/10.1007/s13402-022-00665-w

Alam, A., Herault, J.-P., Barron, P., Favier, B., Fons, P., Delesque-Touchard, N., Senegas, I., Laboudie, P., Bonnin, J., Cassan, C., Savi, P., Ruggeri, B., Carmeliet, P., Bono, F., & Herbert, J.-M. (2004). Heterodimerization with vascular endothelial growth factor receptor-2 (VEGFR-2) is necessary for VEGFR-3 activity. *Biochemical and Biophysical Research Communications, 324*(2), 909-915. https://doi.org/https://doi.org/10.1016/j.bbrc.2004.08.237

Albert, D. H., Tapang, P., Magoc, T. J., Pease, L. J., Reuter, D. R., Wei, R. Q., Li, J., Guo, J., Bousquet, P. F., Ghoreishi-Haack, N. S., Wang, B., Bukofzer, G. T., Wang, Y. C., Stavropoulos, J. A., Hartandi, K., Niquette, A. L., Soni, N., Johnson, E. F., McCall, J. O., Bouska, J. J., Luo, Y., Donawho, C. K., Dai, Y., Marcotte, P. A., Glaser, K. B., Michaelides, M. R., & Davidsen, S. K. (2006). Preclinical activity of ABT-869, a multitargeted receptor tyrosine kinase inhibitor. *Mol Cancer Ther, 5*(4), 995-1006. https://doi.org/10.1158/1535-7163.Mct-05-0410

Albini, A., Pennesi, G., Donatelli, F., Cammarota, R., De Flora, S., & Noonan, D. M. (2010). Cardiotoxicity of anticancer drugs: the need for cardio-oncology and cardio-oncological prevention. *J Natl Cancer Inst, 102*(1), 14-25. https://doi.org/10.1093/jnci/djp440

Allcock, G. H., Warner, T. D., & Vane, J. R. (1995). Roles of endothelin receptors in the regional and systemic vascular responses to ET-1 in the anaesthetized ganglion-blocked rat: use of selective antagonists. *Br J Pharmacol, 116*(5), 2482-2486. https://doi.org/10.1111/j.1476-5381.1995.tb15099.x

Ancker, O. V., Wehland, M., Bauer, J., Infanger, M., & Grimm, D. (2017). The Adverse Effect of Hypertension in the Treatment of Thyroid Cancer with Multi-Kinase Inhibitors. *International Journal of Molecular Sciences, 18*(3), 625. https://www.mdpi.com/1422-0067/18/3/625

Anon. (2001e). ICHS7A: safety pharmacology studies for human pharmaceuticals. *pp CPMP/ICH/ 539-00*.

Ansari, M. J., Bokov, D., Markov, A., Jalil, A. T., Shalaby, M. N., Suksatan, W., Chupradit, S., Al-Ghamdi, H. S., Shomali, N., Zamani, A., Mohammadi, A., & Dadashpour, M. (2022). Cancer combination therapies by angiogenesis inhibitors; a comprehensive review. *Cell Commun Signal, 20*(1), 49. https://doi.org/10.1186/s12964-022-00838-y

Apte, R. S., Chen, D. S., & Ferrara, N. (2019). VEGF in Signaling and Disease: Beyond Discovery and Development. *Cell, 176*(6), 1248-1264. https://doi.org/10.1016/j.cell.2019.01.021

Archer, C. R., Robinson, E. L., Drawnel, F. M., & Roderick, H. L. (2017). Endothelin-1 promotes hypertrophic remodelling of cardiac myocytes by activating sustained signalling and transcription downstream of endothelin type A receptors. *Cell Signal, 36*, 240-254. https://doi.org/10.1016/j.cellsig.2017.04.010

Arjun K Ghosh, J. M. W. (2017). Cardio-oncology. *British Journal of Hospital Medicine, Vol 78, No 1*.

Armulik, A., Genové, G., & Betsholtz, C. (2011). Pericytes: Developmental, Physiological, and Pathological Perspectives, Problems, and Promises. *Developmental Cell, 21*(2), 193-215. https://doi.org/https://doi.org/10.1016/j.devcel.2011.07.001

Asnani, A., Moslehi, J. J., Adhikari, B. B., Baik, A. H., Beyer, A. M., de Boer, R. A., Ghigo, A., Grumbach, I. M., Jain, S., & Zhu, H. (2021). Preclinical Models of Cancer Therapy-Associated Cardiovascular Toxicity: A Scientific Statement From the American Heart

Association. *Circ Res, 129*(1), e21-e34. https://doi.org/10.1161/res.0000000000000473

Authier, S., Pugsley, M. K., & Curtis, M. J. (2015). Haemodynamic Assessment in Safety Pharmacology. *Handb Exp Pharmacol, 229*, 221-241. https://doi.org/10.1007/978-3-662-46943-9_9

Autiero, M., Luttun, A., Tjwa, M., & Carmeliet, P. (2003). Placental growth factor and its receptor, vascular endothelial growth factor receptor-1: novel targets for stimulation of ischemic tissue revascularization and inhibition of angiogenic and inflammatory disorders. *Journal of Thrombosis and Haemostasis, 1*(7), 1356-1370. https://doi.org/https://doi.org/10.1046/j.1538-7836.2003.00263.x

Baek Moller, N., Budolfsen, C., Grimm, D., Kruger, M., Infanger, M., Wehland, M., & N, E. M. (2019). Drug-Induced Hypertension Caused by Multikinase Inhibitors (Sorafenib, Sunitinib, Lenvatinib and Axitinib) in Renal Cell Carcinoma Treatment. *Int J Mol Sci, 20*(19). https://doi.org/10.3390/ijms20194712

Baghban, R., Roshangar, L., Jahanban-Esfahlan, R., Seidi, K., Ebrahimi-Kalan, A., Jaymand, M., Kolahian, S., Javaheri, T., & Zare, P. (2020). Tumor microenvironment complexity and therapeutic implications at a glance. *Cell Communication and Signaling, 18*(1), 59. https://doi.org/10.1186/s12964-020-0530-4

Bagnato, A., & Spinella, F. (2003). Emerging role of endothelin-1 in tumor angiogenesis. *Trends Endocrinol Metab, 14*(1), 44-50. https://doi.org/10.1016/s1043-2760(02)00010-3

Bair, S. M., Choueiri, T. K., & Moslehi, J. (2013). Cardiovascular complications associated with novel angiogenesis inhibitors: emerging evidence and evolving perspectives. *Trends Cardiovasc Med, 23*(4), 104-113. https://doi.org/10.1016/j.tcm.2012.09.008

Ball, S. G., Shuttleworth, C. A., & Kielty, C. M. (2007). Vascular endothelial growth factor can signal through platelet-derived growth factor receptors. *The Journal of cell biology, 177*(3), 489-500. https://doi.org/10.1083/jcb.200608093

Ballmer-Hofer, K., Andersson, A. E., Ratcliffe, L. E., & Berger, P. (2011). Neuropilin-1 promotes VEGFR-2 trafficking through Rab11 vesicles thereby specifying signal output. *Blood, 118*(3), 816-826. https://doi.org/10.1182/blood-2011-01-328773

Banchereau, J., Briere, F., Caux, C., Davoust, J., Lebecque, S., Liu, Y. J., Pulendran, B., & Palucka, K. (2000). Immunobiology of dendritic cells. *Annu Rev Immunol, 18*, 767-811. https://doi.org/10.1146/annurev.immunol.18.1.767

Banfor, P. N., Franklin, P. A., Segreti, J. A., Widomski, D. L., Davidsen, S. K., Albert, D. H., Cox, B. F., Fryer, R. M., & Gintant, G. A. (2009). ETA receptor blockade with atrasentan prevents hypertension with the multitargeted tyrosine kinase inhibitor ABT-869 in telemetry-instrumented rats. *J Cardiovasc Pharmacol, 53*(2), 173-178. https://doi.org/10.1097/FJC.0b013e3181993493

Barac, A., Murtagh, G., Carver, J. R., Chen, M. H., Freeman, A. M., Herrmann, J., Iliescu, C., Ky, B., Mayer, E. L., Okwuosa, T. M., Plana, J. C., Ryan, T. D., Rzeszut, A. K., & Douglas, P.

S. (2015). Cardiovascular Health of Patients With Cancer and Cancer Survivors: A Roadmap to the Next Level. *J Am Coll Cardiol, 65*(25), 2739-2746. https://doi.org/10.1016/j.jacc.2015.04.059

Barrasa-Ramos, S., Dessalles, C. A., Hautefeuille, M., & Barakat, A. I. (2022). Mechanical regulation of the early stages of angiogenesis. *Journal of The Royal Society Interface, 19*(197), 20220360. https://doi.org/doi:10.1098/rsif.2022.0360

Basagiannis, D., Zografou, S., Murphy, C., Fotsis, T., Morbidelli, L., Ziche, M., Bleck, C., Mercer, J., & Christoforidis, S. (2016). VEGF induces signalling and angiogenesis by directing VEGFR2 internalisation through macropinocytosis. *J Cell Sci, 129*(21), 4091-4104. https://doi.org/10.1242/jcs.188219

Bass, A., Kinter, L., & Williams, P. (2004). Origins, practices and future of safety pharmacology. *Journal of Pharmacological and Toxicological Methods, 49*(3), 145-151. https://doi.org/https://doi.org/10.1016/j.vascn.2004.02.007

Bass, A. S., Hombo, T., Kasai, C., Kinter, L. B., & Valentin, J. P. (2015). A Historical View and Vision into the Future of the Field of Safety Pharmacology. *Handb Exp Pharmacol, 229*, 3-45. https://doi.org/10.1007/978-3-662-46943-9_1

Bastos, M. B., Burkhoff, D., Maly, J., Daemen, J., den Uil, C. A., Ameloot, K., Lenzen, M., Mahfoud, F., Zijlstra, F., Schreuder, J. J., & Van Mieghem, N. M. (2020). Invasive left ventricle pressure-volume analysis: overview and practical clinical implications. *Eur Heart J, 41*(12), 1286-1297. https://doi.org/10.1093/eurheartj/ehz552

Bates, D. O. (2010). Vascular endothelial growth factors and vascular permeability. *Cardiovasc Res, 87*(2), 262-271. https://doi.org/10.1093/cvr/cvq105

Bates, D. O., Cui, T. G., Doughty, J. M., Winkler, M., Sugiono, M., Shields, J. D., Peat, D., Gillatt, D., & Harper, S. J. (2002). VEGF165b, an inhibitory splice variant of vascular endothelial growth factor, is down-regulated in renal cell carcinoma. *Cancer Res, 62*(14), 4123-4131.

Battistini, B., Berthiaume, N., Kelland, N. F., Webb, D. J., & Kohan, D. E. (2006). Profile of past and current clinical trials involving endothelin receptor antagonists: the novel "-sentan" class of drug. *Exp Biol Med (Maywood), 231*(6), 653-695.

Belcik, J. T., Qi, Y., Kaufmann, B. A., Xie, A., Bullens, S., Morgan, T. K., Bagby, S. P., Kolumam, G., Kowalski, J., Oyer, J. A., Bunting, S., & Lindner, J. R. (2012). Cardiovascular and systemic microvascular effects of anti-vascular endothelial growth factor therapy for cancer. *J Am Coll Cardiol, 60*(7), 618-625. https://doi.org/10.1016/j.jacc.2012.02.053

Bellesoeur, A., Carton, E., Alexandre, J., Goldwasser, F., & Huillard, O. (2017). Axitinib in the treatment of renal cell carcinoma: design, development, and place in therapy. *Drug Des Devel Ther, 11*, 2801-2811. https://doi.org/10.2147/dddt.S109640

Bellinger, A. M., Arteaga, C. L., Force, T., Humphreys, B. D., Demetri, G. D., Druker, B. J., & Moslehi, J. J. (2015). Cardio-Oncology: How New Targeted Cancer Therapies and Precision Medicine Can Inform Cardiovascular Discovery. *Circulation, 132*(23), 2248-2258. https://doi.org/10.1161/CIRCULATIONAHA.115.010484

Benetos, A., Rudnichi, A., Safar, M., & Guize, L. (1998). Pulse pressure and cardiovascular mortality in normotensive and hypertensive subjects. *Hypertension, 32*(3), 560-564. https://doi.org/10.1161/01.hyp.32.3.560

Bergers, G., & Benjamin, L. E. (2003). Tumorigenesis and the angiogenic switch. *Nat Rev Cancer, 3*(6), 401-410. https://doi.org/10.1038/nrc1093

Bhargava, P. (2009). VEGF kinase inhibitors: how do they cause hypertension? *Am J Physiol Regul Integr Comp Physiol, 297*(1), R1-5. https://doi.org/10.1152/ajpregu.90502.2008

Bhargava, P., & Robinson, M. O. (2011). Development of Second-Generation VEGFR Tyrosine Kinase Inhibitors: Current Status. *Current Oncology Reports, 13*(2), 103-111. https://doi.org/10.1007/s11912-011-0154-3

Bhatt, S., Northcott, C., Wisialowski, T., Li, D., & Steidl-Nichols, J. (2019). Preclinical to Clinical Translation of Hemodynamic Effects in Cardiovascular Safety Pharmacology Studies. *Toxicol Sci, 169*(1), 272-279. https://doi.org/10.1093/toxsci/kfz035

Bhullar, K. S., Lagarón, N. O., McGowan, E. M., Parmar, I., Jha, A., Hubbard, B. P., & Rupasinghe, H. P. V. (2018). Kinase-targeted cancer therapies: progress, challenges and future directions. *Molecular Cancer, 17*(1), 48. https://doi.org/10.1186/s12943-018-0804-2

Binder, N. K., Evans, J., Salamonsen, L. A., Gardner, D. K., Kaitu'u-Lino, T. J., & Hannan, N. J. (2016). Placental Growth Factor Is Secreted by the Human Endometrium and Has Potential Important Functions during Embryo Development and Implantation. *PLoS One, 11*(10), e0163096. https://doi.org/10.1371/journal.pone.0163096

Blanco, R., & Gerhardt, H. (2013). VEGF and Notch in tip and stalk cell selection. *Cold Spring Harb Perspect Med, 3*(1), a006569. https://doi.org/10.1101/cshperspect.a006569

Blasi, E., Heyen, J., Patyna, S., Hemkens, M., Ramirez, D., John-Baptiste, A., Steidl-Nichols, J., & McHarg, A. (2012). Sunitinib, a receptor tyrosine kinase inhibitor, increases blood pressure in rats without associated changes in cardiac structure and function. *Cardiovasc Ther, 30*(5), 287-294. https://doi.org/10.1111/j.1755-5922.2011.00278.x

Bolli, M. H., Marfurt, J., Grisostomi, C., Boss, C., Binkert, C., Hess, P., Treiber, A., Thorin, E., Morrison, K., Buchmann, S., Bur, D., Ramuz, H., Clozel, M., Fischli, W., & Weller, T. (2004). Novel benzo[1,4]diazepin-2-one derivatives as endothelin receptor antagonists. *J Med Chem, 47*(11), 2776-2795. https://doi.org/10.1021/jm031115r

Boucher, J. M., Clark, R. P., Chong, D. C., Citrin, K. M., Wylie, L. A., & Bautch, V. L. (2017). Dynamic alterations in decoy VEGF receptor-1 stability regulate angiogenesis. *Nature Communications, 8*(1), 15699. https://doi.org/10.1038/ncomms15699

Boulanger, C., & Lüscher, T. F. (1990). Release of endothelin from the porcine aorta. Inhibition by endothelium-derived nitric oxide. *J Clin Invest, 85*(2), 587-590. https://doi.org/10.1172/jci114477

Bowes, J., Brown, A. J., Hamon, J., Jarolimek, W., Sridhar, A., Waldron, G., & Whitebread, S. (2012). Reducing safety-related drug attrition: the use of in vitro pharmacological profiling. *Nat Rev Drug Discov, 11*(12), 909-922. https://doi.org/10.1038/nrd3845

Braile, M., Marcella, S., Cristinziano, L., Galdiero, M. R., Modestino, L., Ferrara, A. L., Varricchi, G., Marone, G., & Loffredo, S. (2020). VEGF-A in Cardiomyocytes and Heart Diseases. *Int J Mol Sci, 21*(15). https://doi.org/10.3390/ijms21155294

Bray, F., Laversanne, M., Weiderpass, E., & Soerjomataram, I. (2021). The ever-increasing importance of cancer as a leading cause of premature death worldwide. *Cancer, 127*(16), 3029-3030. https://doi.org/https://doi.org/10.1002/cncr.33587

Bridgett, S., Dellett, M., & Simpson, D. A. (2017). RNA-Sequencing data supports the existence of novel VEGFA splicing events but not of VEGFA(xxx)b isoforms. *Sci Rep, 7*(1), 58. https://doi.org/10.1038/s41598-017-00100-3

Brini, M., & Carafoli, E. (2011). The plasma membrane Ca^{2}+ ATPase and the plasma membrane sodium calcium exchanger cooperate in the regulation of cell calcium. *Cold Spring Harb Perspect Biol, 3*(2). https://doi.org/10.1101/cshperspect.a004168

Bronte, E., Galvano, A., Novo, G., & Russo, A. (2017). Chapter 5 - Cardiotoxic Effects of Anti-VEGFR Tyrosine Kinase Inhibitors. In R. A. Gottlieb & P. K. Mehta (Eds.), *Cardio-Oncology* (pp. 69-89). Academic Press. https://doi.org/https://doi.org/10.1016/B978-0-12-803547-4.00005-7

Brown, S. A., Ray, J. C., & Herrmann, J. (2020). Precision Cardio-Oncology: a Systems-Based Perspective on Cardiotoxicity of Tyrosine Kinase Inhibitors and Immune Checkpoint Inhibitors. *Journal of cardiovascular translational research, 13*(3), 402-416. https://doi.org/10.1007/s12265-020-09992-5

Brown, Z. W., Amit, Z., & Weeks, J. R. (1976). Simple flow-thru swivel for infusions into unrestrained animals. *Pharmacology Biochemistry and Behavior, 5*(3), 363-365. https://doi.org/https://doi.org/10.1016/0091-3057(76)90090-3

Budnitz, D. S., Pollock, D. A., Weidenbach, K. N., Mendelsohn, A. B., Schroeder, T. J., & Annest, J. L. (2006). National surveillance of emergency department visits for outpatient adverse drug events. *JAMA, 296*(15), 1858-1866. https://doi.org/10.1001/jama.296.15.1858

Bui, H. M., Enis, D., Robciuc, M. R., Nurmi, H. J., Cohen, J., Chen, M., Yang, Y., Dhillon, V., Johnson, K., Zhang, H., Kirkpatrick, R., Traxler, E., Anisimov, A., Alitalo, K., & Kahn, M. L. (2016). Proteolytic activation defines distinct lymphangiogenic mechanisms for VEGFC and VEGFD. *J Clin Invest, 126*(6), 2167-2180. https://doi.org/10.1172/jci83967

Bukowski, R. M. (2012). Third generation tyrosine kinase inhibitors and their development in advanced renal cell carcinoma. *Front Oncol, 2*, 13. https://doi.org/10.3389/fonc.2012.00013

Butlin, M., Tan, I., Spronck, B., & Avolio, A. P. (2020). Measuring Arterial Stiffness in Animal Experimental Studies. *Arteriosclerosis, Thrombosis, and Vascular Biology, 40*(5), 1068-1077. https://doi.org/doi:10.1161/ATVBAHA.119.313861

Byzova, T. V., Goldman, C. K., Pampori, N., Thomas, K. A., Bett, A., Shattil, S. J., & Plow, E. F. (2000). A mechanism for modulation of cellular responses to VEGF: activation of the integrins. *Mol Cell, 6*(4), 851-860.

Cabanillas, M. E., & Habra, M. A. (2016). Lenvatinib: Role in thyroid cancer and other solid tumors. *Cancer Treat Rev, 42*, 47-55. https://doi.org/10.1016/j.ctrv.2015.11.003

Camarda, N., Travers, R., Yang, V. K., London, C., & Jaffe, I. Z. (2022). VEGF Receptor Inhibitor-Induced Hypertension: Emerging Mechanisms and Clinical Implications. *Curr Oncol Rep, 24*(4), 463-474. https://doi.org/10.1007/s11912-022-01224-0

Campia, U., Moslehi, J. J., Amiri-Kordestani, L., Barac, A., Beckman, J. A., Chism, D. D., Cohen, P., Groarke, J. D., Herrmann, J., Reilly, C. M., & Weintraub, N. L. (2019). Cardio-Oncology: Vascular and Metabolic Perspectives: A Scientific Statement From the American Heart Association. *Circulation, 139*(13), e579-e602. https://doi.org/10.1161/CIR.0000000000000641

Car, B. (2006). Enabling technologies in reducing drug attrition due to safety failures. *Am Drug Discov, 1(1)*, 53–56.

Carmeliet, P., & Jain, R. K. (2011). Molecular mechanisms and clinical applications of angiogenesis. *Nature, 473*(7347), 298-307. https://doi.org/10.1038/nature10144

Carmeliet, P., Moons, L., Luttun, A., Vincenti, V., Compernolle, V., De Mol, M., Wu, Y., Bono, F., Devy, L., Beck, H., Scholz, D., Acker, T., DiPalma, T., Dewerchin, M., Noel, A., Stalmans, I., Barra, A., Blacher, S., VandenDriessche, T., Ponten, A., Eriksson, U., Plate, K. H., Foidart, J. M., Schaper, W., Charnock-Jones, D. S., Hicklin, D. J., Herbert, J. M., Collen, D., & Persico, M. G. (2001). Synergism between vascular endothelial growth factor and placental growth factor contributes to angiogenesis and plasma extravasation in pathological conditions. *Nat Med, 7*(5), 575-583. https://doi.org/10.1038/87904

Carter, J. J., Fretwell, L. V., & Woolard, J. (2017). Effects of 4 multitargeted receptor tyrosine kinase inhibitors on regional hemodynamics in conscious, freely moving rats. *FASEB J, 31*(3), 1193-1203. https://doi.org/10.1096/fj.201600749R

Carter, J. J., Wheal, A. J., Hill, S. J., & Woolard, J. (2015). Effects of receptor tyrosine kinase inhibitors on VEGF165 a- and VEGF165 b-stimulated gene transcription in HEK-293 cells expressing human VEGFR2. *Br J Pharmacol, 172*(12), 3141-3150. https://doi.org/10.1111/bph.13116

Casanovas, O., Hicklin, D. J., Bergers, G., & Hanahan, D. (2005). Drug resistance by evasion of antiangiogenic targeting of VEGF signaling in late-stage pancreatic islet tumors. *Cancer Cell, 8*(4), 299-309. https://doi.org/10.1016/j.ccr.2005.09.005

Catino, A. B., Hubbard, R. A., Chirinos, J. A., Townsend, R., Keefe, S., Haas, N. B., Puzanov, I., Fang, J. C., Agarwal, N., Hyman, D., Smith, A. M., Gordon, M., Plappert, T., Englefield, V., Narayan, V., Ewer, S., ElAmm, C., Lenihan, D., & Ky, B. (2018). Longitudinal Assessment of Vascular Function With Sunitinib in Patients With Metastatic Renal

Cell Carcinoma. *Circ Heart Fail, 11*(3), e004408. https://doi.org/10.1161/circheartfailure.117.004408

Ceci, C., Atzori, M. G., Lacal, P. M., & Graziani, G. (2020). Role of VEGFs/VEGFR-1 Signaling and Its Inhibition in Modulating Tumor Invasion: Experimental Evidence in Different Metastatic Cancer Models. *International Journal of Molecular Sciences, 21*(4), 1388. https://www.mdpi.com/1422-0067/21/4/1388

Chaar, M., Kamta, J., & Ait-Oudhia, S. (2018). Mechanisms, monitoring, and management of tyrosine kinase inhibitors-associated cardiovascular toxicities. *Onco Targets Ther, 11*, 6227-6237. https://doi.org/10.2147/OTT.S170138

Chae, Y. K., Chiec, L., Adney, S. K., Waitzman, J., Costa, R., Carneiro, B., Matsangou, M., Agulnik, M., Kopp, P., & Giles, F. (2018). Posterior reversible encephalopathy syndrome and takotsubo cardiomyopathy associated with lenvatinib therapy for thyroid cancer: a case report and review. *Oncotarget, 9*(46), 28281-28289. https://doi.org/10.18632/oncotarget.25606

Chan, J. K., Deng, W., Higgins, R. V., Tewari, K. S., Bonebrake, A. J., Hicks, M., Gaillard, S., Ramirez, P. T., Chafe, W., Monk, B. J., & Aghajanian, C. (2017). A phase II evaluation of brivanib in the treatment of persistent or recurrent carcinoma of the cervix: An NRG Oncology/Gynecologic Oncology Group study. *Gynecol Oncol, 146*(3), 554-559. https://doi.org/10.1016/j.ygyno.2017.05.033

Chen, J., & Wang, J. (2018). Risk of regorafenib-induced cardiovascular events in patients with solid tumors: A systematic review and meta-analysis. *Medicine (Baltimore), 97*(41), e12705. https://doi.org/10.1097/md.0000000000012705

Chen, M. H., Kerkelä, R., & Force, T. (2008). Mechanisms of cardiac dysfunction associated with tyrosine kinase inhibitor cancer therapeutics. *Circulation, 118*(1), 84-95. https://doi.org/10.1161/circulationaha.108.776831

Chen, W., Xia, P., Wang, H., Tu, J., Liang, X., Zhang, X., & Li, L. (2019). The endothelial tip-stalk cell selection and shuffling during angiogenesis. *J Cell Commun Signal, 13*(3), 291-301. https://doi.org/10.1007/s12079-019-00511-z

Chen, Y., Tortorici, M. A., Garrett, M., Hee, B., Klamerus, K. J., & Pithavala, Y. K. (2013). Clinical pharmacology of axitinib. *Clin Pharmacokinet, 52*(9), 713-725. https://doi.org/10.1007/s40262-013-0068-3

Cheng, H., & Force, T. (2010). Molecular mechanisms of cardiovascular toxicity of targeted cancer therapeutics. *Circ Res, 106*(1), 21-34. https://doi.org/10.1161/circresaha.109.206920

Cheng, H., Kari, G., Dicker, A. P., Rodeck, U., Koch, W. J., & Force, T. (2011). A Novel Preclinical Strategy for Identifying Cardiotoxic Kinase Inhibitors and Mechanisms of Cardiotoxicity. *Circulation Research, 109*(12), 1401-1409. https://doi.org/doi:10.1161/CIRCRESAHA.111.255695

Cheng, R., & Ma, J. X. (2015). Angiogenesis in diabetes and obesity. *Rev Endocr Metab Disord, 16*(1), 67-75. https://doi.org/10.1007/s11154-015-9310-7

Chiodelli, P., Mitola, S., Ravelli, C., Oreste, P., Rusnati, M., & Presta, M. (2011). Heparan Sulfate Proteoglycans Mediate the Angiogenic Activity of the Vascular Endothelial Growth Factor Receptor-2 Agonist Gremlin. *Arteriosclerosis, Thrombosis, and Vascular Biology, 31*(12), e116-e127. https://doi.org/doi:10.1161/ATVBAHA.111.235184

Chirinos, J. A. (2012). Arterial Stiffness: Basic Concepts and Measurement Techniques. *Journal of cardiovascular translational research, 5*(3), 243-255. https://doi.org/10.1007/s12265-012-9359-6

Chirinos, J. A., Segers, P., Hughes, T., & Townsend, R. (2019). Large-Artery Stiffness in Health and Disease: JACC State-of-the-Art Review. *J Am Coll Cardiol, 74*(9), 1237-1263. https://doi.org/10.1016/j.jacc.2019.07.012

Choueiri, T. K., & Motzer, R. J. (2017). Systemic Therapy for Metastatic Renal-Cell Carcinoma. *N Engl J Med, 376*(4), 354-366. https://doi.org/10.1056/NEJMra1601333

Choueiri, T. K., Schutz, F. A., Je, Y., Rosenberg, J. E., & Bellmunt, J. (2010). Risk of arterial thromboembolic events with sunitinib and sorafenib: a systematic review and meta-analysis of clinical trials. *J Clin Oncol, 28*(13), 2280-2285. https://doi.org/10.1200/jco.2009.27.2757

Chu, T. F., Rupnick, M. A., Kerkela, R., Dallabrida, S. M., Zurakowski, D., Nguyen, L., Woulfe, K., Pravda, E., Cassiola, F., Desai, J., George, S., Harris, D. M., Ismail, N. S., Chen, J.-H., Schoen, F. J., Van den Abbeele, A. D., Demetri, G. D., Force, T., Chen, M. H., & Morgan, J. A. (2007). Cardiotoxicity associated with tyrosine kinase inhibitor sunitinib. *The Lancet, 370*(9604), 2011-2019. https://doi.org/10.1016/s0140-6736(07)61865-0

Chui, R. W., Fosdick, A., Conner, R., Jiang, J., Bruenner, B. A., & Vargas, H. M. (2009). Assessment of two external telemetry systems (PhysioJacket and JET) in beagle dogs with telemetry implants. *J Pharmacol Toxicol Methods, 60*(1), 58-68. https://doi.org/10.1016/j.vascn.2009.04.196

Chung, R., Tyebally, S., Chen, D., Kapil, V., Walker, J. M., Addison, D., Ismail-Khan, R., Guha, A., & Ghosh, A. K. (2020). Hypertensive Cardiotoxicity in Cancer Treatment—Systematic Analysis of Adjunct, Conventional Chemotherapy, and Novel Therapies—Epidemiology, Incidence, and Pathophysiology. *Journal of Clinical Medicine, 9*(10), 3346. https://www.mdpi.com/2077-0383/9/10/3346

Claassen, V. (2013). *Neglected factors in pharmacology and neuroscience research: biopharmaceutics, animal characteristics, maintenance, testing conditions* (Vol. 12). Elsevier.

Claude, J. R., & Claude, N. (2004). Safety pharmacology: an essential interface of pharmacology and toxicology in the non-clinical assessment of new pharmaceuticals. *Toxicol Lett, 151*(1), 25-28. https://doi.org/10.1016/j.toxlet.2004.02.017

Clozel, M., Breu, V., Gray, G. A., Kalina, B., Löffler, B. M., Burri, K., Cassal, J. M., Hirth, G., Müller, M., Neidhart, W., & et al. (1994). Pharmacological characterization of

bosentan, a new potent orally active nonpeptide endothelin receptor antagonist. *J Pharmacol Exp Ther, 270*(1), 228-235.

Cohen, J. B., Brown, N. J., Brown, S. A., Dent, S., van Dorst, D. C. H., Herrmann, S. M., Lang, N. N., Oudit, G. Y., & Touyz, R. M. (2023). Cancer Therapy-Related Hypertension: A Scientific Statement From the American Heart Association. *Hypertension, 80*(3), e46-e57. https://doi.org/10.1161/hyp.0000000000000224

Colatsky, T., Fermini, B., Gintant, G., Pierson, J. B., Sager, P., Sekino, Y., Strauss, D. G., & Stockbridge, N. (2016). The Comprehensive in Vitro Proarrhythmia Assay (CiPA) initiative - Update on progress. *J Pharmacol Toxicol Methods, 81*, 15-20. https://doi.org/10.1016/j.vascn.2016.06.002

Collins, T., Gray, K., Bista, M., Skinner, M., Hardy, C., Wang, H., Mettetal, J. T., & Harmer, A. R. (2018). Quantifying the relationship between inhibition of VEGF receptor 2, drug-induced blood pressure elevation and hypertension. *Br J Pharmacol, 175*(4), 618-630. https://doi.org/10.1111/bph.14103

Constantinides, C., Mean, R., & Janssen, B. J. (2011). Effects of isoflurane anesthesia on the cardiovascular function of the C57BL/6 mouse. *Ilar j, 52*(3), e21-31.

Cooper, S. L., Wragg, E. S., Pannucci, P., Soave, M., Hill, S. J., & Woolard, J. (2022). Regionally selective cardiovascular responses to adenosine A2A and A2B receptor activation. *The FASEB Journal, 36*(4), e22214. https://doi.org/https://doi.org/10.1096/fj.202101945R

Copur, M. S., & Obermiller, A. (2011). An Algorithm for the Management of Hypertension in the Setting of Vascular Endothelial Growth Factor Signaling Inhibition. *Clinical Colorectal Cancer, 10*(3), 151-156. https://doi.org/https://doi.org/10.1016/j.clcc.2011.03.021

Costa, R., Carneiro, B. A., Chandra, S., Pai, S. G., Chae, Y. K., Kaplan, J. B., Garrett, H. B., Agulnik, M., Kopp, P. A., & Giles, F. J. (2016). Spotlight on lenvatinib in the treatment of thyroid cancer: patient selection and perspectives. *Drug Des Devel Ther, 10*, 873-884. https://doi.org/10.2147/dddt.S93459

D'Orléans-Juste, P., Claing, A., Warner, T. D., Yano, M., & Télémaque, S. (1993). Characterization of receptors for endothelins in the perfused arterial and venous mesenteric vasculatures of the rat. *Br J Pharmacol, 110*(2), 687-692. https://doi.org/10.1111/j.1476-5381.1993.tb13866.x

Davenport, A. P., Hyndman, K. A., Dhaun, N., Southan, C., Kohan, D. E., Pollock, J. S., Pollock, D. M., Webb, D. J., & Maguire, J. J. (2016). Endothelin. *Pharmacol Rev, 68*(2), 357-418. https://doi.org/10.1124/pr.115.011833

Davis, M. I., Hunt, J. P., Herrgard, S., Ciceri, P., Wodicka, L. M., Pallares, G., Hocker, M., Treiber, D. K., & Zarrinkar, P. P. (2011). Comprehensive analysis of kinase inhibitor selectivity. *Nat Biotechnol, 29*(11), 1046-1051. https://doi.org/10.1038/nbt.1990

de Aguiar, R. B., & de Moraes, J. Z. (2019). Exploring the Immunological Mechanisms Underlying the Anti-vascular Endothelial Growth Factor Activity in Tumors. *Front Immunol, 10*, 1023. https://doi.org/10.3389/fimmu.2019.01023

De Falco, S. (2012). The discovery of placenta growth factor and its biological activity. *Exp Mol Med, 44*(1), 1-9. https://doi.org/10.3858/emm.2012.44.1.025

De Moudt, S., Leloup, A., & Fransen, P. (2021). Aortic Stiffness Hysteresis in Isolated Mouse Aortic Segments Is Intensified by Contractile Stimuli, Attenuated by Age, and Reversed by Elastin Degradation. *Front Physiol, 12*, 723972. https://doi.org/10.3389/fphys.2021.723972

De Moudt, S., Leloup, A., Van Hove, C., De Meyer, G., & Fransen, P. (2017). Isometric Stretch Alters Vascular Reactivity of Mouse Aortic Segments. *Front Physiol, 8*, 157. https://doi.org/10.3389/fphys.2017.00157

De Munck, D., Leloup, A., De Meyer, G., Martinet, W., & Fransen, P. (2020). Defective autophagy in vascular smooth muscle cells increases passive stiffness of the mouse aortic vessel wall. *Pflügers Archiv - European Journal of Physiology, 472*. https://doi.org/10.1007/s00424-020-02408-y

Dehghanian, F., Hojati, Z., & Kay, M. (2014). New Insights into VEGF-A Alternative Splicing: Key Regulatory Switching in the Pathological Process. *Avicenna J Med Biotechnol, 6*(4), 192-199.

Del Prete, A., Salvi, V., Soriani, A., Laffranchi, M., Sozio, F., Bosisio, D., & Sozzani, S. (2023). Dendritic cell subsets in cancer immunity and tumor antigen sensing. *Cellular & Molecular Immunology, 20*(5), 432-447. https://doi.org/10.1038/s41423-023-00990-6

Delicce, A. V., & Makaryus, A. N. (2023). Physiology, Frank Starling Law. [Updated 2023 Jan 30]. *In: StatPearls [Internet]. Treasure Island (FL): StatPearls Publishing*. https://www.ncbi.nlm.nih.gov/books/NBK470295/#

Deng, L. Y., Li, J. S., & Schiffrin, E. L. (1995). Endothelin receptor subtypes in resistance arteries from humans and rats. *Cardiovasc Res, 29*(4), 532-535.

Deng, Y., Zhang, X., & Simons, M. (2015). Molecular Controls of Lymphatic VEGFR3 Signaling. *Arteriosclerosis, Thrombosis, and Vascular Biology, 35*(2), 421-429. https://doi.org/doi:10.1161/ATVBAHA.114.304881

Déry, M. A., Michaud, M. D., & Richard, D. E. (2005). Hypoxia-inducible factor 1: regulation by hypoxic and non-hypoxic activators. *Int J Biochem Cell Biol, 37*(3), 535-540. https://doi.org/10.1016/j.biocel.2004.08.012

Dhaun, N., & Webb, D. J. (2010). Receptor Tyrosine Kinase Inhibition, Hypertension, and Proteinuria. *Hypertension, 56*(4), 575-577. https://doi.org/doi:10.1161/HYPERTENSIONAHA.110.155762

di Somma, M., Vliora, M., Grillo, E., Castro, B., Dakou, E., Schaafsma, W., Vanparijs, J., Corsini, M., Ravelli, C., Sakellariou, E., & Mitola, S. (2020). Role of VEGFs in metabolic

disorders. *Angiogenesis, 23*(2), 119-130. https://doi.org/10.1007/s10456-019-09700-1

Dimmeler, S., & Zeiher, A. M. (2000). Endothelial Cell Apoptosis in Angiogenesis and Vessel Regression. *Circulation Research, 87*(6), 434-439. https://doi.org/doi:10.1161/01.RES.87.6.434

Dirix, L. (2010). Arterial hypertension induced by vascular endothelial growth factor interfering agents: mechanisms and management. *Belgian Journal of Medical Oncology volume, 4*(4), 160.

Diwan, A., & Gerald W. Dorn, I. (2007). Decompensation of Cardiac Hypertrophy: Cellular Mechanisms and Novel Therapeutic Targets. *Physiology, 22*(1), 56-64. https://doi.org/10.1152/physiol.00033.2006

Dobbin, S. J. H., Cameron, A. C., Petrie, M. C., Jones, R. J., Touyz, R. M., & Lang, N. N. (2018). Toxicity of cancer therapy: what the cardiologist needs to know about angiogenesis inhibitors. *Heart, 104*(24), 1995-2002. https://doi.org/10.1136/heartjnl-2018-313726

Dobbin, S. J. H., Petrie, M. C., Myles, R. C., Touyz, R. M., & Lang, N. N. (2021). Cardiotoxic effects of angiogenesis inhibitors. *Clin Sci (Lond), 135*(1), 71-100. https://doi.org/10.1042/cs20200305

Dong, J., & Chen, H. (2018). Cardiotoxicity of Anticancer Therapeutics. *Front Cardiovasc Med, 5*, 9. https://doi.org/10.3389/fcvm.2018.00009

Dong, S. J., MacGregor, J. H., Crawley, A. P., McVeigh, E., Belenkie, I., Smith, E. R., Tyberg, J. V., & Beyar, R. (1994). Left ventricular wall thickness and regional systolic function in patients with hypertrophic cardiomyopathy. A three-dimensional tagged magnetic resonance imaging study. *Circulation, 90*(3), 1200-1209. https://doi.org/10.1161/01.cir.90.3.1200

Dorst, D. C. H. v., Dobbin, S. J. H., Neves, K. B., Herrmann, J., Herrmann, S. M., Versmissen, J., Mathijssen, R. H. J., Danser, A. H. J., & Lang, N. N. (2021). Hypertension and Prohypertensive Antineoplastic Therapies in Cancer Patients. *Circulation Research, 128*(7), 1040-1061. https://doi.org/doi:10.1161/CIRCRESAHA.121.318051

Duffy AM, B.-H. D., Harmey JH. . (2000–2013). Vascular endothelial growth factor (VEGF) and its role in non-endothelial cells: autocrine signalling by VEGF. *In: Madame Curie Bioscience Database (formerly, Eurekah Bioscience Database). Angio- genesis. Landes Bioscience, Austin (TX), USA*. https://www.ncbi.nlm.nih.gov/books/NBK6482/

Dumor, K., Shoemaker-Moyle, M., Nistala, R., & Whaley-Connell, A. (2018). Arterial Stiffness in Hypertension: an Update. *Curr Hypertens Rep, 20*(8), 72. https://doi.org/10.1007/s11906-018-0867-x

Duong, C. N., & Vestweber, D. (2020). Mechanisms Ensuring Endothelial Junction Integrity Beyond VE-Cadherin. *Front Physiol, 11*, 519. https://doi.org/10.3389/fphys.2020.00519

Dvorak, H. F., Brown, L. F., Detmar, M., & Dvorak, A. M. (1995). Vascular permeability factor/vascular endothelial growth factor, microvascular hyperpermeability, and angiogenesis. *The American journal of pathology, 146*(5), 1029-1039. https://pubmed.ncbi.nlm.nih.gov/7538264
https://www.ncbi.nlm.nih.gov/pmc/articles/PMC1869291/

Eechoute, K., Van Der Veldt, A. A. M., Oosting, S., Kappers, M. H. W., Wessels, J. A. M., Gelderblom, H., Guchelaar, H. J., Reyners, A. K. L., Van Herpen, C. M. L., Haanen, J. B., Mathijssen, R. H. J., & Boven, E. (2012). Polymorphisms in endothelial nitric oxide synthase (eNOS) and vascular endothelial growth factor (VEGF) predict sunitinib-induced hypertension [Article]. *Clinical Pharmacology and Therapeutics, 92*(4), 503-510. https://doi.org/10.1038/clpt.2012.136

Eelen, G., Treps, L., Li, X., & Carmeliet, P. (2020). Basic and Therapeutic Aspects of Angiogenesis Updated. *Circulation Research, 127*(2), 310-329. https://doi.org/doi:10.1161/CIRCRESAHA.120.316851

Elebiyo, T. C., Rotimi, D., Evbuomwan, I. O., Maimako, R. F., Iyobhebhe, M., Ojo, O. A., Oluba, O. M., & Adeyemi, O. S. (2022). Reassessing vascular endothelial growth factor (VEGF) in anti-angiogenic cancer therapy. *Cancer Treatment and Research Communications, 32*, 100620. https://doi.org/https://doi.org/10.1016/j.ctarc.2022.100620

Ellis, L. M., & Hicklin, D. J. (2008). VEGF-targeted therapy: mechanisms of anti-tumour activity. *Nat Rev Cancer, 8*(8), 579-591. https://doi.org/10.1038/nrc2403

Elorza Ridaura, I., Sorrentino, S., & Moroni, L. (2021). Parallels between the Developing Vascular and Neural Systems: Signaling Pathways and Future Perspectives for Regenerative Medicine. *Adv Sci (Weinh), 8*(23), e2101837. https://doi.org/10.1002/advs.202101837

Emami Nejad, A., Najafgholian, S., Rostami, A., Sistani, A., Shojaeifar, S., Esparvarinha, M., Nedaeinia, R., Haghjooy Javanmard, S., Taherian, M., Ahmadlou, M., Salehi, R., Sadeghi, B., & Manian, M. (2021). The role of hypoxia in the tumor microenvironment and development of cancer stem cell: a novel approach to developing treatment. *Cancer Cell International, 21*(1), 62. https://doi.org/10.1186/s12935-020-01719-5

Enevoldsen, F. C., Sahana, J., Wehland, M., Grimm, D., Infanger, M., & Krüger, M. (2020). Endothelin Receptor Antagonists: Status Quo and Future Perspectives for Targeted Therapy. *Journal of Clinical Medicine, 9*(3), 824. https://www.mdpi.com/2077-0383/9/3/824

Fabian, M. A., Biggs, W. H., Treiber, D. K., Atteridge, C. E., Azimioara, M. D., Benedetti, M. G., Carter, T. A., Ciceri, P., Edeen, P. T., Floyd, M., Ford, J. M., Galvin, M., Gerlach, J. L., Grotzfeld, R. M., Herrgard, S., Insko, D. E., Insko, M. A., Lai, A. G., Lélias, J.-M., Mehta, S. A., Milanov, Z. V., Velasco, A. M., Wodicka, L. M., Patel, H. K., Zarrinkar, P. P., & Lockhart, D. J. (2005). A small molecule–kinase interaction map for clinical kinase inhibitors. *Nature Biotechnology, 23*(3), 329-336. https://doi.org/10.1038/nbt1068

Facemire, C. S., Nixon, A. B., Griffiths, R., Hurwitz, H., & Coffman, T. M. (2009). Vascular endothelial growth factor receptor 2 controls blood pressure by regulating nitric oxide synthase expression. *Hypertension, 54*(3), 652-658. https://doi.org/10.1161/hypertensionaha.109.129973

Faggiano, A., Avallone, C., Gentile, D., Provenzale, G., Toriello, F., Merlo, M., Sinagra, G., & Carugo, S. (2021). Echocardiographic Advances in Dilated Cardiomyopathy. *J Clin Med, 10*(23). https://doi.org/10.3390/jcm10235518

FDA. (2006). SU011248/Sutent: Pharmacology/toxicology review and evaluation. https://www.accessdata.fda.gov/drugsatfda_docs/nda/2006/021938_S000_Sutent_PharmR.pdf

Ferlay, J., Shin, H.-R., Bray, F., Forman, D., Mathers, C., & Parkin, D. M. (2010). Estimates of worldwide burden of cancer in 2008: GLOBOCAN 2008. *International Journal of Cancer, 127*(12), 2893-2917. https://doi.org/https://doi.org/10.1002/ijc.25516

Ferrara, N. (2004a). Vascular endothelial growth factor as a target for anticancer therapy. *Oncologist, 9 Suppl 1*, 2-10. https://doi.org/10.1634/theoncologist.9-suppl_1-2

Ferrara, N. (2004b). Vascular endothelial growth factor: basic science and clinical progress. *Endocr Rev, 25*(4), 581-611. https://doi.org/10.1210/er.2003-0027

Ferrara, N., & Adamis, A. P. (2016). Ten years of anti-vascular endothelial growth factor therapy. *Nature Reviews Drug Discovery, 15*(6), 385-403. https://doi.org/10.1038/nrd.2015.17

Ferrara, N., & Alitalo, K. (1999). Clinical applications of angiogenic growth factors and their inhibitors. *Nat Med, 5*(12), 1359-1364. https://doi.org/10.1038/70928

Ferrara, N., & Davis-Smyth, T. (1997). The biology of vascular endothelial growth factor. *Endocr Rev, 18*(1), 4-25. https://doi.org/10.1210/edrv.18.1.0287

Ferrara, N., Gerber, H. P., & LeCouter, J. (2003). The biology of VEGF and its receptors. *Nat Med, 9*(6), 669-676. https://doi.org/10.1038/nm0603-669

Ferri, N., Siegl, P., Corsini, A., Herrmann, J., Lerman, A., & Benghozi, R. (2013). Drug attrition during pre-clinical and clinical development: understanding and managing drug-induced cardiotoxicity. *Pharmacol Ther, 138*(3), 470-484. https://doi.org/10.1016/j.pharmthera.2013.03.005

Finlayson, K., Witchel, H. J., McCulloch, J., & Sharkey, J. (2004). Acquired QT interval prolongation and HERG: implications for drug discovery and development. *European Journal of Pharmacology, 500*(1), 129-142. https://doi.org/https://doi.org/10.1016/j.ejphar.2004.07.019

Flecknell, P. (2015). *Laboratory Animal Anaesthesia*. Elsevier Science. https://books.google.com/books?id=2NuoBAAAQBAJ

Folkman, J. (1971). Tumor Angiogenesis: Therapeutic Implications. *New England Journal of Medicine, 285*(21), 1182-1186. https://doi.org/10.1056/nejm197111182852108

Folkman, J. (1995). Angiogenesis in cancer, vascular, rheumatoid and other disease. *Nat Med, 1*(1), 27-31. https://doi.org/10.1038/nm0195-27

Folkman, J. (2002). Role of angiogenesis in tumor growth and metastasis. *Semin Oncol, 29*(6 Suppl 16), 15-18. https://doi.org/10.1053/sonc.2002.37263

Force, T., & Kerkelä, R. (2008). Cardiotoxicity of the new cancer therapeutics--mechanisms of, and approaches to, the problem. *Drug Discov Today, 13*(17-18), 778-784. https://doi.org/10.1016/j.drudis.2008.05.011

Force, T., Krause, D. S., & Van Etten, R. A. (2007). Molecular mechanisms of cardiotoxicity of tyrosine kinase inhibition. *Nat Rev Cancer, 7*(5), 332-344. https://doi.org/10.1038/nrc2106

Franczyk, B., Rysz, J., Ławiński, J., Ciałkowska-Rysz, A., & Gluba-Brzózka, A. (2023). Cardiotoxicity of Selected Vascular Endothelial Growth Factor Receptor Tyrosine Kinase Inhibitors in Patients with Renal Cell Carcinoma. *Biomedicines, 11*(1), 181. https://www.mdpi.com/2227-9059/11/1/181

Fransen, P., Van Hove, C. E., Leloup, A. J. A., Martinet, W., De Meyer, G. R. Y., Lemmens, K., Bult, H., & Schrijvers, D. M. (2015). Dissecting out the Complex Ca2+-Mediated Phenylephrine-Induced Contractions of Mouse Aortic Segments. *PLoS One, 10*(3), e0121634. https://doi.org/10.1371/journal.pone.0121634

French, K. J., Coatney, R. W., Renninger, J. P., Hu, C. X., Gales, T. L., Zhao, S., Storck, L. M., Davis, C. B., McSurdy-Freed, J., Chen, E., & Frazier, K. S. (2010). Differences in effects on myocardium and mitochondria by angiogenic inhibitors suggest separate mechanisms of cardiotoxicity. *Toxicol Pathol, 38*(5), 691-702. https://doi.org/10.1177/0192623310373775

Friehs, I., Margossian, R. E., Moran, A. M., Cao-Danh, H., Moses, M. A., & del Nido, P. J. (2006). Vascular endothelial growth factor delays onset of failure in pressure-overload hypertrophy through matrix metalloproteinase activation and angiogenesis. *Basic Res Cardiol, 101*(3), 204-213. https://doi.org/10.1007/s00395-005-0581-0

Fuh, G., Garcia, K. C., & de Vos, A. M. (2000). The interaction of neuropilin-1 with vascular endothelial growth factor and its receptor flt-1. *J Biol Chem, 275*(35), 26690-26695. https://doi.org/10.1074/jbc.M003955200

Fuh, G., Li, B., Crowley, C., Cunningham, B., & Wells, J. A. (1998). Requirements for binding and signaling of the kinase domain receptor for vascular endothelial growth factor. *J Biol Chem, 273*(18), 11197-11204. https://doi.org/10.1074/jbc.273.18.11197

Fukuroda, T., Fujikawa, T., Ozaki, S., Ishikawa, K., Yano, M., & Nishikibe, M. (1994). Clearance of circulating endothelin-1 by ETB receptors in rats. *Biochem Biophys Res Commun, 199*(3), 1461-1465. https://doi.org/10.1006/bbrc.1994.1395

Gaasch, W. H., & Little, W. C. (2007). Assessment of Left Ventricular Diastolic Function and Recognition of Diastolic Heart Failure. *Circulation, 116*(6), 591-593. https://doi.org/doi:10.1161/CIRCULATIONAHA.107.716647

Gabrilovich, D. I., Chen, H. L., Girgis, K. R., Cunningham, H. T., Meny, G. M., Nadaf, S., Kavanaugh, D., & Carbone, D. P. (1996). Production of vascular endothelial growth factor by human tumors inhibits the functional maturation of dendritic cells. *Nat Med, 2*(10), 1096-1103. https://doi.org/10.1038/nm1096-1096

Galiè, N., Hoeper, M. M., Gibbs, J. S., & Simonneau, G. (2011). Liver toxicity of sitaxentan in pulmonary arterial hypertension. *Eur Respir J, 37*(2), 475-476. https://doi.org/10.1183/09031936.00194810

García-Caballero, M., Sokol, L., Cuypers, A., & Carmeliet, P. (2022). Metabolic Reprogramming in Tumor Endothelial Cells. *International Journal of Molecular Sciences, 23*(19), 11052. https://www.mdpi.com/1422-0067/23/19/11052

Gardiner, S. M., & Bennett, T. (1988). Regional hemodynamic responses to adrenoceptor antagonism in conscious rats. *Am J Physiol, 255*(4 Pt 2), H813-824. https://doi.org/10.1152/ajpheart.1988.255.4.H813

Gardiner, S. M., Bennett, T., & Kemp, P. A. (1980). Systemic arterial hypertension in rats exposed to short-term isolation; intra-arterial systolic and diastolic blood pressure and baroreflex sensitivity. *Med Biol, 58*(4), 232-239.

Gardiner, S. M., Compton, A. M., & Bennett, T. (1990). Regional haemodynamic effects of endothelin-1 and endothelin-3 in conscious Long Evans and Brattleboro rats. *British Journal of Pharmacology, 99*(1), 107-112. https://doi.org/https://doi.org/10.1111/j.1476-5381.1990.tb14662.x

Gardiner, S. M., Compton, A. M., Bennett, T., & Hartley, C. J. (1990). Can pulsed Doppler technique measure changes in aortic blood flow in conscious rats? *American Journal of Physiology-Heart and Circulatory Physiology, 259*(2), H448-H456. https://doi.org/10.1152/ajpheart.1990.259.2.H448

Gardiner, S. M., Kemp, P. A., March, J. E., Bennett, T., Davenport, A. P., & Edvinsson, L. (1994). Effects of an ET1-receptor antagonist, FR139317, on regional haemodynamic responses to endothelin-1 and [Ala11,15]Ac-endothelin-1 (6-21) in conscious rats. *Br J Pharmacol, 112*(2), 477-486. https://doi.org/10.1111/j.1476-5381.1994.tb13098.x

Gast, R. E., König, S., Rose, K., Ferenz, K. B., & Krieglstein, J. (2011). Binding of ATP to vascular endothelial growth factor isoform VEGF-A165 is essential for inducing proliferation of human umbilical vein endothelial cells. *BMC Biochemistry, 12*(1), 28. https://doi.org/10.1186/1471-2091-12-28

Geller, J. I., Fox, E., Turpin, B. K., Goldstein, S. L., Liu, X., Minard, C. G., Kudgus, R. A., Reid, J. M., Berg, S. L., & Weigel, B. J. (2018). A study of axitinib, a VEGF receptor tyrosine kinase inhibitor, in children and adolescents with recurrent or refractory solid tumors: A Children's Oncology Group phase 1 and pilot consortium trial (ADVL1315). *Cancer, 124*(23), 4548-4555. https://doi.org/10.1002/cncr.31725

Georgakopoulos, D., & Kass, D. A. (2000). Estimation of parallel conductance by dual-frequency conductance catheter in mice. *Am J Physiol Heart Circ Physiol, 279*(1), H443-450. https://doi.org/10.1152/ajpheart.2000.279.1.H443

Georgakopoulos, D., Mitzner, W. A., Chen, C. H., Byrne, B. J., Millar, H. D., Hare, J. M., & Kass, D. A. (1998). In vivo murine left ventricular pressure-volume relations by miniaturized conductance micromanometry. *Am J Physiol, 274*(4), H1416-1422. https://doi.org/10.1152/ajpheart.1998.274.4.H1416

Gerber, D. E. (2008). Targeted therapies: a new generation of cancer treatments. *Am Fam Physician, 77*(3), 311-319.

Gerber, H. P., McMurtrey, A., Kowalski, J., Yan, M., Keyt, B. A., Dixit, V., & Ferrara, N. (1998). Vascular endothelial growth factor regulates endothelial cell survival through the phosphatidylinositol 3'-kinase/Akt signal transduction pathway. Requirement for Flk-1/KDR activation. *J Biol Chem, 273*(46), 30336-30343. https://doi.org/10.1074/jbc.273.46.30336

Ghatalia, P., Morgan, C. J., Je, Y., Nguyen, P. L., Trinh, Q.-D., Choueiri, T. K., & Sonpavde, G. (2015). Congestive heart failure with vascular endothelial growth factor receptor tyrosine kinase inhibitors. *Critical Reviews in Oncology/Hematology, 94*(2), 228-237. https://doi.org/https://doi.org/10.1016/j.critrevonc.2014.12.008

Ghorab, M. M., Alsaid, M. S., Soliman, A. M., & Ragab, F. A. (2017). VEGFR-2 inhibitors and apoptosis inducers: synthesis and molecular design of new benzo[g]quinazolin bearing benzenesulfonamide moiety. *Journal of Enzyme Inhibition and Medicinal Chemistry, 32*(1), 893-907. https://doi.org/10.1080/14756366.2017.1334650

Ghoreschi, K., Laurence, A., & O'Shea, J. J. (2009). Selectivity and therapeutic inhibition of kinases: to be or not to be? *Nat Immunol, 10*(4), 356-360. https://doi.org/10.1038/ni.1701

Giannotta, M., Trani, M., & Dejana, E. (2013). VE-Cadherin and Endothelial Adherens Junctions: Active Guardians of Vascular Integrity. *Developmental Cell, 26*(5), 441-454. https://doi.org/https://doi.org/10.1016/j.devcel.2013.08.020

Giordano, F. J., Gerber, H. P., Williams, S. P., VanBruggen, N., Bunting, S., Ruiz-Lozano, P., Gu, Y., Nath, A. K., Huang, Y., Hickey, R., Dalton, N., Peterson, K. L., Ross, J., Jr., Chien, K. R., & Ferrara, N. (2001). A cardiac myocyte vascular endothelial growth factor paracrine pathway is required to maintain cardiac function. *Proc Natl Acad Sci U S A, 98*(10), 5780-5785. https://doi.org/10.1073/pnas.091415198

Gochfeld, M. (2017). Sex Differences in Human and Animal Toxicology:Toxicokinetics. *Toxicologic Pathology, 45*(1), 172-189. https://doi.org/10.1177/0192623316677327

Goel, A., & Singla, A. (2021). Lenvatinib: A narrative drug review. *Cancer Research, Statistics, and Treatment, 4*(4), 709-720. https://doi.org/10.4103/crst.crst_151_21

Goel, H. L., & Mercurio, A. M. (2013). VEGF targets the tumour cell. *Nature reviews. Cancer, 13*(12), 871-882. https://doi.org/10.1038/nrc3627

Goel, S., Duda, D. G., Xu, L., Munn, L. L., Boucher, Y., Fukumura, D., & Jain, R. K. (2011). Normalization of the vasculature for treatment of cancer and other diseases. *Physiol Rev, 91*(3), 1071-1121. https://doi.org/10.1152/physrev.00038.2010

Gorski, P. A., Ceholski, D. K., & Young, H. S. (2017). Structure-Function Relationship of the SERCA Pump and Its Regulation by Phospholamban and Sarcolipin. *Adv Exp Med Biol, 981*, 77-119. https://doi.org/10.1007/978-3-319-55858-5_5

Gosselin, R. D. (2019). Guidelines on statistics for researchers using laboratory animals: the essentials. *Lab Anim, 53*(1), 28-42. https://doi.org/10.1177/0023677218783223

Gotink, K. J., & Verheul, H. M. W. (2010). Anti-angiogenic tyrosine kinase inhibitors: what is their mechanism of action? *Angiogenesis, 13*(1), 1-14. https://doi.org/10.1007/s10456-009-9160-6

Graham, F. L., Smiley, J., Russell, W. C., & Nairn, R. (1977). Characteristics of a human cell line transformed by DNA from human adenovirus type 5. *J Gen Virol, 36*(1), 59-74. https://doi.org/10.1099/0022-1317-36-1-59

Greenberg, J. I., Shields, D. J., Barillas, S. G., Acevedo, L. M., Murphy, E., Huang, J., Scheppke, L., Stockmann, C., Johnson, R. S., Angle, N., & Cheresh, D. A. (2008). A role for VEGF as a negative regulator of pericyte function and vessel maturation. *Nature, 456*(7223), 809-813. https://doi.org/10.1038/nature07424

Grossman, W., McLaurin, L. P., Moos, S. P., Stefadouros, M., & Young, D. T. (1974). Wall Thickness and Diastolic Properties of the Left Ventricle. *Circulation, 49*(1), 129-135. https://doi.org/doi:10.1161/01.CIR.49.1.129

Grünewald, F. S., Prota, A. E., Giese, A., & Ballmer-Hofer, K. (2010). Structure-function analysis of VEGF receptor activation and the role of coreceptors in angiogenic signaling. *Biochim Biophys Acta, 1804*(3), 567-580. https://doi.org/10.1016/j.bbapap.2009.09.002

Guha, A., Armanious, M., & Fradley, M. G. (2019). Update on cardio-oncology: Novel cancer therapeutics and associated cardiotoxicities. *Trends Cardiovasc Med, 29*(1), 29-39. https://doi.org/10.1016/j.tcm.2018.06.001

Guns, P.-J. D., Guth, B. D., Braam, S., Kosmidis, G., Matsa, E., Delaunois, A., Gryshkova, V., Bernasconi, S., Knot, H. J., Shemesh, Y., Chen, A., Markert, M., Fernández, M. A., Lombardi, D., Grandmont, C., Cillero-Pastor, B., Heeren, R. M. A., Martinet, W., Woolard, J., Skinner, M., Segers, V. F. M., Franssen, C., Van Craenenbroeck, E. M., Volders, P. G. A., Pauwelyn, T., Braeken, D., Yanez, P., Correll, K., Yang, X., Prior, H., Kismihók, G., De Meyer, G. R. Y., & Valentin, J.-P. (2020). INSPIRE: A European training network to foster research and training in cardiovascular safety pharmacology. *Journal of Pharmacological and Toxicological Methods, 105*, 106889. https://doi.org/https://doi.org/10.1016/j.vascn.2020.106889

Guo, B. Q., & Lu, W. Q. (2018). The prognostic significance of high/positive expression of tissue VEGF in ovarian cancer. *Oncotarget, 9*(55), 30552-30560. https://doi.org/10.18632/oncotarget.25702

Gupta, A., Jarzab, B., Capdevila, J., Shumaker, R., & Hussein, Z. (2016). Population pharmacokinetic analysis of lenvatinib in healthy subjects and patients with cancer. *Br J Clin Pharmacol, 81*(6), 1124-1133. https://doi.org/10.1111/bcp.12907

Haibe, Y., Kreidieh, M., El Hajj, H., Khalifeh, I., Mukherji, D., Temraz, S., & Shamseddine, A. (2020). Resistance Mechanisms to Anti-angiogenic Therapies in Cancer. *Front Oncol, 10*, 221. https://doi.org/10.3389/fonc.2020.00221

Haigh, J. J. (2008). Role of VEGF in organogenesis. *Organogenesis, 4*(4), 247-256. https://doi.org/10.4161/org.4.4.7415

Harmey, J. H., & Bouchier-Hayes, D. (2002). Vascular endothelial growth factor (VEGF), a survival factor for tumour cells: implications for anti-angiogenic therapy. *Bioessays, 24*(3), 280-283. https://doi.org/10.1002/bies.10043

Harris, I. S., Zhang, S., Treskov, I., Kovacs, A., Weinheimer, C., & Muslin, A. J. (2004). Raf-1 Kinase Is Required for Cardiac Hypertrophy and Cardiomyocyte Survival in Response to Pressure Overload. *Circulation, 110*(6), 718-723. https://doi.org/doi:10.1161/01.CIR.0000138190.50127.6A

Hartley, C. J., & Cole, J. S. (1974). An ultrasonic pulsed Doppler system for measuring blood flow in small vessels. *J Appl Physiol, 37*(4), 626-629. https://doi.org/10.1152/jappl.1974.37.4.626

Haywood, J. R., Shaffer, R. A., Fastenow, C., Fink, G. D., & Brody, M. J. (1981). Regional blood flow measurement with pulsed Doppler flowmeter in conscious rat. *American Journal of Physiology-Heart and Circulatory Physiology, 241*(2), H273-H278. https://doi.org/10.1152/ajpheart.1981.241.2.H273

Herbert, S. P., & Stainier, D. Y. (2011). Molecular control of endothelial cell behaviour during blood vessel morphogenesis. *Nat Rev Mol Cell Biol, 12*(9), 551-564. https://doi.org/10.1038/nrm3176

Herzog, B., Pellet-Many, C., Britton, G., Hartzoulakis, B., & Zachary, I. C. (2011). VEGF binding to NRP1 is essential for VEGF stimulation of endothelial cell migration, complex formation between NRP1 and VEGFR2, and signaling via FAK Tyr407 phosphorylation. *Mol Biol Cell, 22*(15), 2766-2776. https://doi.org/10.1091/mbc.E09-12-1061

Higazi, D. R., Fearnley, C. J., Drawnel, F. M., Talasila, A., Corps, E. M., Ritter, O., McDonald, F., Mikoshiba, K., Bootman, M. D., & Roderick, H. L. (2009). Endothelin-1-stimulated InsP3-induced Ca2+ release is a nexus for hypertrophic signaling in cardiac myocytes. *Mol Cell, 33*(4), 472-482. https://doi.org/10.1016/j.molcel.2009.02.005

Hill, S. J., Baker, J. G., & Rees, S. (2001). Reporter-gene systems for the study of G-protein-coupled receptors. *Curr Opin Pharmacol, 1*(5), 526-532. https://doi.org/10.1016/s1471-4892(01)00091-1

Hoeben, A., Landuyt, B., Highley, M. S., Wildiers, H., Van Oosterom, A. T., & De Bruijn, E. A. (2004). Vascular endothelial growth factor and angiogenesis. *Pharmacol Rev, 56*(4), 549-580. https://doi.org/10.1124/pr.56.4.3

Holmes, D. I. R., & Zachary, I. (2005). The vascular endothelial growth factor (VEGF) family: angiogenic factors in health and disease. *Genome Biology, 6*(2), 209. https://doi.org/10.1186/gb-2005-6-2-209

Homan, T. D., Bordes, S., & Cichowski, E. (2022). Physiology, Pulse Pressure. In *StatPearls*. StatPearls Publishing
Copyright © 2022, StatPearls Publishing LLC.

Houck, K. A., Ferrara, N., Winer, J., Cachianes, G., Li, B., & Leung, D. W. (1991). The vascular endothelial growth factor family: identification of a fourth molecular species and characterization of alternative splicing of RNA. *Mol Endocrinol, 5*(12), 1806-1814. https://doi.org/10.1210/mend-5-12-1806

Hsieh, P. C., Davis, M. E., Lisowski, L. K., & Lee, R. T. (2006). Endothelial-cardiomyocyte interactions in cardiac development and repair. *Annu Rev Physiol, 68*, 51-66. https://doi.org/10.1146/annurev.physiol.68.040104.124629

Hu-Lowe, D. D., Zou, H. Y., Grazzini, M. L., Hallin, M. E., Wickman, G. R., Amundson, K., Chen, J. H., Rewolinski, D. A., Yamazaki, S., Wu, E. Y., McTigue, M. A., Murray, B. W., Kania, R. S., O'Connor, P., Shalinsky, D. R., & Bender, S. L. (2008). Nonclinical antiangiogenesis and antitumor activities of axitinib (AG-013736), an oral, potent, and selective inhibitor of vascular endothelial growth factor receptor tyrosine kinases 1, 2, 3. *Clin Cancer Res, 14*(22), 7272-7283. https://doi.org/10.1158/1078-0432.Ccr-08-0652

Hulvat, M. C. (2020). Cancer Incidence and Trends. *Surg Clin North Am, 100*(3), 469-481. https://doi.org/10.1016/j.suc.2020.01.002

Hussein, Z., Mizuo, H., Hayato, S., Namiki, M., & Shumaker, R. (2017). Clinical Pharmacokinetic and Pharmacodynamic Profile of Lenvatinib, an Orally Active, Small-Molecule, Multitargeted Tyrosine Kinase Inhibitor. *Eur J Drug Metab Pharmacokinet, 42*(6), 903-914. https://doi.org/10.1007/s13318-017-0403-4

Iacovelli, R., Sternberg, C. N., Porta, C., Verzoni, E., de Braud, F., Escudier, B., & Procopio, G. (2015). Inhibition of the VEGF/VEGFR pathway improves survival in advanced kidney cancer: a systematic review and meta-analysis. *Curr Drug Targets, 16*(2), 164-170. https://doi.org/10.2174/1389450115666141120120145

Iglarz, M., Binkert, C., Morrison, K., Fischli, W., Gatfield, J., Treiber, A., Weller, T., Bolli, M. H., Boss, C., Buchmann, S., Capeleto, B., Hess, P., Qiu, C., & Clozel, M. (2008). Pharmacology of macitentan, an orally active tissue-targeting dual endothelin receptor antagonist. *J Pharmacol Exp Ther, 327*(3), 736-745. https://doi.org/10.1124/jpet.108.142976

Ikeda, M., Okusaka, T., Mitsunaga, S., Ueno, H., Tamai, T., Suzuki, T., Hayato, S., Kadowaki, T., Okita, K., & Kumada, H. (2016). Safety and Pharmacokinetics of Lenvatinib in Patients with Advanced Hepatocellular Carcinoma. *Clinical Cancer Research, 22*(6), 1385-1394. https://doi.org/10.1158/1078-0432.Ccr-15-1354

Inlyta., E. C. C. f. M. P. f. H. U. C. a. r. (24 May 2012).

Iruela-Arispe, M. L., & Davis, G. E. (2009). Cellular and molecular mechanisms of vascular lumen formation. *Dev Cell, 16*(2), 222-231. https://doi.org/10.1016/j.devcel.2009.01.013

Isenberg, J. S., Qin, Y., Maxhimer, J. B., Sipes, J. M., Despres, D., Schnermann, J., Frazier, W. A., & Roberts, D. D. (2009). Thrombospondin-1 and CD47 regulate blood pressure and cardiac responses to vasoactive stress. *Matrix Biol, 28*(2), 110-119. https://doi.org/10.1016/j.matbio.2009.01.002

Iyer, S., & Acharya, K. R. (2011). Tying the knot: The cystine signature and molecular-recognition processes of the vascular endothelial growth factor family of angiogenic cytokines. *The FEBS Journal, 278*(22), 4304-4322. https://doi.org/https://doi.org/10.1111/j.1742-4658.2011.08350.x

Izumiya, Y., Shiojima, I., Sato, K., Sawyer, D. B., Colucci, W. S., & Walsh, K. (2006). Vascular endothelial growth factor blockade promotes the transition from compensatory cardiac hypertrophy to failure in response to pressure overload. *Hypertension, 47*(5), 887-893. https://doi.org/10.1161/01.Hyp.0000215207.54689.31

Jakobsson, L., Franco, C. A., Bentley, K., Collins, R. T., Ponsioen, B., Aspalter, I. M., Rosewell, I., Busse, M., Thurston, G., Medvinsky, A., Schulte-Merker, S., & Gerhardt, H. (2010). Endothelial cells dynamically compete for the tip cell position during angiogenic sprouting. *Nature Cell Biology, 12*(10), 943-953. https://doi.org/10.1038/ncb2103

Jakobsson, L., Kreuger, J., Holmborn, K., Lundin, L., Eriksson, I., Kjellén, L., & Claesson-Welsh, L. (2006). Heparan sulfate in trans potentiates VEGFR-mediated angiogenesis. *Dev Cell, 10*(5), 625-634. https://doi.org/10.1016/j.devcel.2006.03.009

Janssen, B. J., De Celle, T., Debets, J. J., Brouns, A. E., Callahan, M. F., & Smith, T. L. (2004). Effects of anesthetics on systemic hemodynamics in mice. *Am J Physiol Heart Circ Physiol, 287*(4), H1618-1624. https://doi.org/10.1152/ajpheart.01192.2003

Jespersen, B., Tykocki, N. R., Watts, S. W., & Cobbett, P. J. (2015). Measurement of smooth muscle function in the isolated tissue bath-applications to pharmacology research. *J Vis Exp*(95), 52324. https://doi.org/10.3791/52324

Jiang, L., Ping, L., Yan, H., Yang, X., He, Q., Xu, Z., & Luo, P. (2020). Cardiovascular toxicity induced by anti-VEGF/VEGFR agents: a special focus on definitions, diagnoses, mechanisms and management. *Expert Opin Drug Metab Toxicol, 16*(9), 823-835. https://doi.org/10.1080/17425255.2020.1787986

Jin, Y., Xu, Z., Yan, H., He, Q., Yang, X., & Luo, P. (2020). A Comprehensive Review of Clinical Cardiotoxicity Incidence of FDA-Approved Small-Molecule Kinase Inhibitors. *Frontiers in pharmacology, 11*, 891. https://doi.org/10.3389/fphar.2020.00891

Kadowaki, H., Ishida, J., Akazawa, H., Yagi, H., Saga-Kamo, A., Umei, M., Matsuoka, R., Liu, Q., Matsunaga, H., Maki, H., Sato, Y., Kume, H., & Komuro, I. (2021). Axitinib Induces and Aggravates Hypertension Regardless of Prior Treatment With Tyrosine Kinase Inhibitors. *Circ Rep, 3*(4), 234-240. https://doi.org/10.1253/circrep.CR-21-0008

Kaess, B. M., Rong, J., Larson, M. G., Hamburg, N. M., Vita, J. A., Levy, D., Benjamin, E. J., Vasan, R. S., & Mitchell, G. F. (2012). Aortic stiffness, blood pressure progression, and incident hypertension. *JAMA, 308*(9), 875-881. https://doi.org/10.1001/2012.jama.10503

Kamba, T., & McDonald, D. M. (2007). Mechanisms of adverse effects of anti-VEGF therapy for cancer. *Br J Cancer, 96*(12), 1788-1795. https://doi.org/10.1038/sj.bjc.6603813

Kannankeril, P., Roden, D. M., & Darbar, D. (2010). Drug-induced long QT syndrome. *Pharmacol Rev, 62*(4), 760-781. https://doi.org/10.1124/pr.110.003723

Kanthou, C., & Tozer, G. (2019). Targeting the vasculature of tumours: combining VEGF pathway inhibitors with radiotherapy. *Br J Radiol, 92*(1093), 20180405. https://doi.org/10.1259/bjr.20180405

Kappers, M. H., de Beer, V. J., Zhou, Z., Danser, A. H., Sleijfer, S., Duncker, D. J., van den Meiracker, A. H., & Merkus, D. (2012). Sunitinib-induced systemic vasoconstriction in swine is endothelin mediated and does not involve nitric oxide or oxidative stress. *Hypertension, 59*(1), 151-157. https://doi.org/10.1161/hypertensionaha.111.182220

Kappers, M. H., Smedts, F. M., Horn, T., van Esch, J. H., Sleijfer, S., Leijten, F., Wesseling, S., Strevens, H., Jan Danser, A. H., & van den Meiracker, A. H. (2011). The vascular endothelial growth factor receptor inhibitor sunitinib causes a preeclampsia-like syndrome with activation of the endothelin system. *Hypertension, 58*(2), 295-302. https://doi.org/10.1161/HYPERTENSIONAHA.111.173559

Kappers, M. H., van Esch, J. H., Sluiter, W., Sleijfer, S., Danser, A. H., & van den Meiracker, A. H. (2010). Hypertension induced by the tyrosine kinase inhibitor sunitinib is associated with increased circulating endothelin-1 levels. *Hypertension, 56*(4), 675-681. https://doi.org/10.1161/HYPERTENSIONAHA.109.149690

Kappers, M. H. W., Smedts, F. M. M., Horn, T., Van Esch, J. H. M., Sleijfer, S., Leijten, F., Wesseling, S., Strevens, H., Danser, A. H. J., & Van Den Meiracker, A. H. (2011). The vascular endothelial growth factor receptor inhibitor sunitinib causes a preeclampsia-like syndrome with activation of the endothelin system [Article]. *Hypertension, 58*(2), 295-302. https://doi.org/10.1161/HYPERTENSIONAHA.111.173559

Karaman, M. W., Herrgard, S., Treiber, D. K., Gallant, P., Atteridge, C. E., Campbell, B. T., Chan, K. W., Ciceri, P., Davis, M. I., Edeen, P. T., Faraoni, R., Floyd, M., Hunt, J. P., Lockhart, D. J., Milanov, Z. V., Morrison, M. J., Pallares, G., Patel, H. K., Pritchard, S., Wodicka, L. M., & Zarrinkar, P. P. (2008). A quantitative analysis of kinase inhibitor selectivity. *Nature Biotechnology, 26*(1), 127-132. https://doi.org/10.1038/nbt1358

Kass, D. A., Yamazaki, T., Burkhoff, D., Maughan, W. L., & Sagawa, K. (1986). Determination of left ventricular end-systolic pressure-volume relationships by the conductance (volume) catheter technique. *Circulation, 73*(3), 586-595. https://doi.org/10.1161/01.cir.73.3.586

Kaumann, A. J., & Levy, F. O. (2006). 5-hydroxytryptamine receptors in the human cardiovascular system. *Pharmacol Ther, 111*(3), 674-706. https://doi.org/10.1016/j.pharmthera.2005.12.004

Kelly, R. P., Ting, C. T., Yang, T. M., Liu, C. P., Maughan, W. L., Chang, M. S., & Kass, D. A. (1992). Effective arterial elastance as index of arterial vascular load in humans. *Circulation, 86*(2), 513-521. https://doi.org/doi:10.1161/01.CIR.86.2.513

Kerkelä, R., Ulvila, J., & Magga, J. (2015). Natriuretic Peptides in the Regulation of Cardiovascular Physiology and Metabolic Events. *Journal of the American Heart Association, 4*(10), e002423. https://doi.org/doi:10.1161/JAHA.115.002423

Kerkela, R., Woulfe, K. C., Durand, J. B., Vagnozzi, R., Kramer, D., Chu, T. F., Beahm, C., Chen, M. H., & Force, T. (2009). Sunitinib-induced cardiotoxicity is mediated by off-target inhibition of AMP-activated protein kinase. *Clin Transl Sci, 2*(1), 15-25. https://doi.org/10.1111/j.1752-8062.2008.00090.x

Khakoo, A. Y., Kassiotis, C. M., Tannir, N., Plana, J. C., Halushka, M., Bickford, C., Trent, J., 2nd, Champion, J. C., Durand, J. B., & Lenihan, D. J. (2008). Heart failure associated with sunitinib malate: a multitargeted receptor tyrosine kinase inhibitor. *Cancer, 112*(11), 2500-2508. https://doi.org/10.1002/cncr.23460

Kilkenny, C., Browne, W., Cuthill, I. C., Emerson, M., & Altman, D. G. (2010). Animal research: reporting in vivo experiments: the ARRIVE guidelines. *Br J Pharmacol, 160*(7), 1577-1579. https://doi.org/10.1111/j.1476-5381.2010.00872.x

Killock, D. (2015). SELECT—lenvatinib in thyroid cancer. *Nature Reviews Clinical Oncology, 12*(4), 189-189. https://doi.org/10.1038/nrclinonc.2015.30

Kim, C. W., Pokutta-Paskaleva, A., Kumar, S., Timmins, L. H., Morris, A. D., Kang, D.-W., Dalal, S., Chadid, T., Kuo, K. M., Raykin, J., Li, H., Yanagisawa, H., Gleason, R. L., Jo, H., & Brewster, L. P. (2017). Disturbed Flow Promotes Arterial Stiffening Through Thrombospondin-1. *Circulation, 136*(13), 1217-1232. https://doi.org/doi:10.1161/CIRCULATIONAHA.116.026361

Kim, J.-E., Choi, B.-K., Choi, J.-Y., Ryu, T., Roh, W. S., & Song, S.-Y. (2014). Role of calcium channels responsible for phenylephrine-induced contraction in rat aorta 3 days after acute myocardial infarction. *Korean J Anesthesiol, 66*(2), 143-152. https://doi.org/10.4097/kjae.2014.66.2.143

Kim, J.-W., Koh, Y., Kim, D.-W., Ahn, Y.-O., Kim, T. M., Han, S.-W., Oh, D.-Y., Lee, S.-H., Im, S.-A., Kim, T.-Y., Heo, D. S., & Bang, Y.-J. (2013). Clinical Implications of VEGF, TGF-β1, and IL-1β in Patients with Advanced Non-small Cell Lung Cancer. *Cancer research and treatment, 45*(4), 325-333. https://doi.org/10.4143/crt.2013.45.4.325

Kim, M. K., Kim, B., Lee, J. Y., Kim, J. S., Han, B. G., Choi, S. O., & Yang, J. W. (2013). Tissue Doppler-derived E/e' ratio as a parameter for assessing diastolic heart failure and as a predictor of mortality in patients with chronic kidney disease. *Korean J Intern Med, 28*(1), 35-44. https://doi.org/10.3904/kjim.2013.28.1.35

King, J., & Lowery, D. R. (2023). Physiology, Cardiac Output. In *StatPearls*. StatPearls Publishing

King, J. M., Bergeron, C. A., & Taylor, C. E. (2019). Finite state machine implementation for left ventricle modeling and control. *BioMedical Engineering OnLine, 18*(1), 10. https://doi.org/10.1186/s12938-019-0628-3

Kirkby, N. S., Hadoke, P. W., Bagnall, A. J., & Webb, D. J. (2008). The endothelin system as a therapeutic target in cardiovascular disease: great expectations or bleak house? *Br J Pharmacol, 153*(6), 1105-1119. https://doi.org/10.1038/sj.bjp.0707516

Kiselyov, A. S., Semenova, M., Semenov, V. V., Piatnitski, E., & Ouyang, S. (2006). Hetaryl imidazoles: a novel dual inhibitors of VEGF receptors I and II. *Bioorg Med Chem Lett, 16*(5), 1440-1444. https://doi.org/10.1016/j.bmcl.2005.11.033

Klaeboe, L. G., & Edvardsen, T. (2019). Echocardiographic assessment of left ventricular systolic function. *Journal of Echocardiography, 17*(1), 10-16. https://doi.org/10.1007/s12574-018-0405-5

Klagsbrun, M., & D'Amore, P. A. (1996). Vascular endothelial growth factor and its receptors. *Cytokine Growth Factor Rev, 7*(3), 259-270. https://doi.org/10.1016/s1359-6101(96)00027-5

Knight, Z. A., Lin, H., & Shokat, K. M. (2010). Targeting the cancer kinome through polypharmacology. *Nat Rev Cancer, 10*(2), 130-137. https://doi.org/10.1038/nrc2787

Knowles, J., Loizidou, M., & Taylor, I. (2005). Endothelin-1 and Angiogenesis in Cancer. *Current Vascular Pharmacology, 3*(4), 309-314. https://doi.org/http://dx.doi.org/10.2174/157016105774329462

Kobayashi, M., Nishita, M., Mishima, T., Ohashi, K., & Mizuno, K. (2006). MAPKAPK-2-mediated LIM-kinase activation is critical for VEGF-induced actin remodeling and cell migration. *Embo j, 25*(4), 713-726. https://doi.org/10.1038/sj.emboj.7600973

Koch, S., & Claesson-Welsh, L. (2012). Signal transduction by vascular endothelial growth factor receptors. *Cold Spring Harb Perspect Med, 2*(7), a006502. https://doi.org/10.1101/cshperspect.a006502

Koch, S., Tugues, S., Li, X., Gualandi, L., & Claesson-Welsh, L. (2011). Signal transduction by vascular endothelial growth factor receptors. *Biochem J, 437*(2), 169-183. https://doi.org/10.1042/bj20110301

Kohan, D. E., Rossi, N. F., Inscho, E. W., & Pollock, D. M. (2011). Regulation of blood pressure and salt homeostasis by endothelin. *Physiol Rev, 91*(1), 1-77. https://doi.org/10.1152/physrev.00060.2009

Kosaraju, A., Goyal, A., Grigorova, Y., & Makatyus, A. N. (2023). Left Ventricular Ejection Fraction. [Updated 2023 Apr 24]. . *In: StatPearls [Internet]. Treasure Island (FL): StatPearls Publishing; 2023 Jan-. Available from: https://www.ncbi.nlm.nih.gov/books/NBK459131/*.

Kostakou, P. M., Kouris, N. T., Kostopoulos, V. S., Damaskos, D. S., & Olympios, C. D. (2019). Cardio-oncology: a new and developing sector of research and therapy in the field of

cardiology. *Heart Fail Rev, 24*(1), 91-100. https://doi.org/10.1007/s10741-018-9731-y

Krejsa, C. M., Horvath, D., Rogalski, S. L., Penzotti, J. E., Mao, B., Barbosa, F., & Migeon, J. C. (2003). Predicting ADME properties and side effects: the BioPrint approach. *Curr Opin Drug Discov Devel, 6*(4), 470-480.

Kuei, A., & Wu, S. (2013). The risk of proteinuria with the angiogenesis inhibitor axitinib in patients with cancer. *Journal of Clinical Oncology, 31*(6_suppl), 439-439. https://doi.org/10.1200/jco.2013.31.6_suppl.439

Lal, N., Puri, K., & Rodrigues, B. (2018). Vascular Endothelial Growth Factor B and Its Signaling. *Front Cardiovasc Med, 5*, 39. https://doi.org/10.3389/fcvm.2018.00039

Lamalice, L., Boeuf, F. L., & Huot, J. (2007). Endothelial Cell Migration During Angiogenesis. *Circulation Research, 100*(6), 782-794. https://doi.org/doi:10.1161/01.RES.0000259593.07661.1e

Lamore, S. D., Kohnken, R. A., Peters, M. F., & Kolaja, K. L. (2020). Cardiovascular Toxicity Induced by Kinase Inhibitors: Mechanisms and Preclinical Approaches. *Chemical Research in Toxicology, 33*(1), 125-136. https://doi.org/10.1021/acs.chemrestox.9b00387

Lampugnani, M. G., Orsenigo, F., Gagliani, M. C., Tacchetti, C., & Dejana, E. (2006). Vascular endothelial cadherin controls VEGFR-2 internalization and signaling from intracellular compartments. *The Journal of cell biology, 174*(4), 593-604. https://doi.org/10.1083/jcb.200602080

Lankhorst, S., Baelde, H. J., Kappers, M. H., Smedts, F. M., Hansen, A., Clahsen-van Groningen, M. C., Sleijfer, S., Mathijssen, R. H., Danser, A. H., & van den Meiracker, A. H. (2015). Greater Sensitivity of Blood Pressure Than Renal Toxicity to Tyrosine Kinase Receptor Inhibition With Sunitinib. *Hypertension, 66*(3), 543-549. https://doi.org/10.1161/hypertensionaha.115.05435

Lankhorst, S., Danser, A. H. J., & Meiracker, A. H. v. d. (2016). Endothelin-1 and antiangiogenesis. *American Journal of Physiology-Regulatory, Integrative and Comparative Physiology, 310*(3), R230-R234. https://doi.org/10.1152/ajpregu.00373.2015

Lankhorst, S., Kappers, M. H., van Esch, J. H., Danser, A. H., & van den Meiracker, A. H. (2014). Hypertension during vascular endothelial growth factor inhibition: focus on nitric oxide, endothelin-1, and oxidative stress. *Antioxid Redox Signal, 20*(1), 135-145. https://doi.org/10.1089/ars.2013.5244

Lankhorst, S., Kappers, M. H., van Esch, J. H., Smedts, F. M., Sleijfer, S., Mathijssen, R. H., Baelde, H. J., Danser, A. H., & van den Meiracker, A. H. (2014a). Treatment of hypertension and renal injury induced by the angiogenesis inhibitor sunitinib: preclinical study. *Hypertension, 64*(6), 1282-1289. https://doi.org/10.1161/HYPERTENSIONAHA.114.04187

Lankhorst, S., Kappers, M. H. W., Van Esch, J. H. M., Smedts, F. M. M., Sleijfer, S., Mathijssen, R. H. J., Baelde, H. J., Danser, A. H. J., & Van Den Meiracker, A. H. (2014b). Treatment of hypertension and renal injury induced by the angiogenesis inhibitor sunitinib preclinical study [Article]. *Hypertension, 64*(6), 1282-1289. https://doi.org/10.1161/HYPERTENSIONAHA.114.04187

Lankhorst, S., Saleh, L., Danser, A. H. J., & van den Meiracker, A. H. (2015a). Etiology of angiogenesis inhibition-related hypertension. *Current Opinion in Pharmacology, 21*, 7-13. https://doi.org/https://doi.org/10.1016/j.coph.2014.11.010

Lankhorst, S., Saleh, L., Danser, A. J., & van den Meiracker, A. H. (2015b). Etiology of angiogenesis inhibition-related hypertension. *Curr Opin Pharmacol, 21*, 7-13. https://doi.org/10.1016/j.coph.2014.11.010

Larivière, R., Deng, L. Y., Day, R., Sventek, P., Thibault, G., & Schiffrin, E. L. (1995). Increased endothelium-1 gene expression in the endothelium of coronary arteries and endocardium in the DOCA-salt hypertensive rat. *Journal of Molecular and Cellular Cardiology, 27*(10), 2123-2131. https://doi.org/10.1016/S0022-2828(95)91263-0

Laurent, S., & Boutouyrie, P. (2020). Arterial Stiffness and Hypertension in the Elderly [Review]. *Frontiers in Cardiovascular Medicine, 7*. https://www.frontiersin.org/articles/10.3389/fcvm.2020.544302

Laurent, S., Boutouyrie, P., Asmar, R., Gautier, I., Laloux, B., Guize, L., Ducimetiere, P., & Benetos, A. (2001). Aortic Stiffness Is an Independent Predictor of All-Cause and Cardiovascular Mortality in Hypertensive Patients. *Hypertension, 37*(5), 1236-1241. https://doi.org/doi:10.1161/01.HYP.37.5.1236

Laverty, H. G., Benson, C., Cartwright, E. J., Cross, M. J., Garland, C., Hammond, T., Holloway, C., McMahon, N., Milligan, J., Park, B. K., Pirmohamed, M., Pollard, C., Radford, J., Roome, N., Sager, P., Singh, S., Suter, T., Suter, W., Trafford, A., Volders, P. G. A., Wallis, R., Weaver, R., York, M., & Valentin, J. P. (2011). How can we improve our understanding of cardiovascular safety liabilities to develop safer medicines? *British Journal of Pharmacology, 163*(4), 675-693. https://doi.org/10.1111/j.1476-5381.2011.01255.x

Lee, A. (2022). Clazosentan: First Approval. *Drugs, 82*(6), 697-702. https://doi.org/10.1007/s40265-022-01708-0

Lee, K., Jeong, K. W., Lee, Y., Song, J. Y., Kim, M. S., Lee, G. S., & Kim, Y. (2010). Pharmacophore modeling and virtual screening studies for new VEGFR-2 kinase inhibitors. *Eur J Med Chem, 45*(11), 5420-5427. https://doi.org/10.1016/j.ejmech.2010.09.002

Lee, Y. T., Tan, Y. J., & Oon, C. E. (2018). Molecular targeted therapy: Treating cancer with specificity. *European Journal of Pharmacology, 834*, 188-196. https://doi.org/https://doi.org/10.1016/j.ejphar.2018.07.034

Leloup, A. J., Van Hove, C. E., Kurdi, A., De Moudt, S., Martinet, W., De Meyer, G. R., Schrijvers, D. M., De Keulenaer, G. W., & Fransen, P. (2016). A novel set-up for the ex vivo analysis of mechanical properties of mouse aortic segments stretched at

physiological pressure and frequency. *J Physiol, 594*(21), 6105-6115. https://doi.org/10.1113/jp272623

Lemmon, M. A., & Schlessinger, J. (2010). Cell signaling by receptor tyrosine kinases. *Cell, 141*(7), 1117-1134. https://doi.org/10.1016/j.cell.2010.06.011

Lessen, M. v., Nakayama, M., Kato, K., Kim, J. M., Kaibuchi, K., & Adams, R. H. (2015). Regulation of Vascular Endothelial Growth Factor Receptor Function in Angiogenesis by Numb and Numb-Like. *Arteriosclerosis, Thrombosis, and Vascular Biology, 35*(8), 1815-1825. https://doi.org/doi:10.1161/ATVBAHA.115.305473

Li, M., & Ramos, L. G. (2017). Drug-Induced QT Prolongation And Torsades de Pointes. *P t, 42*(7), 473-477.

Li, R. X., Luo, J., Balaram, S. K., Chaudhry, F. A., Shahmirzadi, D., & Konofagou, E. E. (2013). Pulse wave imaging in normal, hypertensive and aneurysmal human aortas in vivo: a feasibility study. *Phys Med Biol, 58*(13), 4549-4562. https://doi.org/10.1088/0031-9155/58/13/4549

Li, W., Croce, K., Steensma, D. P., McDermott, D. F., Ben-Yehuda, O., & Moslehi, J. (2015). Vascular and Metabolic Implications of Novel Targeted Cancer Therapies: Focus on Kinase Inhibitors. *J Am Coll Cardiol, 66*(10), 1160-1178. https://doi.org/10.1016/j.jacc.2015.07.025

Li, X., Lee, C., Tang, Z., Zhang, F., Arjunan, P., Li, Y., Hou, X., Kumar, A., & Dong, L. (2009). VEGF-B: a survival, or an angiogenic factor? *Cell Adh Migr, 3*(4), 322-327. https://doi.org/10.4161/cam.3.4.9459

Li, Y. L., Zhao, H., & Ren, X. B. (2016). Relationship of VEGF/VEGFR with immune and cancer cells: staggering or forward? *Cancer Biol Med, 13*(2), 206-214. https://doi.org/10.20892/j.issn.2095-3941.2015.0070

Liang, C., Zhu, D., Xia, W., Hong, Z., Wang, Q.-S., Sun, Y., Yang, Y.-C., Han, S.-Q., Tang, L.-L., Lou, J., Wu, M.-M., & Zhang, Z.-R. (2023). Inhibition of YAP by lenvatinib in endothelial cells increases blood pressure through ferroptosis. *Biochimica et Biophysica Acta (BBA) - Molecular Basis of Disease, 1869*(1), 166586. https://doi.org/https://doi.org/10.1016/j.bbadis.2022.166586

Liang, J., Wang, S., Zhang, G., He, B., Bie, Q., & Zhang, B. (2021). A New Antitumor Direction: Tumor-Specific Endothelial Cells. *Front Oncol, 11*, 756334. https://doi.org/10.3389/fonc.2021.756334

Lin, A., Giuliano, C. J., Palladino, A., John, K. M., Abramowicz, C., Yuan, M. L., Sausville, E. L., Lukow, D. A., Liu, L., Chait, A. R., Galluzzo, Z. C., Tucker, C., & Sheltzer, J. M. (2019). Off-target toxicity is a common mechanism of action of cancer drugs undergoing clinical trials. *Sci Transl Med, 11*(509). https://doi.org/10.1126/scitranslmed.aaw8412

Lindsay, C. R., MacPherson, I. R., & Cassidy, J. (2009). Current status of cediranib: the rapid development of a novel anti-angiogenic therapy. *Future Oncol, 5*(4), 421-432. https://doi.org/10.2217/fon.09.18

Liu, Y., Li, Y., Wang, Y., Lin, C., Zhang, D., Chen, J., Ouyang, L., Wu, F., Zhang, J., & Chen, L. (2022). Recent progress on vascular endothelial growth factor receptor inhibitors with dual targeting capabilities for tumor therapy. *Journal of hematology & oncology, 15*(1), 89. https://doi.org/10.1186/s13045-022-01310-7

Liu, Y., Zhou, L., Chen, Y., Liao, B., Ye, D., Wang, K., & Li, H. (2019). Hypertension as a prognostic factor in metastatic renal cell carcinoma treated with tyrosine kinase inhibitors: a systematic review and meta-analysis. *BMC Urology, 19*(1), 49. https://doi.org/10.1186/s12894-019-0481-5

Liu, Z.-L., Chen, H.-H., Zheng, L.-L., Sun, L.-P., & Shi, L. (2023). Angiogenic signaling pathways and anti-angiogenic therapy for cancer. *Signal Transduction and Targeted Therapy, 8*(1), 198. https://doi.org/10.1038/s41392-023-01460-1

Louis, N., Evelegh, C., & Graham, F. L. (1997). Cloning and sequencing of the cellular-viral junctions from the human adenovirus type 5 transformed 293 cell line. *Virology, 233*(2), 423-429. https://doi.org/10.1006/viro.1997.8597

Lubos, E., Handy, D. E., & Loscalzo, J. (2008). Role of oxidative stress and nitric oxide in atherothrombosis. *Front Biosci, 13*, 5323-5344. https://doi.org/10.2741/3084

Lugano, R., Ramachandran, M., & Dimberg, A. (2020). Tumor angiogenesis: causes, consequences, challenges and opportunities. *Cellular and Molecular Life Sciences, 77*(9), 1745-1770. https://doi.org/10.1007/s00018-019-03351-7

Lüscher, T. F., & Barton, M. (2000). Endothelins and Endothelin Receptor Antagonists. *Circulation, 102*(19), 2434-2440. https://doi.org/doi:10.1161/01.CIR.102.19.2434

Lyu, Z., Jin, H., Yan, Z., Hu, K., Jiang, H., Peng, H., & Zhuo, H. (2020). Effects of NRP1 on angiogenesis and vascular maturity in endothelial cells are dependent on the expression of SEMA4D. *Int J Mol Med, 46*(4), 1321-1334. https://doi.org/10.3892/ijmm.2020.4692

Mac Gabhann, F., & Popel, A. S. (2007). Dimerization of VEGF receptors and implications for signal transduction: a computational study. *Biophys Chem, 128*(2-3), 125-139. https://doi.org/10.1016/j.bpc.2007.03.010

MacIntyre, I. M., Dhaun, N., Lilitkarntakul, P., Melville, V., Goddard, J., & Webb, D. J. (2010). Greater functional ETB receptor antagonism with bosentan than sitaxsentan in healthy men. *Hypertension, 55*(6), 1406-1411. https://doi.org/10.1161/hypertensionaha.109.148569

Magnussen, A. L., & Mills, I. G. (2021). Vascular normalisation as the stepping stone into tumour microenvironment transformation. *British Journal of Cancer, 125*(3), 324-336. https://doi.org/10.1038/s41416-021-01330-z

Maguire, J. J., & Davenport, A. P. (1998). Increased response to big endothelin-1 in atherosclerotic human coronary artery: functional evidence for up-regulation of endothelin-converting enzyme activity in disease. *British Journal of Pharmacology, 125*(2), 238-240. https://doi.org/https://doi.org/10.1038/sj.bjp.0702102

Maguire, J. J., & Davenport, A. P. (2015). Endothelin receptors and their antagonists. *Seminars in nephrology, 35*(2), 125-136. https://doi.org/10.1016/j.semnephrol.2015.02.002

Maguire, J. J., Johnson, C. M., Mockridge, J. W., & Davenport, A. P. (1997). Endothelin converting enzyme (ECE) activity in human vascular smooth muscle. *British Journal of Pharmacology, 122*(8), 1647-1654. https://doi.org/https://doi.org/10.1038/sj.bjp.0701564

Mäki-Petäjä, K. M., McGeoch, A., Yang, L. L., Hubsch, A., McEniery, C. M., Meyer, P. A. R., Mir, F., Gajendragadkar, P., Ramenatte, N., Anandappa, G., Franco, S. S., Bond, S. J., Schönlieb, C.-B., Boink, Y., Brune, C., Wilkinson, I. B., Jodrell, D. I., & Cheriyan, J. (2021). Mechanisms Underlying Vascular Endothelial Growth Factor Receptor Inhibition–Induced Hypertension. *Hypertension, 77*(5), 1591-1599. https://doi.org/doi:10.1161/HYPERTENSIONAHA.120.16454

Makker, V., Colombo, N., Casado Herráez, A., Santin, A. D., Colomba, E., Miller, D. S., Fujiwara, K., Pignata, S., Baron-Hay, S., Ray-Coquard, I., Shapira-Frommer, R., Ushijima, K., Sakata, J., Yonemori, K., Kim, Y. M., Guerra, E. M., Sanli, U. A., McCormack, M. M., Smith, A. D., Keefe, S., Bird, S., Dutta, L., Orlowski, R. J., & Lorusso, D. (2022). Lenvatinib plus Pembrolizumab for Advanced Endometrial Cancer. *New England Journal of Medicine, 386*(5), 437-448. https://doi.org/10.1056/NEJMoa2108330

Malone, E. R., Oliva, M., Sabatini, P. J. B., Stockley, T. L., & Siu, L. L. (2020). Molecular profiling for precision cancer therapies. *Genome Medicine, 12*(1), 8. https://doi.org/10.1186/s13073-019-0703-1

Mamer, S. B., Chen, S., Weddell, J. C., Palasz, A., Wittenkeller, A., Kumar, M., & Imoukhuede, P. I. (2017). Discovery of High-Affinity PDGF-VEGFR Interactions: Redefining RTK Dynamics. *Sci Rep, 7*(1), 16439. https://doi.org/10.1038/s41598-017-16610-z

Mandela, P., & Ordway, G. A. (2006). The norepinephrine transporter and its regulation. *Journal of Neurochemistry, 97*(2), 310-333. https://doi.org/https://doi.org/10.1111/j.1471-4159.2006.03717.x

Marciscano, A. E., & Anandasabapathy, N. (2021). The role of dendritic cells in cancer and anti-tumor immunity. *Semin Immunol, 52*, 101481. https://doi.org/10.1016/j.smim.2021.101481

Markman, T. M., & Markman, M. (2018). Cardio-Oncology: mechanisms of cardiovascular toxicity. *F1000Res, 7*, 113. https://doi.org/10.12688/f1000research.12598.1

Markó, L., Dörr, A., Linz, P., Meiracker, A. H. v. d., Garrelds, I. M., Kuehne, T., Dechend, R., Danser, A. H. J., Flörcken, A., & Müller, D. N. (2022). Effect of Sunitinib Treatment on Skin Sodium Accumulation in Patients With Renal Cancer: a Pilot Study. *Hypertension, 79*(5), e103-e105. https://doi.org/doi:10.1161/HYPERTENSIONAHA.122.19079

Marmé, D. (2018). Tumor Angiogenesis: A Key Target for Cancer Therapy. *Oncology Research and Treatment, 41*(4), 164-164. https://doi.org/10.1159/000488340

Martin, P. L. (2015). Safety Pharmacology of Anticancer Agents. *Handb Exp Pharmacol, 229*, 405-431. https://doi.org/10.1007/978-3-662-46943-9_16

Martin-Aragon Baudel, M., Espinosa-Tanguma, R., Nieves-Cintron, M., & Navedo, M. F. (2020). Purinergic Signaling During Hyperglycemia in Vascular Smooth Muscle Cells. *Front Endocrinol (Lausanne), 11*, 329. https://doi.org/10.3389/fendo.2020.00329

Martínez-Díaz, I., Martos, N., Llorens-Cebrià, C., Álvarez, F. J., Bedard, P. W., Vergara, A., Jacobs-Cachá, C., & Soler, M. J. (2023). Endothelin Receptor Antagonists in Kidney Disease. *Int J Mol Sci, 24*(4). https://doi.org/10.3390/ijms24043427

Masoumi Moghaddam, S., Amini, A., Morris, D. L., & Pourgholami, M. H. (2012). Significance of vascular endothelial growth factor in growth and peritoneal dissemination of ovarian cancer. *Cancer and Metastasis Reviews, 31*(1), 143-162. https://doi.org/10.1007/s10555-011-9337-5

Matsuki, M., Hoshi, T., Yamamoto, Y., Ikemori-Kawada, M., Minoshima, Y., Funahashi, Y., & Matsui, J. (2018). Lenvatinib inhibits angiogenesis and tumor fibroblast growth factor signaling pathways in human hepatocellular carcinoma models. *Cancer medicine, 7*(6), 2641-2653. https://doi.org/10.1002/cam4.1517

Matsumoto, K., & Ema, M. (2014). Roles of VEGF-A signalling in development, regeneration, and tumours. *J Biochem, 156*(1), 1-10. https://doi.org/10.1093/jb/mvu031

Matsumoto, T., & Claesson-Welsh, L. (2001). VEGF Receptor Signal Transduction. *Science's STKE, 2001*(112), re21-re21. https://doi.org/10.1126/stke.2001.112.re21

Matsuo, M., Wakasaki, T., Yasumatsu, R., & Nakagawa, T. (2020). A case of cardiotoxicity developed under the administration of lenvatinib in a thyroid cancer patient. *Practica Oto-Rhino-Laryngologica 113*, 309-314. https://doi.org/https://doi.org/10.5631/jibirin.113.309

Matsuura, A., Yamochi, W., Hirata, K., Kawashima, S., & Yokoyama, M. (1998). Stimulatory interaction between vascular endothelial growth factor and endothelin-1 on each gene expression. *Hypertension, 32*(1), 89-95. https://doi.org/10.1161/01.hyp.32.1.89

Maurea, N., Coppola, C., Piscopo, G., Galletta, F., Riccio, G., Esposito, E., De Lorenzo, C., De Laurentiis, M., Spallarossa, P., & Mercuro, G. (2016). Pathophysiology of cardiotoxicity from target therapy and angiogenesis inhibitors. *Journal of Cardiovascular Medicine, 17*, e19-e26. https://doi.org/10.2459/jcm.0000000000000377

Mayer, E. L., Dallabrida, S. M., Rupnick, M. A., Redline, W. M., Hannagan, K., Ismail, N. S., Burstein, H. J., & Beckman, J. A. (2011). Contrary effects of the receptor tyrosine kinase inhibitor vandetanib on constitutive and flow-stimulated nitric oxide elaboration in humans. *Hypertension, 58*(1), 85-92. https://doi.org/10.1161/hypertensionaha.110.168120

Mayet, J., & Hughes, A. (2003). Cardiac and vascular pathophysiology in hypertension. *Heart, 89*(9), 1104-1109. https://doi.org/10.1136/heart.89.9.1104

Mazzuca, M. Q., & Khalil, R. A. (2012). Vascular endothelin receptor type B: structure, function and dysregulation in vascular disease. *Biochem Pharmacol, 84*(2), 147-162. https://doi.org/10.1016/j.bcp.2012.03.020

Mazzuca, M. Q., Li, W., Reslan, O. M., Yu, P., Mata, K. M., & Khalil, R. A. (2014). Downregulation of microvascular endothelial type B endothelin receptor is a central vascular mechanism in hypertensive pregnancy. *Hypertension, 64*(3), 632-643. https://doi.org/10.1161/hypertensionaha.114.03315

McGrath, J. C., & Lilley, E. (2015). Implementing guidelines on reporting research using animals (ARRIVE etc.): new requirements for publication in BJP. *Br J Pharmacol, 172*(13), 3189-3193. https://doi.org/10.1111/bph.12955

McKay, R. R., Bossé, D., & Choueiri, T. K. (2018). Evolving Systemic Treatment Landscape for Patients With Advanced Renal Cell Carcinoma. *Journal of Clinical Oncology, 36*(36), 3615-3623. https://doi.org/10.1200/jco.2018.79.0253

Meiracker, A. H. v. d., & Danser, A. H. J. (2016). Mechanisms of Hypertension and Renal Injury During Vascular Endothelial Growth Factor Signaling Inhibition. *Hypertension, 68*(1), 17-23. https://doi.org/doi:10.1161/HYPERTENSIONAHA.116.07618

Melincovici, C. S., Boşca, A. B., Şuşman, S., Mărginean, M., Mihu, C., Istrate, M., Moldovan, I. M., Roman, A. L., & Mihu, C. M. (2018). Vascular endothelial growth factor (VEGF) - key factor in normal and pathological angiogenesis. *Rom J Morphol Embryol, 59*(2), 455-467.

Mellor, H. R., Bell, A. R., Valentin, J. P., & Roberts, R. R. (2011). Cardiotoxicity associated with targeting kinase pathways in cancer. *Toxicol Sci, 120*(1), 14-32. https://doi.org/10.1093/toxsci/kfq378

Mercurio, A. M. (2019). VEGF/Neuropilin Signaling in Cancer Stem Cells. *Int J Mol Sci, 20*(3). https://doi.org/10.3390/ijms20030490

Merkus, D., Houweling, B., Mirza, A., Boomsma, F., van den Meiracker, A. H., & Duncker, D. J. (2003). Contribution of endothelin and its receptors to the regulation of vascular tone during exercise is different in the systemic, coronary and pulmonary circulation. *Cardiovascular Research, 59*(3), 745-754. https://doi.org/10.1016/s0008-6363(03)00479-6

Mickley, E. J., Gray, G. A., & Webb, D. J. (1997). Activation of endothelin ETA receptors masks the constrictor role of endothelin ETB receptors in rat isolated small mesenteric arteries. *Br J Pharmacol, 120*(7), 1376-1382. https://doi.org/10.1038/sj.bjp.0701036

Mihalcea, D., Memis, H., Mihaila, S., & Vinereanu, D. (2023). Cardiovascular Toxicity Induced by Vascular Endothelial Growth Factor Inhibitors. *Life, 13*(2), 366. https://www.mdpi.com/2075-1729/13/2/366

Miller, K. D., Nogueira, L., Devasia, T., Mariotto, A. B., Yabroff, K. R., Jemal, A., Kramer, J., & Siegel, R. L. (2022). Cancer treatment and survivorship statistics, 2022. *CA: A Cancer*

Journal for Clinicians, 72(5), 409-436. https://doi.org/https://doi.org/10.3322/caac.21731

Min, H. Y., & Lee, H. Y. (2022). Molecular targeted therapy for anticancer treatment. *Exp Mol Med, 54*(10), 1670-1694. https://doi.org/10.1038/s12276-022-00864-3

Minotti, G., Salvatorelli, E., & Menna, P. (2010). Pharmacological foundations of cardio-oncology. *J Pharmacol Exp Ther, 334*(1), 2-8. https://doi.org/10.1124/jpet.110.165860

Mirabito Colafella, K. M., Neves, K. B., Montezano, A. C., Garrelds, I. M., van Veghel, R., de Vries, R., Uijl, E., Baelde, H. J., van den Meiracker, A. H., Touyz, R. M., Danser, A. H. J., & Versmissen, J. (2020). Selective ETA vs. dual ETA/B receptor blockade for the prevention of sunitinib-induced hypertension and albuminuria in WKY rats. *Cardiovasc Res, 116*(10), 1779-1790. https://doi.org/10.1093/cvr/cvz260

Mirabito Colafella, K. M., van Dorst, D. C. H., Neuman, R. I., Doorn, L. V., Neves, K. B., Montezano, A. C., Garrelds, I. M., van Veghel, R., de Vries, R., Uijl, E., Clahsen-van Groningen, M. C., Baelde, H. J., van den Meiracker, A. H., Touyz, R. M., Visser, W., Danser, A. H. J., & Versmissen, J. (2022). Differential effects of cyclo-oxygenase 1 and 2 inhibition on angiogenesis inhibitor-induced hypertension and kidney damage. *Clin Sci (Lond), 136*(9), 675-694. https://doi.org/10.1042/cs20220182

Mitter, S. S., Shah, S. J., & Thomas, J. D. (2017). A Test in Context. *Journal of the American College of Cardiology, 69*(11), 1451-1464. https://doi.org/doi:10.1016/j.jacc.2016.12.037

Modi, S. J., & Kulkarni, V. M. (2019). Vascular Endothelial Growth Factor Receptor (VEGFR-2)/KDR Inhibitors: Medicinal Chemistry Perspective. *Medicine in Drug Discovery, 2*, 100009. https://doi.org/https://doi.org/10.1016/j.medidd.2019.100009

Moeller, B. J., Cao, Y., Li, C. Y., & Dewhirst, M. W. (2004). Radiation activates HIF-1 to regulate vascular radiosensitivity in tumors: role of reoxygenation, free radicals, and stress granules. *Cancer Cell, 5*(5), 429-441. https://doi.org/10.1016/s1535-6108(04)00115-1

Mohammed, T., Parekh, T., & Desai, A. (2021). Cardiovascular risk management in cancer survivors: Are we doing it right? *World J Clin Oncol, 12*(3), 144-149. https://doi.org/10.5306/wjco.v12.i3.144

Mohammed, T., Singh, M., Tiu, J. G., & Kim, A. S. (2021). Etiology and management of hypertension in patients with cancer. *Cardiooncology, 7*(1), 14. https://doi.org/10.1186/s40959-021-00101-2

Molife, L. R., Dean, E. J., Blanco-Codesido, M., Krebs, M. G., Brunetto, A. T., Greystoke, A. P., Daniele, G., Lee, L., Kuznetsov, G., Myint, K. T., Wood, K., de Las Heras, B., & Ranson, M. R. (2014). A phase I, dose-escalation study of the multitargeted receptor tyrosine kinase inhibitor, golvatinib, in patients with advanced solid tumors. *Clin Cancer Res, 20*(24), 6284-6294. https://doi.org/10.1158/1078-0432.Ccr-14-0409

Monaghan, R. M., Page, D. J., Ostergaard, P., & Keavney, B. D. (2021). The physiological and pathological functions of VEGFR3 in cardiac and lymphatic development and related diseases. *Cardiovasc Res, 117*(8), 1877-1890. https://doi.org/10.1093/cvr/cvaa291

Monitillo, F., Leone, M., Rizzo, C., Passantino, A., & Iacoviello, M. (2016). Ventricular repolarization measures for arrhythmic risk stratification. *World J Cardiol, 8*(1), 57-73. https://doi.org/10.4330/wjc.v8.i1.57

Morimoto, B. H., Castelloe, E., & Fox, A. W. (2015). Safety Pharmacology in Drug Discovery and Development. *Handb Exp Pharmacol, 229*, 65-80. https://doi.org/10.1007/978-3-662-46943-9_3

Moslehi, J. J. (2016). Cardiovascular Toxic Effects of Targeted Cancer Therapies. *N Engl J Med, 375*(15), 1457-1467. https://doi.org/10.1056/NEJMra1100265

Mottram, P. M., & Marwick, T. H. (2005). Assessment of diastolic function: what the general cardiologist needs to know. *Heart, 91*(5), 681-695. https://doi.org/10.1136/hrt.2003.029413

Motzer, R. J., Taylor, M. H., Evans, T. R. J., Okusaka, T., Glen, H., Lubiniecki, G. M., Dutcus, C., Smith, A. D., Okpara, C. E., Hussein, Z., Hayato, S., Tamai, T., & Makker, V. (2022). Lenvatinib dose, efficacy, and safety in the treatment of multiple malignancies. *Expert Rev Anticancer Ther, 22*(4), 383-400. https://doi.org/10.1080/14737140.2022.2039123

Mourad, J.-J., & Levy, B. I. (2011). Mechanisms of Antiangiogenic-Induced Arterial Hypertension. *Current Hypertension Reports, 13*(4), 289-293. https://doi.org/10.1007/s11906-011-0206-y

Mozafari, H., Zhou, C., & Gu, L. (2019). Mechanical contribution of vascular smooth muscle cells in the tunica media of artery. *Nanotechnology Reviews, 8*(1), 50-60. https://doi.org/doi:10.1515/ntrev-2019-0005

Muller, Y. A., Li, B., Christinger, H. W., Wells, J. A., Cunningham, B. C., & de Vos, A. M. (1997). Vascular endothelial growth factor: crystal structure and functional mapping of the kinase domain receptor binding site. *Proc Natl Acad Sci U S A, 94*(14), 7192-7197. https://doi.org/10.1073/pnas.94.14.7192

Murakami, M., Zheng, Y., Hirashima, M., Suda, T., Morita, Y., Ooehara, J., Ema, H., Fong, G.-H., & Shibuya, M. (2008). VEGFR1 Tyrosine Kinase Signaling Promotes Lymphangiogenesis as Well as Angiogenesis Indirectly via Macrophage Recruitment. *Arteriosclerosis, Thrombosis, and Vascular Biology, 28*(4), 658-664. https://doi.org/doi:10.1161/ATVBAHA.107.150433

Musumeci, F., Radi, M., Brullo, C., & Schenone, S. (2012). Vascular endothelial growth factor (VEGF) receptors: drugs and new inhibitors. *J Med Chem, 55*(24), 10797-10822. https://doi.org/10.1021/jm301085w

Nagai, H., & Kim, Y. H. (2017). Cancer prevention from the perspective of global cancer burden patterns. *J Thorac Dis, 9*(3), 448-451. https://doi.org/10.21037/jtd.2017.02.75

Nagueh, S. F., Smiseth, O. A., Appleton, C. P., Byrd, B. F., 3rd, Dokainish, H., Edvardsen, T., Flachskampf, F. A., Gillebert, T. C., Klein, A. L., Lancellotti, P., Marino, P., Oh, J. K., Popescu, B. A., & Waggoner, A. D. (2016). Recommendations for the Evaluation of Left Ventricular Diastolic Function by Echocardiography: An Update from the American Society of Echocardiography and the European Association of Cardiovascular Imaging. *J Am Soc Echocardiogr, 29*(4), 277-314. https://doi.org/10.1016/j.echo.2016.01.011

Nagy, J. A., Chang, S. H., Dvorak, A. M., & Dvorak, H. F. (2009). Why are tumour blood vessels abnormal and why is it important to know? *Br J Cancer, 100*(6), 865-869. https://doi.org/10.1038/sj.bjc.6604929

Nahm, F. S. (2016). Nonparametric statistical tests for the continuous data: the basic concept and the practical use. *Korean J Anesthesiol, 69*(1), 8-14. https://doi.org/10.4097/kjae.2016.69.1.8

Narayan, V., Keefe, S., Haas, N., Wang, L., Puzanov, I., Putt, M., Catino, A., Fang, J., Agarwal, N., Hyman, D., Smith, A. M., Finkelman, B. S., Narayan, H. K., Ewer, S., ElAmm, C., Lenihan, D., & Ky, B. (2017). Prospective Evaluation of Sunitinib-Induced Cardiotoxicity in Patients with Metastatic Renal Cell Carcinoma. *Clinical Cancer Research, 23*(14), 3601-3609. https://doi.org/10.1158/1078-0432.Ccr-16-2869

National Research Council Committee for the Update of the Guide for the, C., & Use of Laboratory, A. (2011). The National Academies Collection: Reports funded by National Institutes of Health. In *Guide for the Care and Use of Laboratory Animals*. National Academies Press (US)
Copyright © 2011, National Academy of Sciences. https://doi.org/10.17226/12910

Neagoe, P. E., Lemieux, C., & Sirois, M. G. (2005). Vascular endothelial growth factor (VEGF)-A165-induced prostacyclin synthesis requires the activation of VEGF receptor-1 and -2 heterodimer. *J Biol Chem, 280*(11), 9904-9912. https://doi.org/10.1074/jbc.M412017200

Neishi, Y., Mochizuki, S., Miyasaka, T., Kawamoto, T., Kume, T., Sukmawan, R., Tsukiji, M., Ogasawara, Y., Kajiya, F., Akasaka, T., Yoshida, K., & Goto, M. (2005). Evaluation of bioavailability of nitric oxide in coronary circulation by direct measurement of plasma nitric oxide concentration. *Proc Natl Acad Sci U S A, 102*(32), 11456-11461. https://doi.org/10.1073/pnas.0501392102

Neufeld, G., Cohen, T., Gengrinovitch, S., & Poltorak, Z. (1999). Vascular endothelial growth factor (VEGF) and its receptors. *FASEB J, 13*(1), 9-22.

Neves, K. B., Montezano, A. C., Lang, N. N., & Touyz, R. M. (2020). Vascular toxicity associated with anti-angiogenic drugs. *Clin Sci (Lond), 134*(18), 2503-2520. https://doi.org/10.1042/cs20200308

Neves, K. B., Rios, F. J., van der Mey, L., Alves-Lopes, R., Cameron, A. C., Volpe, M., Montezano, A. C., Savoia, C., & Touyz, R. M. (2018). VEGFR (Vascular Endothelial Growth Factor Receptor) Inhibition Induces Cardiovascular Damage via Redox-

Sensitive Processes. *Hypertension, 71*(4), 638-647. https://doi.org/10.1161/HYPERTENSIONAHA.117.10490

Nieves, B. J., D'Amore, P. A., & Bryan, B. A. (2009). The function of vascular endothelial growth factor. *Biofactors, 35*(4), 332-337. https://doi.org/10.1002/biof.46

Niu, G., & Chen, X. (2010). Vascular endothelial growth factor as an anti-angiogenic target for cancer therapy. *Curr Drug Targets, 11*(8), 1000-1017. https://doi.org/10.2174/138945010791591395

Noble, F. A. C. l., Mourad, J.-J., Levy, B. I., & Struijker-Boudier, H. A. J. (2023). VEGF (Vascular Endothelial Growth Factor) Inhibition and Hypertension: Does Microvascular Rarefaction Play a Role? *Hypertension, 80*(5), 901-911. https://doi.org/doi:10.1161/HYPERTENSIONAHA.122.19427

Norgall, S., Papoutsi, M., Rössler, J., Schweigerer, L., Wilting, J., & Weich, H. A. (2007). Elevated expression of VEGFR-3 in lymphatic endothelial cells from lymphangiomas. *BMC Cancer, 7*(1), 105. https://doi.org/10.1186/1471-2407-7-105

Nowak, D. G., Woolard, J., Amin, E. M., Konopatskaya, O., Saleem, M. A., Churchill, A. J., Ladomery, M. R., Harper, S. J., & Bates, D. O. (2008). Expression of pro- and anti-angiogenic isoforms of VEGF is differentially regulated by splicing and growth factors. *J Cell Sci, 121*(Pt 20), 3487-3495. https://doi.org/10.1242/jcs.016410

Okamoto, K., Ikemori-Kawada, M., Jestel, A., von König, K., Funahashi, Y., Matsushima, T., Tsuruoka, A., Inoue, A., & Matsui, J. (2014). Distinct binding mode of multikinase inhibitor lenvatinib revealed by biochemical characterization. *ACS medicinal chemistry letters, 6*(1), 89-94. https://doi.org/10.1021/ml500394m

Olson, H., Betton, G., Robinson, D., Thomas, K., Monro, A., Kolaja, G., Lilly, P., Sanders, J., Sipes, G., Bracken, W., Dorato, M., Van Deun, K., Smith, P., Berger, B., & Heller, A. (2000). Concordance of the toxicity of pharmaceuticals in humans and in animals. *Regul Toxicol Pharmacol, 32*(1), 56-67. https://doi.org/10.1006/rtph.2000.1399

Olsson, A. K., Dimberg, A., Kreuger, J., & Claesson-Welsh, L. (2006). VEGF receptor signalling - in control of vascular function. *Nat Rev Mol Cell Biol, 7*(5), 359-371. https://doi.org/10.1038/nrm1911

Pacher, P., Nagayama, T., Mukhopadhyay, P., Bátkai, S., & Kass, D. A. (2008). Measurement of cardiac function using pressure-volume conductance catheter technique in mice and rats. *Nat Protoc, 3*(9), 1422-1434. https://doi.org/10.1038/nprot.2008.138

Palmieri, E. A., Benincasa, G., Rella, F. D., Casaburi, C., Monti, M. G., Simone, G. D., Chiariotti, L., Palombini, L., Bruni, C. B., Saccà, L., & Cittadini, A. (2002). Differential expression of TNF-α, IL-6, and IGF-1 by graded mechanical stress in normal rat myocardium. *American Journal of Physiology-Heart and Circulatory Physiology, 282*(3), H926-H934. https://doi.org/10.1152/ajpheart.00436.2001

Panesar, D. K., & Burch, M. (2017). Assessment of Diastolic Function in Congenital Heart Disease. *Front Cardiovasc Med, 4*, 5. https://doi.org/10.3389/fcvm.2017.00005

Park, S. A., Jeong, M. S., Ha, K.-T., & Jang, S. B. (2018). Structure and function of vascular endothelial growth factor and its receptor system. *BMB reports, 51*(2), 73-78. https://doi.org/10.5483/bmbrep.2018.51.2.233

Parmar, A., & Bjarnason, G. A. (2019). Individualization of Dose and Schedule Based On Toxicity for Oral VEGF Drugs in Kidney Cancer. *Kidney Cancer, 3*, 213-225. https://doi.org/10.3233/KCA-190077

Parsons, M., Young, L., Lee, J. E., Jacobson, K. A., & Liang, B. T. (2000). Distinct cardioprotective effects of adenosine mediated by differential coupling of receptor subtypes to phospholipases C and D. *The FASEB Journal, 14*(10), 1423-1431. https://doi.org/https://doi.org/10.1096/fasebj.14.10.1423

Patel, S. A., Nilsson, M. B., Le, X., Cascone, T., Jain, R. K., & Heymach, J. V. (2023). Molecular Mechanisms and Future Implications of VEGF/VEGFR in Cancer Therapy. *Clinical Cancer Research, 29*(1), 30-39. https://doi.org/10.1158/1078-0432.Ccr-22-1366

Patyna, S., Laird, A. D., Mendel, D. B., O'Farrell A, M., Liang, C., Guan, H., Vojkovsky, T., Vasile, S., Wang, X., Chen, J., Grazzini, M., Yang, C. Y., Haznedar, J. O., Sukbuntherng, J., Zhong, W. Z., Cherrington, J. M., & Hu-Lowe, D. (2006). SU14813: a novel multiple receptor tyrosine kinase inhibitor with potent antiangiogenic and antitumor activity. *Mol Cancer Ther, 5*(7), 1774-1782. https://doi.org/10.1158/1535-7163.Mct-05-0333

Pavlakovic, H., Becker, J., Albuquerque, R., Wilting, J., & Ambati, J. (2010). Soluble VEGFR-2: an antilymphangiogenic variant of VEGF receptors. *Ann N Y Acad Sci, 1207 Suppl 1*(Suppl 1), E7-15. https://doi.org/10.1111/j.1749-6632.2010.05714.x

Peach, C. J., Mignone, V. W., Arruda, M. A., Alcobia, D. C., Hill, S. J., Kilpatrick, L. E., & Woolard, J. (2018). Molecular Pharmacology of VEGF-A Isoforms: Binding and Signalling at VEGFR2. *Int J Mol Sci, 19*(4). https://doi.org/10.3390/ijms19041264

Peng, X., Haldar, S., Deshpande, S., Irani, K., & Kass, D. A. (2003). Wall stiffness suppresses Akt/eNOS and cytoprotection in pulse-perfused endothelium. *Hypertension, 41*(2), 378-381. https://doi.org/10.1161/01.hyp.0000049624.99844.3d

Phng, L. K., & Gerhardt, H. (2009). Angiogenesis: a team effort coordinated by notch. *Dev Cell, 16*(2), 196-208. https://doi.org/10.1016/j.devcel.2009.01.015

Pollard, C. E., Abi Gerges, N., Bridgland-Taylor, M. H., Easter, A., Hammond, T. G., & Valentin, J. P. (2010). An introduction to QT interval prolongation and non-clinical approaches to assessing and reducing risk. *Br J Pharmacol, 159*(1), 12-21. https://doi.org/10.1111/j.1476-5381.2009.00207.x

Poon, R. T., Fan, S. T., & Wong, J. (2001). Clinical implications of circulating angiogenic factors in cancer patients. *J Clin Oncol, 19*(4), 1207-1225. https://doi.org/10.1200/jco.2001.19.4.1207

Porterfield, J. E., Kottam, A. T., Raghavan, K., Escobedo, D., Jenkins, J. T., Larson, E. R., Treviño, R. J., Valvano, J. W., Pearce, J. A., & Feldman, M. D. (2009). Dynamic correction for parallel conductance, GP, and gain factor, alpha, in invasive murine left ventricular

volume measurements. *J Appl Physiol (1985), 107*(6), 1693-1703. https://doi.org/10.1152/japplphysiol.91322.2008

Pottier, C., Fresnais, M., Gilon, M., Jérusalem, G., Longuespée, R., & Sounni, N. E. (2020). Tyrosine Kinase Inhibitors in Cancer: Breakthrough and Challenges of Targeted Therapy. *Cancers (Basel), 12*(3). https://doi.org/10.3390/cancers12030731

Prins, B. A., Hu, R. M., Nazario, B., Pedram, A., Frank, H. J., Weber, M. A., & Levin, E. R. (1994). Prostaglandin E2 and prostacyclin inhibit the production and secretion of endothelin from cultured endothelial cells. *J Biol Chem, 269*(16), 11938-11944.

Pugh, C. W., & Ratcliffe, P. J. (2003). Regulation of angiogenesis by hypoxia: role of the HIF system. *Nat Med, 9*(6), 677-684. https://doi.org/10.1038/nm0603-677

Pugsley, M. K., & Curtis, M. J. (Eds.). (2015). Principles of Safety Pharmacology. Handbook of Experimental Pharmacology. https://doi.org/doi:10.1007/978-3-662-46943-9

Pugsley, M. K., Authier, S., Stonerook, M., & Curtis, M. J. (2015). The shifting landscape of safety pharmacology in 2015. *J Pharmacol Toxicol Methods, 75*, 5-9. https://doi.org/10.1016/j.vascn.2015.05.013

Qi, S., Deng, S., Lian, Z., & Yu, K. (2022). Novel Drugs with High Efficacy against Tumor Angiogenesis. *Int J Mol Sci, 23*(13). https://doi.org/10.3390/ijms23136934

Qi, W.-X., Shen, Z., Tang, L.-N., & Yao, Y. (2014). Risk of arterial thromboembolic events with vascular endothelial growth factor receptor tyrosine kinase inhibitors: An up-to-date meta-analysis. *Critical Reviews in Oncology/Hematology, 92*(2), 71-82. https://doi.org/https://doi.org/10.1016/j.critrevonc.2014.04.004

Rahimi, N. (2006). VEGFR-1 and VEGFR-2: two non-identical twins with a unique physiognomy. *Front Biosci, 11*, 818-829. https://doi.org/10.2741/1839

Rajabi, M., & Mousa, S. A. (2017). The Role of Angiogenesis in Cancer Treatment. *Biomedicines, 5*(2). https://doi.org/10.3390/biomedicines5020034

Räsänen, M., Sultan, I., Paech, J., Hemanthakumar, K. A., Yu, W., He, L., Tang, J., Sun, Y., Hlushchuk, R., Huan, X., Armstrong, E., Khoma, O.-Z., Mervaala, E., Djonov, V., Betsholtz, C., Zhou, B., Kivelä, R., & Alitalo, K. (2021). VEGF-B Promotes Endocardium-Derived Coronary Vessel Development and Cardiac Regeneration. *Circulation, 143*(1), 65-77. https://doi.org/doi:10.1161/CIRCULATIONAHA.120.050635

Raza, A., Franklin, M. J., & Dudek, A. Z. (2010). Pericytes and vessel maturation during tumor angiogenesis and metastasis. *American Journal of Hematology, 85*(8), 593-598. https://doi.org/https://doi.org/10.1002/ajh.21745

Razandi, M., Pedram, A., Rubin, T., & Levin, E. R. (1996). PGE2 and PGI2 inhibit ET-1 secretion from endothelial cells by stimulating particulate guanylate cyclase. *Am J Physiol, 270*(4 Pt 2), H1342-1349. https://doi.org/10.1152/ajpheart.1996.270.4.H1342

Redfern WS, E. L., Hammond TG, Bialecki R, Kinter L, Lindgren S (2010). Impact and frequency of different toxicities throughout the pharmaceutical life cycle. *The Toxicologist 114: 1081*.

Reid, H. M., & Kinsella, B. T. (2015). Prostacyclin receptors: Transcriptional regulation and novel signalling mechanisms. *Prostaglandins Other Lipid Mediat, 121*(Pt A), 70-82. https://doi.org/10.1016/j.prostaglandins.2015.04.008

Ribatti, D. (2022). Immunosuppressive effects of vascular endothelial growth factor. *Oncol Lett, 24*(4), 369. https://doi.org/10.3892/ol.2022.13489

Richards, C. J., Je, Y., Schutz, F. A., Heng, D. Y., Dallabrida, S. M., Moslehi, J. J., & Choueiri, T. K. (2011). Incidence and risk of congestive heart failure in patients with renal and nonrenal cell carcinoma treated with sunitinib. *J Clin Oncol, 29*(25), 3450-3456. https://doi.org/10.1200/jco.2010.34.4309

Riedel, F., Götte, K., Goessler, U., Sadick, H., & Hörmann, K. (2004). Targeting chemotherapy-induced VEGF up-regulation by VEGF antisense oligonucleotides in HNSCC cell lines. *Anticancer Res, 24*(4), 2179-2183.

Rini, B., Rixe, O., Bukowski, R., Michaelson, M. D., Wilding, G., Hudes, G., Bolte, O., Steinfeldt, H., Reich, S. D., & Motzer, R. (2005). AG-013736, a multi-target tyrosine kinase receptor inhibitor, demonstrates anti-tumor activity in a Phase 2 study of cytokine-refractory, metastatic renal cell cancer (RCC). *Journal of Clinical Oncology, 23*(16_suppl), 4509-4509. https://doi.org/10.1200/jco.2005.23.16_suppl.4509

Rini, B. I., Escudier, B., Tomczak, P., Kaprin, A., Szczylik, C., Hutson, T. E., Michaelson, M. D., Gorbunova, V. A., Gore, M. E., Rusakov, I. G., Negrier, S., Ou, Y. C., Castellano, D., Lim, H. Y., Uemura, H., Tarazi, J., Cella, D., Chen, C., Rosbrook, B., Kim, S., & Motzer, R. J. (2011). Comparative effectiveness of axitinib versus sorafenib in advanced renal cell carcinoma (AXIS): a randomised phase 3 trial. *Lancet, 378*(9807), 1931-1939. https://doi.org/10.1016/s0140-6736(11)61613-9

Rini, B. I., Quinn, D. I., Baum, M., Wood, L. S., Tarazi, J., Rosbrook, B., Arruda, L. S., Cisar, L., Roberts, W. G., Kim, S., & Motzer, R. J. (2015). Hypertension among patients with renal cell carcinoma receiving axitinib or sorafenib: analysis from the randomized phase III AXIS trial. *Target Oncol, 10*(1), 45-53. https://doi.org/10.1007/s11523-014-0307-z

Rivera-Lebron, B. N., & Risbano, M. G. (2017). Ambrisentan: a review of its use in pulmonary arterial hypertension. *Ther Adv Respir Dis, 11*(6), 233-244. https://doi.org/10.1177/1753465817696040

Rixe, O., Bukowski, R. M., Michaelson, M. D., Wilding, G., Hudes, G. R., Bolte, O., Motzer, R. J., Bycott, P., Liau, K. F., Freddo, J., Trask, P. C., Kim, S., & Rini, B. I. (2007). Axitinib treatment in patients with cytokine-refractory metastatic renal-cell cancer: a phase II study. *Lancet Oncol, 8*(11), 975-984. https://doi.org/10.1016/s1470-2045(07)70285-1

Roberts, D. D., Miller, T. W., Rogers, N. M., Yao, M., & Isenberg, J. S. (2012). The matricellular protein thrombospondin-1 globally regulates cardiovascular function and responses

to stress via CD47. *Matrix Biology, 31*(3), 162-169. https://doi.org/https://doi.org/10.1016/j.matbio.2012.01.005

Robinson, C. J., & Stringer, S. E. (2001). The splice variants of vascular endothelial growth factor (VEGF) and their receptors. *J Cell Sci, 114*(Pt 5), 853-865.

Rodriguez, D., Watts, D., Gaete, D., Sormendi, S., & Wielockx, B. (2021). Hypoxia Pathway Proteins and Their Impact on the Blood Vasculature. *International Journal of Molecular Sciences, 22*(17), 9191. https://www.mdpi.com/1422-0067/22/17/9191

Rogers, N. M., Seeger, F., Garcin, E. D., Roberts, D. D., & Isenberg, J. S. (2014). Regulation of soluble guanylate cyclase by matricellular thrombospondins: implications for blood flow. *Front Physiol, 5*, 134. https://doi.org/10.3389/fphys.2014.00134

Rogers, N. M., Sharifi-Sanjani, M., Csányi, G., Pagano, P. J., & Isenberg, J. S. (2014). Thrombospondin-1 and CD47 regulation of cardiac, pulmonary and vascular responses in health and disease. *Matrix Biology, 37*, 92-101. https://doi.org/https://doi.org/10.1016/j.matbio.2014.01.002

Rosen, L. S. (2002). Clinical experience with angiogenesis signaling inhibitors: focus on vascular endothelial growth factor (VEGF) blockers. *Cancer Control, 9*(2 Suppl), 36-44. https://doi.org/10.1177/107327480200902s05

Roskoski, R. (2020). Properties of FDA-approved small molecule protein kinase inhibitors: A 2020 update. *Pharmacological Research, 152*, 104609. https://doi.org/https://doi.org/10.1016/j.phrs.2019.104609

Rottman, J. N., Ni, G., & Brown, M. (2007). Echocardiographic evaluation of ventricular function in mice. *Echocardiography, 24*(1), 83-89. https://doi.org/10.1111/j.1540-8175.2006.00356.x

Roviello, G., Polom, K., Roviello, F., Marrelli, D., Multari, A. G., Paganini, G., Pacifico, C., & Generali, D. (2017). Targeting VEGFR-2 in Metastatic Gastric Cancer: Results From a Literature-Based Meta-Analysis. *Cancer Investigation, 35*(3), 187-194. https://doi.org/10.1080/07357907.2016.1276185

Rugo, H. S., Herbst, R. S., Liu, G., Park, J. W., Kies, M. S., Steinfeldt, H. M., Pithavala, Y. K., Reich, S. D., Freddo, J. L., & Wilding, G. (2005). Phase I trial of the oral antiangiogenesis agent AG-013736 in patients with advanced solid tumors: pharmacokinetic and clinical results. *J Clin Oncol, 23*(24), 5474-5483. https://doi.org/10.1200/jco.2005.04.192

Rumjahn, S. M., Yokdang, N., Baldwin, K. A., Thai, J., & Buxton, I. L. (2009). Purinergic regulation of vascular endothelial growth factor signaling in angiogenesis. *Br J Cancer, 100*(9), 1465-1470. https://doi.org/10.1038/sj.bjc.6604998

Russignan, A., Dal Collo, G., Bagnato, A., Tamassia, N., Bugatti, M., Belleri, M., Lorenzi, L., Borsi, E., Bazzoni, R., Gottardi, M., Terragna, C., Vermi, W., Giacomini, A., Presta, M., Cassatella, M. A., Krampera, M., & Tecchio, C. (2020). Targeting the Endothelin-1 Receptors Curtails Tumor Growth and Angiogenesis in Multiple Myeloma. *Front Oncol, 10*, 600025. https://doi.org/10.3389/fonc.2020.600025

Safar, M. E., & Laurent, P. (2003). Pulse pressure and arterial stiffness in rats: comparison with humans. *American Journal of Physiology-Heart and Circulatory Physiology, 285*(4), H1363-H1369. https://doi.org/10.1152/ajpheart.00513.2003

Safar, M. E., Levy, B. I., & Struijker-Boudier, H. (2003). Current perspectives on arterial stiffness and pulse pressure in hypertension and cardiovascular diseases. *Circulation, 107*(22), 2864-2869. https://doi.org/10.1161/01.Cir.0000069826.36125.B4

Saito, H., Tsujitani, S., Ikeguchi, M., Maeta, M., & Kaibara, N. (1998). Relationship between the expression of vascular endothelial growth factor and the density of dendritic cells in gastric adenocarcinoma tissue. *British Journal of Cancer, 78*(12), 1573-1577. https://doi.org/10.1038/bjc.1998.725

Saman, H., Raza, S. S., Uddin, S., & Rasul, K. (2020). Inducing Angiogenesis, a Key Step in Cancer Vascularization, and Treatment Approaches. *Cancers (Basel), 12*(5). https://doi.org/10.3390/cancers12051172

Sandhu, H., Cooper, S., Hussain, A., Mee, C., & Maddock, H. (2017). Attenuation of Sunitinib-induced cardiotoxicity through the A3 adenosine receptor activation. *Eur J Pharmacol, 814*, 95-105. https://doi.org/10.1016/j.ejphar.2017.08.011

Sanguinetti, M., & Keating, M. (1997). Role of Delayed Rectifier Potassium Channels in Cardiac Repolarization and Arrhythmias. *Physiology, 12*(4), 152-157. https://doi.org/10.1152/physiologyonline.1997.12.4.152

Sarkar, J., Luo, Y., Zhou, Q., Ivakhnitskaia, E., Lara, D., Katz, E., Sun, M. G., Guaiquil, V., & Rosenblatt, M. (2022). VEGF receptor heterodimers and homodimers are differentially expressed in neuronal and endothelial cell types. *PLoS One, 17*(7), e0269818. https://doi.org/10.1371/journal.pone.0269818

Savage, D. G., & Antman, K. H. (2002). Imatinib Mesylate — A New Oral Targeted Therapy. *New England Journal of Medicine, 346*(9), 683-693. https://doi.org/10.1056/NEJMra013339

Savoji, H., Mohammadi, M. H., Rafatian, N., Toroghi, M. K., Wang, E. Y., Zhao, Y., Korolj, A., Ahadian, S., & Radisic, M. (2019). Cardiovascular disease models: A game changing paradigm in drug discovery and screening. *Biomaterials, 198*, 3-26. https://doi.org/https://doi.org/10.1016/j.biomaterials.2018.09.036

Schenk, J., Hebden, A., & McNeill, J. H. (1992). Measurement of cardiac left ventricular pressure in conscious rats using a fluid-filled catheter. *J Pharmacol Toxicol Methods, 27*(3), 171-175. https://doi.org/10.1016/1056-8719(92)90037-2

Schiffrin, E. L. (1999). Role of Endothelin-1 in Hypertension. *Hypertension, 34*(4), 876-881. https://doi.org/doi:10.1161/01.HYP.34.4.876

Schiller, J. H., Larson, T., Ou, S. H., Limentani, S., Sandler, A., Vokes, E., Kim, S., Liau, K., Bycott, P., Olszanski, A. J., & von Pawel, J. (2009). Efficacy and safety of axitinib in patients with advanced non-small-cell lung cancer: results from a phase II study. *J Clin Oncol, 27*(23), 3836-3841. https://doi.org/10.1200/jco.2008.20.8355

Schlumberger, M. J., Elisei, R., Bastholt, L., Wirth, L. J., Martins, R. G., Locati, L. D., Jarzab, B., Pacini, F., Daumerie, C., Droz, J. P., Eschenberg, M. J., Sun, Y. N., Juan, T., Stepan, D. E., & Sherman, S. I. (2009). Phase II study of safety and efficacy of motesanib in patients with progressive or symptomatic, advanced or metastatic medullary thyroid cancer. *J Clin Oncol, 27*(23), 3794-3801. https://doi.org/10.1200/jco.2008.18.7815

Schmidinger, M. (2013). Understanding and managing toxicities of vascular endothelial growth factor (VEGF) inhibitors. *EJC Suppl, 11*(2), 172-191. https://doi.org/10.1016/j.ejcsup.2013.07.016

Schneider, M. P., Boesen, E. I., & Pollock, D. M. (2007). Contrasting actions of endothelin ET(A) and ET(B) receptors in cardiovascular disease. *Annu Rev Pharmacol Toxicol, 47*, 731-759. https://doi.org/10.1146/annurev.pharmtox.47.120505.105134

Scott, A. M., Wolchok, J. D., & Old, L. J. (2012). Antibody therapy of cancer. *Nat Rev Cancer, 12*(4), 278-287. https://doi.org/10.1038/nrc3236

Scott, E. N., Meinhardt, G., Jacques, C., Laurent, D., & Thomas, A. L. (2007). Vatalanib: the clinical development of a tyrosine kinase inhibitor of angiogenesis in solid tumours. *Expert Opin Investig Drugs, 16*(3), 367-379. https://doi.org/10.1517/13543784.16.3.367

Sebestyén, A., Kopper, L., Dankó, T., & Tímár, J. (2021). Hypoxia Signaling in Cancer: From Basics to Clinical Practice. *Pathol Oncol Res, 27*, 1609802. https://doi.org/10.3389/pore.2021.1609802

Seed, A., Kuc, R. E., Maguire, J. J., Hillier, C., Johnston, F., Essers, H., de Voogd, H. J., McMurray, J., & Davenport, A. P. (2012). The dual endothelin converting enzyme/neutral endopeptidase inhibitor SLV-306 (daglutril), inhibits systemic conversion of big endothelin-1 in humans. *Life Sciences, 91*(13), 743-748. https://doi.org/https://doi.org/10.1016/j.lfs.2012.03.022

Semenza, G. (2002). Signal transduction to hypoxia-inducible factor 1. *Biochem Pharmacol, 64*(5-6), 993-998. https://doi.org/10.1016/s0006-2952(02)01168-1

Senger, D. R., & Davis, G. E. (2011). Angiogenesis. *Cold Spring Harb Perspect Biol, 3*(8), a005090. https://doi.org/10.1101/cshperspect.a005090

Seo, Y., Baba, H., Fukuda, T., Takashima, M., & Sugimachi, K. (2000). High expression of vascular endothelial growth factor is associated with liver metastasis and a poor prognosis for patients with ductal pancreatic adenocarcinoma. *Cancer, 88*(10), 2239-2245. https://doi.org/10.1002/(sici)1097-0142(20000515)88:10<2239::aid-cncr6>3.0.co;2-v

Shah, R. R., & Morganroth, J. (2015a). Update on Cardiovascular Safety of Tyrosine Kinase Inhibitors: With a Special Focus on QT Interval, Left Ventricular Dysfunction and Overall Risk/Benefit. *Drug Saf, 38*(8), 693-710. https://doi.org/10.1007/s40264-015-0300-1

Shah, R. R., & Morganroth, J. (2015b). Update on Cardiovascular Safety of Tyrosine Kinase Inhibitors: With a Special Focus on QT Interval, Left Ventricular Dysfunction and Overall Risk/Benefit. *Drug Safety, 38*(8), 693-710. https://doi.org/10.1007/s40264-015-0300-1

Shaik, F., Cuthbert, G. A., Homer-Vanniasinkam, S., Muench, S. P., Ponnambalam, S., & Harrison, M. A. (2020). Structural Basis for Vascular Endothelial Growth Factor Receptor Activation and Implications for Disease Therapy. *Biomolecules, 10*(12). https://doi.org/10.3390/biom10121673

Sharma, M., Subbiah, V., Shapiro, G., Pal, S. K., Agarwal, N., Wentzel, K., Hazra, S., Vora, R., Waldes, J., Cha, E., Mehr, K. T., & Patnaik, A. (2022). A phase 1 first-in-human study of XL092 administered alone or in combination with immune checkpoint inhibitors (ICIs) in patients (pts) with inoperable locally advanced or metastatic solid tumors: Description of genitourinary (GU) expansion cohorts. *Journal of Clinical Oncology, 40*(6_suppl), TPS401-TPS401. https://doi.org/10.1200/JCO.2022.40.6_suppl.TPS401

Sheng, C. C., Amiri-Kordestani, L., Palmby, T., Force, T., Hong, C. C., Wu, J. C., Croce, K., Kim, G., & Moslehi, J. (2016). 21st Century Cardio-Oncology: Identifying Cardiac Safety Signals in the Era of Personalized Medicine. *JACC: Basic to Translational Science, 1*(5), 386-398. https://doi.org/https://doi.org/10.1016/j.jacbts.2016.05.008

Shibuya, M. (2011). Vascular Endothelial Growth Factor (VEGF) and Its Receptor (VEGFR) Signaling in Angiogenesis: A Crucial Target for Anti- and Pro-Angiogenic Therapies. *Genes Cancer, 2*(12), 1097-1105. https://doi.org/10.1177/1947601911423031

Shibuya, M. (2012). Vascular endothelial growth factor and its receptor system: physiological functions in angiogenesis and pathological roles in various diseases. *The Journal of Biochemistry, 153*(1), 13-19. https://doi.org/10.1093/jb/mvs136

Sibille, M., Deigat, N., Janin, A., Kirkesseli, S., & Durand, D. V. (1998). Adverse events in phase-I studies: a report in 1015 healthy volunteers. *Eur J Clin Pharmacol, 54*(1), 13-20. https://doi.org/10.1007/s002280050413

Siegel, E. M., Jacobsen, P. B., Malafa, M., Fulp, W., Fletcher, M., Lee, J. H., Smith, J. C., Brown, R., Levine, R., Cartwright, T., Abesada-Terk, G., Jr., Kim, G., Alemany, C., Faig, D., Sharp, P., Markham, M. J., & Shibata, D. (2012). Evaluating the quality of colorectal cancer care in the state of Florida: results from the Florida Initiative for Quality Cancer Care. *J Oncol Pract, 8*(4), 239-245. https://doi.org/10.1200/JOP.2011.000477

Siegel, R., DeSantis, C., Virgo, K., Stein, K., Mariotto, A., Smith, T., Cooper, D., Gansler, T., Lerro, C., Fedewa, S., Lin, C., Leach, C., Cannady, R. S., Cho, H., Scoppa, S., Hachey, M., Kirch, R., Jemal, A., & Ward, E. (2012). Cancer treatment and survivorship statistics, 2012. *CA Cancer J Clin, 62*(4), 220-241. https://doi.org/10.3322/caac.21149

Simons, M., Gordon, E., & Claesson-Welsh, L. (2016). Mechanisms and regulation of endothelial VEGF receptor signalling. *Nat Rev Mol Cell Biol, 17*(10), 611-625. https://doi.org/10.1038/nrm.2016.87

Simons, M., Gordon, E., & Claesson-Welsh, L. (2016). Mechanisms and regulation of endothelial VEGF receptor signalling. *Nature Reviews Molecular Cell Biology, 17*(10), 611-625. https://doi.org/10.1038/nrm.2016.87

Sitohy, B., Nagy, J. A., & Dvorak, H. F. (2012). Anti-VEGF/VEGFR therapy for cancer: reassessing the target. *Cancer Res, 72*(8), 1909-1914. https://doi.org/10.1158/0008-5472.Can-11-3406

Small, H. Y., Montezano, A. C., Rios, F. J., Savoia, C., & Touyz, R. M. (2014). Hypertension due to antiangiogenic cancer therapy with vascular endothelial growth factor inhibitors: understanding and managing a new syndrome. *Can J Cardiol, 30*(5), 534-543. https://doi.org/10.1016/j.cjca.2014.02.011

Smiseth, O. A., Donal, E., Boe, E., Ha, J.-W., Fernandes, J. F., & Lamata, P. (2023). Phenotyping heart failure by echocardiography: imaging of ventricular function and haemodynamics at rest and exercise. *European Heart Journal - Cardiovascular Imaging, 24*(10), 1329-1342. https://doi.org/10.1093/ehjci/jead196

Smith, G. A., Fearnley, G. W., Tomlinson, D. C., Harrison, M. A., & Ponnambalam, S. (2015). The cellular response to vascular endothelial growth factors requires co-ordinated signal transduction, trafficking and proteolysis. *Biosci Rep, 35*(5). https://doi.org/10.1042/BSR20150171

Smith, N. R., Baker, D., James, N. H., Ratcliffe, K., Jenkins, M., Ashton, S. E., Sproat, G., Swann, R., Gray, N., Ryan, A., Jürgensmeier, J. M., & Womack, C. (2010). Vascular endothelial growth factor receptors VEGFR-2 and VEGFR-3 are localized primarily to the vasculature in human primary solid cancers. *Clin Cancer Res, 16*(14), 3548-3561. https://doi.org/10.1158/1078-0432.Ccr-09-2797

Sobczuk, P., Brodziak, A., Khan, M. I., Chhabra, S., Fiedorowicz, M., Wełniak-Kamińska, M., Synoradzki, K., Bartnik, E., Cudnoch-Jędrzejewska, A., & Czarnecka, A. M. (2020). Choosing The Right Animal Model for Renal Cancer Research. *Transl Oncol, 13*(3), 100745. https://doi.org/10.1016/j.tranon.2020.100745

Soker, S., Takashima, S., Miao, H. Q., Neufeld, G., & Klagsbrun, M. (1998). Neuropilin-1 is expressed by endothelial and tumor cells as an isoform-specific receptor for vascular endothelial growth factor. *Cell, 92*(6), 735-745. https://doi.org/10.1016/s0092-8674(00)81402-6

Soldin, O. P., & Mattison, D. R. (2009). Sex differences in pharmacokinetics and pharmacodynamics. *Clin Pharmacokinet, 48*(3), 143-157. https://doi.org/10.2165/00003088-200948030-00001

Somanath, P. R., Malinin, N. L., & Byzova, T. V. (2009). Cooperation between integrin alphavbeta3 and VEGFR2 in angiogenesis. *Angiogenesis, 12*(2), 177-185. https://doi.org/10.1007/s10456-009-9141-9

Song, M., & Finley, S. D. (2020). ERK and Akt exhibit distinct signaling responses following stimulation by pro-angiogenic factors. *Cell Communication and Signaling, 18*(1), 114. https://doi.org/10.1186/s12964-020-00595-w

Song, M., & Finley, S. D. (2022). Mechanistic characterization of endothelial sprouting mediated by pro-angiogenic signaling. *Microcirculation, 29*(2), e12744. https://doi.org/https://doi.org/10.1111/micc.12744

Sopo, M., Anttila, M., Hämäläinen, K., Kivelä, A., Ylä-Herttuala, S., Kosma, V.-M., Keski-Nisula, L., & Sallinen, H. (2019). Expression profiles of VEGF-A, VEGF-D and VEGFR1 are higher in distant metastases than in matched primary high grade epithelial ovarian cancer. *BMC Cancer, 19*(1), 584. https://doi.org/10.1186/s12885-019-5757-3

Sounni, N. E., Paye, A., Host, L., & Noël, A. (2011). MT-MMPS as Regulators of Vessel Stability Associated with Angiogenesis. *Frontiers in pharmacology, 2*, 111-111. https://doi.org/10.3389/fphar.2011.00111

Steeghs, N., Gelderblom, H., Roodt, J. O. t., Christensen, O., Rajagopalan, P., Hovens, M., Putter, H., Rabelink, T. J., & de Koning, E. (2008). Hypertension and rarefaction during treatment with telatinib, a small molecule angiogenesis inhibitor. *Clinical cancer research : an official journal of the American Association for Cancer Research, 14*(11), 3470-3476. https://doi.org/10.1158/1078-0432.ccr-07-5050

Steingart, R. M., Bakris, G. L., Chen, H. X., Chen, M. H., Force, T., Ivy, S. P., Leier, C. V., Liu, G., Lenihan, D., Lindenfeld, J., Maitland, M. L., Remick, S. C., & Tang, W. H. (2012). Management of cardiac toxicity in patients receiving vascular endothelial growth factor signaling pathway inhibitors. *Am Heart J, 163*(2), 156-163. https://doi.org/10.1016/j.ahj.2011.10.018

Stevens, J. L., & Baker, T. K. (2009). The future of drug safety testing: expanding the view and narrowing the focus. *Drug Discov Today, 14*(3-4), 162-167. https://doi.org/10.1016/j.drudis.2008.11.009

Stevens, M., & Oltean, S. (2019). Modulation of Receptor Tyrosine Kinase Activity through Alternative Splicing of Ligands and Receptors in the VEGF-A/VEGFR Axis. *Cells, 8*(4), 288. https://www.mdpi.com/2073-4409/8/4/288

Stevens, M., Star, E., Lee, M., Innes, E., Li, L., Bowler, E., Harper, S., Bates, D. O., & Oltean, S. (2019). The VEGF-A exon 8 splicing-sensitive fluorescent reporter mouse is a novel tool to assess the effects of splicing regulatory compounds in vivo. *RNA biology, 16*(12), 1672-1681. https://doi.org/10.1080/15476286.2019.1652522

Sung, H., Ferlay, J., Siegel, R. L., Laversanne, M., Soerjomataram, I., Jemal, A., & Bray, F. (2021). Global Cancer Statistics 2020: GLOBOCAN Estimates of Incidence and Mortality Worldwide for 36 Cancers in 185 Countries. *CA Cancer J Clin, 71*(3), 209-249. https://doi.org/10.3322/caac.21660

Takahashi, H., & Shibuya, M. (2005). The vascular endothelial growth factor (VEGF)/VEGF receptor system and its role under physiological and pathological conditions. *Clin Sci (Lond), 109*(3), 227-241. https://doi.org/10.1042/cs20040370

Tan, E., Chin, C. S. H., Lim, Z. F. S., & Ng, S. K. (2021). HEK293 Cell Line as a Platform to Produce Recombinant Proteins and Viral Vectors. *Front Bioeng Biotechnol, 9*, 796991. https://doi.org/10.3389/fbioe.2021.796991

Tan, I., Butlin, M., Spronck, B., Xiao, H., & Avolio, A. (2018). Effect of Heart Rate on Arterial Stiffness as Assessed by Pulse Wave Velocity. *Curr Hypertens Rev, 14*(2), 107-122. https://doi.org/10.2174/1573402113666170724100418

Tan, L.-L., & Lyon, A. R. (2021). Cardio-oncology for the general cardiologist. *Heart, 107*(15), 1254-1266. https://doi.org/10.1136/heartjnl-2020-317871

Thomas, P., & Smart, T. G. (2005). HEK293 cell line: a vehicle for the expression of recombinant proteins. *J Pharmacol Toxicol Methods, 51*(3), 187-200. https://doi.org/10.1016/j.vascn.2004.08.014

Thorin, E., & Webb, D. J. (2010). Endothelium-derived endothelin-1. *Pflugers Arch, 459*(6), 951-958. https://doi.org/10.1007/s00424-009-0763-y

Tian, X., Song, S., Wu, J., Meng, L., Dong, Z., & Shou, C. (2001). Vascular endothelial growth factor: acting as an autocrine growth factor for human gastric adenocarcinoma cell MGC803. *Biochem Biophys Res Commun, 286*(3), 505-512. https://doi.org/10.1006/bbrc.2001.5409

Tischer, E., Mitchell, R., Hartman, T., Silva, M., Gospodarowicz, D., Fiddes, J. C., & Abraham, J. A. (1991). The human gene for vascular endothelial growth factor. Multiple protein forms are encoded through alternative exon splicing. *J Biol Chem, 266*(18), 11947-11954.

Tocci, P., Blandino, G., & Bagnato, A. (2021). YAP and endothelin-1 signaling: an emerging alliance in cancer. *Journal of Experimental & Clinical Cancer Research, 40*(1), 27. https://doi.org/10.1186/s13046-021-01827-8

Tohyama, O., Matsui, J., Kodama, K., Hata-Sugi, N., Kimura, T., Okamoto, K., Minoshima, Y., Iwata, M., & Funahashi, Y. (2014). Antitumor activity of lenvatinib (e7080): an angiogenesis inhibitor that targets multiple receptor tyrosine kinases in preclinical human thyroid cancer models. *J Thyroid Res, 2014*, 638747. https://doi.org/10.1155/2014/638747

Touyz, R. M. (2004). Reactive oxygen species, vascular oxidative stress, and redox signaling in hypertension: what is the clinical significance? *Hypertension, 44*(3), 248-252. https://doi.org/10.1161/01.HYP.0000138070.47616.9d

Touyz, R. M., & Herrmann, J. (2018). Cardiotoxicity with vascular endothelial growth factor inhibitor therapy. *NPJ Precis Oncol, 2*, 13. https://doi.org/10.1038/s41698-018-0056-z

Touyz, R. M., Herrmann, S. M. S., & Herrmann, J. (2018). Vascular toxicities with VEGF inhibitor therapies-focus on hypertension and arterial thrombotic events. *J Am Soc Hypertens, 12*(6), 409-425. https://doi.org/10.1016/j.jash.2018.03.008

Touyz, R. M., Lang, N. N., Herrmann, J., Meiracker, A. H. v. d., & Danser, A. H. J. (2017). Recent Advances in Hypertension and Cardiovascular Toxicities With Vascular Endothelial Growth Factor Inhibition. *Hypertension, 70*(2), 220-226. https://doi.org/doi:10.1161/HYPERTENSIONAHA.117.08856

Touyz, R. M., Lang, N. N., Herrmann, J., van den Meiracker, A. H., & Danser, A. H. J. (2017). Recent Advances in Hypertension and Cardiovascular Toxicities With Vascular Endothelial Growth Factor Inhibition. *Hypertension, 70*(2), 220-226. https://doi.org/10.1161/hypertensionaha.117.08856

Townsend, D. (2016). Measuring Pressure Volume Loops in the Mouse. *J Vis Exp*(111). https://doi.org/10.3791/53810

Trame, M. N., Biliouris, K., Lesko, L. J., & Mettetal, J. T. (2016). Systems pharmacology to predict drug safety in drug development. *Eur J Pharm Sci, 94*, 93-95. https://doi.org/10.1016/j.ejps.2016.05.027

Tyler, T. (2012). Axitinib: newly approved for renal cell carcinoma. *J Adv Pract Oncol, 3*(5), 333-335. https://doi.org/10.6004/jadpro.2012.3.5.7

Ucuzian, A. A., Gassman, A. A., East, A. T., & Greisler, H. P. (2010). Molecular mediators of angiogenesis. *J Burn Care Res, 31*(1), 158-175. https://doi.org/10.1097/BCR.0b013e3181c7ed82

Valentin, J. P., Keisu, M. and Hammond, T.G. (2010). Predicting Human Adverse Drug Reactions from Nonclinical Safety Studies. In *Pharmaceutical Sciences Encyclopedia* (pp. 1-27). https://doi.org/https://doi.org/10.1002/9780470571224.pse203

Van Daele, M., Kilpatrick, L. E., Woolard, J., & Hill, S. J. (2023). Characterisation of tyrosine kinase inhibitor-receptor interactions at VEGFR2 using sunitinib-red and nanoBRET. *Biochem Pharmacol, 214*, 115672. https://doi.org/10.1016/j.bcp.2023.115672

van der Veldt, A. A., de Boer, M. P., Boven, E., Eringa, E. C., van den Eertwegh, A. J., van Hinsbergh, V. W., Smulders, Y. M., & Serné, E. H. (2010). Reduction in skin microvascular density and changes in vessel morphology in patients treated with sunitinib. *Anticancer Drugs, 21*(4), 439-446. https://doi.org/10.1097/CAD.0b013e3283359c79

van Geel, R. M., Beijnen, J. H., & Schellens, J. H. (2012). Concise drug review: pazopanib and axitinib. *Oncologist, 17*(8), 1081-1089. https://doi.org/10.1634/theoncologist.2012-0055

van Varik, B. J., Rennenberg, R. J., Reutelingsperger, C. P., Kroon, A. A., de Leeuw, P. W., & Schurgers, L. J. (2012). Mechanisms of arterial remodeling: lessons from genetic diseases. *Front Genet, 3*, 290. https://doi.org/10.3389/fgene.2012.00290

Van Vliet, B. N., Chafe, L. L., Antic, V., Schnyder-Candrian, S., & Montani, J. P. (2000). Direct and indirect methods used to study arterial blood pressure. *J Pharmacol Toxicol Methods, 44*(2), 361-373. https://doi.org/10.1016/s1056-8719(00)00126-x

Vasudev, N. S., & Reynolds, A. R. (2014). Anti-angiogenic therapy for cancer: current progress, unresolved questions and future directions. *Angiogenesis, 17*(3), 471-494. https://doi.org/10.1007/s10456-014-9420-y

Verheul, H. M. W., & Pinedo, H. M. (2007). Possible molecular mechanisms involved in the toxicity of angiogenesis inhibition. *Nature Reviews Cancer, 7*(6), 475-485. https://doi.org/10.1038/nrc2152

Veronese, M. L., Mosenkis, A., Flaherty, K. T., Gallagher, M., Stevenson, J. P., Townsend, R. R., & O'Dwyer, P. J. (2006). Mechanisms of hypertension associated with BAY 43-9006. *J Clin Oncol, 24*(9), 1363-1369. https://doi.org/10.1200/JCO.2005.02.0503

Versmissen, J., Mirabito Colafella, K. M., Koolen, S. L. W., & Danser, A. H. J. (2019). Vascular Cardio-Oncology: Vascular Endothelial Growth Factor inhibitors and hypertension. *Cardiovasc Res, 115*(5), 904-914. https://doi.org/10.1093/cvr/cvz022

Viallard, C., & Larrivee, B. (2017). Tumor angiogenesis and vascular normalization: alternative therapeutic targets. *Angiogenesis, 20*(4), 409-426. https://doi.org/10.1007/s10456-017-9562-9

Vieira, J. M., Ruhrberg, C., & Schwarz, Q. (2010). VEGF receptor signaling in vertebrate development. *Organogenesis, 6*(2), 97-106. https://doi.org/10.4161/org.6.2.11686

Vlachopoulos, C., & O'Rourke, M. (2000). Diastolic pressure, systolic pressure, or pulse pressure? *Curr Hypertens Rep, 2*(3), 271-279. https://doi.org/10.1007/s11906-000-0010-6

Vlahakis, N. E., Young, B. A., Atakilit, A., Hawkridge, A. E., Issaka, R. B., Boudreau, N., & Sheppard, D. (2007). Integrin α9β1 Directly Binds to Vascular Endothelial Growth Factor (VEGF)-A and Contributes to VEGF-A-induced Angiogenesis. *Journal of Biological Chemistry, 282*(20), 15187-15196. https://doi.org/10.1074/jbc.M609323200

Voron, T., Colussi, O., Marcheteau, E., Pernot, S., Nizard, M., Pointet, A.-L., Latreche, S., Bergaya, S., Benhamouda, N., Tanchot, C., Stockmann, C., Combe, P., Berger, A., Zinzindohoue, F., Yagita, H., Tartour, E., Taieb, J., & Terme, M. (2015). VEGF-A modulates expression of inhibitory checkpoints on CD8+ T cells in tumors. *Journal of Experimental Medicine, 212*(2), 139-148. https://doi.org/10.1084/jem.20140559

Wagner, O. F., Christ, G., Wojta, J., Vierhapper, H., Parzer, S., Nowotny, P. J., Schneider, B., Waldhäusl, W., & Binder, B. R. (1992). Polar secretion of endothelin-1 by cultured endothelial cells. *J Biol Chem, 267*(23), 16066-16068.

Wang, X., Bove, A. M., Simone, G., & Ma, B. (2020). Molecular Bases of VEGFR-2-Mediated Physiological Function and Pathological Role. *Front Cell Dev Biol, 8*, 599281. https://doi.org/10.3389/fcell.2020.599281

Weaver, R. J., & Valentin, J.-P. (2018). Today's Challenges to De-Risk and Predict Drug Safety in Human "Mind-the-Gap". *Toxicological Sciences, 167*(2), 307-321. https://doi.org/10.1093/toxsci/kfy270

Wellstein, A., Giaccone, G., Atkins, M. B., & E.A., a. S. (2018). Pathway-Targeted Therapies: Monoclonal Antibodies, Protein Kinase Inhibitors, and Various Small Molecules. *Goodman & Gilman's: The Pharmacological Basis of Therapeutics, 13e, Chapter 67*, 1203-1240.

Welti, J., Loges, S., Dimmeler, S., & Carmeliet, P. (2013). Recent molecular discoveries in angiogenesis and antiangiogenic therapies in cancer. *J Clin Invest, 123*(8), 3190-3200. https://doi.org/10.1172/JCI70212

White, D. G., Cannon, T. R., Garratt, H., Mundin, J. W., Sumner, M. J., & Watts, I. S. (1993). Endothelin ETA and ETB receptors mediate vascular smooth-muscle contraction. *J Cardiovasc Pharmacol, 22 Suppl 8*, S144-148. https://doi.org/10.1097/00005344-199322008-00039

Wilkinson, I. B., & McEniery, C. M. (2004). Arterial stiffness, endothelial function and novel pharmacological approaches. *Clin Exp Pharmacol Physiol, 31*(11), 795-799. https://doi.org/10.1111/j.1440-1681.2004.04074.x

Williams, B., Mancia, G., Spiering, W., Agabiti Rosei, E., Azizi, M., Burnier, M., Clement, D. L., Coca, A., de Simone, G., Dominiczak, A., Kahan, T., Mahfoud, F., Redon, J., Ruilope, L., Zanchetti, A., Kerins, M., Kjeldsen, S. E., Kreutz, R., Laurent, S., Lip, G. Y. H., McManus, R., Narkiewicz, K., Ruschitzka, F., Schmieder, R. E., Shlyakhto, E., Tsioufis, C., Aboyans, V., & Desormais, I. (2018). 2018 ESC/ESH Guidelines for the management of arterial hypertension. *Eur Heart J, 39*(33), 3021-3104. https://doi.org/10.1093/eurheartj/ehy339

Williams, P. D. (1990). The role of pharmacological profiling in safety assessment. *Regulatory Toxicology and Pharmacology, 12*(3, Part 1), 238-252. https://doi.org/https://doi.org/10.1016/S0273-2300(05)80061-3

Wilson, D. P. (2011). Vascular Smooth Muscle Structure and Function. In R. Fitridge & M. Thompson (Eds.), *Mechanisms of Vascular Disease: A Reference Book for Vascular Specialists*. University of Adelaide Press

Winkler, F., Kozin, S. V., Tong, R. T., Chae, S. S., Booth, M. F., Garkavtsev, I., Xu, L., Hicklin, D. J., Fukumura, D., di Tomaso, E., Munn, L. L., & Jain, R. K. (2004). Kinetics of vascular normalization by VEGFR2 blockade governs brain tumor response to radiation: role of oxygenation, angiopoietin-1, and matrix metalloproteinases. *Cancer Cell, 6*(6), 553-563. https://doi.org/10.1016/j.ccr.2004.10.011

Winn, M., von Geldern, T. W., Opgenorth, T. J., Jae, H. S., Tasker, A. S., Boyd, S. A., Kester, J. A., Mantei, R. A., Bal, R., Sorensen, B. K., Wu-Wong, J. R., Chiou, W. J., Dixon, D. B., Novosad, E. I., Hernandez, L., & Marsh, K. C. (1996). 2,4-Diarylpyrrolidine-3-carboxylic acids--potent ETA selective endothelin receptor antagonists. 1. Discovery of A-127722. *J Med Chem, 39*(5), 1039-1048. https://doi.org/10.1021/jm9505369

Wiszniak, S., & Schwarz, Q. (2021). Exploring the Intracrine Functions of VEGF-A. *Biomolecules, 11*(1). https://doi.org/10.3390/biom11010128

Wood, J. M., Bold, G., Buchdunger, E., Cozens, R., Ferrari, S., Frei, J., Hofmann, F., Mestan, J., Mett, H., O'Reilly, T., Persohn, E., Rösel, J., Schnell, C., Stover, D., Theuer, A., Towbin, H., Wenger, F., Woods-Cook, K., Menrad, A., Siemeister, G., Schirner, M., Thierauch, K. H., Schneider, M. R., Drevs, J., Martiny-Baron, G., & Totzke, F. (2000). PTK787/ZK 222584, a novel and potent inhibitor of vascular endothelial growth factor receptor

tyrosine kinases, impairs vascular endothelial growth factor-induced responses and tumor growth after oral administration. *Cancer Res, 60*(8), 2178-2189.

Woolard, J., Bennett, T., Dunn, W. R., Heal, D. J., Aspley, S., & Gardiner, S. M. (2004). Acute cardiovascular effects of sibutramine in conscious rats. *J Pharmacol Exp Ther, 308*(3), 1102-1110. https://doi.org/10.1124/jpet.103.061259

Woolard, J., Bevan, H. S., Harper, S. J., & Bates, D. O. (2009). Molecular diversity of VEGF-A as a regulator of its biological activity. *Microcirculation, 16*(7), 572-592. https://doi.org/10.1080/10739680902997333

Woolard, J., Wang, W. Y., Bevan, H. S., Qiu, Y., Morbidelli, L., Pritchard-Jones, R. O., Cui, T. G., Sugiono, M., Waine, E., Perrin, R., Foster, R., Digby-Bell, J., Shields, J. D., Whittles, C. E., Mushens, R. E., Gillatt, D. A., Ziche, M., Harper, S. J., & Bates, D. O. (2004). VEGF165b, an inhibitory vascular endothelial growth factor splice variant: mechanism of action, in vivo effect on angiogenesis and endogenous protein expression. *Cancer Res, 64*(21), 7822-7835. https://doi.org/10.1158/0008-5472.Can-04-0934

Wragg, E. S., Pannucci, P., Hill, S. J., Woolard, J., & Cooper, S. L. (2022). Involvement of β-adrenoceptors in the cardiovascular responses induced by selective adenosine A(2A) and A(2B) receptor agonists. *Pharmacol Res Perspect, 10*(3), e00975. https://doi.org/10.1002/prp2.975

Wu, J. B., Tang, Y. L., & Liang, X. H. (2018). Targeting VEGF pathway to normalize the vasculature: an emerging insight in cancer therapy. *Onco Targets Ther, 11*, 6901-6909. https://doi.org/10.2147/ott.S172042

Wu, S., Chen, J. J., Kudelka, A., Lu, J., & Zhu, X. (2008). Incidence and risk of hypertension with sorafenib in patients with cancer: a systematic review and meta-analysis. *The Lancet Oncology, 9*(2), 117-123. https://doi.org/10.1016/s1470-2045(08)70003-2

Wu, X.-M., Zhang, N., Li, J.-S., Yang, Z.-H., Huang, X.-L., & Yang, X.-F. (2023). Purinergic receptors mediate endothelial dysfunction and participate in atherosclerosis. *Purinergic signalling, 19*(1), 265-272. https://doi.org/10.1007/s11302-021-09839-x

Xia, Y., Jiang, L., & Zhong, T. (2018). The role of HIF-1α in chemo-/radioresistant tumors. *Onco Targets Ther, 11*, 3003-3011. https://doi.org/10.2147/ott.S158206

Yamagishi, N., Teshima-Kondo, S., Masuda, K., Nishida, K., Kuwano, Y., Dang, D. T., Dang, L. H., Nikawa, T., & Rokutan, K. (2013). Chronic inhibition of tumor cell-derived VEGF enhances the malignant phenotype of colorectal cancer cells. *BMC Cancer, 13*(1), 229. https://doi.org/10.1186/1471-2407-13-229

Yamazaki, Y., & Morita, T. (2006). Molecular and functional diversity of vascular endothelial growth factors. *Molecular Diversity, 10*(4), 515. https://doi.org/10.1007/s11030-006-9027-3

Yang, B., & Papoian, T. (2012). Tyrosine kinase inhibitor (TKI)-induced cardiotoxicity: approaches to narrow the gaps between preclinical safety evaluation and clinical outcome. *J Appl Toxicol, 32*(12), 945-951. https://doi.org/10.1002/jat.2813

Yang, B., & Papoian, T. (2018). Preclinical approaches to assess potential kinase inhibitor-induced cardiac toxicity: Past, present and future. *Journal of Applied Toxicology, 38*(6), 790-800. https://doi.org/https://doi.org/10.1002/jat.3584

Yang, J. C., Haworth, L., Sherry, R. M., Hwu, P., Schwartzentruber, D. J., Topalian, S. L., Steinberg, S. M., Chen, H. X., & Rosenberg, S. A. (2003). A randomized trial of bevacizumab, an anti-vascular endothelial growth factor antibody, for metastatic renal cancer. *N Engl J Med, 349*(5), 427-434. https://doi.org/10.1056/NEJMoa021491

Yang, Y., Li, N., Chen, T., Zhang, C., Liu, L., Qi, Y., & Bu, P. (2019). Trimetazidine ameliorates sunitinib-induced cardiotoxicity in mice via the AMPK/mTOR/autophagy pathway. *Pharmaceutical Biology, 57*(1), 625-631. https://doi.org/10.1080/13880209.2019.1657905

Yao, J., Wu, X., Zhuang, G., Kasman, I. M., Vogt, T., Phan, V., Shibuya, M., Ferrara, N., & Bais, C. (2011). Expression of a functional VEGFR-1 in tumor cells is a major determinant of anti-PlGF antibodies efficacy. *Proc Natl Acad Sci U S A, 108*(28), 11590-11595. https://doi.org/10.1073/pnas.1109029108

Ye, X., Gaucher, J. F., Vidal, M., & Broussy, S. (2021). A Structural Overview of Vascular Endothelial Growth Factors Pharmacological Ligands: From Macromolecules to Designed Peptidomimetics. *Molecules, 26*(22). https://doi.org/10.3390/molecules26226759

Yeh, E. T., & Bickford, C. L. (2009). Cardiovascular complications of cancer therapy: incidence, pathogenesis, diagnosis, and management. *J Am Coll Cardiol, 53*(24), 2231-2247. https://doi.org/10.1016/j.jacc.2009.02.050

Yuan, Z., Li, Y., Zhang, S., Wang, X., Dou, H., Yu, X., Zhang, Z., Yang, S., & Xiao, M. (2023). Extracellular matrix remodeling in tumor progression and immune escape: from mechanisms to treatments. *Molecular Cancer, 22*(1), 48. https://doi.org/10.1186/s12943-023-01744-8

Zarrabi, K., Fang, C., & Wu, S. (2017). New treatment options for metastatic renal cell carcinoma with prior anti-angiogenesis therapy. *Journal of hematology & oncology, 10*(1), 38-38. https://doi.org/10.1186/s13045-016-0374-y

Zentilin, L., Puligadda, U., Lionetti, V., Zacchigna, S., Collesi, C., Pattarini, L., Ruozi, G., Camporesi, S., Sinagra, G., Pepe, M., Recchia, F. A., & Giacca, M. (2010). Cardiomyocyte VEGFR-1 activation by VEGF-B induces compensatory hypertrophy and preserves cardiac function after myocardial infarction. *FASEB J, 24*(5), 1467-1478. https://doi.org/10.1096/fj.09-143180

Zhang, D., Zhang, X., & Zhao, C. (2016). Risk of venous and arterial thromboembolic events associated with anti-VEGF agents in advanced non-small-cell lung cancer: a meta-analysis and systematic review. *Onco Targets Ther, 9*, 3695-3704. https://doi.org/10.2147/ott.S103735

Zhang, F., Tang, Z., Hou, X., Lennartsson, J., Li, Y., Koch, A. W., Scotney, P., Lee, C., Arjunan, P., Dong, L., Kumar, A., Rissanen, T. T., Wang, B., Nagai, N., Fons, P., Fariss, R., Zhang, Y., Wawrousek, E., Tansey, G., Raber, J., Fong, G. H., Ding, H., Greenberg, D. A., Becker, K. G., Herbert, J. M., Nash, A., Yla-Herttuala, S., Cao, Y., Watts, R. J., & Li, X. (2009). VEGF-B is dispensable for blood vessel growth but critical for their survival, and VEGF-B targeting inhibits pathological angiogenesis. *Proc Natl Acad Sci U S A, 106*(15), 6152-6157. https://doi.org/10.1073/pnas.0813061106

Zhang, J., Yang, P. L., & Gray, N. S. (2009). Targeting cancer with small molecule kinase inhibitors. *Nature Reviews Cancer, 9*(1), 28-39. https://doi.org/10.1038/nrc2559

Zhang, L., Zhou, F., Han, W., Shen, B., Luo, J., Shibuya, M., & He, Y. (2010). VEGFR-3 ligand-binding and kinase activity are required for lymphangiogenesis but not for angiogenesis. *Cell Research, 20*(12), 1319-1331. https://doi.org/10.1038/cr.2010.116

Zhang, X., Shao, Y., & Wang, K. (2016). Incidence and risk of hypertension associated with cabozantinib in cancer patients: a systematic review and meta-analysis. *Expert Rev Clin Pharmacol, 9*(8), 1109-1115. https://doi.org/10.1080/17512433.2016.1190269

Zhang, Z.-F., Wang, T., Liu, L.-H., & Guo, H.-Q. (2014). Risks of Proteinuria Associated with Vascular Endothelial Growth Factor Receptor Tyrosine Kinase Inhibitors in Cancer Patients: A Systematic Review and Meta-Analysis. *PLoS One, 9*(3), e90135. https://doi.org/10.1371/journal.pone.0090135

Zhao, H., Liu, L., Ma, Y., Fang, J., Fang, W., Ma, H., Zhang, Y., Feng, G., Hong, S., Zeng, S., Xie, B., Ren, J., Lin, X., Zhang, Y., Xi, N., Jiang, Y., Wu, Y., Kang, N., Li, S., & Zhang, L. (2020). A phase Ib study of a novel c-MET, AXL and VEGFR-2 inhibitor ningetinib and gefitinib combination therapy in Chinese EGFR-TKI resistant NSCLC with T790M negative. *Journal of Clinical Oncology, 38*(15_suppl), 9583-9583. https://doi.org/10.1200/JCO.2020.38.15_suppl.9583

Zhao, Z. B., P.E. . (2020). Overview of Current Type I/II Kinase Inhibitors. *In: Shapiro P. (eds) Next Generation Kinase Inhibitors. Springer, Cham*. https://doi.org/https://doi.org/10.1007/978-3-030-48283-1_2

Zhong, L., Li, Y., Xiong, L., Wang, W., Wu, M., Yuan, T., Yang, W., Tian, C., Miao, Z., Wang, T., & Yang, S. (2021). Small molecules in targeted cancer therapy: advances, challenges, and future perspectives. *Signal Transduction and Targeted Therapy, 6*(1), 201. https://doi.org/10.1038/s41392-021-00572-w

Ziche, M., Maglione, D., Ribatti, D., Morbidelli, L., Lago, C. T., Battisti, M., Paoletti, I., Barra, A., Tucci, M., Parise, G., Vincenti, V., Granger, H. J., Viglietto, G., & Persico, M. G. (1997). Placenta growth factor-1 is chemotactic, mitogenic, and angiogenic. *Lab Invest, 76*(4), 517-531.

Ziello, J. E., Jovin, I. S., & Huang, Y. (2007). Hypoxia-Inducible Factor (HIF)-1 regulatory pathway and its potential for therapeutic intervention in malignancy and ischemia. *Yale J Biol Med, 80*(2), 51-60.

Zips, D., Eicheler, W., Geyer, P., Hessel, F., Dörfler, A., Thames, H. D., Haberey, M., & Baumann, M. (2005). Enhanced Susceptibility of Irradiated Tumor Vessels to Vascular Endothelial Growth Factor Receptor Tyrosine Kinase Inhibition. *Cancer Research, 65*(12), 5374-5379. https://doi.org/10.1158/0008-5472.Can-04-3379

Zuppinger, C., & Suter, T. M. (2010). Cancer Therapy-Associated Cardiotoxicity and Signaling in the Myocardium. *Journal of Cardiovascular Pharmacology, 56*(2), 141-146. https://doi.org/10.1097/FJC.0b013e3181e0f89a